Loss of function associated with breakdown of the blood-brain barrier in the central nervous system: an *in vivo* study

-

Grégory Delattre

A thesis submitted with the requirements of

University College London

for the degree of

Doctor of Philosophy

Department of Neuroinflammation

Institute of Neurology

University College London

2013

Declaration

I, Grégory Delattre, confirm that the work presented in this thesis is my own. Where information has been derived from other sources, I confirm this has been indicated. All the histological research has been performed personally, except that resin embedding and sectioning has been performed by Dr. Daniel Morrison.

Acknowledgements

First, I would like to thank my supervisor Prof. Kenneth Smith for having given me the opportunity to work in his laboratory, but also for his invaluable training, guidance and advice without which this work would not have been possible. Ken has always been available and open to discuss when needed. I am very grateful to him for that. I also would like to thank the Brain Research Trust for providing me the funding for this research.

I would also like to thank my colleagues and friends for their support. Particularly, I would like to thank Radha Desai, Helen Crehan and Joseph Jebelli for their friendship. I would also like to say thank you to Dr. Marija Sajic, Dr. Mona Sadeghian, Dr. Roshni Desai, Dr. Damineh Morsali, Dr. Andrew Davies, Dr. Daniel Morrison and Dr. Peter Anderson for their teaching, help and answers to all my questions. Also, thank you to Kim Chisholm, Keila Ida, Dimitra Schiza, Diogo Trigo, Fabian Peters and Mario Amatruda for providing the lab with a nice working environment.

Finally, my utmost gratitude goes to my family and especially my parents, who have always been there for me, providing me with everything I needed and giving me such examples to follow.

Merci pour tout.

Pour Karine.

Abstract

Loss of function associated with breakdown of the blood-brain barrier in the central nervous system: an in vivo study

Blood-brain barrier breakdown is a common feature of neuroinflammatory diseases, such as multiple sclerosis (MS). Indeed, blood proteins may play a role in the pathology of the disease. Here we investigate the link between the presence of blood-borne components in the CNS parenchyma and the expression of neurological deficits.

Male Sprague-Dawley rats were injected intraspinally with vascular endothelial growth factor (VEGF), which causes breakdown of the blood-brain barrier, or saline as control. The injection was made unilaterally at the T13 – L1 junction, namely the spinal level that controls hind limb movement. In VEGF-injected animals alone, hind limb motor and sensory deficits consistently appeared at day two after surgery, but not at days 1 or 3 (onwards), as assessed by behavioural and locomotor tests (horizontal ladder test, walking treadmill, von Frey hair test, inclined plane, burrowing). Histological examination revealed the presence of a blood-brain barrier leakage within the spinal cord as assessed by the presence of extravascular IgG and fibrinogen. Activated microglia/macrophages ($ED1^+$, MHC class II^+ and $OX\text{-}42^+$ cells) were present at the injection site, peaking at day two, along with activated astrocytes. The mechanism responsible for the neurological deficit was investigated by attempting to antagonize specific VEGF signalling pathways, assessing a potential hypoxic

state using immunohistochemical techniques, and characterizing neuronal excitability by electrophysiological methods.

VEGF injection provokes opening of the blood-brain barrier which is temporally and spatially associated with neuroinflammation and loss of function. The findings indicate a potential mechanism underlying loss of function in inflammatory neurological diseases such as MS.

Table of contents

List of figures

Chapter I: Introduction

Chapter II: Materials and Methods

Chapter III: Results – Behavioural analysis

Chapter IV: Results – Immunohistochemical analysis

Chapter V: Results – Mechanism investigation

Abbreviations

ABC	ATP-binding cassette
AD	Alzheimer's disease
ALS	Amyotrophic lateral sclerosis
ATP	Adenosine triphosphate
CD11b	Cluster of differentiation 11b
CNS	Central nervous system
CSF	Cerebrospinal fluid
Cy3	Cyanine 3
DAB	3, 3'-diaminobenzidine
EAE	Experimental autoimmune encephalomyelitis
EAAT	Excitatory amino acid transporter
EMG	Electromyograph
eNOS	Endothelial nitric oxide synthase
FITC	Fluorescein isothiocyanate
fMRI	Functional magnetic resonance imaging
Gd-DTPA	Gadolinium diethylenetriaminepentaacetic acid
GFAP	Glial fibrillary acidic protein
H&E	Haematoxylin and eosin
HIF-1α	Hypoxia inducible factor 1α
HIF-1β	Hypoxia inducible factor 1β
HRE	Hypoxia response element
HRP	Horseradish peroxidase
IFN-γ	Interferon γ

IL-1 β	Interleukin 1β
IL-1	Interleukin 1
IL-2	Interleukin 2
IL-6	Interleukin 6
iNOS	Inducible nitric oxide synthase
JAM	Junctional adhesion molecule
Kir4.1	Potassium inward rectifying channel 4.1
LPS	Lipopolysaccharide
LTP	Long-term potentiation
MAG	Myelin-associated glycoprotein
MCP-1	Monocyte chemoattractant protein 1
MRI	Magnetic resonance imaging
MRP	Multidrug resistant protein
MS	Multiple sclerosis
NMDA	N-methyl-D-aspartate
NO	Nitric oxide
NRP	Neuropilin
PAR	Protease activated receptor
PBS	Phosphate buffer saline
PBST	Phosphate buffer saline with Triton-X
PECAM-1	Platelet endothelial cell adhesion molecule 1
PD	Parkinson’s disease
PFA	Paraformaldehyde
P-gp	P-glycoprotein
PI3K	Phosphoinositide 3-kinase
PNS	Peripheral nervous system

PPMS	Primary progressive multiple sclerosis
PRMS	Progressive relapsing multiple sclerosis
PSD-95	Post-synaptic density 95
PTS	Peptide transport system
RECA-1	Rat endothelial cell antibody 1
rhVEGF	Recombinant human vascular endothelial growth factor
RRMS	Relapsing remitting multiple sclerosis
SAV	Streptavidin
SD	Sprague Dawley
SPMS	Secondary progressive multiple sclerosis
TGF-β	Transforming growth factor β
TLR-4	Toll-like receptor 4
TNF-α	Tumour necrosis factor α
VEGF	Vascular endothelial growth factor
VEGFR	Vascular endothelial growth factor receptor
VHL	Von Hippel-Lindau protein
VPF	Vascular permeability factor
ZO	Zonula occludens

Chapter I: Introduction

Multiple sclerosis (MS) is an inflammation-mediated disease causing non-traumatic disability to 2.5 million people worldwide (Compston and Coles, 2002). This demyelinating disease was first described by Charcot in 1868 (Charcot, 1868) and is usually characterised by a biphasic course. 85% of cases begin with relapsing-remitting MS (RRMS) during which unpredictable relapses occur and are followed by periods of remission. 90% of these patients then switch, after about 25 years, to a secondary-progressive MS (SPMS) form, with a progressive and non-reversible neurological decline. 10% of patients undergo a third type of MS, primary-progressive MS (PPMS), with progressive decline from disease onset without recovery. Finally, 5% of patients have a steady progressive decline punctuated by acute attacks, called progressive relapsing MS (PRMS) (Weinshenker, 1996). A summary of the different courses of the disease observed in patients is provided in figure I.1.

As described in this introduction, the aetiology of MS is complex and has not yet been elucidated. It is thought by many to involve an activation of auto-immunity against myelin proteins. It has traditionally been accepted that the symptoms are mainly due to dysfunction in axonal conduction arising from demyelination, but more recent studies suggest that inflammation may also be involved in the symptoms displayed during the relapses, and an energy deficit is thought to play a role. Attention has also focussed on alterations of the blood-brain barrier following the observation that this breakdown occurs as one of the first events in a new relapse. The aim of this study is to investigate whether breakdown of the blood-brain barrier plays a causative role in the production of neurological deficits in vivo.

I.1- Clinico-pathology of MS

I.1.1- Relapses

The appearance of new symptoms, called a relapse, is caused by neurological dysfunction which can be attributed to several different pathological events.

I.1.1.1- Demyelination

Demyelination is considered to be a primary cause of neurological deficits in MS patients. Loss of myelin exposes the axolemma and leads to conduction failure due to several mechanisms, including a deficit of sodium channels on this newly exposed part of the axon (Waxman et al., 1994; Waxman and Ritchie, 1993). The cause of the demyelination is not understood, but many believe that an immunological reaction is mediated by T-cells directly targeting myelin protein (Ben-Nun et al., 1996; Kerlero de Rosbo et al., 1993). Oligodendrocyte injury may also play a role in the demyelination phenomenon observed in MS (Patel and Balabanov, 2012). In MS lesions, oligodendrocytes express MHC-I molecules and are a potential direct target of the CD8+ T-cells (Hoftberger et al., 2004). Other factors such as inflammation and pro-inflammatory cytokines (Pouly et al., 2000; Vartanian et al., 1995), oxidative injury (Thorburne and Juurlink, 1996) and excitotoxicity (McDonald et al., 1998) also contribute to demyelination by affecting oligodendrocytes.

I.1.1.2- Inflammation

Generally, inflammatory cells such as macrophages, microglia or T lymphocytes are thought to be involved in the axonal injury observed in MS patients (Bitsch et al., 2000). Inflammatory cells enter the central nervous system (CNS) by crossing the blood-brain

barrier and can be deleterious by releasing cytokines. Inflammatory cytokines, such as tumour necrosis factor alpha (TNF-α) or interferon gamma (IFN-γ) have been reported to play a role in MS following the observation that increased levels of these cytokines correlated with the worsening of symptoms and exacerbation of pre-existing symptoms (Moreau et al., 1996). Pro-inflammatory cytokines can also provoke production of inducible nitric oxide synthase (iNOS), an inflammatory mediator thought to play a role in the neurological dysfunction observed in MS and experimental autoimmune encephalomyelitis (EAE), an animal model of MS (Bo et al., 1994; MacMicking et al., 1992; Willenborg et al., 2007). Although demyelination has traditionally been thought to be the cause of loss of conduction, inflammation (Youl et al., 1991) and nitric oxide (Redford et al., 1997) have been shown to be sufficient to affect conduction properties on their own.

I.1.1.3- Excitotoxicity

In RRMS patients, an increase in CSF levels of glutamate and aspartate has been demonstrated in active lesions (Sarchielli et al., 2003) and MRI studies have confirmed these findings (Srinivasan et al., 2005). This increase in excitatory amino acid levels leads to an abnormal activation of ionotropic glutamate receptors (AMPA/kainate and NMDA receptors) and trigger an excessive influx of calcium in neurons and oligodendrocytes where these receptors are present, leading to neuronal degeneration (Arundine and Tymianski, 2003). Immunohistochemical studies show a correlation between axonal and oligodendrocyte damage and abnormal glutamate levels (Werner et al., 2001). Inhibition of glutamate receptors reduces neurological deficits in EAE (Wallstrom et al., 1996), probably by reducing axonal and oligodendrocyte damage (Pitt et al., 2000; Werner et al., 2000). Since oligodendrocytes play a major role in glutamate removal (Pitt et al., 2003), their destruction could further enhance glutamate's deleterious effects.

I.1.2- Remission

Between relapses, patients suffering from MS typically have periods of remission of variable length. The recovery of functions lost during a relapse occurs by several mechanisms, but perhaps most importantly by remyelination, which helps to restore conduction to (formerly) demyelinated axons. This process typically involves recruitment of oligodendrocyte precursor cells (Takahashi et al., 2013) which transform into oligodendrocytes that produce the myelin lipids and protein necessary for remyelination, enabling recovery of saltatory conduction (Nave and Trapp, 2008). Remyelination is not the only way to restore conduction. Resolution of inflammation has also been shown to correlate with recovery of function (Redford et al., 1997; Youl et al., 1991). Compensation by increasing the number of sodium channels has also been shown to restore conduction in demyelinated axons, allowing slower but effective conduction (Black et al., 1997). Finally, adaptive changes of the neural network may contribute to the disappearance of symptoms. Indeed, functional magnetic resonance imaging (fMRI) studies in MS patients (Cerasa et al., 2006; Pantano et al., 2006) showed a reorganization of the functional activity of the brain by modifying the pattern of brain activation, recruiting for parallel pathways to compensate for the pathological impairments.

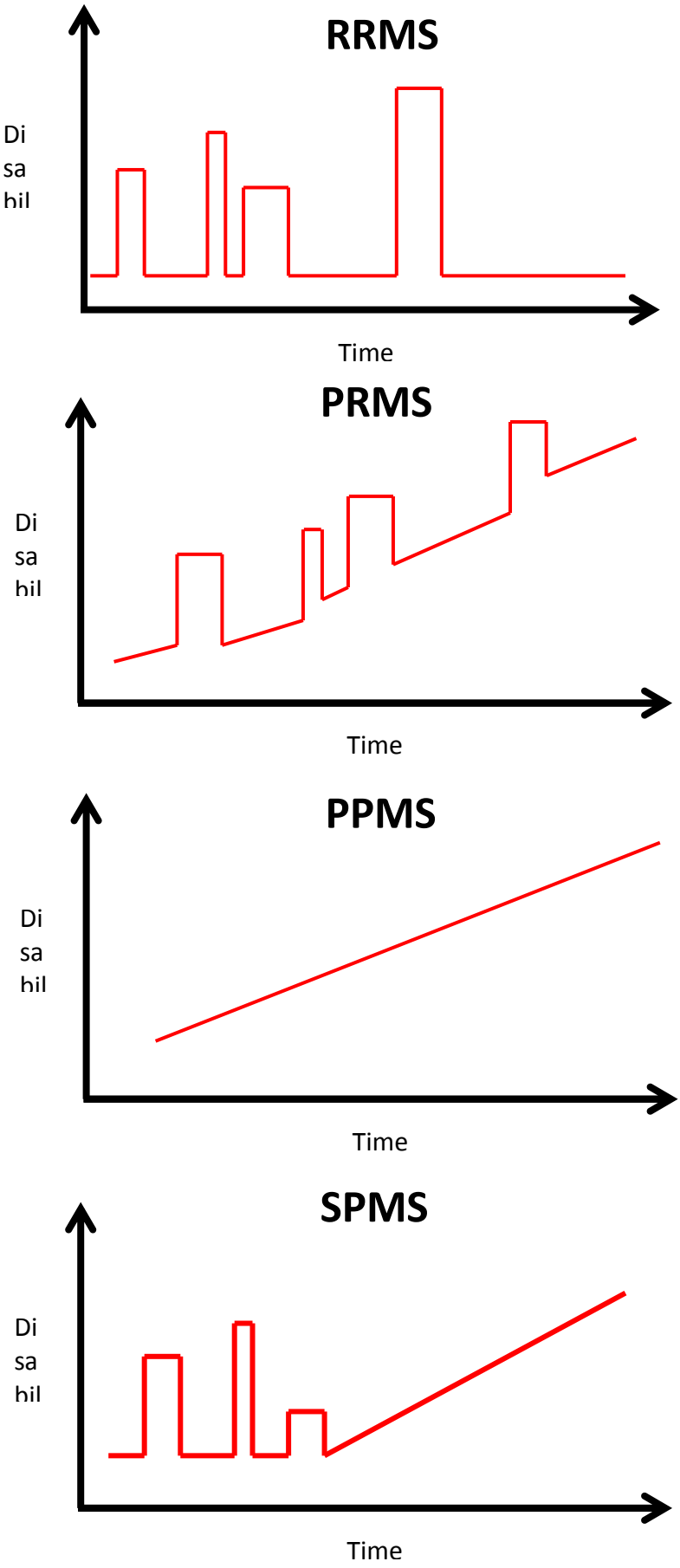

Figure I.1: *Evolution of disability with time for the different courses of disease observed in MS patients. RRMS: Relapsing remitting multiple sclerosis, PRMS: Progressive relapsing multiple sclerosis, PPMS: Primary progressive multiple sclerosis, SPMS: Secondary progressive multiple sclerosis.*

I.1.3- Progression

A relapsing/remitting phase of the disease may evolve into a progressive course in many patients. Others may experience a progressive course from the very beginning. Analysis of the CNS of such patients usually reveals areas of atrophy in both grey and white matter (Hofstetter et al., 2013). The permanent neurological deficit is thought to be caused by this atrophy rather than demyelination.

I.1.4- Heterogeneity of lesions

Pathological studies have revealed that different inflammatory components can play a role in demyelination (Lucchinetti et al., 2000) and axonal injury (Bitsch et al., 2000). Following this view, it has been proposed (Lucchinetti et al., 2000) that four different lesions patterns can be distinguished according to biopsy and autopsy results from patients with MS (Table I.1).

Firstly, Pattern I has been attributed to T-cell- and macrophage-related inflammation. The presence of immunoglobulins and activated astrocytes indicates damage of the blood-brain barrier. Myelin proteins are degraded independently of their identity, contrary to another pattern (see below), and oligodendrocytes are lost in active lesions but seem to be present in inactive lesions, giving rise to the possibility of remyelination of inactive lesions.

Pattern II is very similar to pattern I since it shares all the features described previously. The only difference is a stronger presence of immunoglobulins and the activation of complement, which can indicate a major role for immune activation.

Lesion Pattern	Macrophage and T-cell inflammation	Loss of oligodendrocytes	Immunoglobulin presence	Complement activation	Loss of myelin proteins
I	**Yes**	**No**	**Yes**	**No**	**All**
II	**Yes**	**No**	**Yes (strong)**	**Yes**	**All**
III	**Yes**	**Yes (apoptosis)**	**No**	**No**	**MAG only**
IV	**Yes**	**Yes (not apoptosis)**	**No**	**No**	**All**

Table I.1: *Characteristics of the four main lesion patterns observed in MS patients, according to the classification of Lucchinetti and colleagues.*

In Pattern III, the inflammatory infiltrate is still present but immunoglobulins and bound complement are not observed. However, preferential loss of myelin associated glycoprotein (MAG) occurs. At sites of MAG loss, a pronounced loss of oligodendrocytes is observed, mainly due to apoptosis (as indicated by presence of nuclear condensation and fragmentation (Cotter et al., 1990)). This preferential loss of MAG is associated with hypoxia-like tissue injury, indicated by production of hypoxia inducible factor-1α (HIF-1 α) (Aboul-Enein et al., 2003).

In Pattern IV lesions, T-cells and macrophages constitute the main portion of the inflammatory infiltrate. Demyelination is present in conjunction with oligodendrocyte death which occurs through a non-apoptotic pathway. Finally, there is simultaneous degradation of all myelin proteins.

I.1.5- Impairments of the motor system

In MS patients, lesions often localize within the sensory-motor pathway, causing motor dysfunction. This can be not only the most visible deficit, but also the most common. Weakness of the limbs is often experienced by MS patients during relapses, most commonly affecting the lower limbs. Weakness is usually noticed only after exertion at first, but with time it may be present constantly.

Spasticity is most often due to an amplification of motor reactivity to sensory stimulation, and results in hypertonia, an abnormally high muscle tone which confers unusual stiffness on muscles. Some patients also suffer from uncontrolled tremor (Alusi et al., 2001) in upper and lower limbs, and also in the trunk and head. Limb incoordination and gait ataxia is also a common feature of MS, resulting in clumsiness and poor balance.

I.2- The blood-brain barrier

The concept of the blood brain barrier was discovered in the beginning of the 20th century by Ehrlich who noticed that when injecting intravenously a range of dyes, staining was present in all tissue but the brain (Ehrlich, 1904). One of his students later confirmed his suspicion by injecting the same dyes into the cerebrospinal fluid (CSF) and observing that the dyes did not enter the blood flow (Goldmann, 1913).

I.2.1- Structure

The primary role of the blood brain barrier is to prevent plasma components, red blood cells and most leukocytes from entering the brain where they could be deleterious (Zlokovic, 2008). It also maintains the biochemical environment of the CNS necessary for its normal functioning, especially synaptic transmission. The barrier is mainly created by endothelial cells all along the capillaries in the brain and spinal cord (Abbott et al., 2010). Another interface is present at the epithelial cells of the choroid plexus, constituting the blood-cerebrospinal fluid barrier (Brown et al., 2004). Finally, the avascular arachnoid epithelium constitutes another barrier separating the extracellular fluid of the body from the central nervous system (Abbott et al., 2006). The paragraphs below will focus on the blood-brain barrier created by endothelial cells.

I.2.1.1- Cellular junctions

The blood brain barrier consists at the level of the vasculature of a monolayer of brain endothelial cells that are sealed together in order to prevent free exchange of solutes between the blood and the brain (figure I.2) (Brightman and Reese, 1969; Reese and

Karnovsky, 1967). This interface is characterised by a low paracellular permeability and high electrical resistance (Zlokovic, 2008), and it is achieved by cellular junctions between the brain endothelial cells that prevent free transfer of molecules between the blood and the brain. Indeed, only molecules smaller than 400 Da with less than nine hydrogen bonds can freely cross the blood-brain barrier (Pardridge, 2007). These cellular junctions consist of tight junctions, adherens junctions and proteins linking these junctions to the endothelial cell cytoskeleton.

Tight junctions

Tight junction proteins help to form a continuous membrane between the blood and the brain. The first to be discovered was occludin (Furuse et al., 1993), a 65 kDa integral membrane protein made of two extracellular domains. Whereas tight junctions in occludin-deficient mice do not seem to be altered at the ultrastructural level (Saitou et al., 2000), calcification of the brain is observed in these mice. It has also been shown that phosphorylation of occludin at the tight junction complex (Sakakibara et al., 1997) regulates permeability independently of changes in the cytoskeleton (Hirase et al., 2001). These observations suggest that occludin regulates, rather than contributes to, blood-brain barrier properties.

Claudins are a family of 23 kDa integral membrane proteins responsible for sealing of the blood-brain barrier (Furuse et al., 1998) through the interaction of their extracellular loops (Piontek et al., 2008). Claudin-3, -5 and -12 are localized in the brain (Nitta et al., 2003; Zlokovic, 2008) and prevent the leakage of molecules in a size-specific manner; for instance, claudin-5 deficiency in mice allow the diffusion of molecules smaller than 800 Da (Nitta et al., 2003).

Other proteins, called adhesion molecules, are also present in tight junction complexes. The junctional adhesion molecule family (JAM) plays a role via homophilic and heterophilic interactions (Bazzoni et al., 2000a; Wolburg and Lippoldt, 2002). These 40 kDa transmembrane proteins are involved in leukocyte recruitment into the brain (Del Maschio et al., 1999), and in organizing the intercellular structure via the interaction with occludin (Bazzoni et al., 2000b).

Finally, an endothelial cell-selective adhesion molecule (ESAM) has been found in endothelial cells (Nasdala et al., 2002) but its role in the tight junctional structure is still poorly understood.

Adherens junctions

Adherens junctions are expressed between brain endothelial cells (Schulze and Firth, 1993) and are responsible for adhesion between endothelial cells, as well as the regulation of permeability.

VE-cadherin is the main component of adherens junction proteins and is responsible for cell-cell adhesion via its extracellular loops (Vincent et al., 2004) via homophilic binding (Breviario et al., 1995). The cytoplasmic part is linked to the actin cytoskeleton by catenins (Knudsen et al., 1995) which stabilize the protein in the cell-membrane, because truncated molecules without links to actin do not promote adhesion nor control permeability (Breviario et al., 1995). VE-cadherins are also involved in angiogenesis and maintenance of blood vessels (Lampugnani and Dejana, 2007).

Platelet endothelial cell adhesion molecule 1 (PECAM-1 or CD31) is present on endothelial cells but outside the tight junction complex. It has been shown to play a role in lymphocyte

infiltration in the brain; the use of a soluble form of PECAM-1 impairs lymphocytes entry and diminishes the severity of symptoms in EAE mice (Reinke et al., 2007).

Cytoskeleton links

Tight junction and adherens junction proteins are linked to the cytoskeleton of endothelial cells by cytoplasmic accessory proteins (Hawkins and Davis, 2005). Proteins of the zonula occludens (ZO) family have been shown to interact with tight junction (Stevenson et al., 1986) and adherens junction proteins (Itoh et al., 1993). ZO-1 (220 kDa) is involved in the tight junction communication with the actin cytoskeleton (Fanning et al., 1998) and alteration in ZO-1 cellular localization correlates with inter-cellular permeability (Fischer et al., 2002). ZO-2 is thought to have a redundant function with ZO-1 as it is similarly distributed (Gumbiner et al., 1991) and can replace it to form normal tight junctions in cultured epithelia lacking ZO-1 (Umeda et al., 2004). Finally, ZO-3 is also present (Hawkins and Davis, 2005) but its function remains poorly understood.

I.2.1.2- The neurovascular unit

Several specialized cells communicate with the brain endothelia and form the neurovascular unit (Abbott et al., 2006). These cells are pericytes, astrocytes and microglia. Their close proximity to endothelial cells allows paracrine regulations (Lok et al., 2007).

Pericytes

Pericytes wrap the endothelium with their processes and, along their cytoplasmic processes that encircle 30% to 70% of the capillary wall (Zlokovic, 2008), they communicate directly with endothelial cells through specialized synapses (Bell and Zlokovic, 2009). At points of contact, which are functionally determined, tight junctions and adherens

junctions are present (Allt and Lawrenson, 2001). They are involved in microvessel stability in a mechanical manner (von Tell et al., 2006) but also by promoting endothelial cell differentiation and quiescence (Armulik et al., 2005). Pericytes also control the formation of tight junctions (Daneman et al., 2010), guide endothelial cells during developmental angiogenesis (Virgintino et al., 2007), and their contractile properties allow for the regulation of capillary blood flow (Peppiatt et al., 2006).

Astrocytes

The endfeet of astrocytes make contacts with other cells in the neurovascular unit (figure I.2), which is important in the regulation of the extracellular electrolyte concentration. Their perivascular endfeet express the water channel aquaporin-4 (Nielsen et al., 1997) and the potassium channel Kir 4.1 (Takumi et al., 1995) and contribute to water volume and electrolyte regulation. For example, blood-brain barrier disruption leads to overexpression of aquaporin-4 receptors in perivascular astrocytes presumably to limit oedema formation (Tomas-Camardiel et al., 2005). They also secrete factors able to modify the blood-brain barrier phenotype in vitro by reducing angiogenesis (Lee et al., 2003), and promote maturation of the blood brain barrier via formation of tight junctions induced by glial derived neurotrophic factor (Igarashi et al., 1999). Astrocytes also contribute to neurovascular coupling by adapting cerebral blood flow to the neural metabolic demand, as photolysis of caged Ca^{2+} in astrocytic endfeet leads to vasodilation (Anderson and Nedergaard, 2003). Moreover, inhibition of astrocytic metabotropic glutamate receptor-mediated Ca^{2+} oscillations reduces the vasodilation induced by an increase in neural activity both in vitro and in vivo (Zonta et al., 2003).

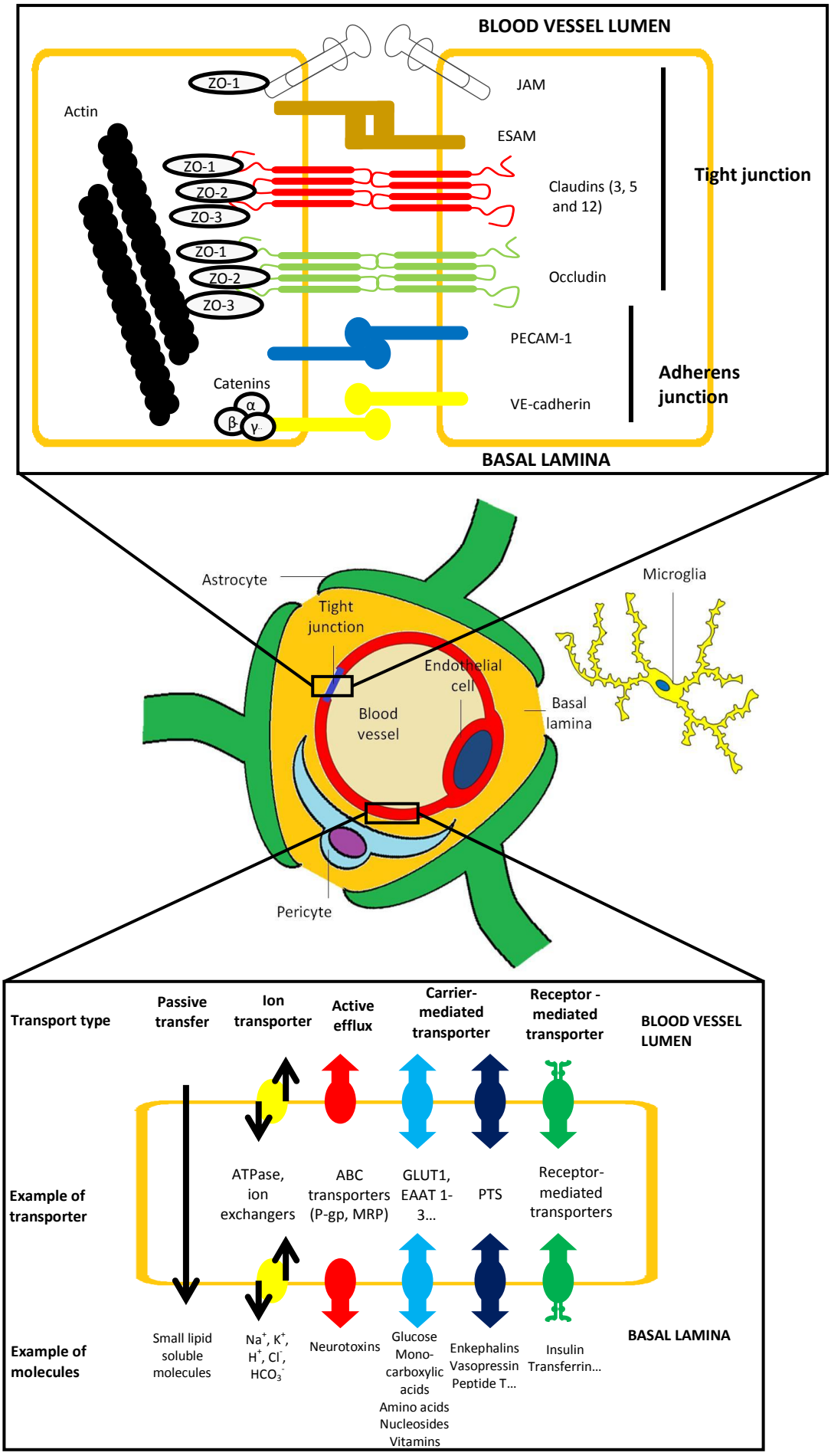

Figure I.2: *Cellular organisation of the blood-brain barrier.*

Microglia

Microglia connect with the brain endothelial cells by making endfeet connections and forming the glia limitans with astrocytes (figure I.2), which constitutes the barrier against mononuclear cell infiltration into the brain (Man et al., 2007). The perivascular microglial cells, endogenous to the CNS, are derived from bone marrow (Hickey and Kimura, 1988) and present antigens to infiltrating lymphocytes. Microglia also communicate with the blood brain barrier via cytokines and chemokines in order to allow the recruitment by the CNS of peripheral mononuclear cells by a process of diapedesis through the cytoplasm of endothelial cells rather than a paracellular route (Abbott et al., 2010). The role of microglia in the breakdown of the blood-brain barrier is discussed below.

Basal lamina

Finally, astrocytes and pericytes are separated from the brain endothelia by the basal lamina (figure I.2) (Zlokovic, 2008). This membrane is made of matrix proteins such as collagen and laminin and provides mechanical support for the neurovascular unit (Desai et al., 2007). The neurovascular unit cells all express matrix adhesion receptors (Del Zoppo et al., 2006), such as the integrin family which regulates endothelial cell migration and vessel formation during angiogenesis (del Zoppo and Milner, 2006).

I.2.2- Function

I.2.2.1- Ion balance

The blood brain barrier regulates the ion concentration in the CSF thanks to specific ion channels and transporters in order to maintain the optimal synaptic activity. For instance, the concentration of potassium in the CSF is maintained at 2.5-2.9 mM independently of

the variations in concentration in plasma (approximately 4.5 mM) (Hansen, 1985). The sodium pump (Na^+-K^+-ATPase) regulates the sodium and potassium gradients at the abluminal membrane (Zlokovic, 2008) while, at the luminal membrane, the Na^+-K^+-$2CL^-$ co-transporter is responsible for the entry of potassium, sodium and chloride into the brain (O'Donnell et al., 2004). Intracellular pH control is performed via sodium-hydrogen exchangers expressed at the luminal surface, and chloride-bicarbonate exchangers present on both sides of the barrier (Taylor et al., 2006). Other ions such as Ca^{2+}, Mg^{2+} are also regulated at the blood brain barrier (Jeong et al., 2006; Nischwitz et al., 2008).

I.2.2.2- Neurotransmitters

Glutamate, a neuroexcitatory amino acid, is present in high concentration in the blood and its level varies significantly after ingestion of food (Abbott et al., 2010). Three excitatory amino acid transporters (EAAT-1, 2 and 3) are localized at the blood brain barrier and are responsible for glutamate and aspartate homeostasis. Depending on the extracellular level of glutamate, influx or efflux of glutamate occurs. For example, the systemic use of a glutamate scavenging agent, which reduces the glutamate level in the blood, leads to efflux of glutamate from the brain and reduces excitotoxicity after brain injury (Zlotnik et al., 2007). The blood brain barrier thus prevents its release into the CNS in an uncontrolled manner and subsequent neurotoxic damage. In this way the barrier allows keeping the central and peripheral neurotransmitter pools separated (Bernacki et al., 2008).

I.2.2.3- Macromolecules

Specific peptide and protein transporters, mainly peptide transport system proteins (PTS), are also present at the blood-brain barrier. PTS-1 and -2 are located at the abluminal

surface and are responsible for efflux of enkephalins (Banks and Kastin, 1997) and arginine-vasopressin (Banks et al., 1987) respectively from the brain. PTS-3 transports peptide T into the brain (Barrera et al., 1987) and PTS-4 can transport macromolecules bi-directionally (Barrera et al., 1991).

Receptor-mediated transport systems are responsible for transfer of larger molecules such as transferrin (Jefferies et al., 1984) or insulin (Pardridge et al., 1985). The characteristics of this receptor-mediated transport can be used for drug delivery: agents that normally do not get into the brain can be conjugated to antibodies against a blood-brain barrier receptor which act as a ligand and allow the crossing of the agent.

Finally, the blood brain barrier prevents macromolecules from the plasma to enter the CNS where they are usually absent. Several individual plasma proteins and their actions on the CNS are described in detail below.

I.2.2.4- Neurotoxins

Neurotoxins (whether they are endogenous metabolites, proteins or xenobiotics) may have a deleterious effect on the neuronal population, which is especially significant because neurons are deprived of significant regenerative capacity. Several adenosine triphosphate (ATP)-binding cassette transporters are located at the blood brain barrier and are able to pump these neurotoxic substances out of the CNS (Abbott et al., 2010). On the other hand, these transporters also play a role in drug resistance, since they are able to transport brain-targeted drugs out of the brain. For instance, the multidrug resistance transporter P-glycoprotein (P-gp) is expressed at the luminal surface of endothelial cells and removes toxic metabolites, mainly cationic drugs (Loscher and Potschka, 2005). Knock-out studies in

mice have shown that a deficiency in P-gp leads to enhanced neurotoxicity of brain-targeted drugs (Schinkel et al., 1994; Schinkel et al., 1996), indicating that drug removal is a defence mechanism in the first place. The multidrug resistance-associated proteins (MRP) can be expressed on both the abluminal and luminal surface and are mainly responsible for anionic compound removal (Loscher and Potschka, 2005).

I.2.2.5- Brain nutrition

Specific transporter proteins are expressed at the blood brain barrier to allow nutrients and metabolites required by the CNS to reach it (Abbott et al., 2006). Specific carrier-mediated transporters allow nutrients such as glucose (Simpson et al., 2007), monocarboxylic acids (lactate, pyruvate) (Simpson et al., 2007), amino acids (Hawkins et al., 2006) and vitamins (Spector and Johanson, 2007) to enter the brain. Some of these transporters are polarised and can be specifically expressed at the luminal or abluminal surface of endothelial cells, thus allowing for a unique direction of transport (blood to brain or brain to blood) (Ohtsuki and Terasaki, 2007). For example, the glucose transporter GLUT-1 is expressed exclusively at the blood brain-barrier with a higher concentration at the abluminal surface (Simpson et al., 2007), preventing accumulation of glucose in the brain.

I.2.3- Breakdown of the blood-brain barrier in MS

Several studies suggest that breakdown of the blood-brain barrier plays a role in disorders involving neuroinflammation such as MS, Alzheimer's disease (AD) or Parkinson's disease (PD) (Leech et al., 2007; Miyakawa, 2010; Stolp and Dziegielewska, 2009). It is still unclear whether these alterations are a causal event, or a consequence of these pathologies.

The development of imaging techniques like magnetic resonance imaging (MRI) have allowed the dysfunction of the blood-brain barrier to be assessed in MS patients. Gadolinium diethylenetriaminepenta-acetate (Gd-DTPA) enhancement MRI techniques have been developed in the past two decades and are commonly used for detection of leakage of the blood-brain barrier in MS patients. Enhancement is consistently found within new lesions in patients suffering from relapsing/remitting MS and secondary progressive MS (Kermode et al., 1990). Because of this early permeability in MS lesions, it has been suggested that leakage of plasma into the CNS may have a role in lesion formation (Cotton et al., 2003; Kermode et al., 1990). Moreover, there is a strong correlation between the duration of Gd-DTPA enhancement and the size and severity of the lesion formed in the area where the breakdown occurred. Tight junction abnormalities (occludin, ZO-1) have also been associated with lesion formation, leakage of the blood-brain barrier and demyelination in MS patients (Kirk et al., 2003; Plumb et al., 2002).

In animal models of MS, breakdown of the blood-brain barrier is also present. In EAE, the leakage occurs at the early onset of neurological deficit, persists during the peak of the disease and disappears at recovery (Floris et al., 2004). Also, the leakage correlates with the duration and severity of neurological signs (Proescholdt et al., 2002b). Correspondingly, Gd-DTPA enhancement in EAE lesions is associated with relapses, and the duration of the leakage correlates with the expression of symptoms (Hawkins et al., 1991). These observations suggest that leakage of the blood-brain barrier is directly implicated in the neurological deficits observed in neuroinflammation (Fabis et al., 2007; Floris et al., 2004; Hawkins et al., 1991).

I.2.4- Breakdown of the blood-brain barrier and inflammation

In most neuroinflammatory diseases, and particularly in MS, alteration of the blood-brain barrier and inflammation are often linked. It has been shown that leukocytes are able to enter the CNS not only via small gaps at intercellular cell junctions, but also via a transcellular pathway through endothelial cells (Engelhardt and Wolburg, 2004). In MS lesions, the breakdown of the blood-brain barrier is associated with infiltration of activated neutrophils, lymphocytes and monocytes (Petty and Lo, 2002). It has also been demonstrated that in knock-out mice lacking pro-inflammatory mediators, EAE still induced a breakdown of the blood-brain barrier but less severely than in wild type mice, suggesting that the breakdown of the blood-brain barrier is at least partly mediated by inflammation (Fabis et al., 2007). A direct correlation has also been made between the disruption of the blood-brain barrier and the localization of inflammatory infiltration sites in mice with EAE (Muller et al., 2005).

Products of inflammatory cells such as cytokines and chemokines have the ability to induce alterations of the blood-brain barrier. In rats intra-cranially injected with interleukin-1β (IL-1β), the increased permeability observed a few hours following injection was dependent on the presence of neutrophils within the CNS (Blamire et al., 2000). In EAE, an increase in IL-1 and TNF-α release has been demonstrated and correlated with the observed alterations of the blood-brain barrier (Abraham et al., 1996; Gijbels et al., 1990). Other interleukins (IL-2 and IL-6) have also been shown to induce permeability (Saija et al., 1995).

Finally, inflammatory cells and their mediators can have a direct effect on the expression of tight junction proteins, either at a post-transcriptional level (Bennett et al., 2010) or by directly inducing their degradation (Kniesel and Wolburg, 2000), thus contributing to an

enhanced permeability. Leukocyte infiltration has also been reported to alter the organization of tight junctions (Bolton et al., 1998), reducing the expression of occludin and ZO-1. Also, TNF-α and IFN-α released by lymphocytes can decrease the occludin gene promoter activity and reduce occludin mRNA expression in epithelial cells (Mankertz et al., 2000).

From the evidence gathered, it is clear that inflammation and the blood-brain barrier are intimately related. However, the mechanism by which this relationship is established is yet to be fully revealed, as well as the sequence of events. Discerning the cause from the consequences is currently the source of many controversies.

I.3- Plasma components in the CNS

I.1.1- Fibrinogen

Fibrinogen is a 340 kDa glycoprotein present in blood and playing a role in the coagulation cascade. After the conversion to fibrinogen monomers by thrombin, it polymerizes to form fibrin. Fibrinogen only reaches tissue in the case of injury, being found only in blood under normal conditions. CNS cells have been shown to express activators of the coagulation cascade that trigger the thrombin-mediated transformation of fibrinogen to fibrin (Smiley et al., 2001). In neuroinflammatory conditions, such as within the lesions in MS patients, fibrinogen is present around the blood vessels where it colocalizes with mononuclear cells (Sobel and Mitchell, 1989) in both acute and chronic MS lesions (Kirk et al., 2003). In pattern III lesions (as described by Lucchinetti and colleagues (Lucchinetti et al., 2000)), fibrinogen binds to nodes of Ranvier and activates microglia probably through toll-like receptor 4 (TLR-4) receptor- or cluster of differentiation 11b (CD11b) receptor-signalling,

and it promotes the release of pro-inflammatory cytokines (Adams et al., 2007; Flick et al., 2004a; Perez et al., 1999; Smiley et al., 2001). In particular, fibrinogen can induce a phagocytic phenotype in microglia (Adams et al., 2007), and this activation occurs before the onset of demyelination (Marik et al., 2007). Similar observations are made in animal models. The mouse transgenic line TgK21, a TNF-α mouse model of MS, presents the same features described above regarding fibrinogen; deposition is present before tissue damage and correlates with sites of demyelination (Akassoglou et al., 2004). Genetic and pharmacological depletion of fibrinogen in this mouse model leads to a decreased inflammation and a later onset of demyelination (Akassoglou et al., 2004). Fibrinogen plays a role in the adhesion and infiltration of inflammatory cells such as leukocytes, neutrophils and macrophages (Flick et al., 2004b; Whitlock et al., 2000). Fibrinogen can also trigger the formation of astrocytic scars and prevent CNS repair following injury (Schachtrup et al., 2010). Regarding alterations of the blood-brain barrier, depletion of fibrinogen in animal models of AD has been shown to reduce permeability and Evans blue leakage (Paul et al., 2007). As a consequence, fibrinogen's interaction with the different cells present in the CNS may have consequences in neuroinflammatory pathologies.

I.2.2- Thrombin

Thrombin is a 70 kDa serine-proteinase involved in the coagulation cascade. Particularly, it catalyses the conversion of fibrinogen to fibrin. In the cell, thrombin signals through G-coupled protein protease-activated receptors (PAR). PARs are normally expressed in the CNS of rats and humans, on neurons and glial cells (Sokolova and Reiser, 2008).

In neuroinflammation, thrombin has been shown to play a role in the induction of the inflammatory process. Thrombin can trigger microglial activation leading to proliferation

and cytokine release (Dheen et al., 2007; Moller et al., 2000) and nitric oxide production (Lee da et al., 2006; Sokolova and Reiser, 2008). In vivo injection of thrombin in the brain results in microglial activation and oxidative and nitrative stress induced by the expression of inducible nitric oxide synthase (iNOS) (Choi et al., 2005b). Thrombin has also been shown to interact with astrocytes and induce nitric oxide production (Meli et al., 2001). PAR receptors have been shown to be upregulated on astrocytes and microglia in EAE, suggesting a potential mechanism for thrombin-induced glial cell activation (Bushell, 2007). Thrombin is also implicated in neurodegeneration, depending on its concentration within the CNS. It has been demonstrated that in ischaemia, low concentrations of thrombin can be neuroprotective whereas high concentrations are neurotoxic in a dose-dependent manner (Lee da et al., 2006; Striggow et al., 2000). Direct injection of thrombin in the CNS results in neurodegeneration in vivo (Lee da et al., 2006). Moreover, inhibition of microglial activation by thrombin protects neurons against this degradation (Choi et al., 2005a). Attenuation of thrombin has also been shown to be neuroprotective in rat models of injured optic nerve, highlighting a deleterious effect of thrombin on axons.

Thrombin can also play a role in alterations of the blood-brain barrier as it can promote monocyte migration and increased permeability of endothelial cells by inducing release of platelet activating factor, an inflammatory transmitter and vasodilator (Nagy et al., 1995; Strukova, 2001).

I.3.3- Albumin

Albumin is a major plasma protein of 66 kDa, accounting for 50% of all plasma proteins (Hooper et al., 2005b). Similarly to thrombin and fibrinogen, it may play role in the neuroinflammatory process, being normally kept out of the CNS by the blood-brain barrier.

It has been shown that in EAE, an influx of albumin occurs at the lesion site where the blood-brain barrier becomes permeable (Butter et al., 1991). Albumin entry into the CNS is able to induce microglial activation and proliferation (Hooper et al., 2005a), resulting in the release of pro-inflammatory cytokines such as TNF-α and IL-1β (Zhao et al., 2009). Albumin also triggers the release of superoxide by microglia (Nakamura et al., 2000) and the induction of iNOS, leading to the production of NO (Hooper et al., 2009). In astrocytes, albumin can cause activation and proliferation (Nadal et al., 1995), and has consequences on neuronal excitability, discussed below. All these interaction can have deleterious effects on the neuronal population. Indeed, activation of microglia by albumin is correlated with neuronal damage and apoptosis (Hooper et al., 2009).

I.4- Hypoxia

I.4.1- CNS perfusion

The CNS is particularly vulnerable to hypoxia and defects in oxygen supply. It is thought to consume 15% of the cardiac output, 20% of the oxygen and 10% of the glucose consumed by the whole body (Afifi, 2005; McKenna, 2006), the two forms of energy consumed by the brain. People lose consciousness within seconds of blood flow interruption and undergo irreversible damage within minutes (Hansen, 1985).

In other tissues of the body, glycogen stores are present in order to cope with periods of high energy demand when oxygen provided by the blood supply is not enough to sustain the energy metabolism. In the brain this store is present in astrocytes (Cataldo and Broadwell, 1986) and is used during periods of hypoglycaemia (Suh et al., 2007). However, in vivo studies in ischaemia have shown that this glycogen store is unable to compensate

for the lack of energy substrate as it is rapidly depleted. As a consequence, the brain is exposed to damage even during short periods of interruption of energy supply.

I.4.2- Potential role of hypoxia in MS

MS is generally thought to be an immune mediated disease, where the immune system wrongly attacks myelin proteins. However, breakdown of the blood-brain barrier occurs before the onset of demyelination in some patients, suggesting that another mechanism may be responsible for lesion formation. Lucchinetti and colleagues (Lucchinetti et al., 2000) categorized the lesions observed in MS patients and distinguished one subtype, pattern III lesions, that were characterized by loss of myelin with almost no T-cell or B-cell infiltration: a similar lesion has been described in detail by Prineas and colleagues (Barnett and Prineas, 2004). A similar pattern of lesion has also been observed in brain ischemic insults such as stroke (Aboul-Enein et al., 2003), suggesting that hypoxia is responsible for the loss of myelin observed. Also, hypoxia can cause an increase in permeability of the blood-brain barrier (Dux et al., 1984), thus providing a potential origin of the leakage observed in early MS lesions. Moreover, a reduced cerebral blood flow has been observed in the brain of patients suffering from MS (Adhya et al., 2006; Law et al., 2004) and areas weakly perfused have been correlated with lesion formation in the white matter, with axon sparing and microglial activation in rats (Farkas et al., 2004). Finally, a higher probability of lesion formation in patients is linked to white matter area with lower perfusion rates (Holland et al., 2012).

I.4.3- Markers of hypoxia

In this report, we used two different methods to detect hypoxia in spinal cord tissue. Both were using specific markers, namely HIF and pimonidazole, which are endogenous and exogenous respectively. The mechanisms of hypoxia detection by these markers are described below.

I.4.3.1- HIF-1α

HIF-1 is a heterodimer consisting of HIF-1α and HIF-1β. HIF-1β is constitutively expressed and located in the nucleus whereas HIF-1α is oxygen sensitive. Both subunits are continuously transcribed and translated but under normal oxygen conditions the HIF-1α subunit is hydroxylated in an oxygen dependant manner by proxyl hydroxylate enzymes (Schofield and Zhang, 1999). The hydroxylated subunit is then recognised by the von Hippel-Lindau (VHL) protein which targets it for proteasomal degradation (Maxwell et al., 1999). Another protein, factor-inhibiting HIF, is also able to hydroxylate it and reduce HIF activity (Lando et al., 2002). Under hypoxia, however, HIF-1α is not recognized by VHL and is therefore not targeted for degradation. It is thus allowed to enter the nucleus and dimerize with HIF-1β to promote transcription of hypoxia response elements (HRE) (Klimova and Chandel, 2008). HIF-1α is therefore a potent marker of hypoxic condition in cells.

I.4.3.2- Pimonidazole

Pimonidazole is a 2-Nitroimidazole molecule which binds to proteins and accumulates in cells under hypoxic conditions. In the presence of adequate oxygen concentration, it is oxidized to pimonidazole N-oxide or conjugated via glucoronyl transferase or

sulfotransferase. These products are then readily metabolized and excreted. On the other hand, oxygen competes with nitroreductases to provide the first electron needed to reduce pimonidazole. Hence, in low oxygen conditions, pimonidazole is reduced to a hydroxylamine which can then irreversibly bind the –SH group of proteins or glutathione and accumulate in the tissue. The bound pimonidazole can then be detected via immunohistochemical techniques and used as a hypoxia marker (figure I.3) (Arteel et al., 1998).

I.4.3.3- Correlation between pimonidazole and HIF-1α labelling

Hutchison and colleagues (Hutchison et al., 2004) compared the viability of both pimonidazole and HIF-1α as markers of hypoxia by performing a correlation study in tumour tissue. They found a weak but significant correlation between pimonidazole and HIF-1α staining and only a weak link between high HIF-1α and oxygen concentration measured with oxygen electrodes. This is at odds with another study showing a strong correlation between HIF-1α labelling and oxygen concentration (Haugland et al., 2002). Some variability in HIF-1α labelling following hypoxia is therefore present. One potential reason explaining this discrepancy is the fact that HIF-1α labelling only detects strong hypoxia and is therefore not useful for milder situations (Haugland et al., 2002). Another possible reason is that, whereas pimonidazole is a hypoxia-specific marker, HIF-1α degradation is regulated by mechanisms other than hypoxia such as the phosphatidylinositol 3'-kinase (PI3K) pathway involving growth factors (Zhong et al., 2000).

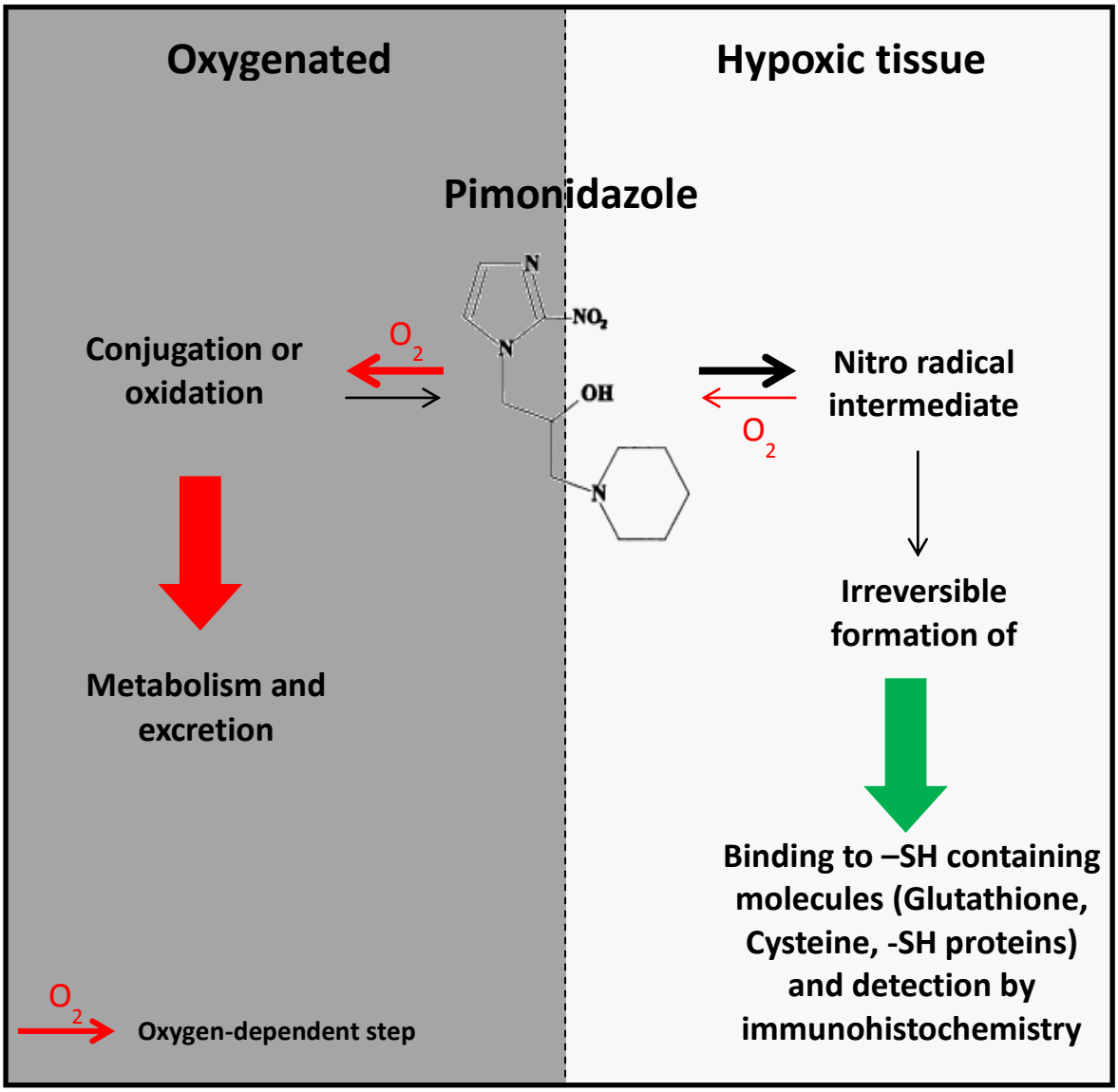

Figure I.3: *Schematic representation of pimonidazole metabolism in hypoxic and non-hypoxic tissue*

I.5- Vascular endothelial growth factor

I.5.1- The protein and its receptors

Vascular endothelial growth factor (VEGF) was first discovered in 1983 as a vascular permeability factor (VPF) (Senger et al., 1983) and was then rediscovered as an endothelial cell mitogen later (Ferrara and Henzel, 1989). It is a homodimeric glycoprotein responsible for blood vessel development and angiogenesis. Five members compose the VEGF family in mammals: VEGF-A, VEGF-B, VEGF-C, VEGF-D and placenta growth factor (PLGF). Two proteins are structurally related: the parapoxvirus Orf VEGF (VEGF-E) and the snake venom VEGF (VEGF-F). VEGF-A is a 46kDa protein and exists in six different isoforms, coming from different splicing: VEGF-A_{121}, VEGF-A_{145}, VEGF-A_{165}, VEGF-A_{183}, VEGF-A_{189} and VEGF-A_{206}. VEGF-A_{165}, named VEGF in this report, is the most abundant form while VEGF-A_{145} and VEGF-A_{206} are rare (Robinson and Stringer, 2001). In mice and rats, VEGF isoforms lack a glycine residue and are therefore one amino acid shorter than the human protein. A broad range of cells are able to produce VEGF, including vascular smooth muscle cells, macrophages and tumour cells (Berse et al., 1992).

VEGF can bind to three different tyrosine kinase receptors (VEGFR-1, VEGFR-2 and VEGFR-3), each being expressed by specific cell types and therefore mediating different biological functions (Holmes et al., 2007). A summary of VEGF receptors and their specific ligands is provided in figure I.4. Upon binding of one of the possible ligands, VEGFRs form either homodimers or heterodimers. Dimerization of receptors leads to the activation of the kinase activity resulting in autophosphorylation. Recruiting of second messengers follows with the activation of the ligand-specific signalling pathway (Olsson et al., 2006).

I.5.1.1- VEGFR-1

VEGFR-1 is a high affinity receptor for VEGF-A, VEGF-B and PLGF of 180 kDa. It is expressed on endothelial cells and is involved in endothelial cells migration (Kanno et al., 2000). These biological activities are thought to occur only in presence of VEGFR-2 as when cross-talk with VEGFR-2 is prevented, VEGFR-1 activation is not capable to promote these responses (Rahimi, 2006). VEGFR-1 may therefore act as a trap for VEGF, regulating VEGFR-2 function by controlling VEGF availability. However, when VEGFR-1 is able to heterodimerize with VEGFR-2, it can promote angiogenesis. At the vascular level, it also enhances VEGFR-2 induced permeability (Takahashi et al., 2004). VEGFR-1 is also expressed on other cell types such as macrophages and monocytes (Sawano et al., 2001) where it has been shown to mediate their migration (Barleon et al., 1996; Hiratsuka et al., 1998) and reduce the production of pro-inflammatory cytokines by macrophages (Autiero et al., 2003). It can also induce the recruitment of haematopoietic stem cells for reconstitution of hematopoiesis (Hattori et al., 2002).

I.5.1.2- VEGFR-2

VEGFR-2 is a 200 kDa protein to which VEGF-A, VEGF-C, VEGF-D and VEGF-E can bind. VEGF has an affinity for VEGFR-2 approximately 10-fold lower than for VEGFR-1 but the triggered kinase activity is much stronger following VEGFR-2 activation (Takahashi and Shibuya, 2005). VEGFR-2 is found mainly at the surface of vascular endothelial cells but is also present on neuronal cells and hematopoietic stem cells. VEGFR-2 is responsible for the migration, proliferation and survival of vascular endothelial cells but also vascular permeability (Holmes et al., 2007). VEGFR-2 specific agonists are able to increase permeability on their own (Hillman et al., 2001) and specific inhibition of VEGFR-2 prevents VEGF-induced permeability (Whittles et al., 2002), confirming the essential role of VEGFR-2.

I.5.1.3- VEGFR-3

VEGFR-3 is a 195 KDa receptor specific for VEGF-C and VEGF-D expressed on lymphatic endothelial cells (Takahashi and Shibuya, 2005). It is thought to be important during embryonic development for migration and sprouting for endothelial lymphatic precursor cells (Olsson et al., 2006). It has been shown that a VEGFR-3 specific mutant of VEGF-C is able to induce lymphangiogenesis in mice without any influence on blood vessels (Veikkola et al., 2001).

I.5.1.4- Neuropilin 1 and 2

Neuropilin-1 (NRP-1) is a 140 kDa cell surface glycoprotein involved in neuronal guidance via semaphorin signalling. NRP-1 also binds VEGF-A_{165}, VEGF-B, PLGF and some VEGF-E variants and NRP-2 binds VEGF-A_{165}, VEGF-A_{145}, PLGF and VEGF-C (Takahashi and Shibuya, 2005). The very short intracellular domain of NRPs prevents any biological activity upon VEGF binding. However, the proliferation and migration of endothelial cells induced by VEGF binding to VEGFR-2 is enhanced in presence of NRP-1 (Soker et al., 1998), suggesting that NRP-1 acts as an enhancer of VEGFR-2 signalling by forming a complex with it (Whitaker et al., 2001). Similarly, NRP-2 seems to play a regulating role in VEGF induced lymphatic development (Yuan et al., 2002).

I.5.2- VEGF-induced permeability mechanism

The mechanism by which VEGF induces permeability has not yet been fully elucidated. However, signalling through VEGFR-2 is required for both angiogenesis and permeability. VEGF-E, which binds to VEGFR-2 but not VEGFR-1 is able to induce angiogenesis without sign of plasma leakage, suggesting that the combined action of VEGFR-1 is required for

permeability to occur (Kiba et al., 2003). NO has been shown to be a mediator of vascular angiogenesis and permeability (Fukumura and Jain, 1998) and VEGF receptor activation leads to activation of endothelial nitric oxide synthase (eNOS) via activation of phospholipase C-γ activation and calcium influx or via phosphorylation of eNOS by AKT/protein kinase B (Bates and Harper, 2002; Fulton et al., 1999). Several studies have confirmed this observation. VEGF has been shown to induce eNOS and inducible nitric oxide synthase (iNOS) in vitro through VEGFR-2 activation (Kroll and Waltenberger, 1999) and studies in knock-out mice showed that VEGF induced permeability was suppressed in eNOS deficient mice, confirming that eNOS plays an important role in permeability (Fukumura et al., 2001). Moreover, a selective eNOS inhibitor, cavtratin, has recently been used to reduce both breakdown of the blood-brain barrier and the severity of lesions in mice with EAE (Argaw et al., 2012).

I.5.3- Activity of VEGF in the CNS

Although the predominant role of VEGF is related to the regulation of angiogenesis, several studies have shown that VEGF can also have direct effects on the CNS. While most of these effects seem to have a positive impact on neurons and other cells composing the CNS, a few studies have also shown that under certain conditions VEGF can be deleterious.

In vitro findings showed that in explant cultures of dorsal root ganglia, VEGF promotes axonal outgrowth and the survival of neurons and Schwann cells. The same effects were observed in satellite cells (Sondell et al., 1999). It has been demonstrated that neurons express VEGFR-2 and for most of them NRP-1 and that the neurotrophic effects of VEGF were mediated by VEGFR-2 signalling (Sondell et al., 2000). At higher doses, a mitogenic effect of VEGF on astrocytes was also observed (Silverman et al., 1999). In several

pathological conditions, VEGF can be neuroprotective, and studies performed in vitro showed that VEGF protected neurons against ischaemia as well as glutamate-induced excitotoxicity (Jin et al., 2000a; Matsuzaki et al., 2001).

In vivo, knock-in mice with spinal VEGF levels reduced by 75% developed symptoms related to motor neuron degeneration at 5 months of age, resulting in loss of motor coordination, muscle atrophy and axonal loss (Oosthuyse et al., 2001), a phenotype very similar to amyotrophic lateral sclerosis (ALS). In AD, VEGF immunoreactivity has been demonstrated in clusters of reactive astrocytes and diffuse perivascular deposits in patients (Kalaria et al., 1998) and it is thought to be part of a repair mechanism against hypoperfusion.

VEGF may however have negative effects on the CNS. Recombinant human VEGF (rhVEGF) injected intravenously less than an hour after focal embolic ischemia can induce disruption of the blood-brain barrier and haemorrhage in ischemic lesions as assessed by MRI techniques (Zhang et al., 2000). Moreover, antagonising VEGF reduces oedema formation and tissue damage after ischaemia in mice brain (van Bruggen et al., 1999). During ischaemic insult, VEGF may also recruit inflammatory cells and promote leukocyte adhesion, thus contributing further to neuronal damage. MRI studies in MS lesions have shown a positive correlation between VEGF expression in the CNS and the length of lesions, suggesting an involvement of VEGF in spinal cord lesions (Su et al., 2006). Furthermore, as discussed before, VEGF may also exacerbate inflammation in MS lesions. An interesting study by Zhu and colleagues (Zhu et al., 2008) revealed that delivery of soluble VEGFR-1, binding VEGF but lacking the signalling activity, is able to reduce the severity of EAE in rats, suggesting that VEGF may play an important role in the pathology of the lesions. Another study aimed at reducing spinal cord injury lesions by injecting rhVEGF intraspinally in rats

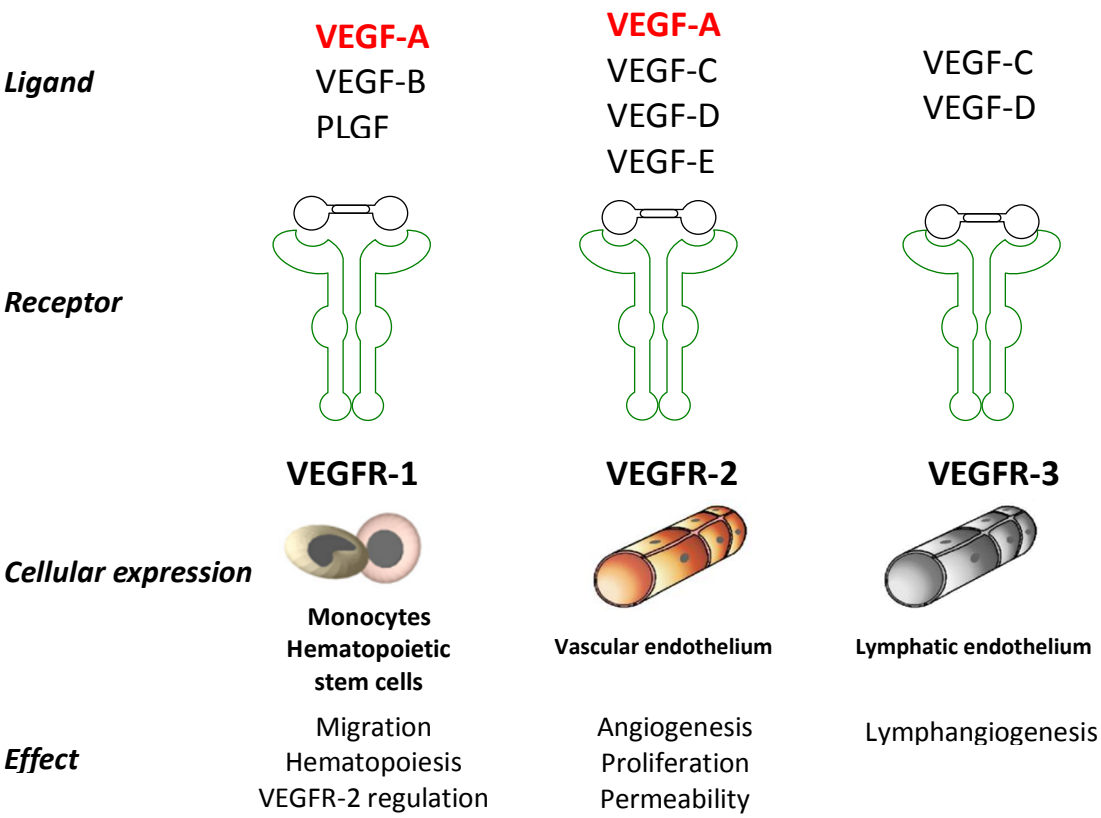

Figure I.4: *Summary of the VEGF-VEGFR system, its ligand specificity, cellular localization and physiological effects.*

revealed that animals treated with VEGF actually experienced an exacerbation of the lesion volume (Benton and Whittemore, 2003). It was suggested that this exacerbation was due to the action of VEGF on vessel permeability.

Finally, VEGF may also play a role in synaptic plasticity. VEGF treatment of hippocampal slice before stimulation of neurons at high-frequency increased the long term potentiation (LTP) effect while antagonizing VEGFR-2 reduces it (Ruiz de Almodovar et al., 2009). This observation combined with the fact that upon NMDA receptor activation, hippocampal neurons release VEGF, suggests that VEGF may be involved in synaptic plasticity.

I.5.4 – Existing models of intraspinal injection of VEGF in rats

To our knowledge, two studies have explored the consequences of injecting VEGF into the spinal cord in rats where no previous injury or pathology can be found. Benton and colleagues (Benton and Whittemore, 2003) studied the effect of recombinant human VEGF in rat spinal cord. This was a side experiment completing their study on the effect of VEGF injection following spinal cord injury. Briefly, they injected 2µg of recombinant human VEGF at the T9 level in the intermediate grey matter at two different sites located 2 mm apart and looked at the induced blood brain barrier leakage 30 min, 24h and 72h following injection. To do so, they injected HRP intravenously 30min before perfusing the animals and removing the cord for immunohistochemical processing. The outcome of this study was that HRP extravasation was apparent at 30min and 24h following injection but not at 72h, indicative of a blood brain barrier leakage resolving before 72h. It is worth noting that the extravasation of neutrophils was correlated with the blood brain barrier leakage observed. Unfortunately, they did not assess any associated behavioural deficit.

On the other hand, Sasaki and colleagues (Sasaki et al., 2010) performed an acute injection of VEGF in rats previously injected with incomplete Freund's adjuvant (i.e. unable to induce EAE on its own) as part of a control experiment aimed at inducing focal EAE. 21 days following injection of incomplete Freund's adjuvant, they injected 1 µL of 0.5 mg/mL of rat recombinant VEGF at the T9 level, at two different depths (0.7 and 0.5 mm) and at two longitudinal sites 2mm apart (thus reaching a total amount of VEGF of 2 x 2 x 0.5µg = 2µg). They then assessed the blood brain barrier leakage by injecting Evans blue immediately after VEGF injection. Animals were perfused at 36h and their cord removed for analysis. Evans blue leakage was present in the VEGF injected animals but not in the non-injected ones, indicative of a blood brain barrier breakdown occurring within 36h (the exact timing is impossible to determine because of the protocol used). As animals were scored with the EAE score system for detection of EAE symptoms, the group injected with VEGF and incomplete Freund's adjuvant displayed some deficit in the first 3 days following injection of VEGF that disappeared further on. This observation was discarded as a surgical trauma. However, we believe that because of its correlation with the Evans blue leakage and the absence of deficit in another group intraspinally injected with saline, further investigation is needed to explain this neurological deficit.

I.6- Spinal cord anatomy

The spinal cord is the means of communication between the brain and the peripheral nervous system (PNS). It is constituted of white matter, made of myelinated axons, and grey matter, the location of most neuronal cell bodies. Both ascending and descending projections connect the brain to the different spinal cord levels to control motor, sensory and proprioceptive functions.

I.6.1 – Link between the spinal cord and the periphery

Magendie, in 1822, showed that the dorsal roots contain afferent sensory fibres whereas the ventral roots contain somatic efferent fibres and presynaptic autonomic fibres.

The majority of fibres composing ventral roots are somatic motor fibres leaving the ventral column of the spinal cord. These are thick myelinated alpha motor axons with high conduction velocity controlling muscle contraction and gamma motor axons mainly controlling muscle spindle fibres.

The dorsal roots contain sensory fibres. According to their type and source, the termination of these fibres within the spinal cord differs. Thin unmyelinated fibres responsible for nociception, temperature and touch are located in the lateral part of the dorsal roots and terminate in the superficial laminae of the dorsal horn. On the other hand, thick myelinated fibres, such as the Ia afferent fibres, carry sensory information from the muscles and are located in the medial part of the dorsal roots, projecting deep into the dorsal and ventral horns. Terminations of primary afferents on dorsal horn neurons are arranged in a somatotopic manner. For example, distal parts of the limbs connect in the medial part of the dorsal horn while proximal parts are located laterally in the dorsal horn (Molander and Grant, 1987; Shortland and Woolf, 1993).

Dorsal and ventral roots join together to form a spinal nerve which is therefore made of somatic and visceral fibres that can be either afferent or efferent. Afferent fibres are made of axons of dorsal ganglia neurons transmitting external or visceral sensations to the spinal cord while efferent fibres are axons of motor neurons or autonomic fibres leaving the spinal cord.

I.6.2 - Ascending spinal projections

Ascending spinal projections transmit sensory information such as pain, temperature, position and touch from somatic input and pressure, pain from internal organs. The fibres composing this pathway are myelinated dorsal root fibres from the dorsal root ganglia and axons. Three areas within the spinal cord contain these projections: the ventrolateral funiculus, the spinocerebellar tracts and the dorsal column (Kayalioglu, 2009).

The ventrolateral funiculus conveys nociceptive, thermal, touch and pressure information to supraspinal levels. One of its major projections is the spinothalamic tract, which connects to several thalamic nuclei. The ventral spinothalamic tract conveys crude touch and pressure sensations while the lateral part transmits pain and temperature. The dorsolateral spinothalamic tract, present in the dorsolateral funiculus, is nociceptive-specific (Martin et al., 1990). Within the tract, axons are arranged somatotopically; fibres from caudal segments are in the medial parts of the tract while more rostral fibres are in the lateral parts. In rats, most of the fibres are positioned contralaterally (Burstein et al., 1990).

Other ventrolateral projections are the spinoreticular tract which are mostly activated by high threshold noxious stimulation but also by low threshold cutaneous stimulation (Sahara et al., 1990). More nociceptive tracts connecting to other parts of the brain are present in the ventrolateral funiculus: these are the spinomesencephalic and the spinohypothalamic tracts.

The spinocerebellar tract carries proprioceptive and cutaneous information to the cerebellum, and it is involved in the coordination of movements. The dorsal spinocerebellar tract projects mainly ipsilaterally and the fibres are excited by Goups Ia and Ib afferents

from muscle spindles and tendon organs respectively (Aoyama et al., 1988) but also by Group II fibres for cutaneous touch and pressure. It signals for proprioceptive information and allows for coordination of hindlimbs.

The fibres within ventral the spinocerebellar tract are also activated by Group Ia and Ib afferents and transmit information about the entire position and coordination of the limbs.

Axons coming from the dorsal root ganglia enter the dorsal column and form the dorsal column pathway by dividing into ascending and descending projections. Long ascending projections form the direct dorsal column pathway responsible for discriminatory touch, proprioception, deep pressure and vibration input. These projections ascend ipsilaterally and are highly organized; fibres from a given segment are lateral to fibres from lower segments and are responsible for innocuous mechanical sensations as well as noxious stimuli. Short fibres also synapse in the dorsal nucleus of the grey matter whose neurons give rise to the spinocerebellar tract. The other neurons coming from dorsal root ganglia synapse onto the dorsal horn neurons whose axons ascend in the dorsal column and form the postsynaptic dorsal column pathway which controls responses to innocuous stimuli, noxious peripheral stimuli as well as visceral nociception. A dorsal intersegmental pathway is also present to allow communication between different segments of the cord.

I.6.3- Descending spinal projections and motor neurons

All mammals possess a very important descending pathway, namely the corticospinal tract (figure I.5), which controls motor and sensory functions. These fibres come mainly from motor, premotor and somatosensory cortical areas. In rats, this tract is located in the dorsal column and its axons connect to the medial parts of the dorsal horns, the intermediate grey matter and also motor neurons in the ventral horn. Other tracts, located in the lateral and

ventral white matter of the spinal cord also control sensory and motor functions by linking brain inputs to the grey matter areas responsible for motor functions (Watson, 2009). Among these, the rubrospinal tract (figure I.5) connects to the intermediate grey matter and the ventral horn in rats to control motor function and skilled motor tasks (Kuchler et al., 2002). The reticulospinal tract (figure I.5), which can be differentiated into the medial and lateral reticulospinal tract, are projections responsible for preparatory and movement activities and terminate in ventral laminae of the grey matter. The vestibulospinal tracts, also split into the lateral and medial tracts (figure I.5), control coordination and posture in the limbs and trunk. The lateral one controls extensor tone during locomotion (Pompeiano, 1972) while the medial one coordinates the head position with that of the body (Wilson et al., 1967). Finally, minor descending tracts also include the tectospinal tract, the cerebellospinal tract, the raphespinal and coeruleospinal tracts.

The somatic motor neurons, responsible for skeletal and voluntary muscle control, and visceral motor neurons (autonomic system) are located in the grey matter of the spinal cord (McHanwell, 2009). Somatic motor neurons are present in the ventral horn and their axons innervate fibres leaving the cord via the ventral roots. The axons controlling the hind limbs leave the spinal cord and form the sciatic nerve, which innervates the appropriate muscles. The sciatic nerve is formed from three spinal nerves that leave the spinal cord at the L4, L5 and L6 levels. Importantly, these spinal cord levels are all within the limits of the L1 vertebra (Gelderd and Chopin, 1977).

I.6.4- Proprioception

Propriospinal neurons are neurons that are intrinsic to the spinal cord; their axons terminate within its boundaries. They account for most of both the white matter and the

grey matter. They modulate afferent and descending input to control locomotion, autonomic signals and sensory functions. Within the lumbosacral enlargement (between T12-L1 vertebrae in rats), they control the hind limb motor neuron pool by integrating peripheral stimuli with muscle contraction and are also involved in hind limb-fore limb coordination (Conta, 2009).

Short propriospinal projections are located in the grey matter (excluding lamina 9) and they projects inter-segmentally towards interneurons or lamina 9 motor neurons. Lumbar short propriospinal projections are differentially located according to the motor neurons they project to (i.e. thigh musculature or distal hindlimb muscles) and these subsets of fibres control locomotion. For instance, involuntary stepping can be elicited by stimulation of the lumbar spinal cord in individuals with complete cord transection, suggesting that these short fibres are able to control lower limb movement (Minassian et al., 2004).

The long descending propriospinal tracts are located in the deep dorsal horn, the intermediate grey matter and dorsal to the central canal and make links between the cervical and the lumbar enlargements, thus playing a key role in reflexes and coordination, especially during quadrupedal locomotion in rats (Stelzner and Cullen, 1991).

The long ascending propriospinal tract is the counterpart of the long descending one, playing a role in lumbocervical coupling and right-left forelimb alternation (Juvin et al., 2005).

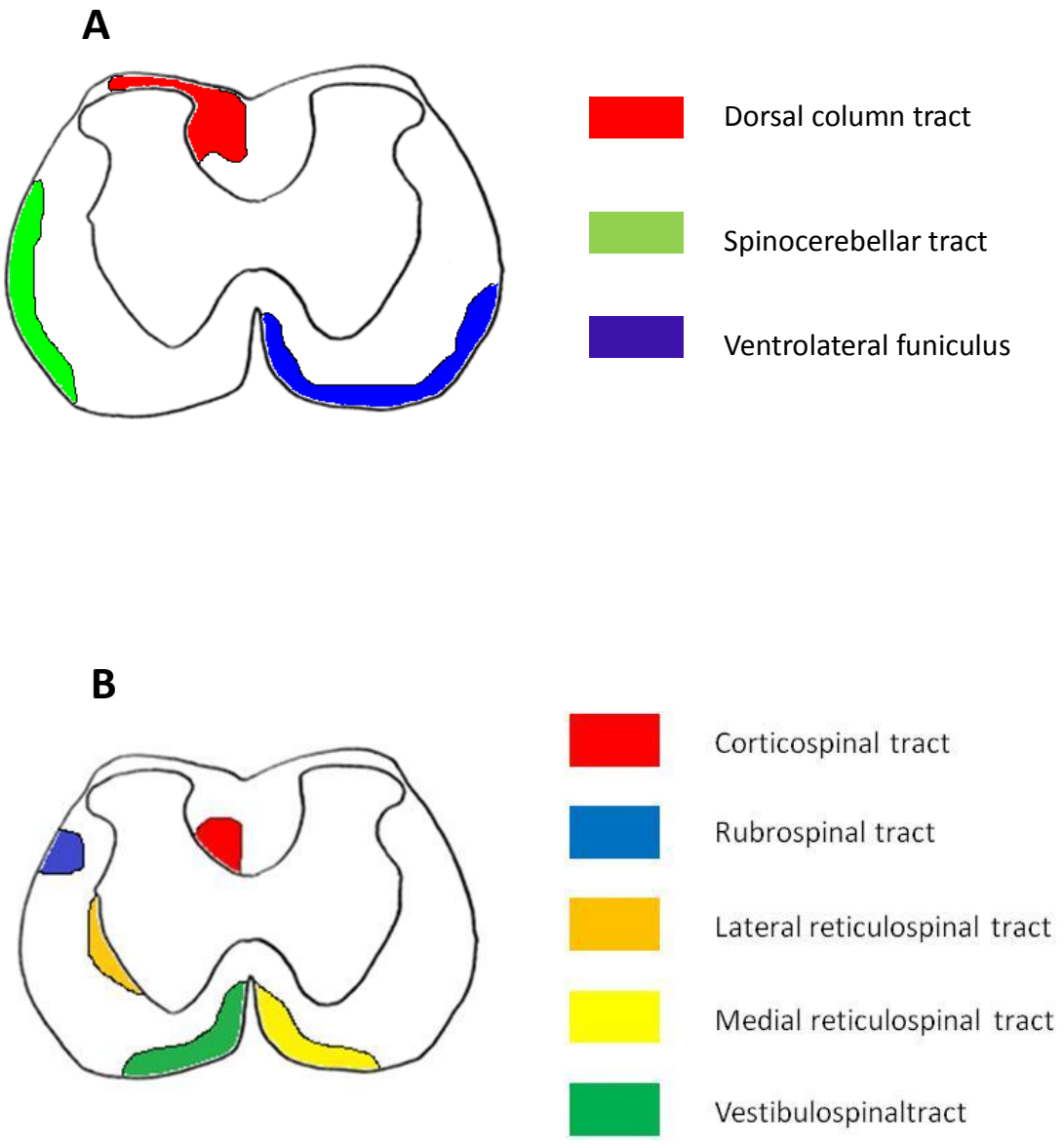

Figure I.5: ***A.*** *Localization of the main ascending tracts in the spinal cord.* ***B.*** *Localization of the main descending tracts in the spinal cord.*

I.7- Neuronal excitability

I.7.1- Astrocytes

There is a bi-directional communication between astrocytes and synapses, which are ensheathed in astrocytic endfeet. Astrocytes can release glutamate upon activation and are thought to regulate pre-synaptic and postsynaptic activity. This glutamate release is thought to be Ca^{2+}-dependent (Bezzi et al., 1998; Pasti et al., 2001) which has been shown to induce post-and pre-synaptic depression evoked by electrical stimulation (Araque et al., 1998). It has also been shown that potentiation of synaptic transmission between inhibitory interneurons and pyramidal cells by repetitive firing of interneurons is mediated by glutamate release from the neighbouring astrocytes (Kang et al., 1998). Astrocytes also use indirect mechanisms to regulate synaptic transmission. Uptake of extracellular glutamate is important for termination of synaptic transmission and is primarily performed by astrocytes (Rothstein et al., 1996). Release of chemical cofactors can also potentiate synaptic transmission. D-serine, released by astrocytes, is an agonist of the glycine-binding site of NMDA receptors and allows its activation (Schell et al., 1995). Finally, regulation of the concentration of extracellular ions such as K^+ and H^+ affects neuronal activity, and is performed by astrocytes (Newman, 1996; Rausche et al., 1990), providing another means by which astrocytes can control neuronal activity.

I.7.2- Inflammation and neuronal excitability

Inflammation can affect neuronal excitability. It has been shown that activated microglia are correlated with the presence of alterations of glutamate re-uptake mechanisms . In MS cortical lesions, loss of excitatory amino acid transporters (EAAT), which are responsible for controlling the extracellular glutamate concentration, is associated with the activation of

microglia (Vercellino et al., 2007). Pro-inflammatory factors such as interleukin-2 (IL-2), TNF-α, IFN-γ and nitric oxide (NO) (D'Arcangelo et al., 1991; Fossier et al., 1999; Park et al., 1995; Tancredi et al., 1992) have been shown to alter synaptic transmission in the CNS. Moreover, pro-inflammatory cytokines produced by microglia, such as IL-1β and TNF-α, reduced astrocyte-mediated glutamate uptake in an in vitro study (Ye and Sontheimer, 1996). Pro-inflammatory molecules derived from microglia can also increase neuronal stimulation and decrease seizure threshold in epilepsy (Devinsky et al., 2013). The intensity of production of these mediators correlates with seizure frequency in epilepsy models (Ravizza et al., 2008). Also, activated microglial cells themselves are a source of glutamate, hence further contributing to an increase in excitability (Patrizio and Levi, 1994; Piani et al., 1991).

I.7.3- Blood-brain barrier and neuronal excitability

Plasma proteins also play a role in excitability alteration in pathological conditions. Entry of albumin into the CNS has been shown to induce over-excitability and leads to epileptogenesis (Frigerio et al., 2012; Heinemann et al., 2012) by modulating astrocyte-mediated K^+ and glutamate homeostasis (Seifert et al., 2006). The latter study has revealed that a focal long-lasting disruption of the blood-brain barrier in the brain leads to activation of astrocytes and induction of neuronal over-excitability.

A role for IgG in neuronal dysfunction induced by epileptic episodes has been suggested based on a correlation study between IgG leakage into the CNS and epileptic activity in patients (Michalak et al., 2012).

Thrombin has also been shown to increase NMDA mediated excitability by binding to neurons via the PAR-1 receptor (Gingrich et al., 2000) and it increases the neuronal response to stimulation (Maggio et al., 2008).

I.7.4- F-wave and H-reflex changes in MS

Spasticity is a very common symptom of MS, reported in 84% of patients (Rizzo et al., 2004). Spasticity is thought to be due to a hyper-excitable state of the stretch reflex arc (Heckmann et al., 2005). H-reflex amplitude (Voerman et al., 2005) and F wave amplitude (Argyriou et al., 2006; Lin and Floeter, 2004) are quantitative methods available to assess over excitability of neurons and thus, spasticity. These methods have already been used in MS patients to detect spasticity (Argyriou et al., 2010; Bischoff et al., 1992; Smith et al., 1989; Voerman et al., 2005).

I.8- Aim of the study

Our hypothesis is that breakdown of the blood-brain barrier can lead to alterations of CNS function, and cause loss of function.

Our aims are

1) to study the direct effects of BBB disruption and plasma leakage in the CNS
2) to determine the behavioural and motor consequences of BBB disruption
3) to explore any structural and metabolic changes following BBB breakdown

Chapter II: Materials and Methods

II.1- Animal procedures

A summary of the animal procedures undergone by each goup of animals is provided at the end of this chapter in figures II.8, II.9, II.10 and II.11.

II.1.1- VEGF intraspinal injection

Adult (250-350g) Sprague Dawley (SD) rats were anaesthetised with 2% isoflurane (Merail, Harlow, UK) in room air and the site of operation was shaved and sterilized with iodine. Subsequently, animals received a quarter laminectomy of the 13th thoracic (T13-L1) vertebra. The T13 vertebra was found by feeling vertebrae through the skin of the animals and counting them starting from the L6 vertebra located at the level of the hips. Once the spinal cord was exposed, a small incision was made in the dura, and injections of 1µl of $VEGF_{164}$ (Rat $VEGF_{164}$, R&D Systems, Minneapolis, MN) at a concentration of 1µg/µl in sterile PBS were performed at each depth of 0.7mm and 0.4mm in the left dorsal column. Injections were made using a drawn glass micropipette held in a micromanipulator, with a trajectory of 24 degrees to the vertical. Injection sites were marked with a small amount of sterile charcoal. Control animals were injected with sterile phosphate buffered saline (PBS). The number of animals per group will be indicated for each experiment reported in the results sections. Injections into the animals were made blind to the content of the needle; the needle used for each injection was filled with PBS or VEGF by a third person and the animal number and the corresponding treatment recorded by this third person. The blinding code was kept secret until the very end of the protocol, i.e. any subsequent

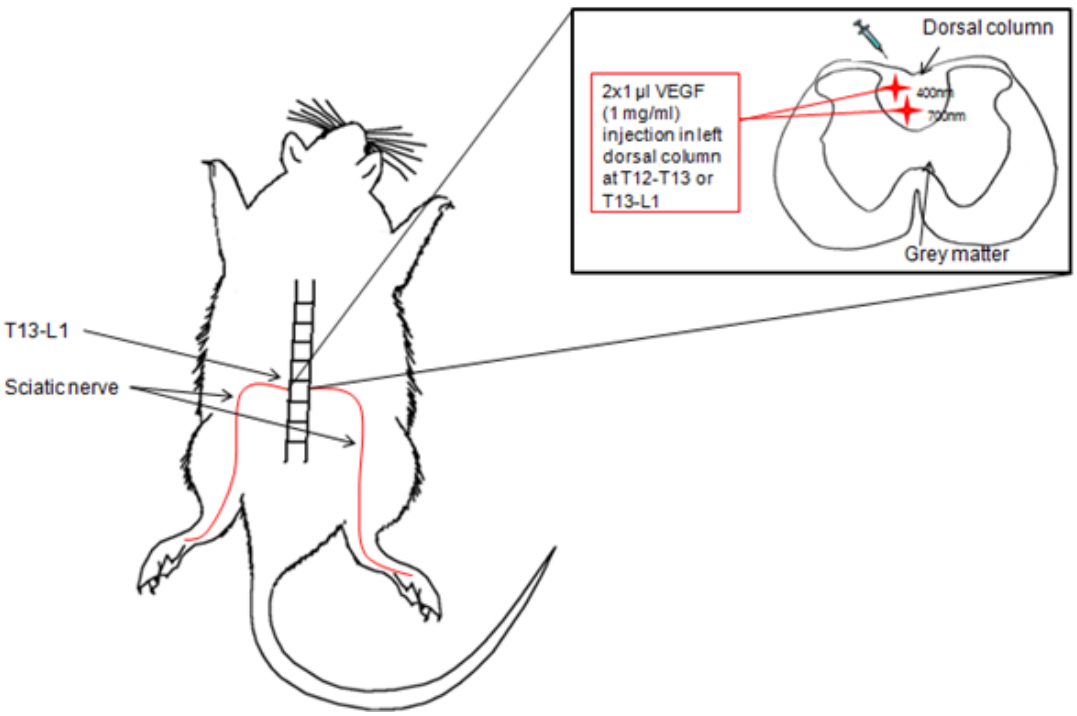

Figure II.1: *Schematic representation of the surgery protocol. Injection sites are represented with red crosses.*

procedure and analysis was performed without knowing whether the animal had been injected with VEGF or PBS.

II.1.2- Evans blue injection

Two days following surgery and injection of either PBS (n=3) or VEGF (n=5), animals were anaesthetised with 2% isoflurane (Merail, Harlow, UK) in room air and, 4% Evans blue (Sigma-Aldrich, St Louis, MO) in sterile saline was injected into the right femoral vein (1ml/kg) 30min before perfusion. The spinal cords were removed and pictures of the injection site were taken using a bright field microscope (Axiophot microscope, Zeiss, Oberkochen, Germany).

II.1.3- Pimonidazole injection

Two days after injection of PBS (n=3) or VEGF (n=5), animals were anaesthetised with 2% isoflurane (Merail, Harlow, UK) in room air and, 60mg/ml pimonidazole hydrochloride (HPI, Burlington, MA) in sterile saline was injected in the right femoral vein (1ml/kg) 4h before perfusion. Spinal cords were removed and prepared as described for immunohistochemical labelling for bound pimonidazole.

II.1.4- Perfusion

Animals were anaesthetised with 3% isoflurane (Merail, Harlow, UK) in room air throughout the procedure. An incision was made to expose the peritoneal cavity and the chest was opened to expose the heart. The right atrium was severed and a needle inserted

into the left ventricle of the heart. A rinse solution (2000U/L heparin, 2% lidocaine, 1% $NaNO_2$ and 2M N-2-hydroxyethylpiperazine-NO-2-ethanesulphonic acid (HEPES; pH 7.4) in 0.9% saline) was perfused through the vasculature until the solution emerging from the atrium was clear. Paraformaldehyde (4% in 0.4M phosphate buffer) was then injected. The spinal cord was dissected free and placed in paraformaldehyde overnight for further processing.

II.1.5- Deficit reversal experiments

II.1.5.1- Cavtratin injection

Animals were anaesthetised with 2% isoflurane (Merail, Harlow, UK) in room air and 2.5 mg/kg of Cavtratin (n=4) (Caveolin-1 scaffolding domain peptide, cell permeable, Calbiochem) or the respective scrambled peptide (n=5) in PBS was injected intraperitoneally 30 min before injection of VEGF and 24h hour later (before the one day time point testing session). Cavtratin is a specific eNOS inhibitor able to block VEGF-induced blood-brain barrier leakage (Argaw et al., 2012). Animals were tested on the horizontal ladder walking test for two days following surgery. At day two, rats were perfused and their spinal cord removed to investigate immunohistochemically a potential IgG leakage.

II.1.5.2- Oxygen treatment

Two days following intraspinal injection of VEGF, animals were blindly and randomly divided in two groups assigned to receive either room air (n=5) or normobaric hyperoxia

(~90% Oxygen, n=5). Animals were first tested on the horizontal ladder test and then housed for one hour in a chamber (BioSpherix, USA) where temperature, oxygen concentration and carbon dioxide concentration were controlled according to the group to which they were allocated. Subsequent to their respective treatments, animals were tested again on the horizontal ladder test to assess the effect of treatment on their hind-limb scores. After the final test, animals were perfused as described in II.1.4.

II.1.6- Electromyographic (EMG) techniques

Animals were anaesthetised with xylazine (Xylacare, AnimalCare Ltd)/ketamine (Ketaset, Fort Dodge Animal Health Ltd) by i.p. injection. The sciatic nerve was electrically stimulated at the sciatic notch and the EMG was recorded at the food dorsum with needle electrodes (figure II.2 Top). For each measurement, ten recordings were taken at 10 seconds intervals with an oscilloscope (Sigma 60, Nicolet Technologies) and the data transferred to Microsoft Excel. Out of these ten recordings, the maximum value of the H reflex amplitude, F and M responses amplitudes were used for analysis and comparison (figure II.2 Bottom). At the end of the protocol, animals were perfused as described in II.1.4.

The EMG curve representing the H reflex was differentiated from that representing the F-wave signals by the absence of M response preceding the H-reflex and the lower stimulus strength used to elicit the signals.

Many parameters (time, temperature, electrode placement) can lead to variability in the measurement of H reflex or F response within an animal. As a consequence, the data presented here are normalised with the maximal M response, much more stable and reproducible.

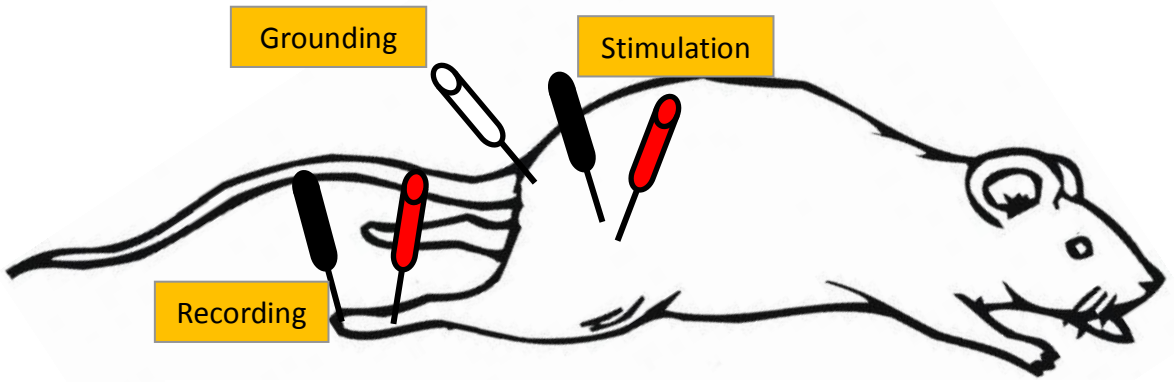

Figure II.2: ***Top.*** *Summary of the electrophysiology setup: stimulation at the sciatic notch, recording at the foot muscle and grounding at the base of the tail.* ***Bottom.*** *Summary of the different responses elicited by electrical stimulation at the sciatic notch and recorded at the foot muscle (Palmieri et al., 2004).*

II.2- Behavioural analysis

II.2.1- Ladder test

Functional deficit was assessed using the ladder test described by Metz and Whishaw (Metz and Whishaw, 2002b, 2009). Briefly, animals walked spontaneously on a horizontal ladder constructed from irregularly spaced rungs (figure II.3) and a video record was prepared. A frame by frame analysis of each step was performed to enable quantification of hind- and fore-limb placement and coordination according to a scaling method described in table II.1. Each rat performed the test five times in a row at the specified time points. Animals had previously been trained for four days before surgery. The last test completed before surgery was used as the baseline for subsequent studies. Foot fault scoring and foot placement accuracy analysis were performed for each limb for each animal using the video recordings. The average of the five trials was then used as the individual measurement for each rat. This test allowed gathering data for each paw separately. The averages of both fore-limbs and both hind-limbs were calculated and used as the main parameters studied to assess the deficit. To assess the potential side-specificity of the deficit, both hind-limbs were analysed separately and compared.

II.2.2- Tail angle analysis

The tail angle is defined as the angle made between a virtual horizontal line and the line joining the base of the tail to the tip of the tail (figure II.4)). The horizontal ladder test videos were used to measure the tail angle. During each of the 5 trials, when the animals was performing 5 consecutive steps on the ladder, a snapshot of the video was taken and used to measure the tail angle using the ImageJ software. An average of the 5 trials was

then calculated to obtain a single angle per animal. This analysis was performed up to two days following injection of VEGF (n=11) or PBS (n=6).

II.2.2- Inclined plane

During the inclined plane test, each animal was placed facing the upper edge in the middle of a wooden rectangular board mounted with a coarse surface and inclined at a specific angle (starting at 40°) (figure II.5). Success to stay on the board was defined as the ability to stay for 5 seconds at a given angle, repeated for 3 out of 5 consecutive trials. If successful, the angle was increased by a 1° increment and the procedure repeated until reaching the angle of first fall (3 falls out of 5 trials). The latter was then recorded for each animal and a comparison was made between animals injected with VEGF (n=6) and PBS (n=5).

Figure II.3: *Snapshot of an animal walking on the horizontal ladder test taken from a video recording*

Score	Type of foot misplacement	Characteristics
0	Total miss	Deep fall after limb missed the rung
1	Deep slip	Deep fall after limb slipped off the rung
2	Slight slip	Slight fall after limb slipped off the rung
3	Replacement	Limb replaced from one rung to another
4	Correction	Limb aimed for one rung but was placed on another or limb position on same rung was corrected
5	Partial placement	Limb placed on rung with either digits/toes or wrist/heel
6	Correct placement	Mid-portion of limb placed on rung

Table II.1: *Ladder test scoring system (Metz and Whishaw, 2002a)*

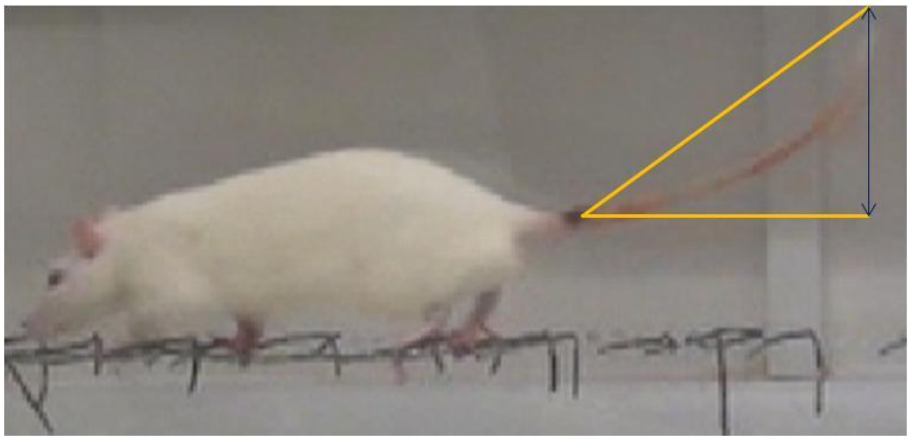

Figure II.4: *Schematic representation of the tail angle measured in this study*

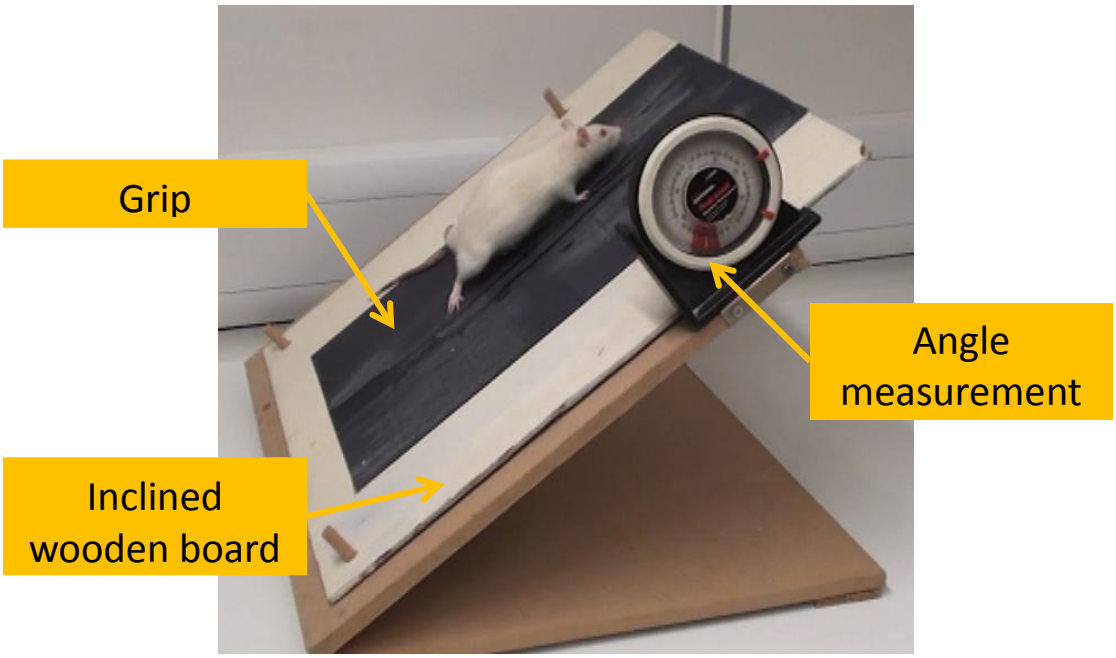

Figure II.5: *Inclined plane apparatus*

II.2.3- Treadmill test – Gait analysis

Treadmill gait assessment was performed using the TreadScan imaging system. The treadmill consisted of a Plexiglas® compartment and a transparent belt with an angled mirror placed below, allowing the recording of videos to visualize paw contact during the testing procedure. Animals were trained once daily for 4 days before the beginning of testing. After being injected with either VEGF (n=5) or PBS (n=5), the testing procedure consisted of a 1 min session of walking at a speed of 10 cm/s. This speed was chosen in order to allow sick animals to be able to walk at their peak of deficit. The last training session was recorded and served as the baseline for normal locomotion. The testing protocol consisted of a 1 min walking session once daily according to the time points to be studied. Videos were taken and analysed using the TreadScan proprietary software (CleverSys), which identifies each individual paw in each frame, outlines them and calculates different parameters such as stance time, stride frequency, animal speed, gait angle, rear track width, minimal longitudinal reach and feet base. Training session videos were used to train the software to correctly use colour and pixel differentiation to identify paw placement.

II.2.4- Burrowing test

Burrowing is a spontaneous natural behaviour in rodents and, as such, an easy test to assess the general well-being of these animals (Deacon, 2009). Burrowing behaviour was thus analysed as an indicator of the effect of VEGF intraspinal injections in injected rats (n=5) compared to the control group (n=4). Burrows were constructed from cardboard cylinders of dimensions 300mm long and 90mm in diameter, and they were filled with woodchips (figure II.6). The open end of the tube was raised 60mm above the cage floor by

two bolts and burrows were filled with woodchip bedding before each test. The test was performed every other day from one week pre-surgery up to one month post-surgery. Briefly, each animal was housed singly from 6pm until 9am with a burrow filled with woodchip bedding. The amount of woodchip bedding burrowed out of the cylinder was calculated by comparing the weight of woodchip bedding in the cylinder before and after the experiment. Results were expressed as a percentage of woodchip ejected over the 15h period.

II.2.5- Von Frey

To evaluate the consequence of VEGF injection on animals' response to tactile stimuli, the Von Frey filament test was performed. These filaments (Touch Test, Semmes Weinstein) are calibrated fibres with ascending force (10g, 15g, 26g, 80g, 100g, 180g, 300g) and the accuracy of the calibration was checked by applying the filaments on a scale. Rats were placed in a red Plexiglas® box on a mesh and filaments were applied sequentially to the plantar surface of both hind paws, one after the other, until either bending of the filament or a withdrawal of the paw was observed (figure II.7). Each filament was tested five times on each paw and a given force was considered as the withdrawing threshold when three out of five trials resulted in paw withdrawal. This threshold was recorded for each paw of each animal at

Figure II.6: *Burrowing apparatus*

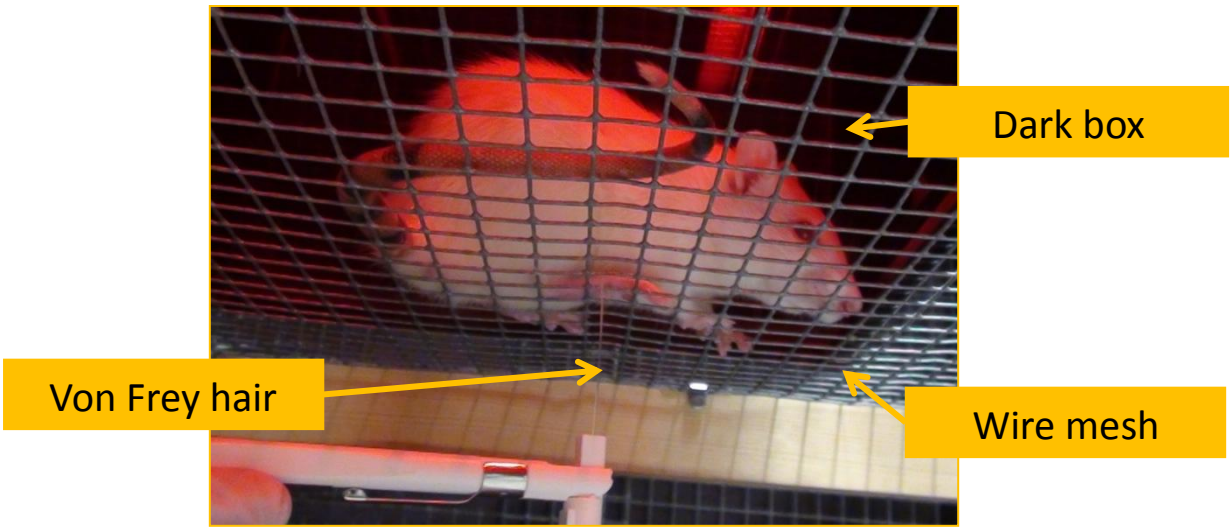

Figure II.7: *Von Frey hair testing apparatus*

each time point and the animals injected with PBS (n=12) were compared to the ones injected with VEGF (n=17).

II.2.6- Statistical analysis

In each group (control and VEGF-injected animals) ladder test scores, treadmill measurement, burrowing scores and inclined plane angles were analysed with a repeated measures ANOVA test when all data was normally distributed. If the normality assumption was not verified, the non-parametric Friedman test was used. Post-hoc analysis was performed with the Student's t-test between different time points when the data were normally distributed. If not the case, the Wilcoxon test was used. Results were accepted as significant at $p < 0.05$.

Since the Von Frey test score is an ordinary measure of strength leading to paw withdrawal, following the non-parametric Friedman test, the non-parametric Wilcoxon test was used to compare results between each time point for each paw and each group of animals. Results were considered significant at $p < 0.05$.

II.3- Immunohistochemistry

Spinal cords for immunohistochemistry were left in 4% paraformaldehyde (PFA) overnight and then put into 30% Sucrose (Sigma-Aldrich, St Louis, MO) and 0.3% sodium azide (Sigma-Aldrich, St Louis, MO) in PBS for 48h minimum. Tissue of interest was cut into 5mm blocks and frozen on dry ice in optimal cutting temperature (OCT) solution (Bright, Huntingdon, UK) and stored at -80°C. 12µm thick transverse sections were cut at -20°C on a

cryostat (CM 1950, Leica, Milton Keynes, UK) and mounted on slides (2 sections/slide). Slides were left to dry overnight and then stored at -20°C.

II.3.1- Localization of the centre of the lesion

Within the 5mm block described above, care was taken to accurately find the centre of the lesion as the block was taken from the spinal cord by hand, giving the opportunity to introduce a slight error of localization during the cutting. The centre of the lesion was then accurately found by labelling several slides covering the whole block at 400 µm intervals for IgG, which was the best marker for blood-brain barrier leakage and, as a consequence, for the presence of the lesion. The section with the most intense IgG labelling was recorded and subsequent immunohistochemical labelling performed on adjacent sections. For each labelling, one section per animal was used and analysed. Thus, for a given study, the n number of sections analysed for quantification is equal to the n number of animals used.

II.3.2- Tissue preparation

Before immunohistochemical processing, slides were dried at room temperature for a minimum of one hour. The area around sections was delimited with a block pen and slides were washed with PBS containing 0.3% Triton-X (PBST) for 3x5 min. Depending on the antibody used, different pre-treatments were used for antigen retrieval and inhibition of endogenous peroxidase activity.

- Tissue meant to be labelled with 3-3’ diaminobenzidine (DAB) was pre-treated with 70% methanol and 10% hydrogen peroxide in water to suppress any endogenous

peroxidase activity (on which the labelling mechanism is based) for 15min at room temperature.

- Tissue meant to be fluorescently labelled was pre-treated with 70% methanol in water for permeabilisation of the tissue.
- For nitrotyrosine labelling, slides were immersed in 10 % target retrieval solution (DAKO) in water at 40°C for 40min.
- For pimonidazole and HIF labelling, slides were immersed in 0.1% sodium borohydride in water for 2x5min to unmask antigens.

Pre-treatment relative to each antibody is summarized in table II.1.

II.3.3- Primary labelling

Tissue was blocked with 10% of the appropriate serum (see table II.2) in PBST for 30 min before incubation overnight at 4°C in 200µl of primary antibody diluted at the optimal concentration (table II.2) in 2% blocking serum in PBST.

II.3.4- Secondary labelling and amplification

- **DAB labelling**

Biotin-coupled secondary antibodies (listed in table II.2) were applied for 1h at room temperature. Amplification was achieved with the Vectastain ABC Elite kit (30min room temperature, Vector Labs, Peterborough, UK) and a triple 5min PBST wash was performed between each step. Labelling with DAB (Vector labs, Peterborough, UK) was timed as appropriate for the relevant antibody (listed in table II.2) and the reaction was stopped with water. Slides were then immersed in ethanol and xylene in ascending concentrations:

70% (5min), 90% (5min), 100% (2min), 100% (2 min), xylene (2min), xylene (2min), mounted in DPX and stored at room temperature.

- **Fluorescent labelling**

Secondary antibodies, consisting of either fluorescently labelled antibody (Cyanine 3 (Cy3) or Fluorescin isothiocyanate (FITC)) or biotin-coupled antibody (listed in table II.2), were applied for 1h at room temperature followed by 1h incubation with Streptavidin (SAV) 488 for biotin-coupled secondary antibodies. After a triple PBST wash, slides were mounted with DAPI fluorescent medium and stored at 4°C.

II.3.5- H&E staining

Slides of transverse sections of the spinal cord were used for haematoxilin and eosin (H&E) staining. After drying for 1 hour at room temperature, a triple 5 min PBS watch was performed. Slides were then incubated for 2 min in a haematoxylin solution and washed again for 15 min under running tap water. They were incubated in eosin for 2 minutes before being washed again for 15 min with running tap water. Slides were then immersed in ethanol and xylene in ascending concentrations: 70% (5min), 90% (5min), 100% (2min), 100% (2 min), xylene (2min), xylene (2min), mounted in DPX and stored at room temperature.

II.3.6- Microscopy analysis

DAB labelled sections and plastic sections were examined by light microscopy (Axiophot microscope, Zeiss, Oberkochen, Germany) and pictures were taken using a Nikon D300 camera (Nikon, Tokyo, Japan). Fluorescent labelling was observed through an LSM 5 Pascal confocal microscope (Zeiss, Oberkochen, Germany) and pictures were recorded and analysed with the Pascal software (Zeiss).

II.3.7- ED1, MHC class II and RECA-1 labelling quantification

Following immunohistochemical labelling of spinal cord sections, low magnification (10x) pictures were taken. Using ImageJ software, pictures were thresholded using the "color threshold" tool in order to differentiate between background and positive labelling. Once the threshold was applied to the image (the value of the threshold was kept constant for all images), they were converted into an 8 bit black and white format and transformed into binary black and white pictures using the "make binary" tool with the white background option selected. Particles to be counted were therefore black, and using the drawing tool, the area of interest was delimited and particles labelled in black were counted using the "Analyze particles" tool. Results were expressed as a number of positive particles per area.

II.3.8- Statistical analysis

To show significance of the results, statistical analysis was performed on ED1 and MHC-II cell counts between the control group and the VEGF injected animals. Student's t-test was performed for normally distributed measurements and the Mann Witney U-test was used for non-parametric evaluations. Results were considered significant for $p < 0.05$.

II.4- Plastic sections

Spinal cords for plastic sectioning were put in 4% (PFA) overnight. Tissue of interest was cut into 1mm thick blocks and left for at least 24h in 4% glutaraldehyde. Tissue was then subjected to three 10min washes in 0.1 M PO4 buffer (pH 7.4) and post-fixed in 1.5% osmium tetroxide for 1h, before undergoing a further set of three 10min washes in 0.1 M PO_4 buffer (pH 7.4). Spinal cords were then dehydrated in 15min washes in 30%, 50%, 70% and 90% ethanol ending with three 20min washes in 100% anhydrous ethanol. For resin infiltration, two 30min washes in 100% propylene oxide were followed by 2h in 75% propylene oxide: 25% resin, 2h in 50% propylene oxide: 50% resin, 2h in 25% propylene oxide: 75% resin and finally overnight at 4ºC in fresh 100% resin. The tissue was embedded in resin, using Beem capsules for longitudinal sections or coffin molds for transverse sections, and heated at 60°C for 48 hours. 0.7µm thick sections were cut and collected onto slides and stained with thionin acetate and acridine orange. These sections were then screened in a light microscope and ultrathin sections from selected blocks were subsequently examined further in an electron microscope.

II.5- Grey matter area ratio

The size of the grey matter on the ipsilateral side of the spinal cord was compared to the contralateral side by using plastic sections or sections stained with H&E. Briefly, 5x pictures were taken with a light microscope (Axiophot microscope, Zeiss, Oberkochen, Germany) and, using ImageJ analysis software, the grey matter was delimited using the drawing tool

and the area measured. The ratio ipsilateral/contralateral area was then calculated and plotted.

Primary antibody	Source	Dilution	Company	Pre-treatment 1	Pre-treatment 2	Blocker	Secondary	Labelling
IgG + HRP	Goat, polyclonal	1/200	Sigma Aldrich	Met + Peroxide		Goat	N/A	DAB: 4min
iNOS	Rabbit, polyclonal	1/200	BD Transduction Lab.	Met + Peroxide		Goat	Goat anti-rabbit biotinylated	DAB: 6min
ED1	Mouse, monoclonal	1/200	AbD Serotec	Met + Peroxide		Horse	Horse anti-mouse biotinylated	DAB: 1min
Pimonidazole	Mouse, monoclonal	1/200	HPI Inc.	Met + Peroxide	Sodium borohydride	Casein	Horse anti-mouse biotinylated	DAB: 30min
Nitrotyrosine	Mouse, monoclonal	1/200	Millipore	Met + Peroxide	DAKO retrieval	Horse	Horse anti-mouse biotinylated	DAB: 5min
Ox-42	Mouse, monoclonal	1/200	Abcam	Met + Peroxide		Horse	Horse anti-mouse biotinylated	DAB: 5min
HIF	Rabbit, polyclonal	1/200	Millipore	Met + Peroxide	Sodium borohydride	Goat	Goat anti-rabbit biotinylated	DAB: 3.5min
Fibrinogen	Goat, polyclonal	1/500	Nordic Immunology	Met		Rabbit	Rabbit anti-goat biotinylated	SAV 488
GFAP	Mouse, monoclonal	1/200	Abcam	Met		Horse	Horse anti-mouse biotinylated	SAV 488
VEGF	Mouse, monoclonal	1/200	Abcam	Met		Horse	Horse anti-mouse biotinylated	SAV 488
MHC class II	Mouse, monoclonal	1/200	Abcam	Met		Horse	Horse anti-mouse biotinylated	SAV 488
CD 3	Rabbit, polyclonal	1/200	Abcam	Met		Goat	Cy-3 conjugated Goat anti-rabbit	
Synaptophysin	Mouse monoclonal	1/100	Abcam	Met	DAKO retrieval	Horse	Horse anti-mouse biotynilated	SAV 488
PSD-95	Rabbit polyclonal	1/1000	Abcam	Met	DAKO retrieval	Goat	Goat anti-rabbit biotinylated	SAV 488
RECA-1	Mouse, monoclonal	1/500	Abcam	Met		Horse	Horse anti-mouse biotinylated	SAV 488

Table II.2: *Primary antibodies used with their respective blocker, dilution and pre-treatment (Met: Methanol 70%, Peroxide: Hydrogen Peroxide). Secondary antibodies are shown with their respective labelling method (time of incubation in DAB is given, SAV 488: Alexa Fluor 488 conjugate).*

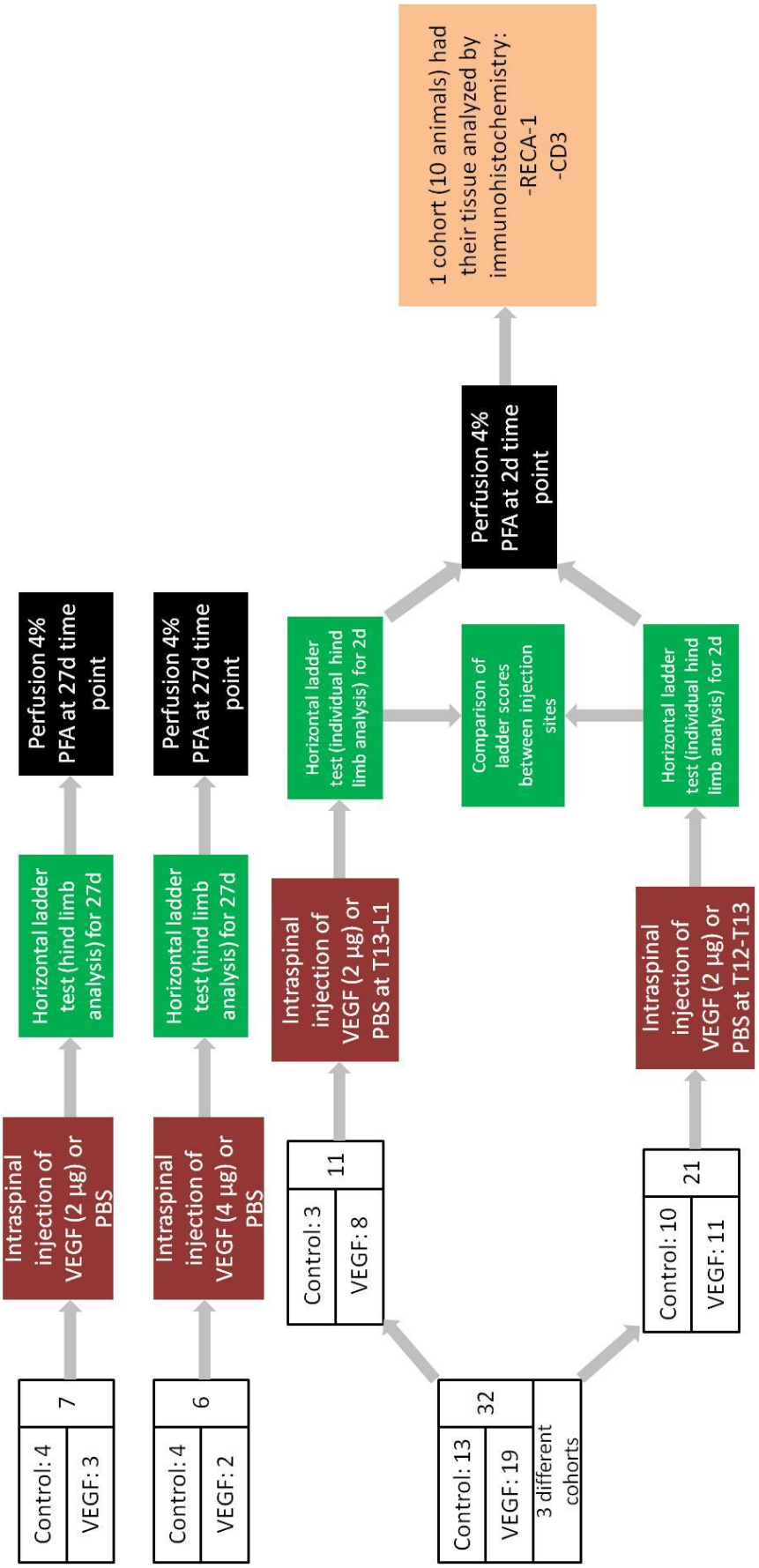

Figure II.8: *Summary of the procedures undergone by each group of animals used in the study (1)*

Figure II.9: *Summary of the procedures undergone by each group of animals used in the study (2)*

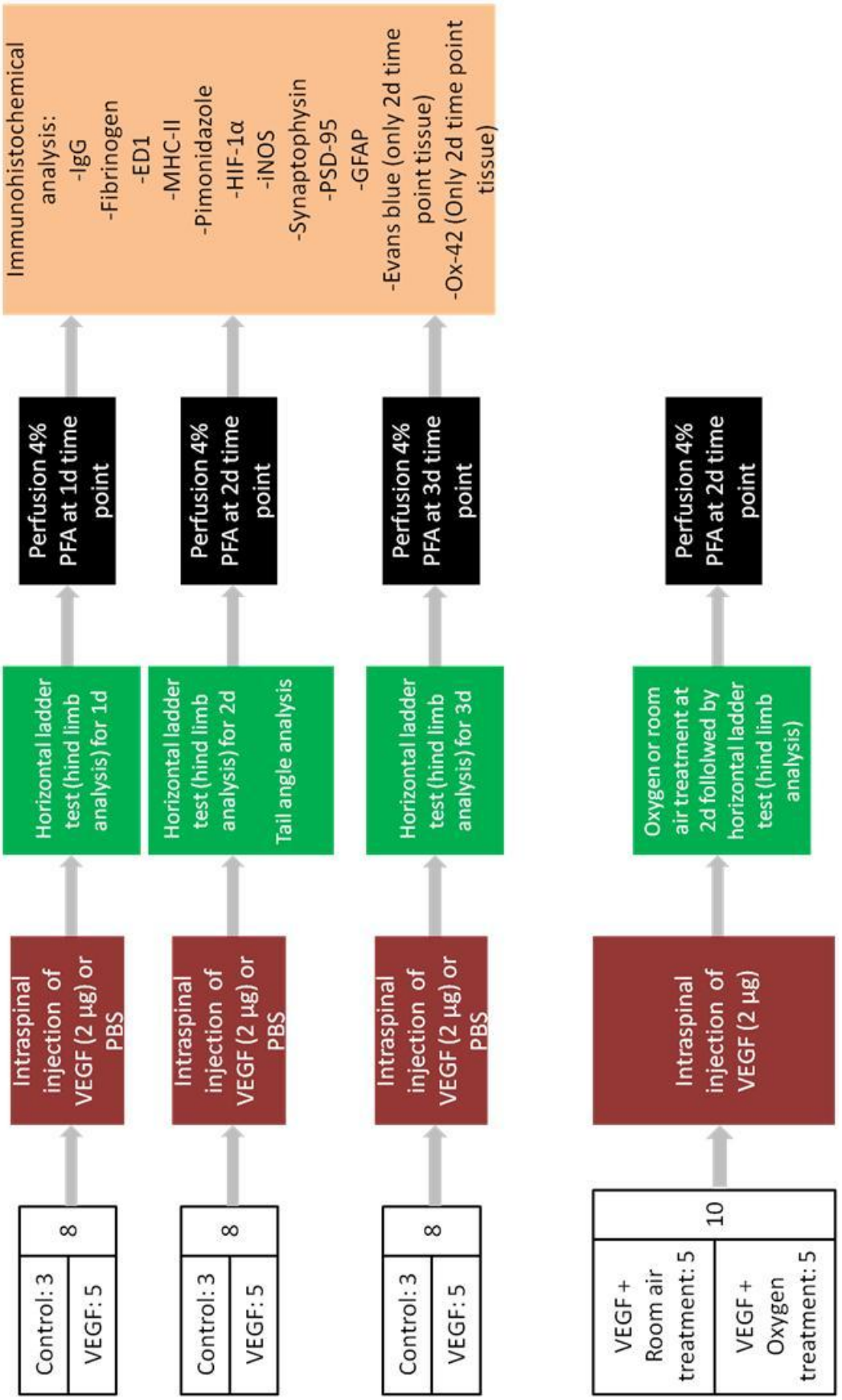

Figure II.10: *Summary of the procedures undergone by each group of animals used in the study (3)*

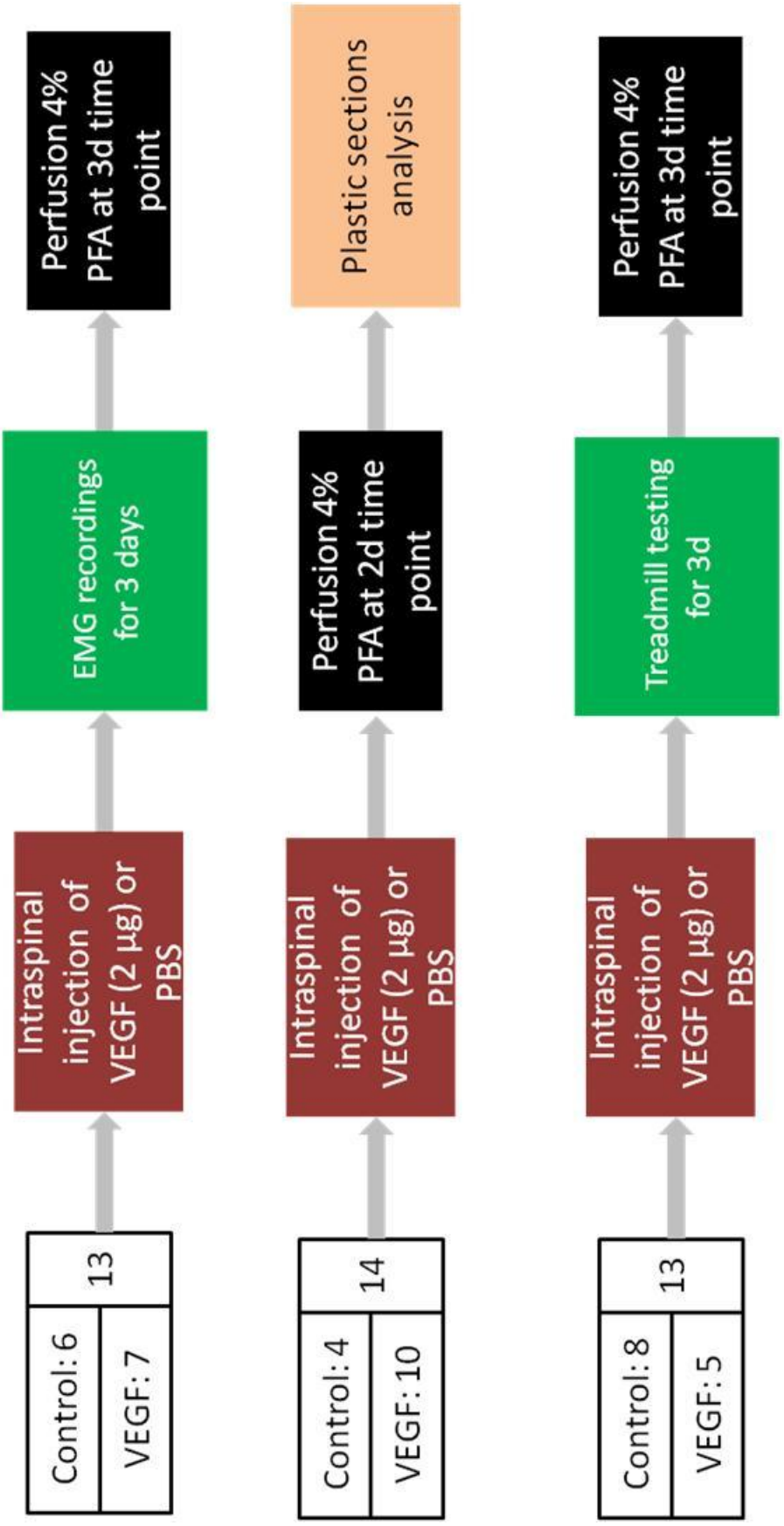

Figure II.11: *Summary of the procedures undergone by each group of animals used in the study (4)*

Chapter III: Results - Behavioural analysis

III.1- Choice of the injection dose

Preliminary studies were necessary to determinate the dose of VEGF to be injected in the spinal cord. One research group, however, has injected directly VEGF intraspinally in rats to provoke a focal EAE lesion (Sasaki et al., 2010). Basing our protocol on their study, we decided to inject rats with VEGF at the T13-L1 vertebral level (where the hind limbs motor neurons pool is located) in the dorsal column at two different doses: 2x1µL at 1 mg/mL VEGF (low dose) and 4x1µL of 1 mg/mL (high dose). We then assessed the motor function of hind limbs of animals for up to one month post-surgery with the horizontal ladder walking test.

Control animals (injected with low (n=4) or high (n=4) dose of PBS) did not demonstrate any deficit on the ladder test for the whole course of the study. In contrast, animals injected with VEGF at both low dose (n=3) and high dose (n=2) (note: these small group sizes were just for determining the dose) showed a transient and reversible deficit starting at day two as shown in figure III.1. The low dose group showed a milder and quantifiable deficit (figure III.1.A) while the high dose animals were paralysed from the hind limbs at day one and two following surgery and recovered from day three onward (figure III.1.B).

A

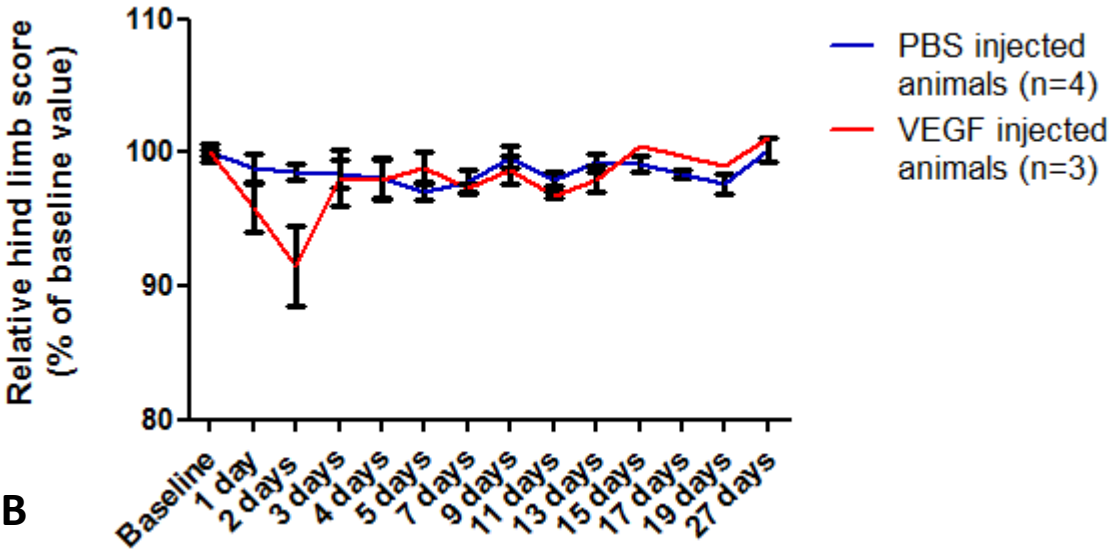

B

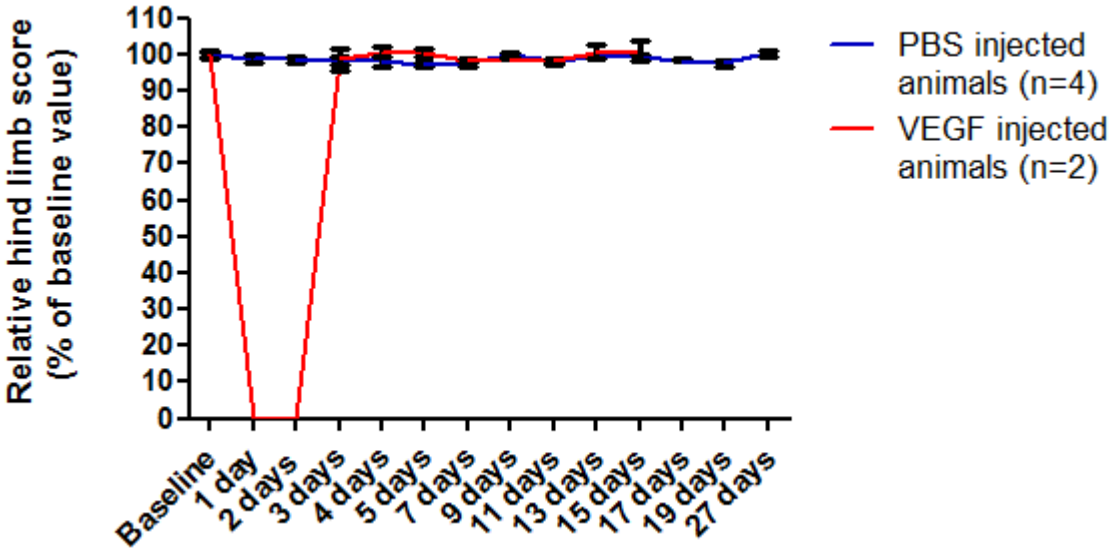

Figure III.1: ***A.*** *Relative hind limb score on the horizontal ladder test of animals injected with PBS (n=4) or a low dose (2x1µg) of VEGF (n=3). Day 0 corresponds to the date of surgery.* ***B.*** *Relative hind limb score on the horizontal ladder test of animals injected with PBS (n=4) or a high dose (4x1µg) of VEGF (n=2).* Animals were tested from seven days before surgery up to 27 days post-surgery. *Day 0 corresponds to the date of surgery. Error bars represent the standard error of the mean.*

It is worth noting that, as expected, only the hind limbs exhibited a deficit after VEGF injection: in another study, the scores for both fore limbs for VEGF-treated animals (n=6) were comparable to control animals (n=4) for the whole period of study (figure III.2). Interestingly, the deficit in the hind limbs had no effect on the ability of the animals to use the fore limbs on the ladder. Because of the ability to quantify the deficit undergone by animals injected with a low dose of VEGF, the low dose protocol was preferred. This choice was justified by the prospect of assessing quantifiable differences between possible mechanisms of actions and causes of deficit. For the rest of the study, the dose injected is a dose corresponding to a low dose of VEGF: 2x1µL at 1 mg/mL.

III.2- Motor deficits induced by injection of VEGF

III.2.1- Horizontal ladder test

Animals injected with VEGF were compared with controls on the horizontal ladder walking test on different days over a month. As expected, control animals did not show any deficiency while performing the task but animals injected with VEGF showed a deficit during days one and two post-surgery, and recovered from day three until the end of the study, as shown by their hind limb score (figure III.1). Noticeably, two animals (not included in the data shown in figure III.1), showed a complete hind-limb paralysis (explained by the subsequent histological discover that the VEGF injection went into the grey matter leading to haemorrhage) and recovered within the same time course as correctly injected animals.

As the deficit was observed within the first three days following surgery, with subsequent recovery, the focus of most subsequent studies has been during the first days of lesion

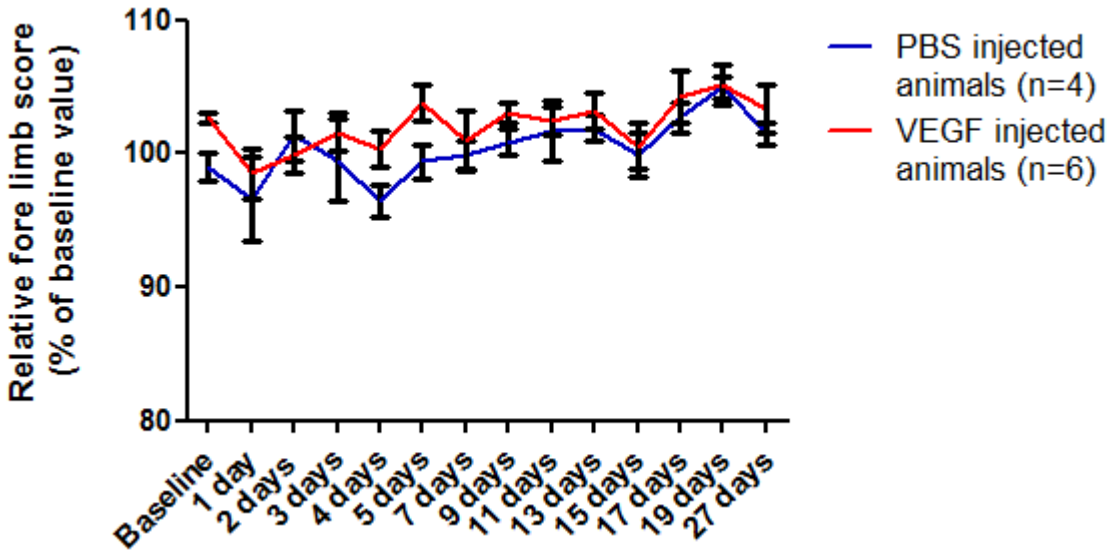

Figure III.2: *Relative fore-limb score on the horizontal ladder test of animals injected with PBS (n=4) or VEGF (n=6). A*nimals were tested from seven days before surgery up to 27 days post-surgery. *Day 0 corresponds to the date of surgery. Error bars represent the standard error of the mean.*

development. Moreover, as described in the introduction, the motor neuron pool and proprioceptive pathway mediating hind limb control is located in the lumbrosacral enlargement, between the T12 and L1 vertebrae. To verify the accuracy of the hind-limb control location, rats were injected at either T12-T13 or T13-L1 levels with VEGF or PBS and tested for three days before perfusion. Data are shown in figure III.3 and show a significant deficit (T12-T13: p=0.003 n=10; T13-L1: p=0.012 n=8) at day two post-surgery in animals injected with VEGF in either injection locations. Control animals did not show any score reduction in any of the injection locations (T12-T13: n=8; T13-L1: n=8). The amplitude of the deficit was similar between animals injected at T12-T13 (23.76 +/- 11.9%, n=8) or T13-L1 (28.4 +/- 11.08%, n=10). Thus for both injection sites, VEGF injection causes a significant neurological deficit at day two post-surgery compared to the baseline and control animals.

The data presented so far are an average of the scores for both hind-limbs. As a consequence, no difference between left and right hind-limbs can be observed from these data. However, the horizontal ladder walking test allows for discrimination between different limbs by analysing them separately (Metz and Whishaw, 2002a, 2009). This limb-specific analysis has been performed on 19 VEGF-injected animals and 13 control animals. Interestingly, whereas VEGF was injected on the left side of the cord, left and right hind-limbs had a similar deficit amplitude as shown in figure III.4. No side-specific effect was observed.

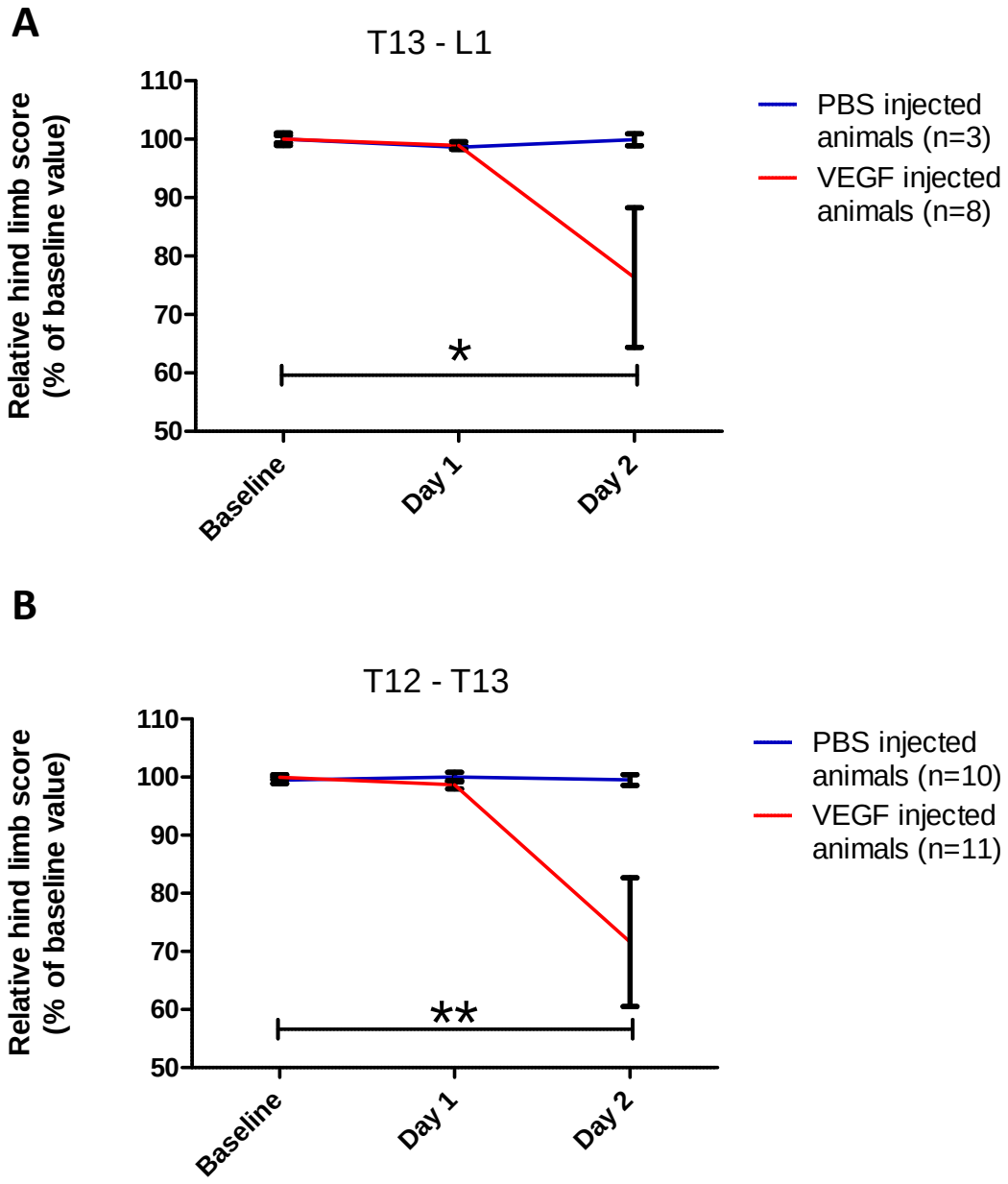

Figure III.3: ***A.*** *Relative hind limb score on the horizontal ladder test of animals injected with PBS (n=3) or VEGF (n=8) at the T13-L1 vertebral level.* ***B.*** *Relative hind limb score on the horizontal ladder test of animals injected with PBS (n=10) or VEGF (n=11) at the T12-T13 vertebral level. A*nimals were tested from one day before surgery up to three days post-surgery. *Day 0 corresponds to the date of surgery. Statistical analysis was performed with a Wilcoxon test. (*: p<0.05). Error bars represent the standard error of the mean.*

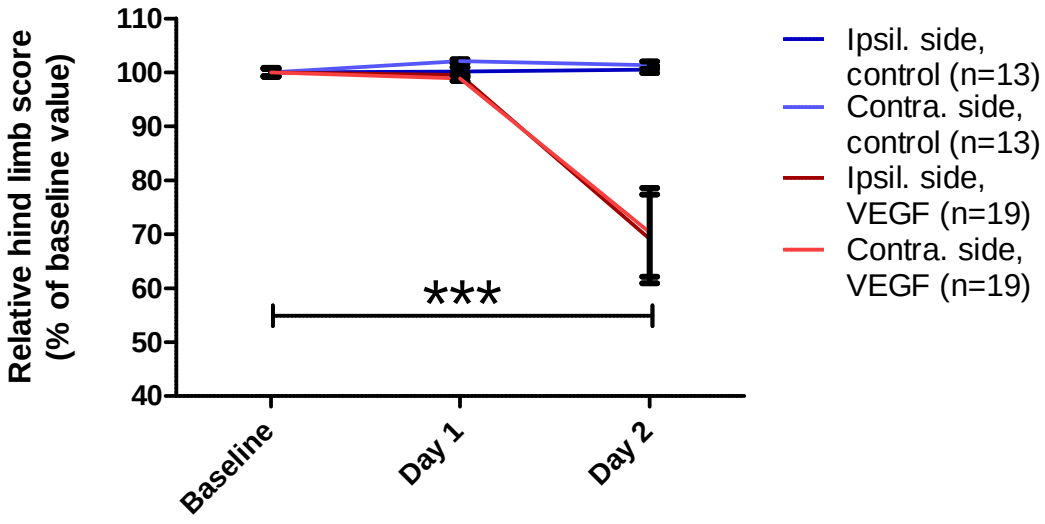

Figure III.4: *Relative hind limb score on the horizontal ladder test of animals injected with PBS (n=13) or VEGF (n19). Left and right hind-limbs scores were assessed separately and are represented. A*nimals were tested from one day before surgery up to three days post-surgery. *Day 0 corresponds to the date of surgery. Statistical analysis was performed with a Wilcoxon test. (***: p<0.001). Error bars represent the standard error of the mean.*

III.2.2- Tail position

During the ladder test it was noticed that some animals held their tail abnormally. Thus, both naïve and saline-injected (n=6) rats walked with the tail lifted high, whereas animals injected with VEGF (n=11) either dragged their tail, or only lifted it slightly. Quantification of the tail angle (figure III.5) confirmed this impression, revealing that at day two following surgery VEGF injected animals carried their tails at a significantly reduced angle compared with baseline values ($p=0.008$). A trend is present at one day. This result reveals that VEGF injection impairs both hind limb and tail function.

III.2.3- Inclined plane test

The inclined plane method was used to explore further the impairment in motor function in the rats injected with VEGF. No difference was observed in the plane angle between one day before (baseline) and after surgery in both control (54.6° +/- 0.84°, n=5) and VEGF-treated animals (55.8° +/- 0.2°, n=5), but there was a significant difference ($p=0.043$) at day two. Thus, slipping occurred at a lower angle compared to baseline in treated animals (45.2° +/- 0.58°, n=5), but not in controls (53.17° +/- 2.41°, n=5) (figure III.6).

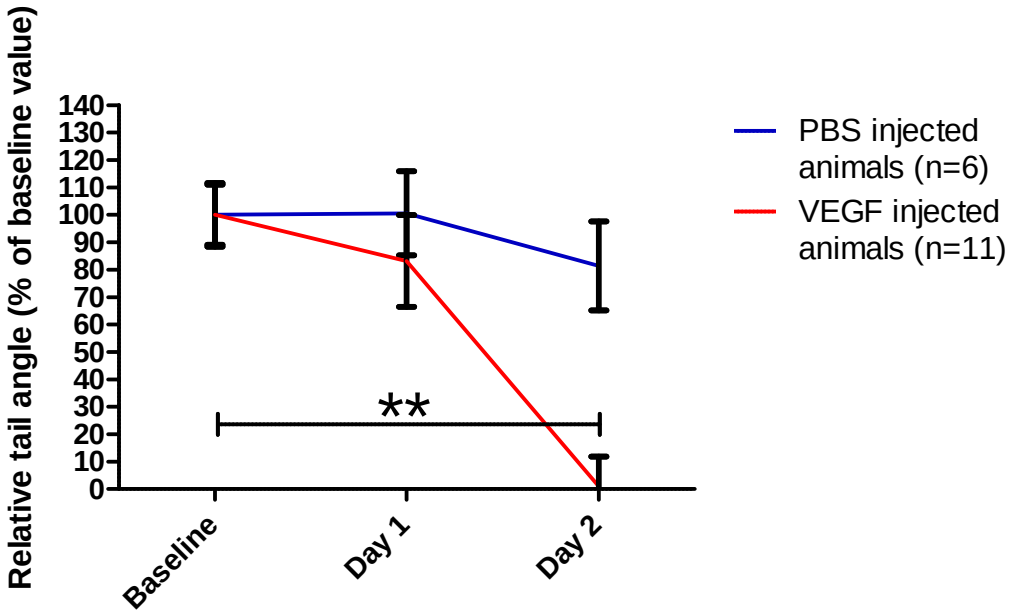

Figure III.5: *Relative tail angle value while walking on the horizontal ladder of animals injected with PBS (n=6) or VEGF (n=11). A*nimals were tested from one day before surgery up to three days post-surgery. *Day 0 corresponds to the date of surgery. Statistical analysis was performed with a Wilcoxon test. (**: p<0.005). Error bars represent the standard error of the mean.*

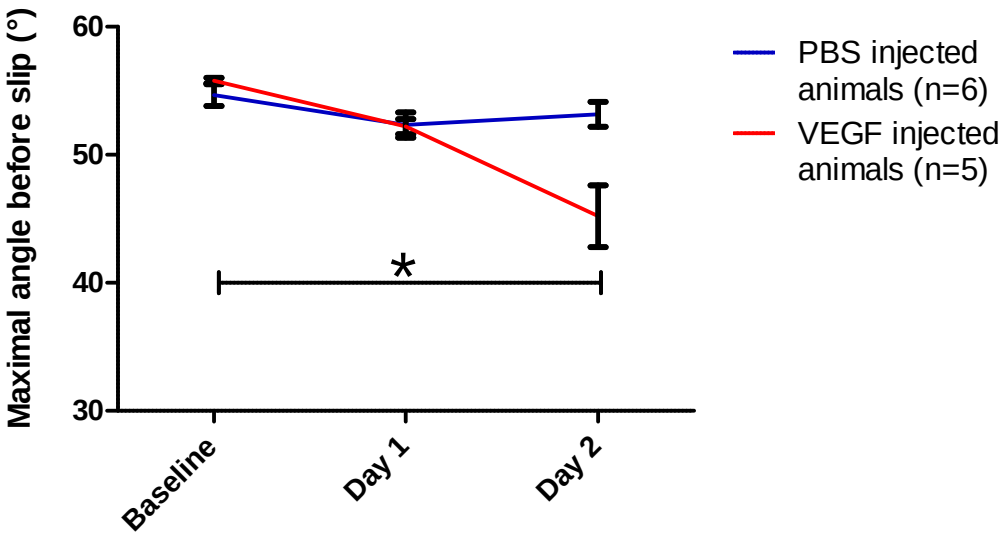

Figure III.6: Inclined plane test. Maximal angle before slip for *animals injected with PBS (n=6) or VEGF (n=5). A*nimals were tested from one day before surgery up to three days post-surgery. *Day 0 corresponds to the date of surgery. Statistical analysis was performed with a Wilcoxon test. (*: p<0.05). Error bars represent the standard error of the mean.*

III.2.4- Treadmill test

The motor deficit resulting from the injection of VEGF was characterized further using an automated treadmill test that assessed a range of measures of locomotor function.

- General observations

On the automated treadmill, videos of the animals could be recorded while walking, allowing for an observation of their gait. As shown in the snapshots presented in figure III.7, a difference could be observed between control animals and animals injected with VEGF. While walking, the hind limbs of control animals were kept at a consistent distance from each other and their toes were constantly spread. In contrast, animals injected with VEGF walked with their hind limbs very close to each other, almost in line along the longitudinal axis, and the spreading of the toes was absent.

- Feet base

The feet base is the side-specific distance between the midpoint of the front paw stride and the midpoint of the rear paw stride. In control animals (n=8), the feet base remained stable from baseline prior to surgery up to three days post-surgery (figure III.8.B). At two days post-surgery, VEGF-treated animals showed a longer feet base measure compared to baseline, one day and three days post-surgery values. This effect was amplified ipsilaterally to the injection side and is in line with the deficit characterized so far.

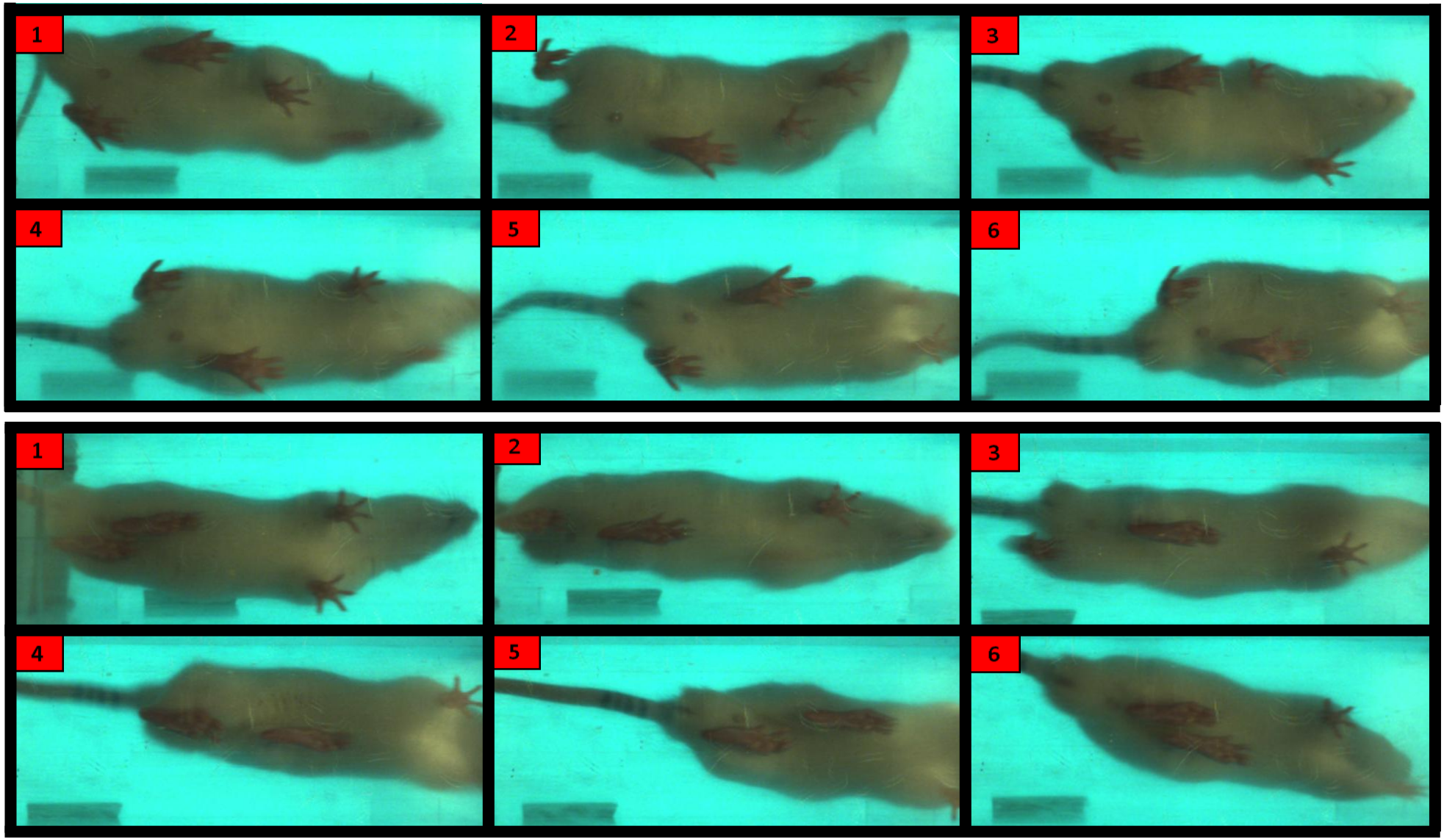

Figure III.7: *Snapshots (1 to 6 in the chronological order) of animals walking on the automated treadmill. Top panel: Control animal. Bottom panel: VEGF injected animal*

- Gait angle

The gait angle is the angle between the line connecting the plantar position of one rear foot to the next plantar position of the same foot and the line connecting the plantar position of that same rear foot to the next plantar position of the opposite rear foot. It is a combined singular measure of stride width and length. No difference between the control group (n=8) and the VEGF treated group (n=5) was observable at baseline, one day or three days post-surgery (figure III.8.A). However, at day two following intraspinal injections, animals that received VEGF showed a decrease in the gait angle compared with animals that received PBS. The change did not reach statistical significance, but a clear trend was apparent. As the gait angle is a combined measure of stride width and length, it is in agreement with both the decrease in track width and the bigger minimal longitudinal reach observed at day two post-surgery (figures III.9.A and III.9.B).

- Rear track width

The rear track width is the distance between the midpoint of the rear left paw stride and the midpoint of the right rear paw stride. As show in figure III.9.A, the rear track width of control animals (n=8) was not affected by injection of PBS. On the contrary, the rear track width of VEGF injected animals (n=5) showed a non-significant trend towards reduction two days post-surgery and went back to a baseline level at day three following the injection of VEGF.

- Minimal longitudinal reach

The minimal longitudinal reach is the closest distance during the stance that the paw attained relative to the waist axis, i.e. it measures how close the paw got to the waist. The minimal longitudinal reach did not change baseline after surgery in control animals (n=8), but there was a trend towards a higher minimal longitudinal reach in VEGF-injected ones.

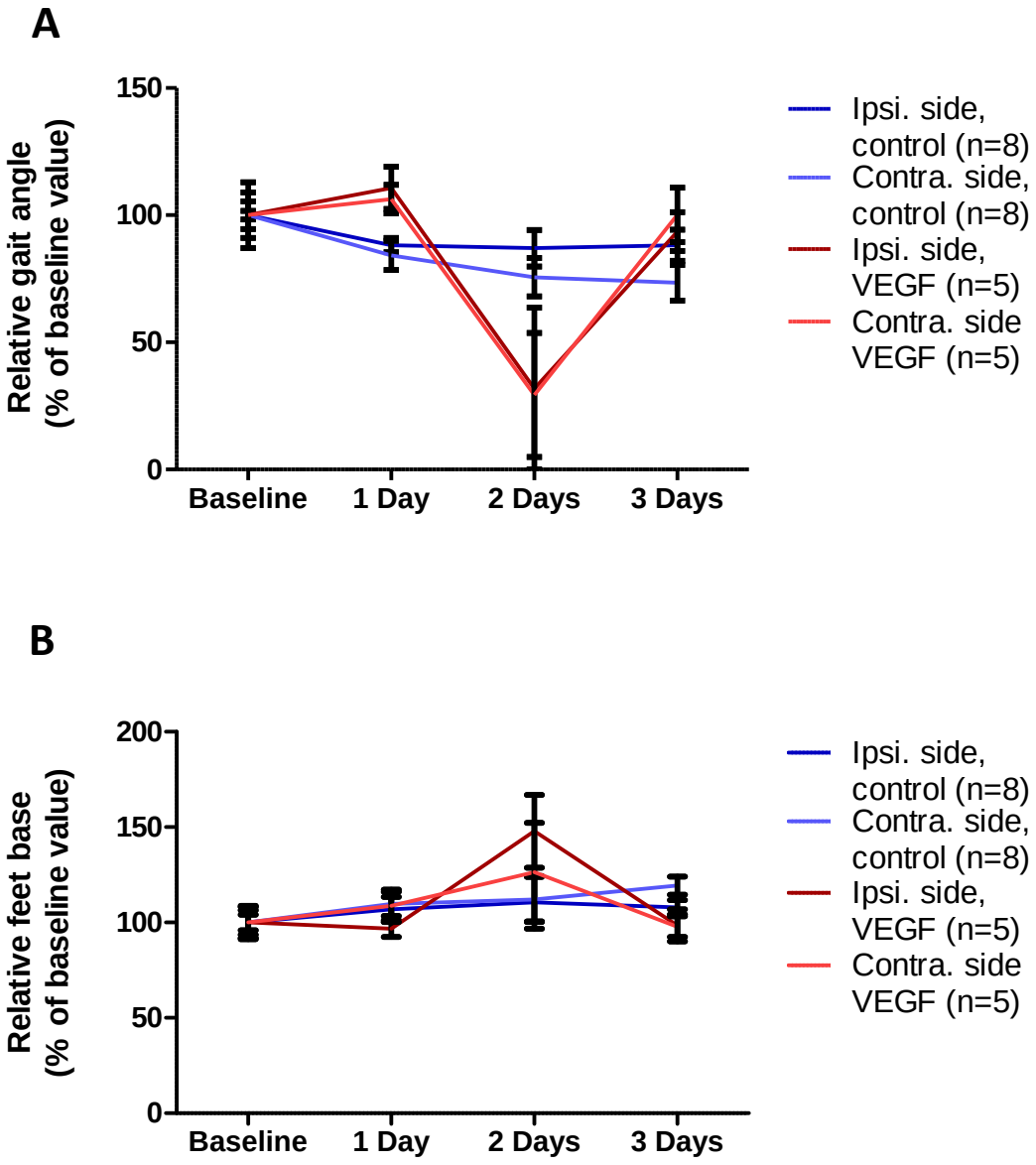

Figure III.8: *Movement parameters of animals tested on an automated treadmill from one day before surgery up to three days post-surgery.* ***A.*** *Relative gait angle of animals injected with PBS (n=8) or VEGF (n=5). Day 0 corresponds to the date of surgery.* ***B.*** *Relative feet base values of animals injected with PBS (n=8) or VEGF (n=5). Day 0 corresponds to the date of surgery. Using a Wilcoxon test, no statistical significance was achieved at any time point. Error bars represent the standard error of the mean.*

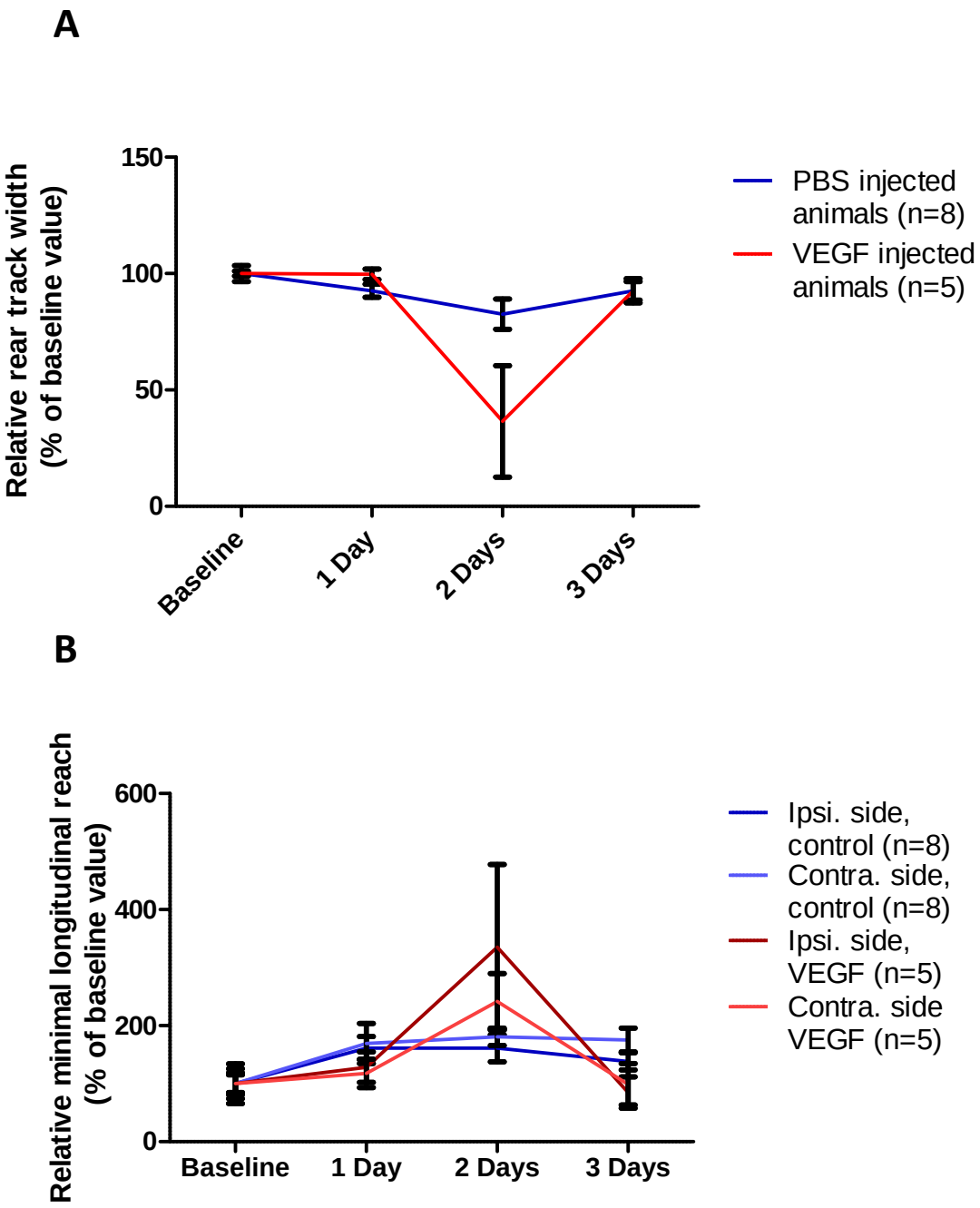

Figure III.9: *Position parameters of animals tested on an automated treadmill from one day before surgery up to three days post-surgery.* ***A.*** *Relative rear track width of animals injected with PBS (n=8) or VEGF (n=5). Day 0 corresponds to the date of surgery.* ***B.*** *Relative minimal longitudinal reach of animals injected with PBS (n=8) or VEGF (n=5). Day 0 corresponds to the date of surgery. Using a Wilcoxon test, no statistical significance could be achieved at any time point. Error bars represent the standard error of the mean.*

- Overall running speed

The overall running speed is obtained by dividing the total distance travelled by the centre of the animal by the time it took to travel that distance. As shown in figure III.10.C, through the three days of testing after injection of PBS (n=8) or VEGF (n=5), no change in overall speed was observable for any of the groups.

- Stance time

The stance time is the time elapsed while the paw is in contact with the treadmill, in its stance phase. At day two following surgery, animals injected with VEGF (n=5) had a lower stance time compared with PBS-injected animals (n=8), while no difference was observable at any other time point, showing a recovery to baseline level at day three post-surgery. Although present on both sides, this trend was not statistically significant. Within a given group, no difference was observable between the left and right paw (figure III.10.A).

- Stride frequency

The stride frequency is the ratio of the number of strides to the sum of the stride times of these strides. This yields the number of strides per second (Hz) for the given paw. An increase in stride frequency was present at day two post-surgery for the VEGF treated group (n=5) but not in the PBS injected group (n=8) (figure III.10.B). At other time points, no difference between the groups could be observed. Similarly to the stance time, no difference between left and right paws was present within a given group. This result is in line with the decrease in stance time and the absence of change in overall speed, leading to a higher stride frequency to keep the same pace.

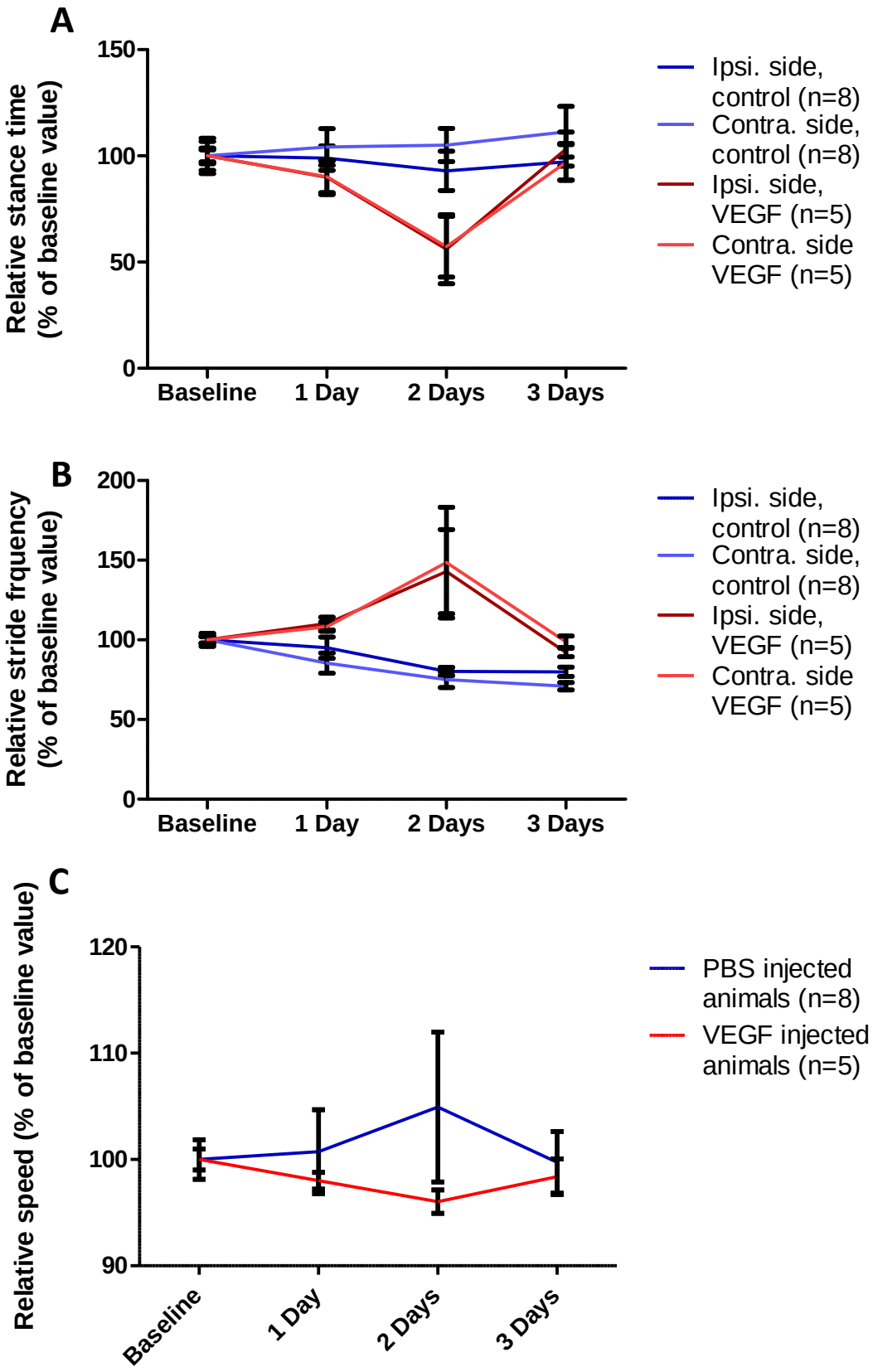

Figure III.10: *Speed parameters of animals tested on an automated treadmill from one day before surgery up to three days post-surgery.* ***A.*** *Relative stance time of animals injected with PBS (n=8) or VEGF (n=5). Day 0 corresponds to the date of surgery.* ***B.*** *Relative stride frequency of animals injected with PBS (n=8) or VEGF (n=5). Day 0 corresponds to the date of surgery.* ***C.*** *Relative speed of animals injected with PBS (n=8) or VEGF (n=5). Day 0 corresponds to the date of surgery. Using a Wilcoxon test, no statistical significance was achieved at any time point. Error bars represent the standard error of the mean.*

III.3- Behavioural deficits induced by injection of VEGF

It is a natural behaviour for rodents to burrow (Deacon, 2006), so burrowing activity can be used as a sensitive method to assess general behavioural dysfunction. To make the assessment, five rats injected with VEGF, and four controls, were housed singly in cages overnight (and put back with their cage mates during the day). The cages contained a burrow filled with wood chip bedding, and the burrowing activity was measured by weighing the remaining contents. A significant reduction in burrowing behaviour was observed with VEGF-treated animals at one ($p=0.043$), two ($p=0.043$) and three ($p=0.043$) days post-surgery compared with their pre-surgery baseline (figure III.11). The decreased burrowing activity correlated with their decreased motor dysfunction (compare figures III.3 and III.11). No significant difference was observed between the control- and VEGF-injected groups after the first three days following surgery (figure III.11).

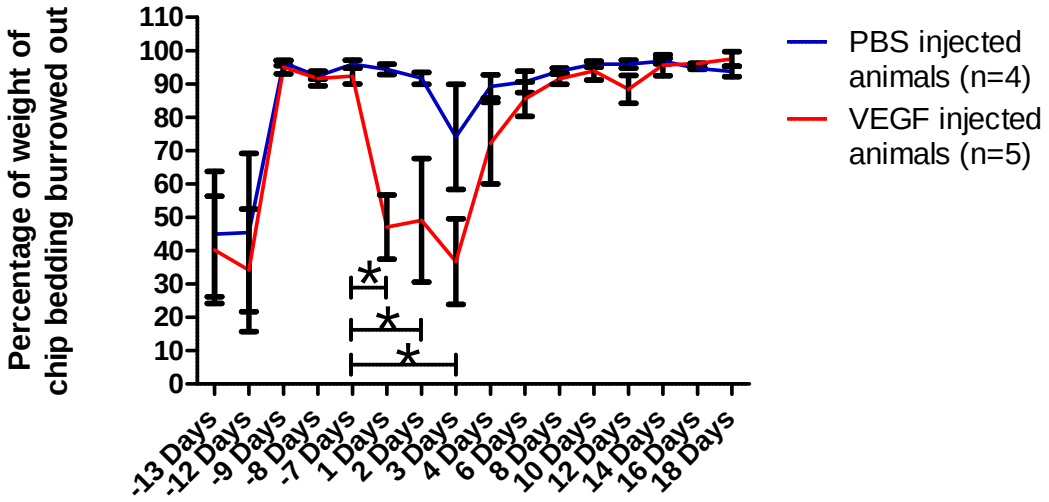

Figure III.11: *Burrowing activity of animals injected with PBS (n=4) or VEGF (n=5).Animals were tested from 13 days before surgery up to 18 days post-surgery. Day 0 corresponds to the date of surgery. Statistical analysis was performed with a Wilcoxon test. (*: p<0.05). Error bars represent the standard error of the mean.*

III.4- Sensory deficits induced by injection of VEGF

The sensory pathway from the hind limbs may be affected by the spinal lesion (at the T12-L1 vertebrae), so it was of interest to determine whether the injection of VEGF changed the responsiveness of the hind limbs to touch stimuli. The von Frey hair test was performed on the hind paws of 17 animals injected with VEGF and 12 control animals injected with PBS. The results displayed in figure III.12 show a decrease in sensitivity from baseline of both the left ($p=0.002$) and right ($p=0.003$) hind-paws in VEGF-treated animals, whereas no significant change was observed in controls. Thus, in animals injected with VEGF, the ipsilateral hind paw required a greater stimulus (115 g) to elicit withdrawal than the contralateral paw (105 g). This finding indicates that the injection of VEGF desensitizes the hind paws to tactile stimuli.

III.5- Long term effect of injection of VEGF

To assess whether the intraspinal injection of VEGF can have any long term effect on animals, we used the horizontal ladder test and assessed animals injected with PBS or VEGF for one year following surgery. As expected, a hind limb deficit was observable at day two post-surgery in VEGF-injected animals ($n=6$) compared to controls ($n=3$) ($p=0.043$) (figure III.13). During the following year, no difference in behaviour or ladder score could be observed, the animals injected with VEGF did not show any sign of deficit, indicating that injection of VEGF did not have any long term effect on motor function.

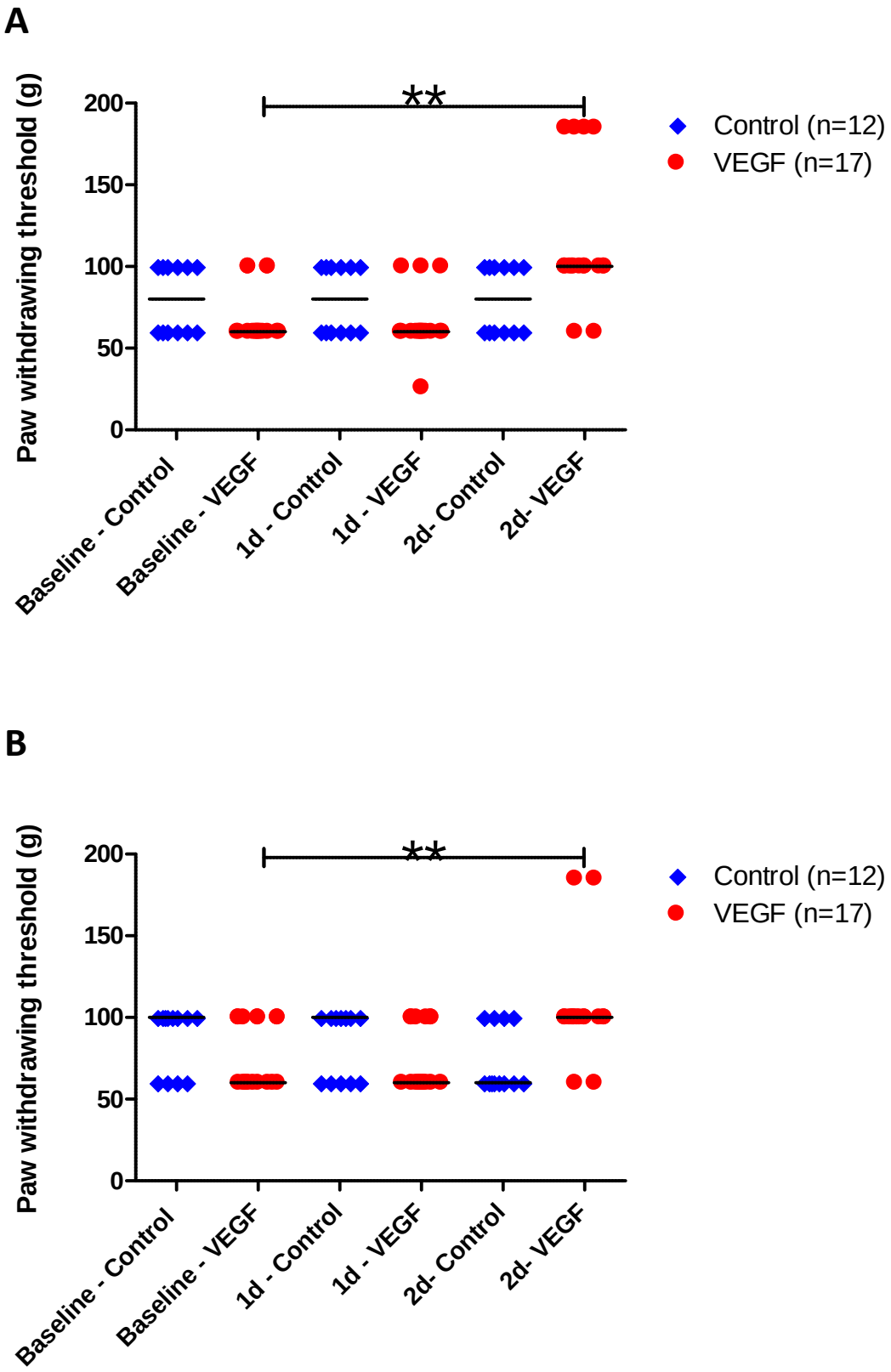

Figure III.12: *Paw withdrawal threshold in grams of animals injected with PBS (n=12) or VEGF (n=17).* ***A.*** *Left hind limb.* ***B.*** *Right hind limb. Animals were tested from one day before surgery up to two days post-surgery. Statistical analysis was performed with a Wilcoxon test. (**: p< 0.005). Horizontal bars represent the median of each group. Each point represents the measurement for one animal.*

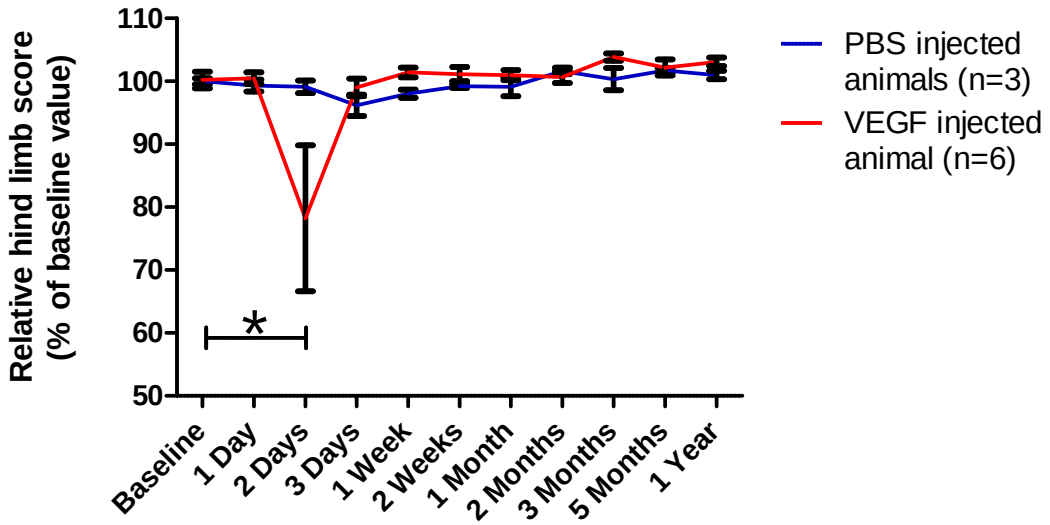

Figure III.13: *Relative hind limb score on the horizontal ladder test of animals injected with PBS (n=3) or VEGF (n=6) from one day before surgery up to a year following injection. Note that the abscissa is non-linear. Day 0 corresponds to the date of injection. Statistical analysis was performed with a Wilcoxon test. (*: p<0.05). Error bars represent the standard error of the mean.*

Chapter IV: Results - Immunohistochemical analysis

IV.1- Blood-brain barrier breakdown

IV.1.1- Evans blue leakage

Evans blue is a dye commonly used to assess leakage of blood vessels in the CNS (Olsson et al., 2006; Sasaki et al., 2010). The dye binds to blood albumin irreversibly (Veikkola et al., 2001) and gives a blue colour to any tissue into which labelled albumin may have leaked. On the second day following VEGF injection, Evans blue was administered intravenously in both animal groups (5 rats injected with VEGF and 3 with PBS) 30 minutes before perfusion. As shown in figure IV.1.A, all animals treated with VEGF (n=5) showed a focal blue staining specifically at the lesion site, indicating the presence of labelled albumin in the spinal cord. Control animals (n=3) did not show any sign of leakage (figure IV.1.A). The staining was consistently present around the injection site and extended longitudinally over an average of 5 to 6 mm, suggesting that a blood-brain barrier breakdown occurs over up to 3 mm away from the injection site. The extent of the lesion (measured by Evans blue leakage) was long enough to occur at the zone of entry of the sciatic nerve into the spinal cord (figure IV.1.B), confirming that the location chosen for VEGF injection is appropriate for targeting the motor function of the hind limbs.

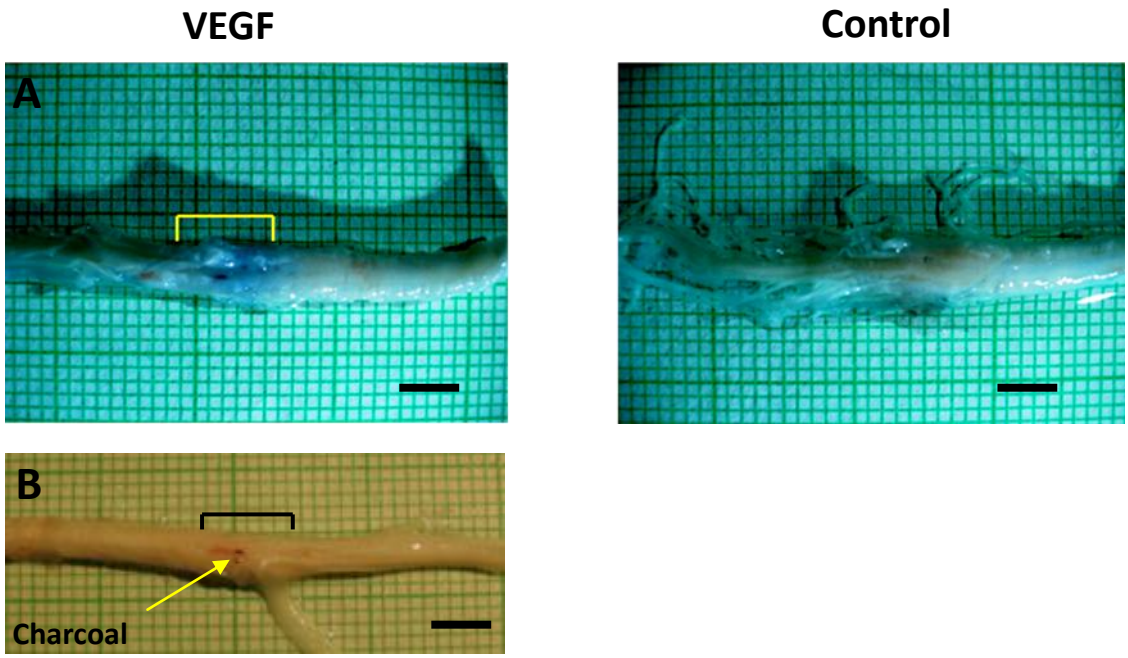

Figure IV.1: ***A.*** *Spinal cord of animals injected with VEGF (Left) or PBS (right) and intravenous Evans blue 30 min before perfusion at day two following surgery.* ***B.*** *Spinal cord of an animal injected with VEGF (the injection site is located by putting sterile charcoal where the needle was inserted) removed altogether with the spinal roots projecting to the left sciatic nerve. The black bar represents the extent of the lesion observed with Evans blue leakage, and covers the zone of entry of the roots from the sciatic nerve into the spinal cord. Scale bar: 5mm.*

IV.1.2- IgG leakage

Blood-brain barrier disruption within the spinal cord was also assessed by IgG immunohistochemical labelling in spinal cord sections. Spinal cords of rats injected with VEGF or PBS were taken at different time points (one day, two days and three days following surgery) and processed to investigate the presence of IgG. Results (figure IV.2) show the presence of IgG in VEGF-injected spinal cords, but not in PBS-injected tissue, indicative of a breakdown of the blood-brain barrier. Interestingly, the highest amount of IgG was found at one and two days post-surgery. IgG was still present at three days post-injection although in a lesser extent. The IgG peak during the first two days following surgery is in agreement with previous studies showing that VEGF induces blood-brain barrier breakdown from day one to day three (Benton and Whittemore, 2003). Labelling was present throughout the whole spinal cord cross section although a higher labelling for IgG was found in the grey matter compared with the white matter.

IV.1.3- Fibrinogen extravasation

We investigated whether fibrinogen is present within the rat spinal cord as a consequence of VEGF injection. Similarly to IgG, we looked for infiltration of fibrinogen at different time points (one, two and three days following surgery) and at different locations within the cord, namely the dorsal column, both dorsal horns, both ventral horns and the base of the dorsal column. Fibrinogen was present in the spinal cords of animals treated with VEGF but absent from control tissue (figure IV.3 and IV.4). All the areas examined showed fibrinogen extravasation at all time points, with a tendency to diminish at day three post-surgery. Moreover, a tendency for a higher intensity in the ipsilateral side is detectable in VEGF-injected animals (figures IV.3 and IV.4).

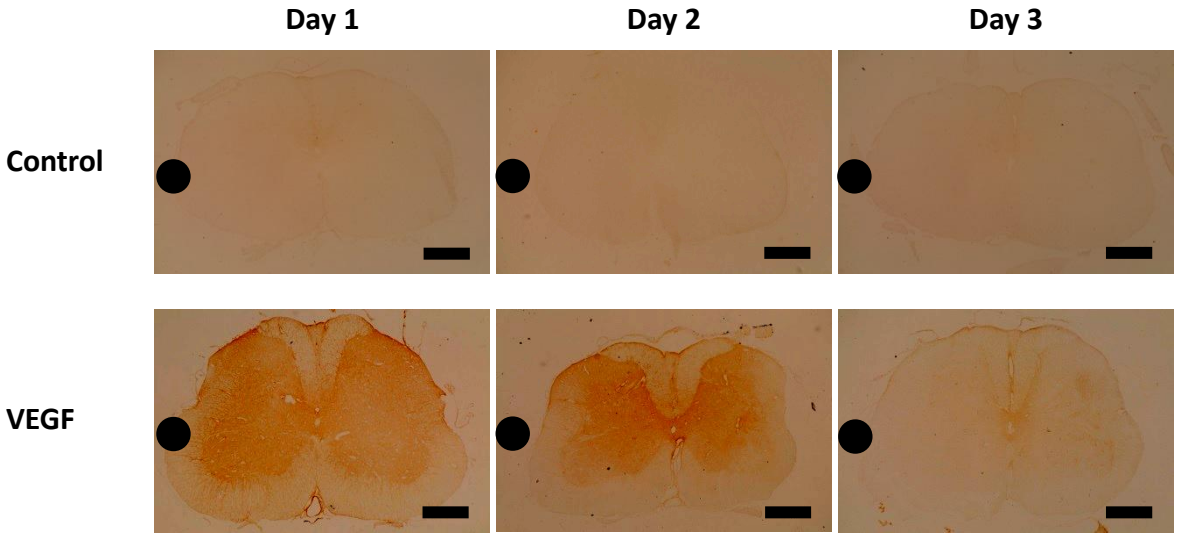

Figure IV.2: *IgG labelling in spinal cords of animals treated with VEGF (bottom row) or PBS (top row) at one day (left column), two days (middle column) and three days (right column) post-surgery. Scale: 600µm. Injections were made on the left side of the dorsal column. The black dot shows the side of injection.*

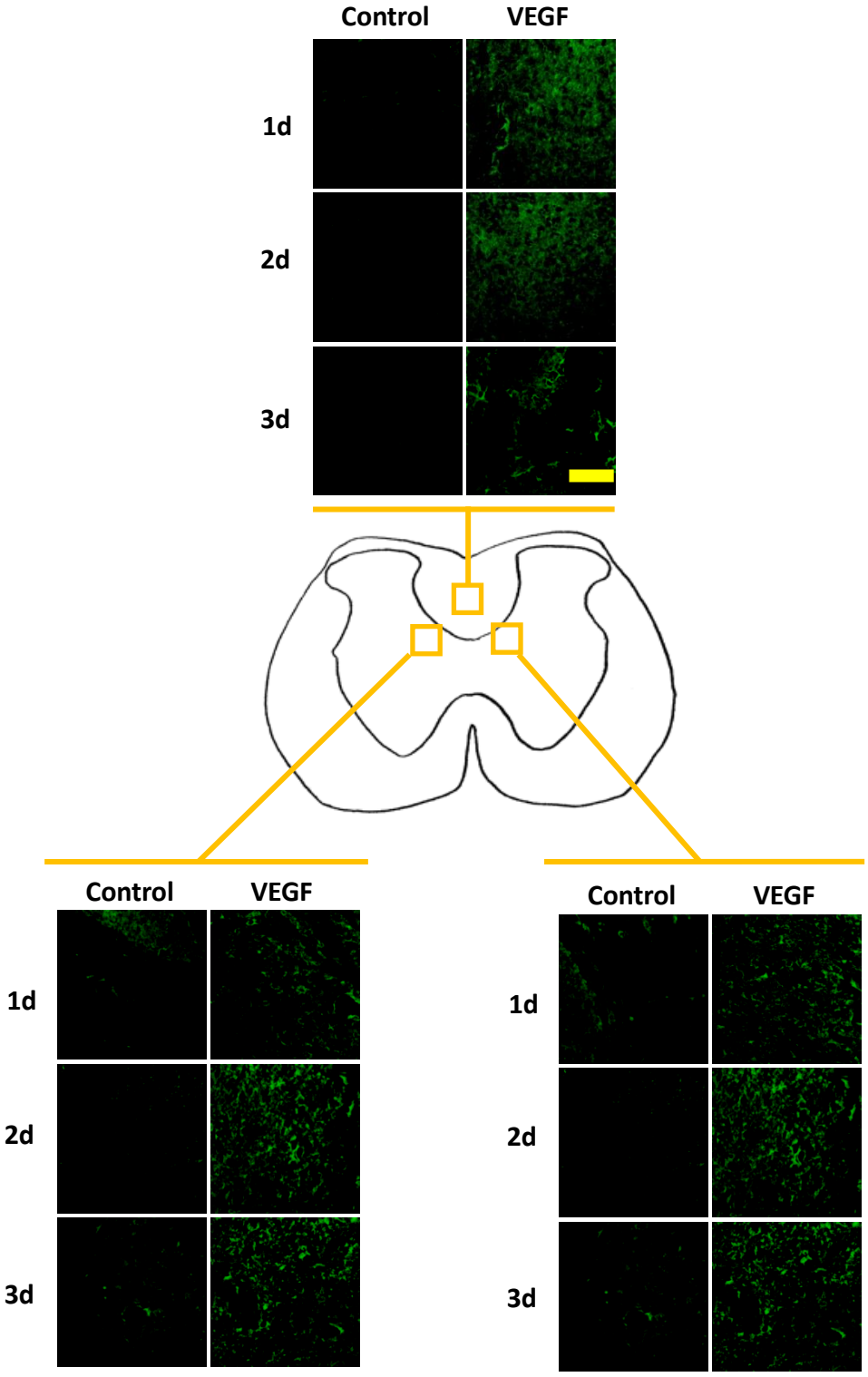

Figure IV.3: *Fibrinogen labelling in spinal cords of animals treated with VEGF (right column) or PBS (left column) at one day (top row), two days (middle row) and three days (bottom row) post-surgery. Pictures were taken in the dorsal column (top panel), the left base of the dorsal column (bottom left panel) and the right base of the dorsal column (bottom right panel). Scale: 20µm. Injections were made on the left side of the dorsal column.*

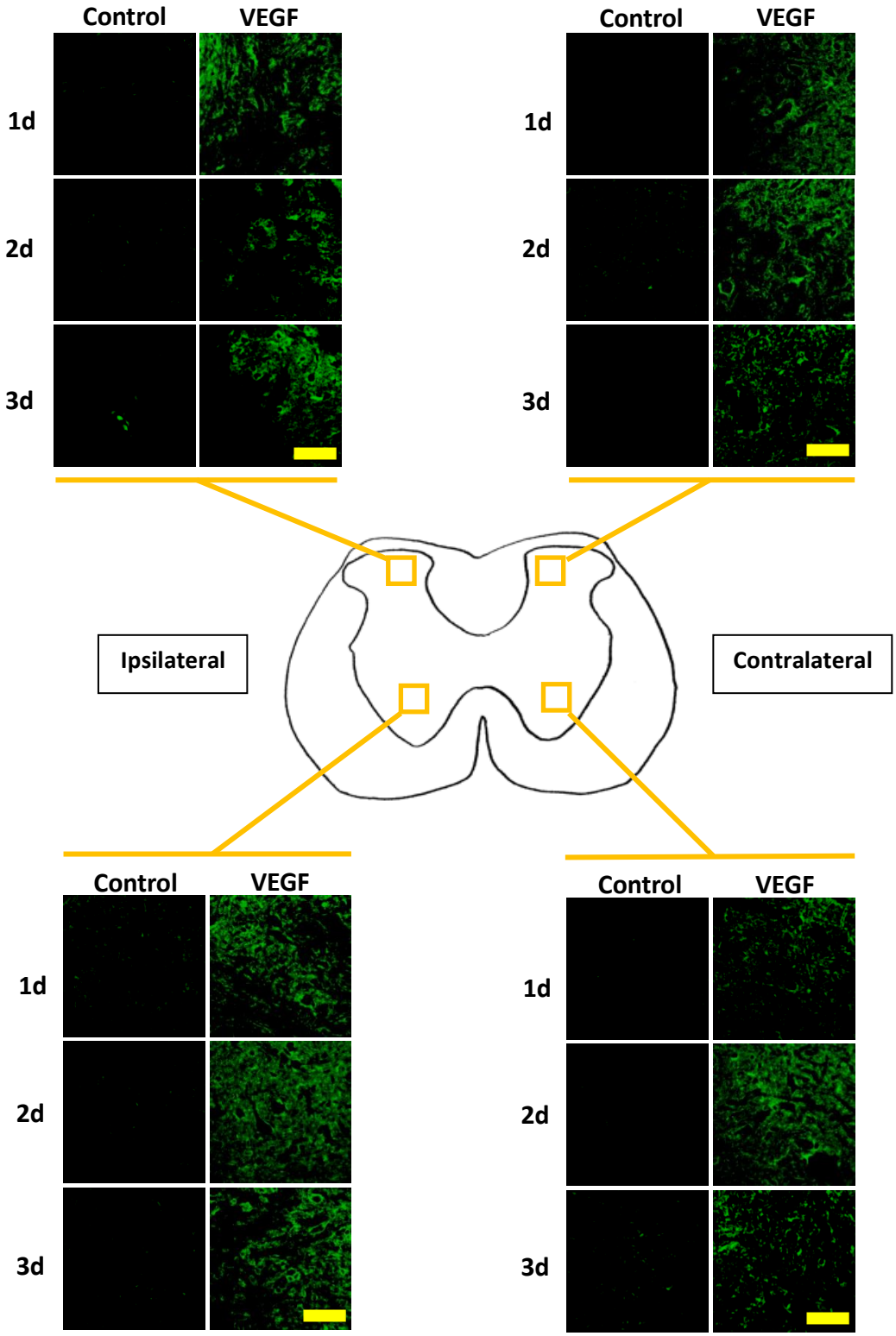

Figure IV.4: *Fibrinogen labelling in spinal cords of animals treated with VEGF (right column) or PBS (left column) at one day (top row), two days (middle row) and three days (bottom row) post-surgery. Pictures were taken in the left dorsal horn (top left panel), the right dorsal horn (top right panel), the left ventral horn (bottom left panel) and the right ventral horn (bottom right panel). Scale: 20µm. Injections were made on the left side of the dorsal column.*

IV.2- Structural changes induced by injection of VEGF

To assess the effect of VEGF on the spinal cord tissue, plastic sections of VEGF-injected spinal cords were analysed. Sections were taken at two days post-surgery (during the peak of deficit of VEGF-treated animals) at the injection site of animals treated with VEGF (n=10) and compared with control tissue (PBS-injected, n=4). Changes in neuron structure, demyelination, degeneration or presence of oedema were investigated in the whole spinal cord with a focus on the dorsal column where the injection was made. In both VEGF- and PBS-treated groups, no oedema could be observed two days following injection (figure IV.5, top and middle row). Also, no degeneration or demyelination was present after injection, indicating that VEGF injection (and PBS) has no obvious effect on the structure of the spinal cord. The motor nuclei of the ventral horn did not show any structural change following injection of VEGF. Motor neurons in tissue injected with VEGF had a similar appearance to the motor neurons of PBS-injected tissue (figure IV.5, bottom row). Moreover, the ratio between in ipsilateral and contralateral grey matter was measured. Results are presented in figure IV.6. For both groups, VEGF-injected (n=10) and control (n=4), the ratio was very close to 1, indicating that no difference between the ipsilateral and contralateral side was present (figure IV.6).

The same study has been performed one month (VEGF: n=6, PBS: n=4) after surgery to assess any long term change due to VEGF. Analysis of plastic sections led to the same conclusion as the two days post-surgery tissue, i.e. that no structural changes were apparent in any part of the spinal cord.

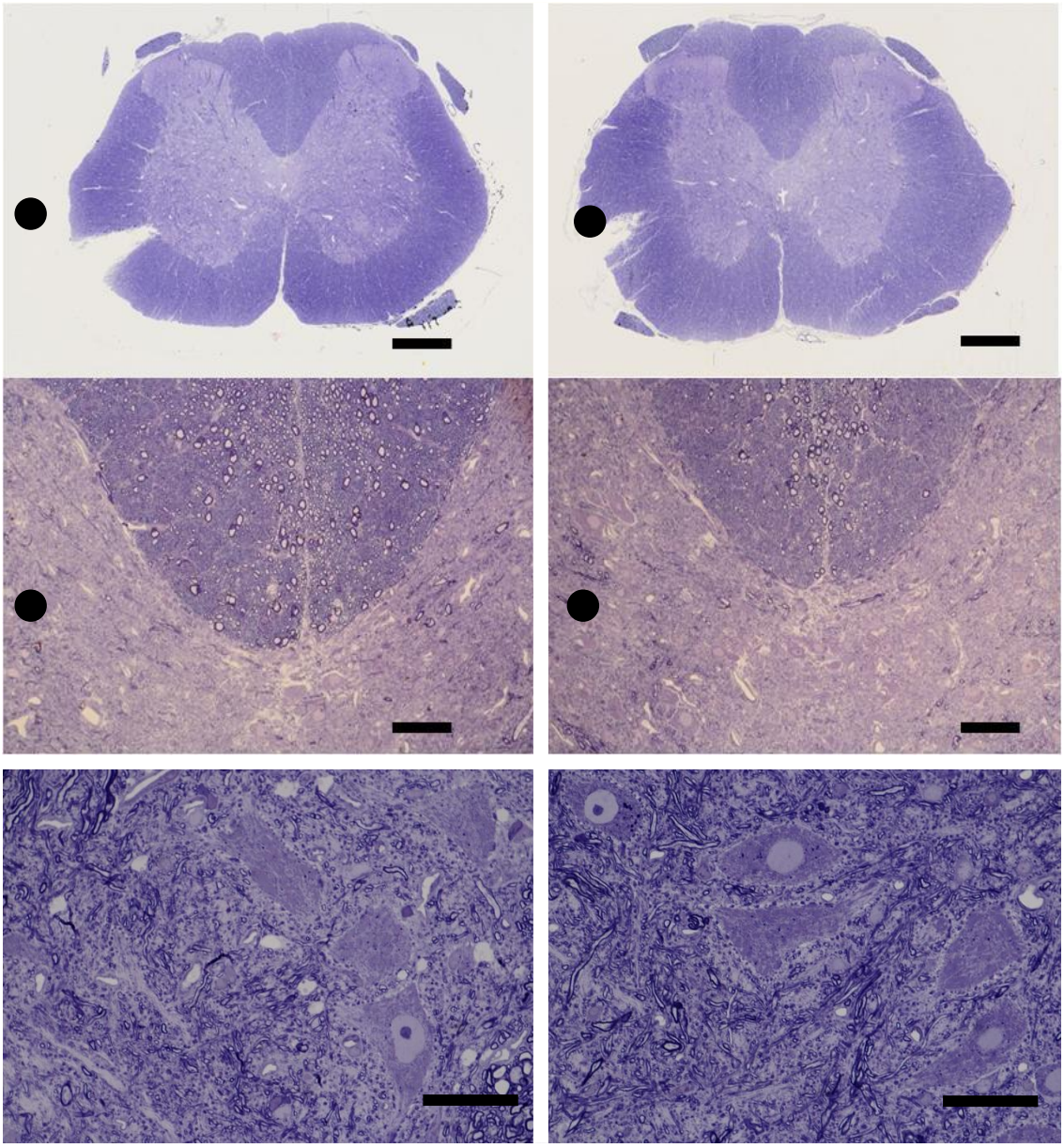

Figure IV.5: *Plastic transverse sections of spinal cords of animals injected with VEGF (right column) or PBS (left column) at 5x (top row, scale: 600µm). Middle row shows the base of the dorsal column (20x, scale: 75µm) and bottom row shows the ipsilateral motor nuclei of the ventral horn (100x, scale: 40µm) two days after surgery. Injections were made on the left side of the dorsal column. The black dot shows the side of injection.*

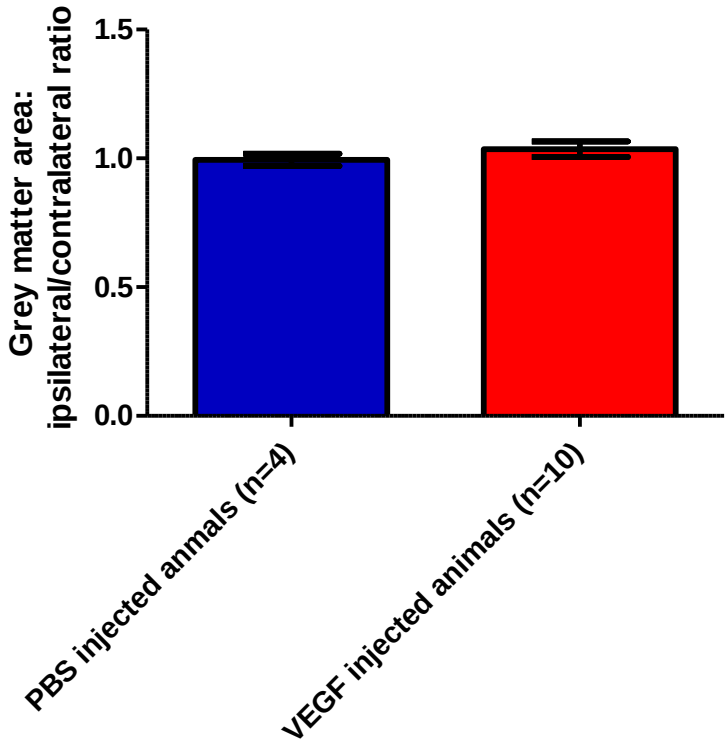

Figure IV.6: *Grey matter area ratio measured two days after surgery between the ipsilateral side of injection and the contralateral side of injection in PBS- (n=4) and VEGF- (n=6) injected animals. Error bars represent the standard error of the mean.*

IV.3- Angiogenic effects of injection of VEGF

Since VEGF is a vascular endothelial growth factor involved in angiogenesis, the effect of VEGF on blood vessels has been assessed by labelling of blood vessel density with the rat endothelial cell antibody (RECA-1). Blood vessels were counted and their shape qualitatively examined in the dorsal column and in the grey matter bordering the dorsal column. Examination of the blood vessel structure and number showed that a single injection of the dose used in this study is not sufficient to induce any change at two days-post surgery in terms of blood vessel number (figure IV.7.B) or shape (figure IV.7.A).

IV.4- Inflammatory response following injection of VEGF

Since the deficit observed in behavioural tests could not be explained by any structural change within the spinal cord following VEGF injection, a metabolic explanation was investigated. Tissue was assessed for signs of an inflammatory response. Spinal cord sections were labelled for ED1, a microglia/macrophage marker, MHC class II and OX-42 (CD11b), microglial markers, to explore this hypothesis.

IV.4.1- ED1 response

Sections were taken at the lesion site at one, two and three days after injection of VEGF, labelled immunohistochemically and compared with control animals. VEGF-injected tissue showed strong ED1 labelling localised principally within the dorsal column but also extending to the nearby grey matter (figure IV.8.A), indicating the presence of activated microglia and/or macrophages. In contrast, control tissue did not show as much ED1 labelling. At any time point, VEGF-injected tissue revealed a significantly stronger ED1 labelling at day one and day two following surgery ($p=0.043$ for both time points).

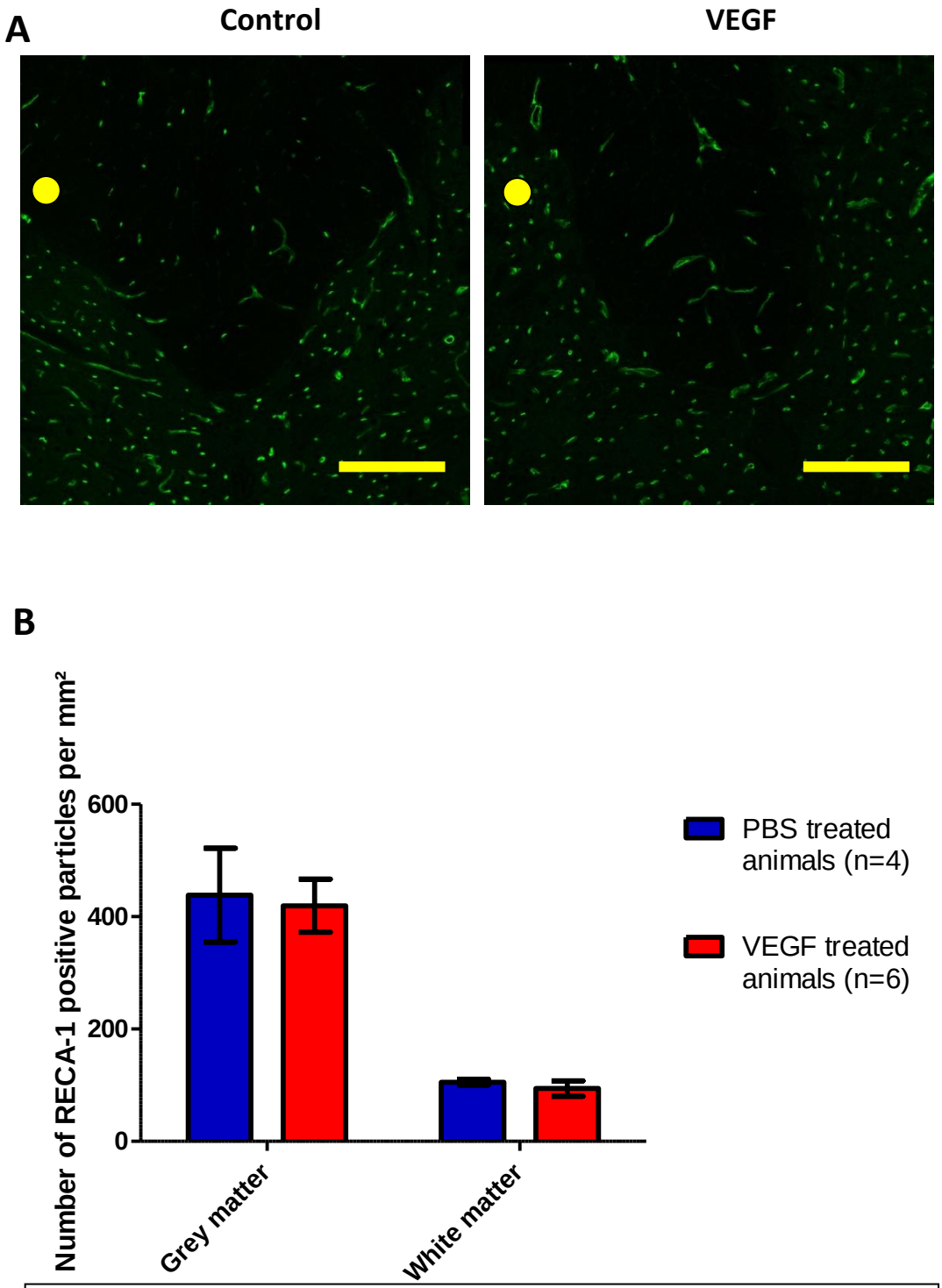

Figure IV.7: ***A.*** *RECA-1 labelling in spinal cords of animals treated with VEGF (right column) or PBS (left column) at 2 days post-surgery showing blood vessels in the base of the dorsal column and its surrounding grey matter. Scale: 150µm. Injections were made on the left side of the dorsal column. The yellow dot shows the side of injection.* ***B.*** *Density of blood vessel in the dorsal column (white matter) and the surrounding grey matter (grey matter) in transverse sections of spinal cord of animals injected with VEGF (n=6) or PBS (n=4). Error bars represent the standard error of the mean.*

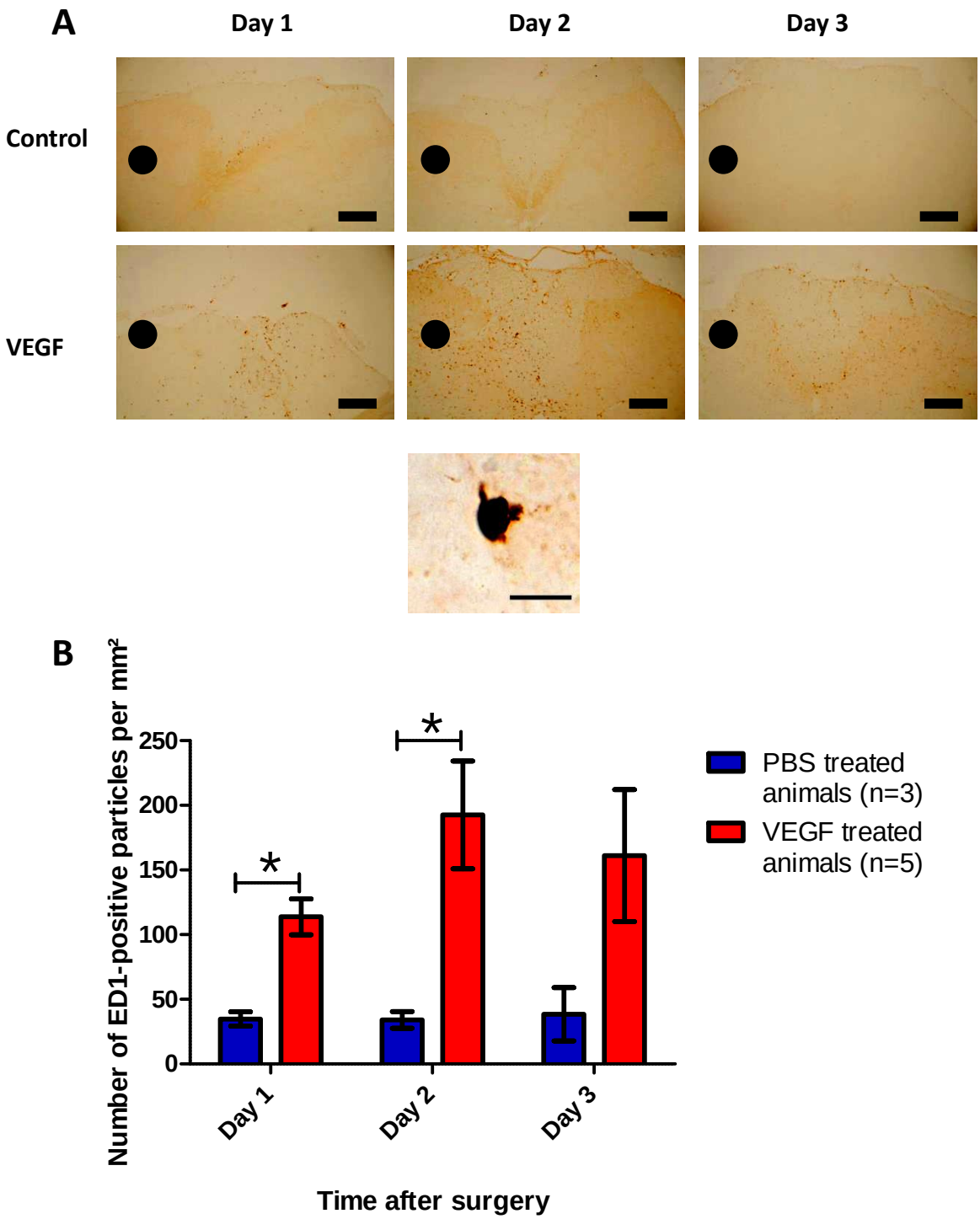

Figure IV.8: ***A.*** *ED1 labelling in spinal cords of animals treated with VEGF (bottom row) or PBS (top row) at one day (left column), two days (medium column) and three days (right column) post-surgery in the dorsal column. Scale: 300µm. Injections were made on the left side of the dorsal column. The black dot shows the side of injection. The bottom pictures shows a single ED1 positive cell, representative of the particles counted during the quantification (Scale: 20 µm)* ***B.*** *Density of ED1-positive cells in transverse sections of spinal cord of animals injected with VEGF (n=5) or PBS (n=3). Statistical analysis was performed with a Mann Whitney U test. (*: p<0.05). Error bars represent the standard error of the mean.*

The same trend was present at day three, although not significant. The highest amount of ED1 labelling was observed two days after VEGF injection and decreased at day three (figure IV.8.B). Moreover the presence of ED1 appeared to be side-specific in VEGF-injected tissue (figure IV.8.*A*), suggesting that macrophages are concentrated ipsilaterally to the injection side.

IV.4.2- MHC-II response

MHC-II-labelling in VEGF-injected tissue showed a broader pattern. Indeed, MHC-II could be found in both white matter (mainly of the dorsal column) and grey matter of the spinal cord: again, control tissue did not show such an intense labelling (figure IV.9.A). Similarly to the labelling pattern with ED1, MHC-II was mainly localised on the same side as the injection (figure IV.9.A) in both the dorsal column and the white matter. Also, the rounded shape of cells labelled (see zoomed-in panels in figure IV.9.A) with MHC-II in VEGF-injected tissue is a hallmark of activated microglia. In contrast, the few cells labelled in control tissue had ramified shape, characteristic of non-activated microglia. Quantification of the MHC-II-positive cells was performed through the whole spinal cord transection, specifically within the dorsal column and within the grey matter. The highest amount of positive cells was found at day two post-surgery (figures IV.9.B, IV.10.A and IV.10.B) in animals treated with VEGF ($p=0.036$ for each area analysed). The same trend, but not statistically significant, was observable at one day and three days following injection (figures IV.9.B, IV.10.A and IV.10.B).

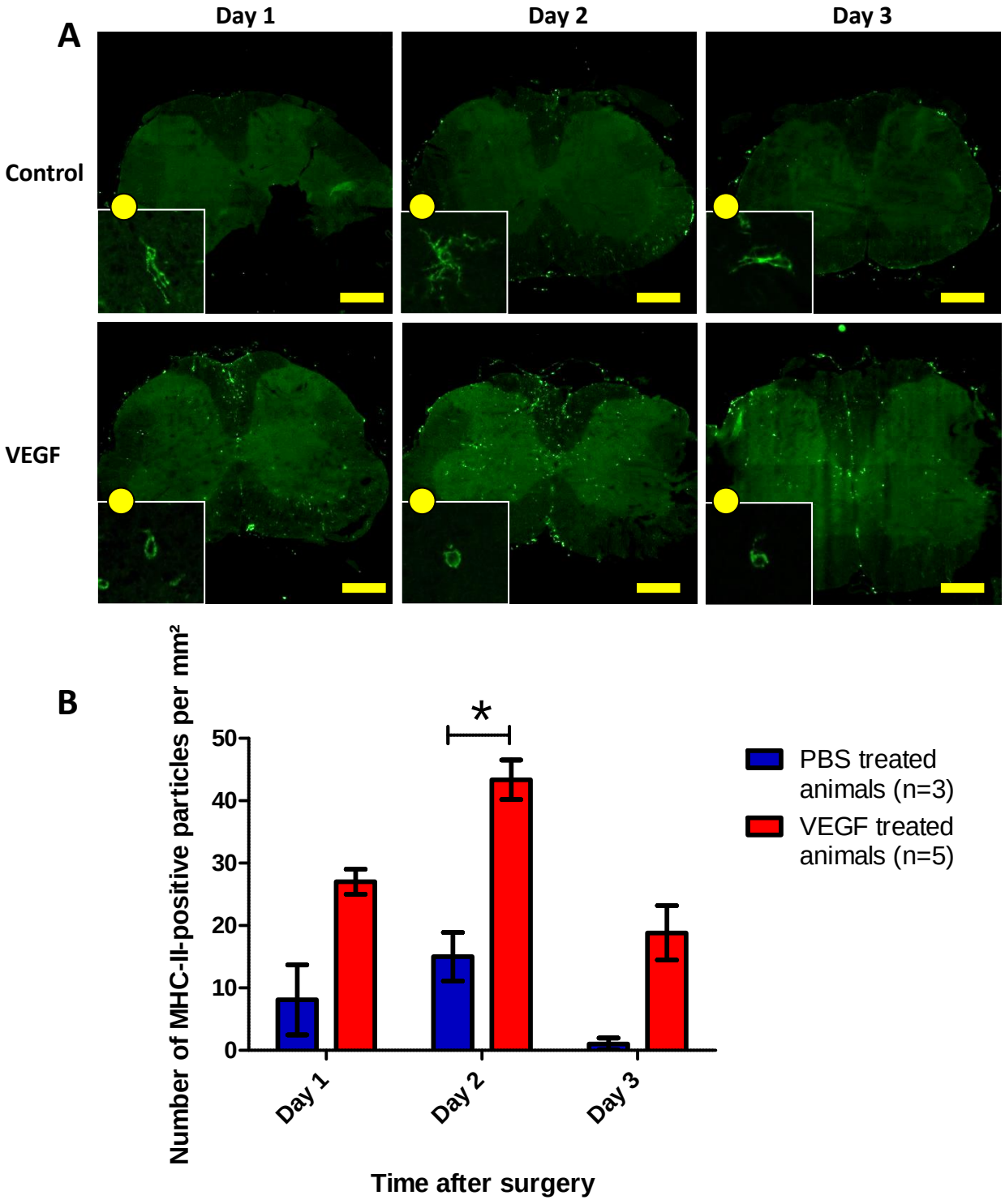

Figure IV.9: ***A.*** *MHC-II labelling in spinal cords of animals treated with VEGF (bottom row) or PBS (top row) at one day (left column), two days (medium column) and three days (right column) post-surgery in the dorsal column. Scale: 200µm. Bottom left panels show a typical MHC-II-positive cell for each section (63x). Injections were made on the left side of the dorsal column. The yellow dot shows the side of injection.* ***B.*** *Density of MHC-II-positive cells in transverse sections of spinal cord of animals injected with VEGF (n=5) or PBS (n=3). Statistical analysis was performed with a Mann Whitney U test. (*: p<0.05). Error bars represent the standard error of the mean.*

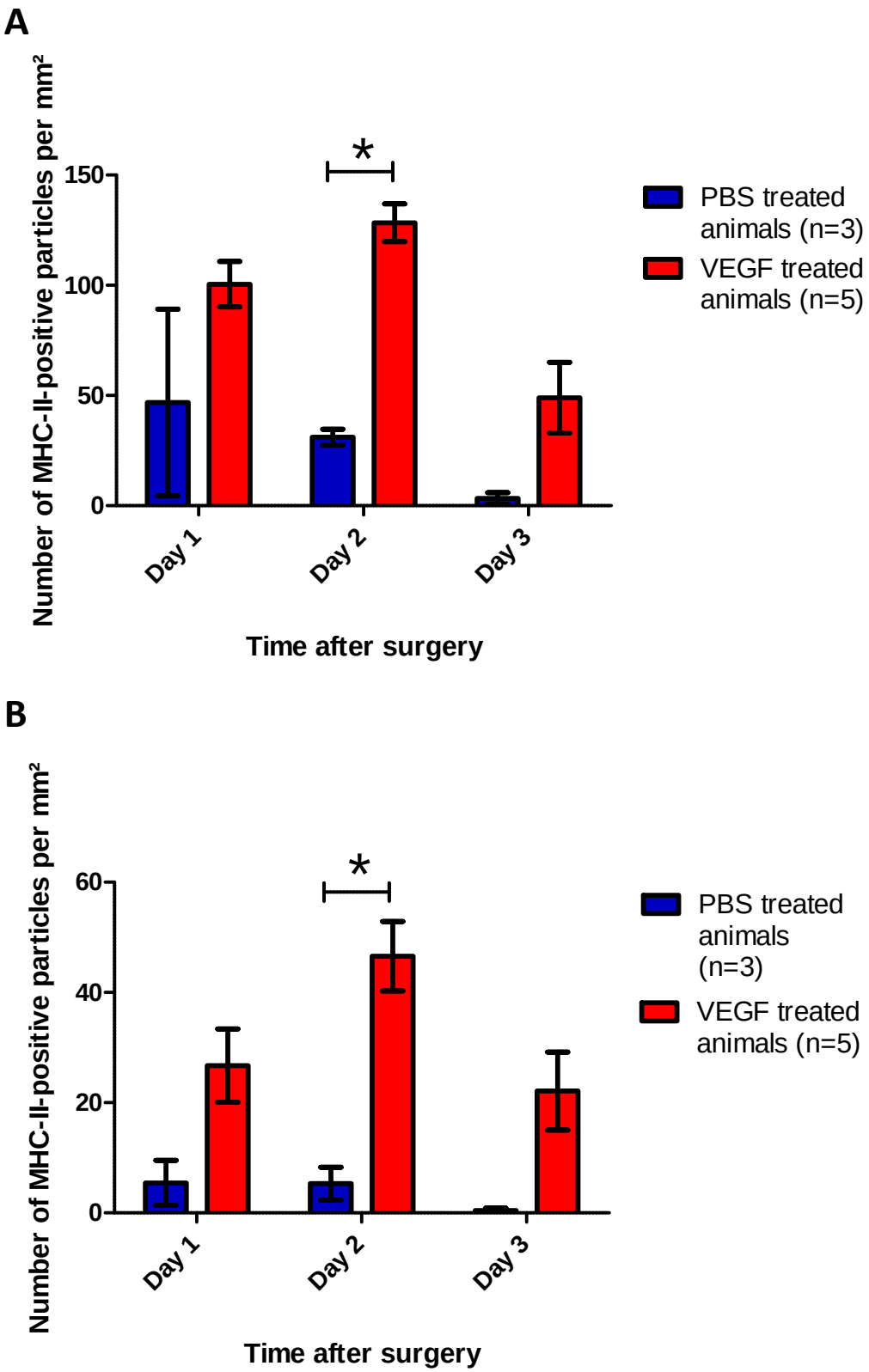

Figure IV.10: ***A.*** *Density of MHC-II-positive cells in the dorsal column of transverse sections of spinal cord of animals injected with VEGF (n=5) or PBS (n=3).* ***B.*** *Density of MHC-II-positive cells in the grey matter of transverse sections of spinal cord of animals injected with VEGF (n=5) or PBS (n=3). Statistical analysis was performed with a Mann Whitney U test. (*: p<0.05). Error bars represent the standard error of the mean.*

IV.4.3- Ox-42 response

Finally, Ox-42, a microglial receptor able to mediate activation by fibrinogen (Angelov et al., 2009) was found sparsely in the grey matter of VEGF-injected animals but not in the control group (figure IV.11) at day two post-surgery, in line with both the presence of inflammatory markers and fibrinogen in VEGF-treated tissue. These strongly Ox-42 labelled cells had a round shape (a hallmark of reactive microglia (Hickey and Kimura, 1988)) compared with the ramified cells present in control groups suggesting activation of microglia in VEGF-treated tissue (contrasting with the ramified inactive microglia (Hickey and Kimura, 1988)).

IV.4.4- T-cell infiltration

The effect of VEGF injection on T-cell infiltration was investigated two days post-surgery by CD3 labelling, a T-cell receptor, in tissue injected with VEGF or PBS. The labelling showed an absence of CD3 labelling in both the VEGF and control groups (figure IV.12) in the dorsal column and the grey matter, suggesting that T-cell infiltration does not occur at this stage.

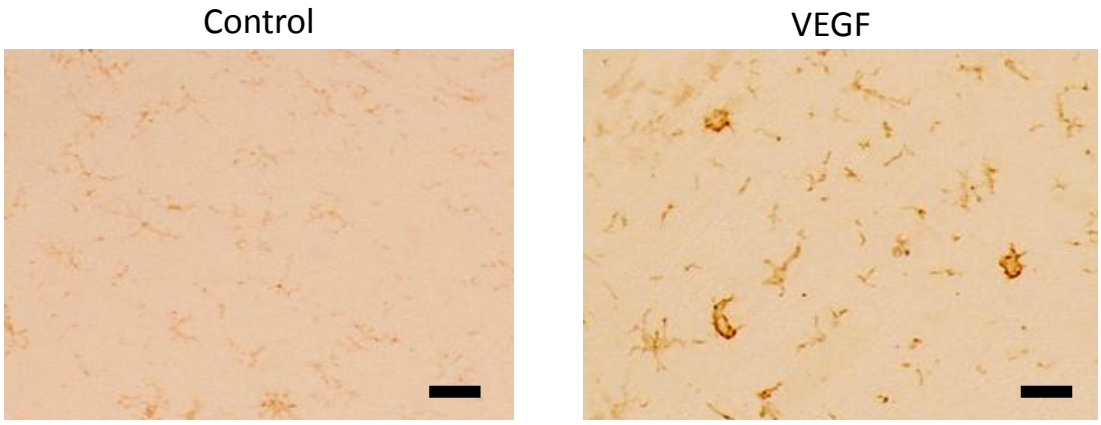

Figure IV.11: OX42 *labelling in spinal cords of animals treated with VEGF (right) or PBS (left) at two days post-surgery the ipsilateral grey matter. Scale: 20µm.*

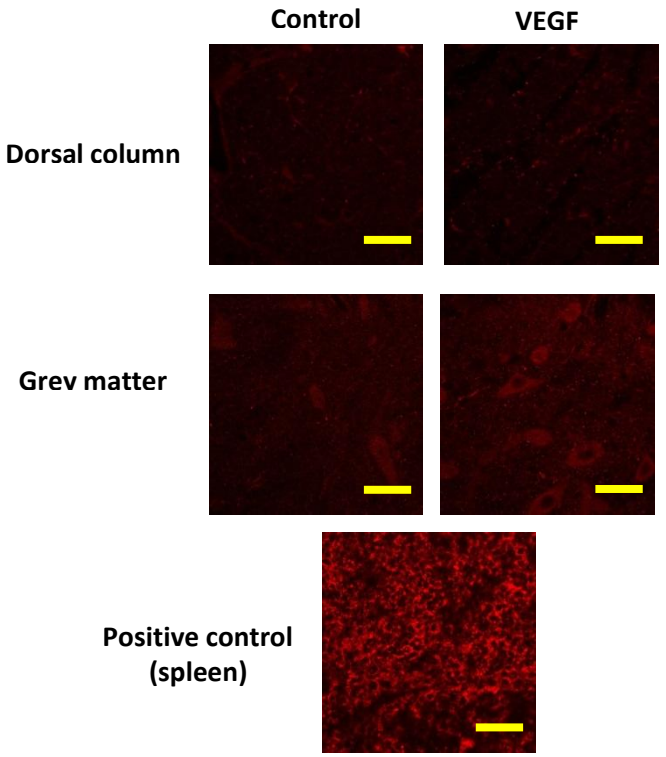

Figure IV.12: CD3 *labelling in the ipsilateral grey matter of spinal cords of animals treated with VEGF (right) or PBS (left) at two days post-surgery. Spleen tissue was used as a positive control. Scale: 20µm.*

IV.5- Long term effect of injection of VEGF

To assess whether injection of VEGF has any long term effect at the immunohistochemical level, we examined the spinal cord of animals one year after injecting VEGF or PBS. One year following surgery, there was no sign of IgG in the animals injected with VEGF or PBS (figure IV.13.A).

Structural changes were assessed by looking at sections stained with H&E. No major change was observable when comparing sections of animals injected with VEGF or PBS. Specifically, no alteration was present in the motor nuclei of the ventral horn (figure IV.14). Moreover, the ratio between the ipsilateral and contralateral grey matter area was measured. Results are presented in figure IV.15. For both groups, VEGF-injected (n=6) and control (n=3), the ratio was very close to 1, indicating that no difference between the ipsilateral and contralateral side was present.

Figure IV.13.B shows ED1 labelling in transverse sections of spinal cord for both the VEGF- and PBS- injected groups. Both pictures show the absence of ED1 in those sections, revealing the absence of activated microglia or macrophages in the tissue. Interestingly, one animal injected with VEGF presented some ED1 positive cells in the dorsal column. The tissue of this animal was thus investigated further, transections were taken along the cord to reach the caudal end (4600 µm away from the entry zone of the sciatic nerve root) and 2200 µm more rostral from the entry zone) and labelled for ED1. As shown in figure IV.16, the ED1 positive cells are spread in the dorsal column in the caudal part of the cord and get more and more centred around the midline of the dorsal column as the sections are more rostral.

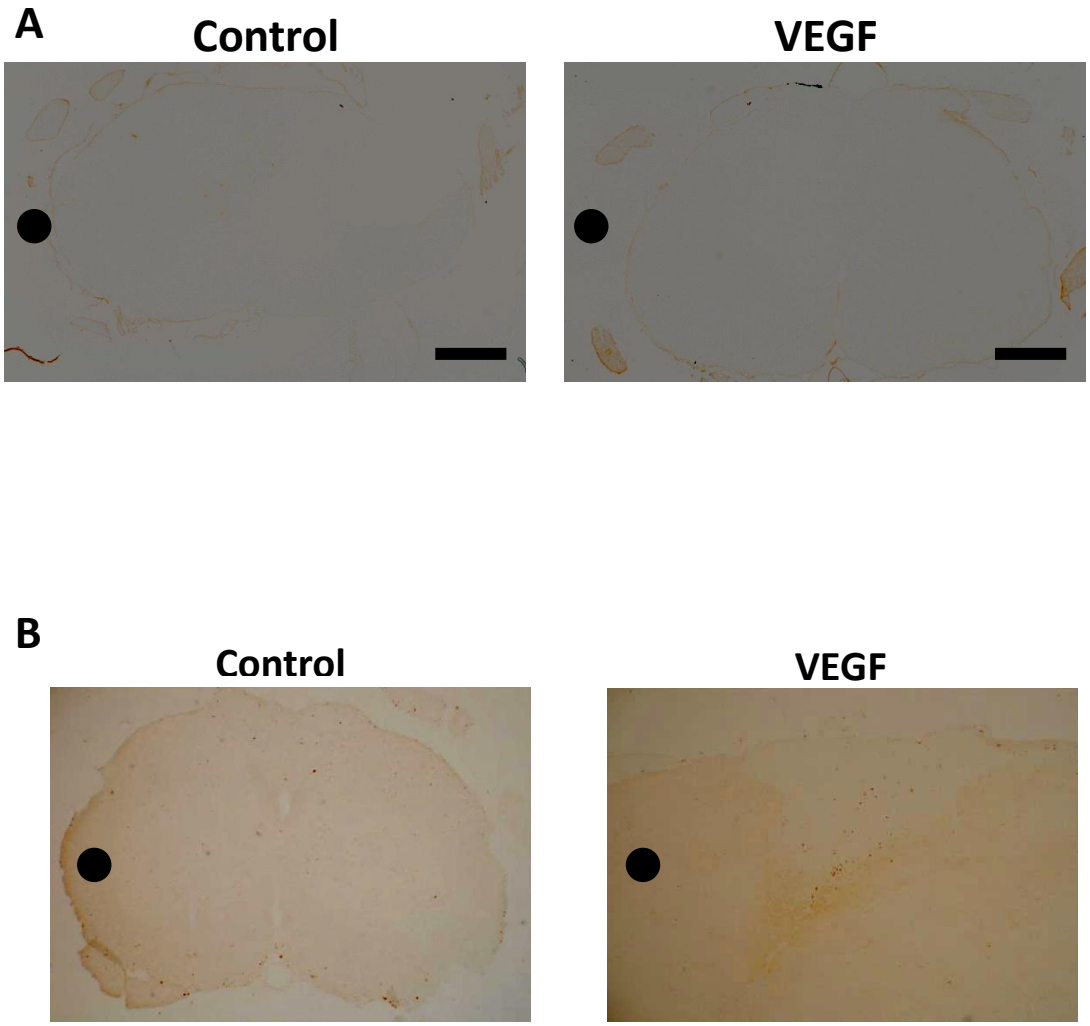

Figure IV.13: ***A.*** *IgG labelling in spinal cords of animals treated with VEGF (right) or PBS (left) 1 year post-surgery. Scale: 600µm. Injections were made on the left side of the dorsal column.* ***B.*** *ED1 labelling in spinal cords of animals treated with VEGF (right) or PBS (left) one year post-surgery. Scale: 600µm. Injections were made on the left side of the dorsal column. The black dot shows the side of injection.*

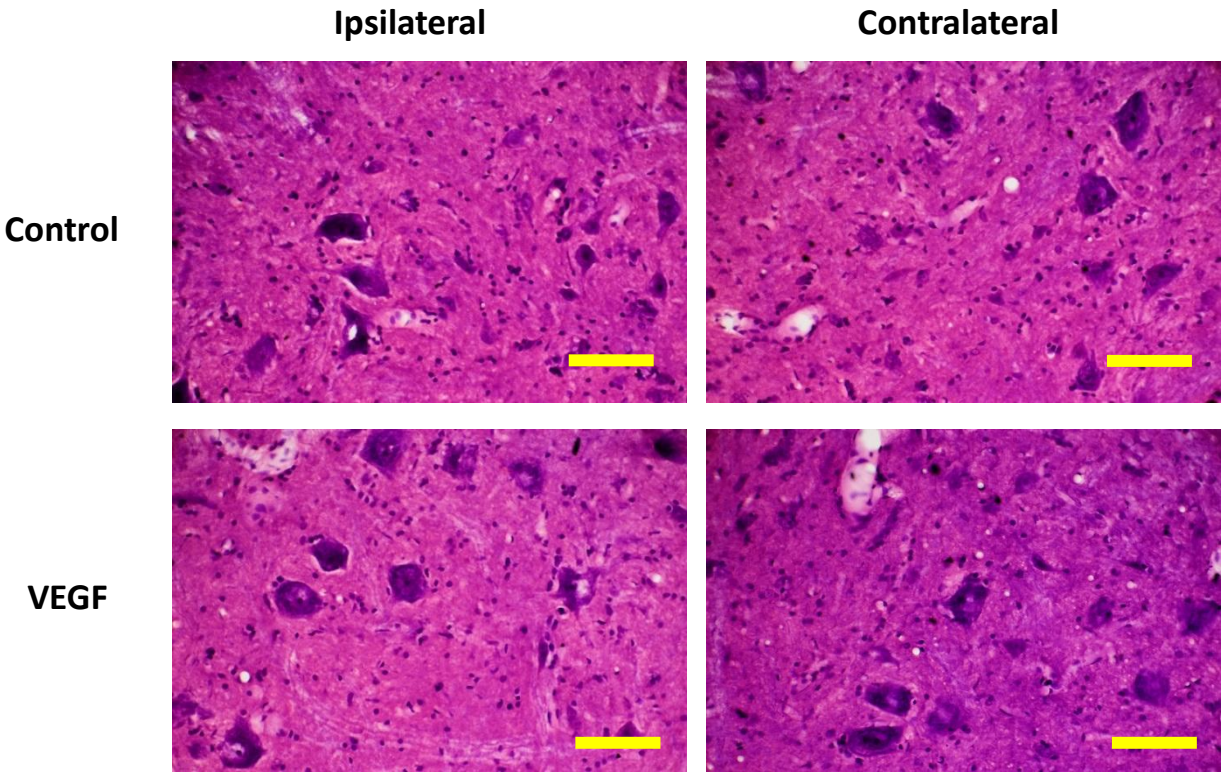

Figure IV.14: *Motor nuclei of spinal cords stained with H&E in the ipsilateral (left) and contralateral (right) ventral horn one year post-surgery. Top row shows tissue treated with PBS. Bottom row corresponds to VEGF-injected tissue. Scale: 20µm.*

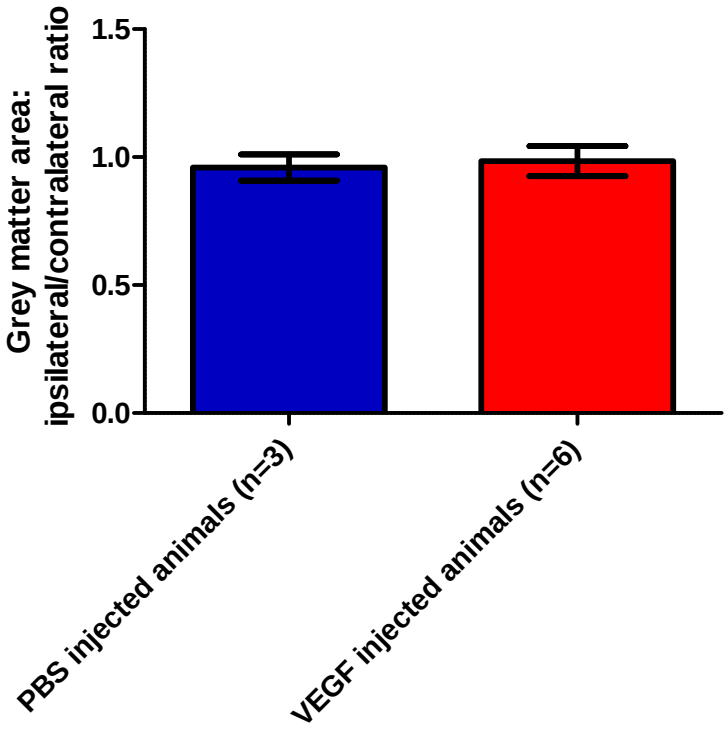

Figure IV.15: *Grey matter area ratio measured one year after surgery between the ipsilateral side of injection and the contralateral side of injection in PBS- and VEGF-injected animals. Error bars represent the standard error of the mean.*

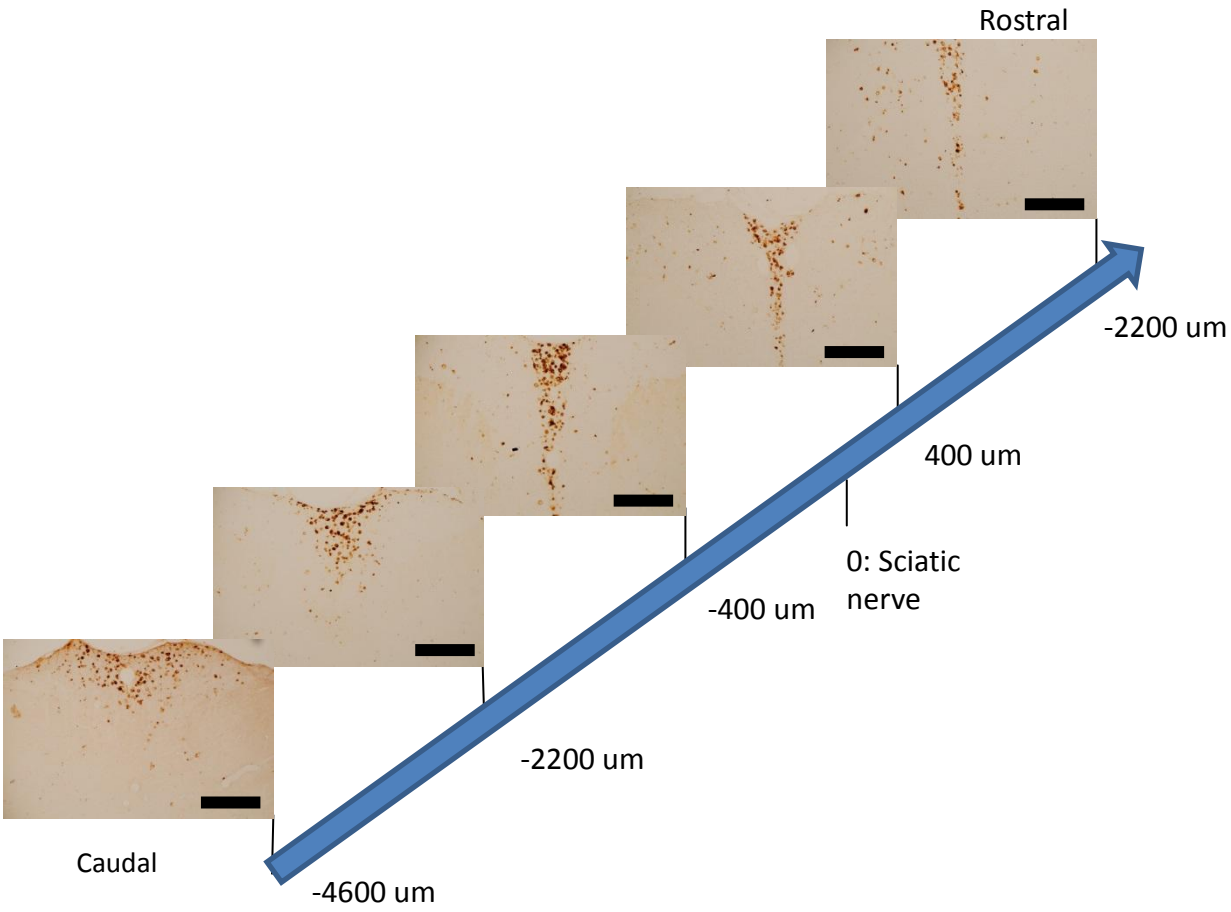

Figure IV.16: ***A.*** *ED1 labelling in spinal cords of an animal treated with VEGF 1 year post-surgery. Scale: 300µm. Injections were made on the left side of the dorsal column.*

Chapter V: Results - Mechanism investigation

V.1- Discrimination between a direct effect of VEGF and a role of the blood-brain barrier breakdown

V.1.1- Motor deficit

The results shown so far suggest that an intraspinal injection of VEGF can cause a deficit of the motor function of hind limbs correlated with immunohistochemical changes indicating inflammation associated with the injection site within the CNS. However, the origin of the neurological deficit is not clear. To try to determine the mechanisms underlying the deficit we investigated a number of potential causes, and, particularly, we aimed to determine whether the loss of function may be a direct action of the injected VEGF on neurons, or other CNS cells, or whether the loss may be due to the blood-brain barrier breakdown following the injection. To do so, we used a selective eNOS inhibitor, cavtratin, to block the blood-brain barrier breakdown induced by VEGF, while leaving other signalling pathways of VEGF intact. An absence of deficit following treatment with cavtratin would thus suggest that the locomotor alterations were due to the leakage of vascular constituents into the spinal cord. A preliminary study was performed only with a small number of animals injected with VEGF in order to assess the potential efficacy of this approach. As shown in figure V.1.A, no difference in the hind limb score on the horizontal test was observed following injection of VEGF and treatment with either cavtratin (n=4) or its scrambled peptide control (n=5), both groups showed a deficit compared to baseline.

V.1.2- Blood-brain barrier breakdown

In view of the failure of cavtratin to prevent the loss of function, we assessed whether it had been effective in preventing the breakdown of the blood-brain barrier as planned. To make this assessment the lesioned tissue was tested immunohistochemically for the parenchymal presence of IgG. As represented in figure V.1.B, IgG leakage occurred in both cavtratin and control peptide-treated tissue, revealing that cavtratin did not block the breakdown of the blood-brain barrier. Given the fact that the highest dose of cavtratin found in the literature was used, and the fact that it did not appear to be effective in protecting against blood-brain barrier breakdown, and given the high purchase price for cavtratin, the negative results led to the discontinuation of this part of the study.

V.2- Investigation of a role of hypoxia

V.2.1- Pimonidazole labelling

We investigated a possible role of hypoxia in the motor dysfunction following the breakdown of the blood-brain barrier in animals injected with VEGF. We assessed the potential hypoxic state of the tissue by labelling spinal cord cross sections of pimonidazole-treated animals for bound pimonidazole, a marker of hypoxic cells, at one, two and three days following surgery. As shown in figure V.2.A, a difference in pimonidazole in the grey matter was observable between tissue injected with VEGF and tissue injected with PBS at day one and two, but no labelling was present three days after injection. Control tissue did not show any labelling (figure V.2.A). This was confirmed by quantification of pimonidazole labelling intensity in the ipsilateral ventral horn (figure V.2.B). A significant difference in intensity was present at day one ($p=0.031$) and day two ($p=0.026$) after surgery. It is worth noting

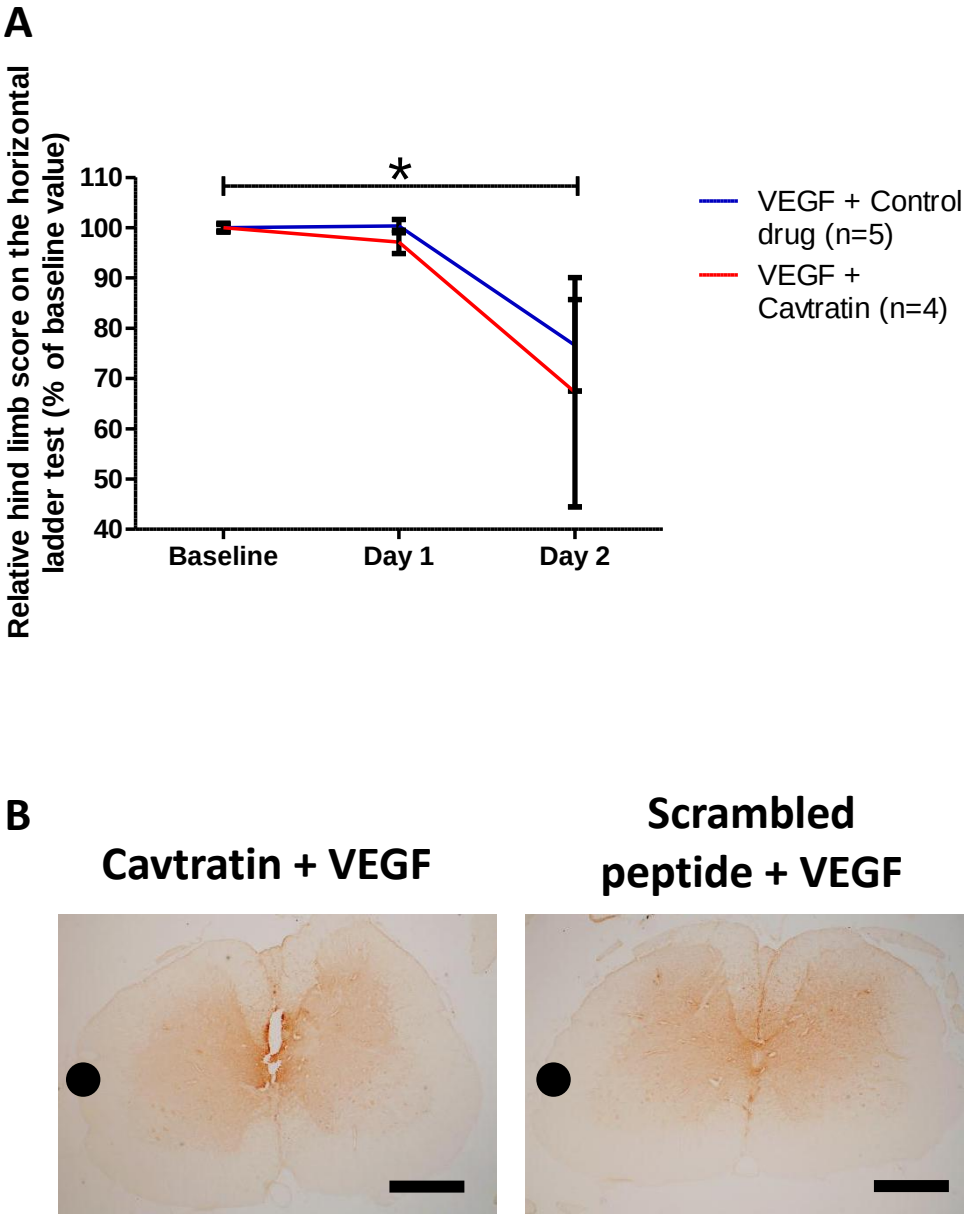

Figure V.1: ***A.*** *Relative hind limb score on the horizontal ladder test of animals injected with VEGF and treated with Cavtratin (n=4) or a scrambled peptide (n=5). Day 0 corresponds to the date of surgery. Statistical analysis was performed with a Wilcoxon test. (*: p<0.05)* ***B.*** *IgG labelling two days following surgery in spinal cords of animals treated with VEGF and cavtratin (left) or a scrambled peptide (right). Scale: 600µm. Injections were made on the left side of the dorsal column. The black dot shows the side of injection.*

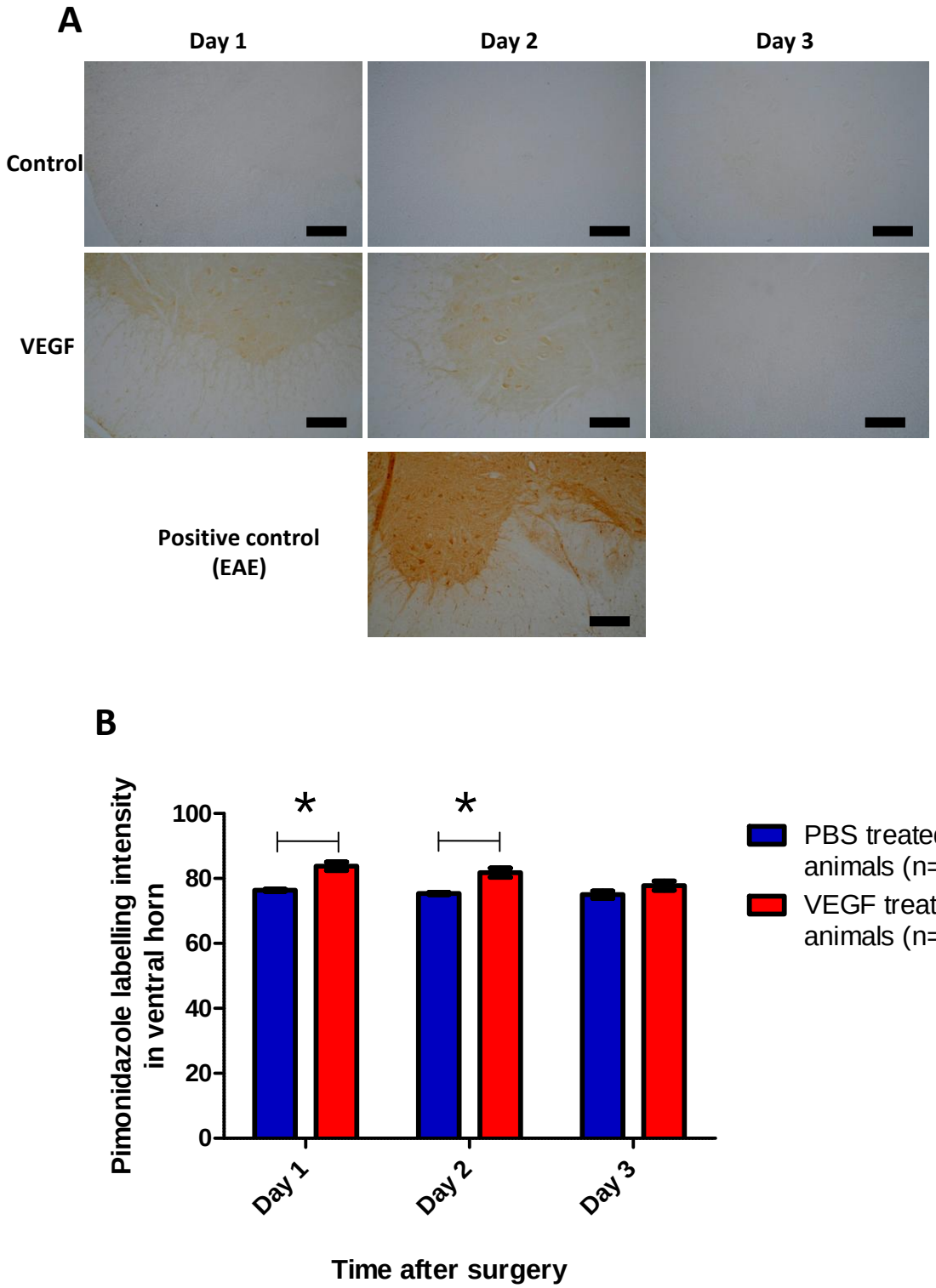

Figure V.2: ***A.*** *Pimonidazole labelling in spinal cords of animals treated with VEGF (middle row) or PBS (top row) at one day (left column), two days (middle column) and three days (right column) post-surgery. For comparison, positive control (EAE) is displayed below. Scale: 150µm. Injections were made on the left side of the dorsal column.* ***B.*** *Intensity of pimonidazole labelling in the ventral horn of animals injected with PBS (n=3 per time point) or VEGF (n=5 per time point). Range: 0 (white) – 255 (black). Statistical analysis was performed with a Mann Whitney U test. (*: p<0.05). Error bars represent the standard error of the mean.*

that the labelling observed in VEGF-injected tissue is weaker than the labelling observed in the positive control tissue (spinal cord of an animal suffering from EAE) (figure V.2). The pimonidazole labelling observed in the grey matter of VEGF-injected tissue suggests that hypoxia is present in the grey matter in the first two days after injection of VEGF.

V.2.2- Oxygen treatment

We investigated further the hypothesis that hypoxia could be the cause for the motor deficit by attempting to reverse this deficit with an oxygen treatment. At day two following surgery, animals were tested on the horizontal ladder test prior to either room air or 100% oxygen treatment for 1h and tested once again to assess the effect of the treatment on their motor function. As shown in figure V.3.A, there is some variation regarding the effect of the treatment in different animals. 100% oxygen treatment led to an improvement of the motor function in some animals undergoing a deficit at day two following surgery. Unexpectedly, the same observation was true for some animals treated with room air suggesting that the repetition of the task (i.e. walking on the horizontal ladder) helped to improve the score the second time. On the other hand, some animals did not show any improvement following oxygen treatment as their score on the ladder did not improve. Again, the same outcome was true for animals left in room air between the two testing sessions. The average score within each group (room air treatment, n=5 and oxygen treatment, n=5) are shown in figure V.3.B. In both groups, the treatment led to an improvement of the motor function on the horizontal ladder test. The deficit observed in the group of animals treated with oxygen was stronger than for the animals treated with room air. This is due to chance since the protocol did not differ between the groups before the onset of deficit. An objective measure eliminating this bias is the percentage of deficit recovered after treatment (i.e. the fraction of improvement after treatment over the

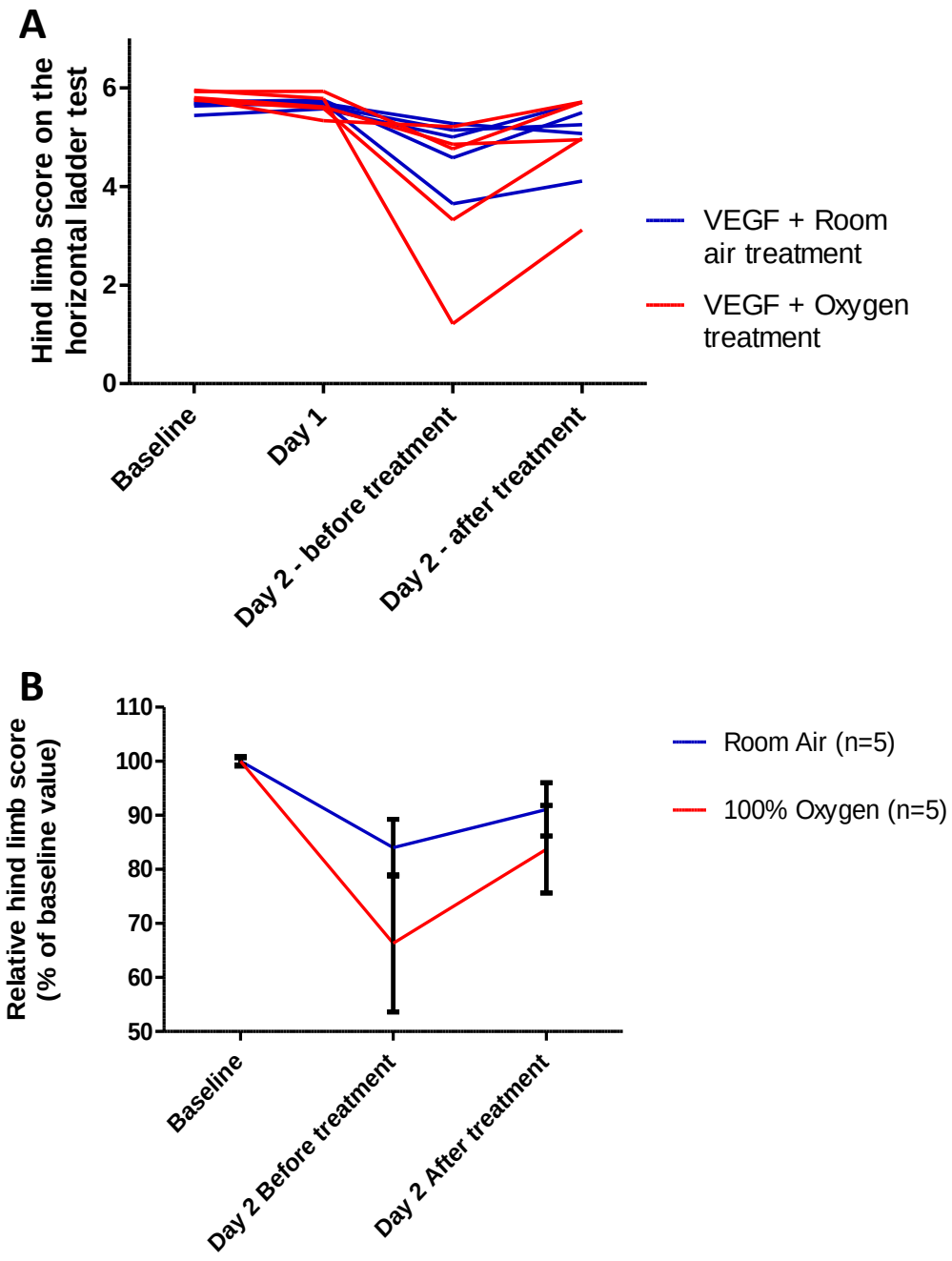

Figure V.3: ***A.*** *Relative hind limb score on the horizontal ladder test of individual animals injected with VEGF and treated with room air (n=5) or oxygen (n=5). Day 0 corresponds to the date of surgery.* ***B.*** *Mean relative hind limb score on the horizontal ladder test of animals injected with VEGF and treated with room air (n=5) or oxygen (n=5). Day 0 corresponds to the date of surgery. Error bars represent the standard error of the mean.*

amplitude of the deficit before treatment). Oxygen treatment led to an average recovery of 57+/-14% of the deficit and the room air treatment led to a recovery of 46+/-35% of the deficit. The data gathered in figure V.3 are thus inconclusive regarding the positive effect of oxygen on the motor deficit induced by VEGF but rather show that repetition of testing within a short period of time (here 1h) leads to an improvement of the ladder test score.

V.2.3- HIF-1α labelling

The pimonidazole labelling of VEGF-injected tissue was rather faint compared to the corresponding positive control. Combined with the failure to observe a clear effect of oxygen on the motor deficit induced by VEGF, this observation poses the question of whether the tissue injected with VEGF is really hypoxic two days following surgery. We explored further our hypothesis by labelling spinal cord cross-sections for HIF-1α, another hypoxia marker. As shown in figure V.4, a stronger labelling was present in VEGF-injected tissue than in control (saline-injected). This observation was confirmed in most of the sections observed. Indeed, HIF-1α-positive tissue was present in the dorsal column, the dorsal horns and the ventral horns of animals injected with VEGF. However, some of the VEGF-injected animals did not show stronger labelling than controls, even though these animals showed a deficit on the horizontal ladder test. Unfortunately, the data obtained from HIF-1α-labelled section is not conclusive regarding the hypothesis that hypoxia is present in lesions induced by VEGF.

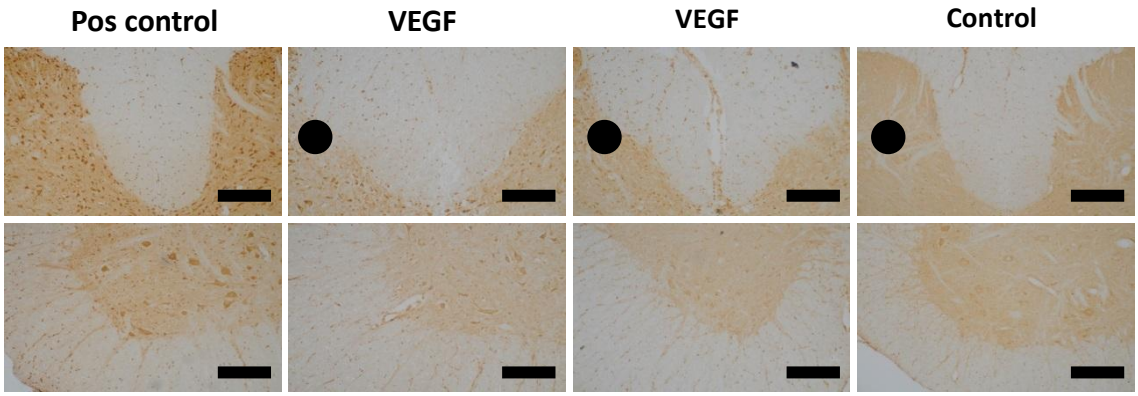

Figure V.4: *HIF-1α labelling 2 days following surgery in spinal cords of animals treated with VEGF (middle) or PBS (right). Pictures were taken in the dorsal column (top) and the ipsilateral ventral horn (bottom). Positive control (EAE tissue, left) is shown for comparison. Scale: 150µm. Injections were made on the left side of the dorsal column. The black dot shows the side of injection.*

V.3- Is nitric oxide involved in the observed motor deficit?

We assessed iNOS expression in the spinal cords of rats treated with VEGF by labelling it immunohistochemically one, two and three days-post surgery. Similar results were found for both VEGF-injected and control groups: there was no expression of iNOS at any time point in any cell type of the spinal cord while the animals were exhibiting a motor deficit (figure V.5.A).

To explore whether NO was nevertheless produced, which might then trigger a cascade of events, we labelled the tissue for nitrotyrosine, a product of tyrosine nitration mediated by reactive nitrogen species which permanently labels proteins, allowing for the detection of a "footprint" of NO formation at two days following surgery. No labelling could be observed in either of the groups (VEGF-treated and controls), confirming that NO is not involved in the motor deficit initiated by the injection of VEGF (figure V.5.B).

V.4- Neuron excitability

V.4.1 - EMG

Observation of the general behaviour of animals during the different studies performed led to the interesting finding that at one day after VEGF injection, the hind limbs of some animals had tremor. It was a high frequency tremor that did not seem to affect their ability to perform on the different behavioural and motor tests described in Chapter 3. Following this observation, we investigated the excitability of neurons in the spinal cord at the site of injection. EMG recordings were performed on animals injected with PBS (n=6) or VEGF (n=7) at one day, two days and three days following surgery. Representative recordings are

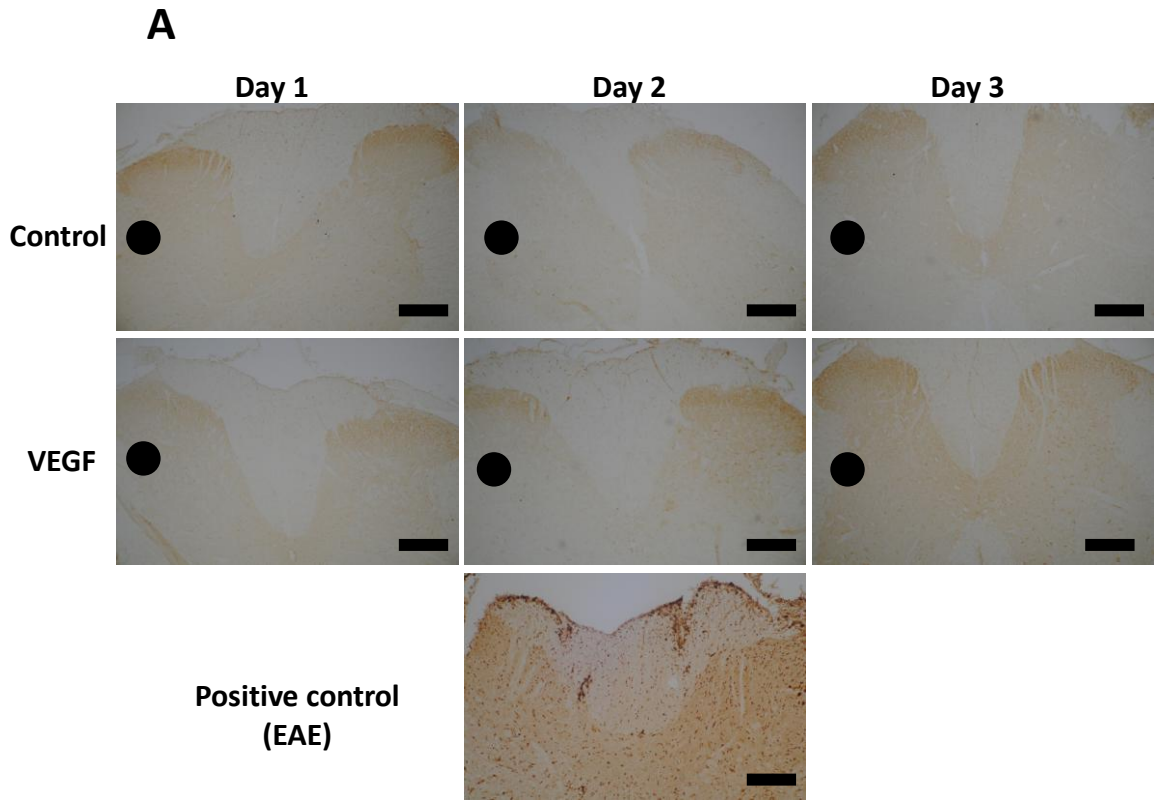

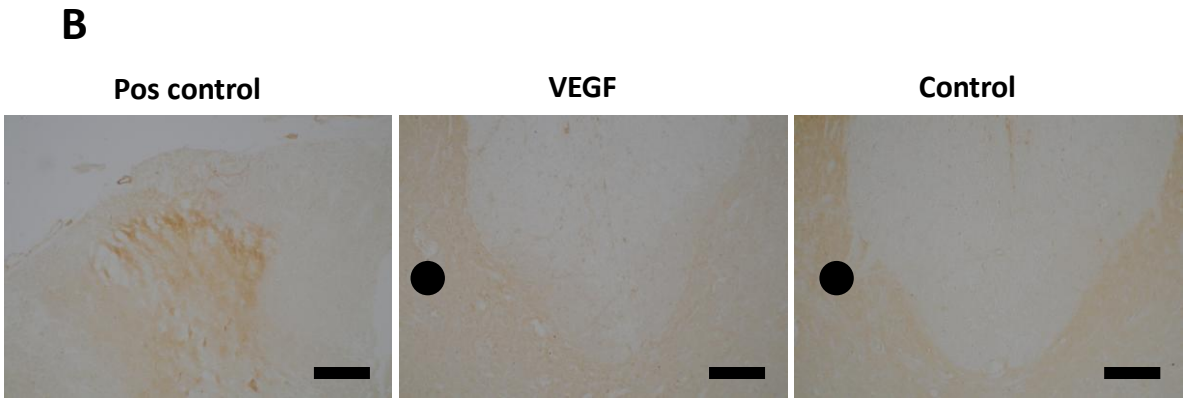

Figure V.5: ***A.*** *iNOS labelling in spinal cords of animals treated with VEGF (bottom row) or PBS (top row) at one day (left column), two days (middle column) and three days (right column) post-surgery. For comparison, positive control (EAE) is displayed below. Pictures of the dorsal column were taken. Scale: 150µm. Injections were made on the left side of the dorsal column.* ***B.*** *Nitrotyrosin labelling two days following surgery in spinal cords of animals treated with VEGF (middle) or PBS (right). Positive control (EAE tissue, left) is shown for comparison. Pictures of the dorsal column were taken. Scale: 150µm. Injections were made on the left side of the dorsal column. The black dot shows the side of injection.*

shown in figure V.6. The results of this study reveal that in animals treated with VEGF, an increase in H/M ratio (left: p=0.043, right: p=0.043) and F/M ratio (left: p=0.043, right: p=0.018) is present at day one following surgery but not in control animals (figures V.7 and V.8). This increase was more marked on the ipsilateral side of injection than on the contralateral side. At day two post-surgery, the H/M and F/M ratio returned to baseline level for the VEGF animals and remained similar to the baseline level of control animals. At three days, in animals injected with VEGF, a non-significant trend towards a decrease (compared to baseline level was present). This was not the case in control animals. We then investigated which components of both H/M and F/M ratio were responsible for the variations observed in animals treated with VEGF. Figures V.9, V.10and V.11 show the individual H reflex, F response and M response respectively of each animals involved in the study. The M response did not show any consistent pattern of change for most of the animals but both the H reflex and F response followed the same pattern as the H/M ratio and F/M ratio respectively, leading to the conclusion that both H reflex and F response are affected by the injection of VEGF.

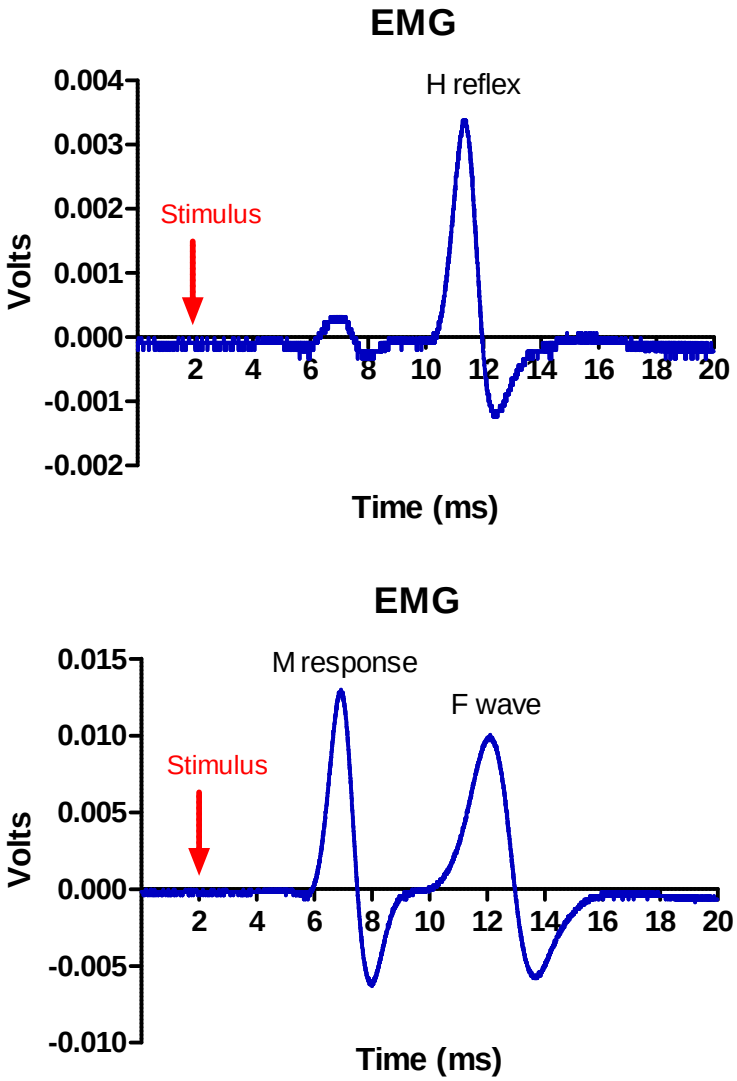

Figure V.6: *Representative recordings of an H reflex (top) and an f-wave obtained at the maximal M response (bottom). Stimulus was sent at a 2 ms latency after the beginning of the recording.*

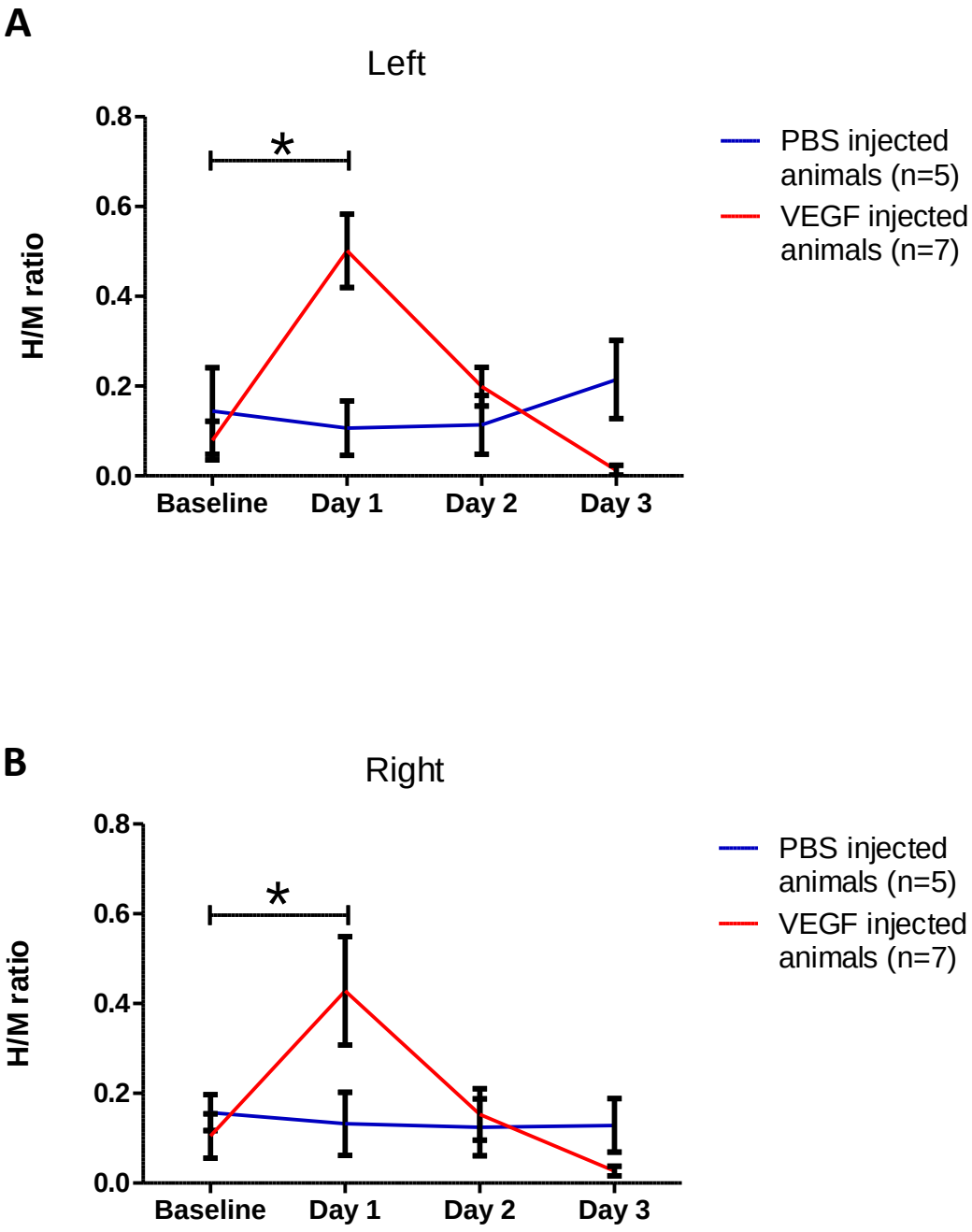

Figure V.7: *H/M ratio recorded in the left (top) and right (bottom) foot muscle in animals injected with PBS (n=5) or VEGF (n=7). Day 0 corresponds to the date of surgery. Statistical analysis was performed with a Wilcoxon test. (*: p<0.05) Error bars represent the standard error of the mean.*

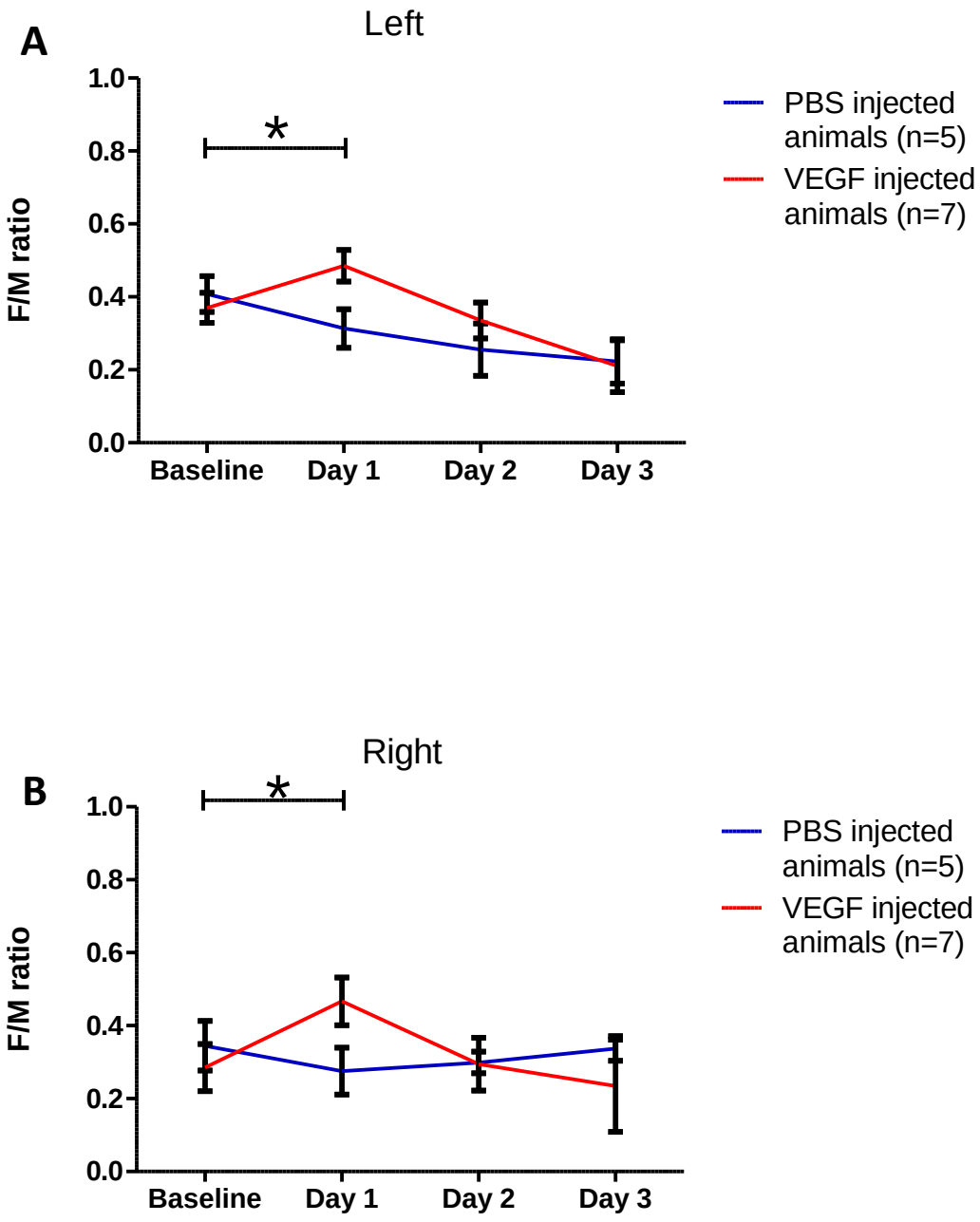

Figure V.8: *F/M ratio recorded in the left (top) and right (bottom) foot muscle in animals injected with PBS (n=5) or VEGF (n=7). Day 0 corresponds to the date of surgery. Statistical analysis was performed with a Wilcoxon test. (*: p<0.05) Error bars represent the standard error of the mean.*

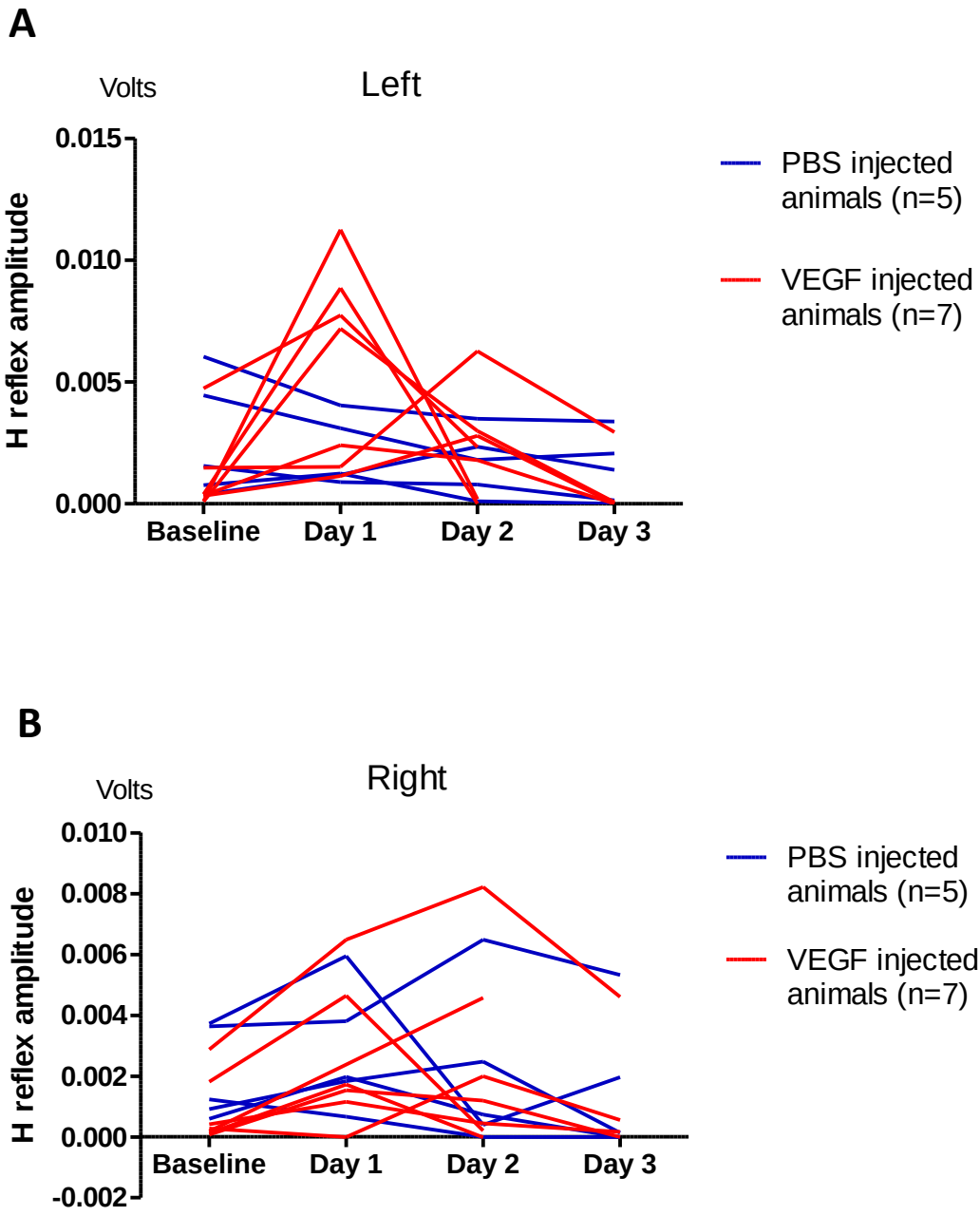

Figure V.9: *H reflex amplitude recorded in the left (top) and right (bottom) foot muscle of individual animals injected with PBS (n=5) or VEGF (n=7). Day 0 corresponds to the date of surgery.*

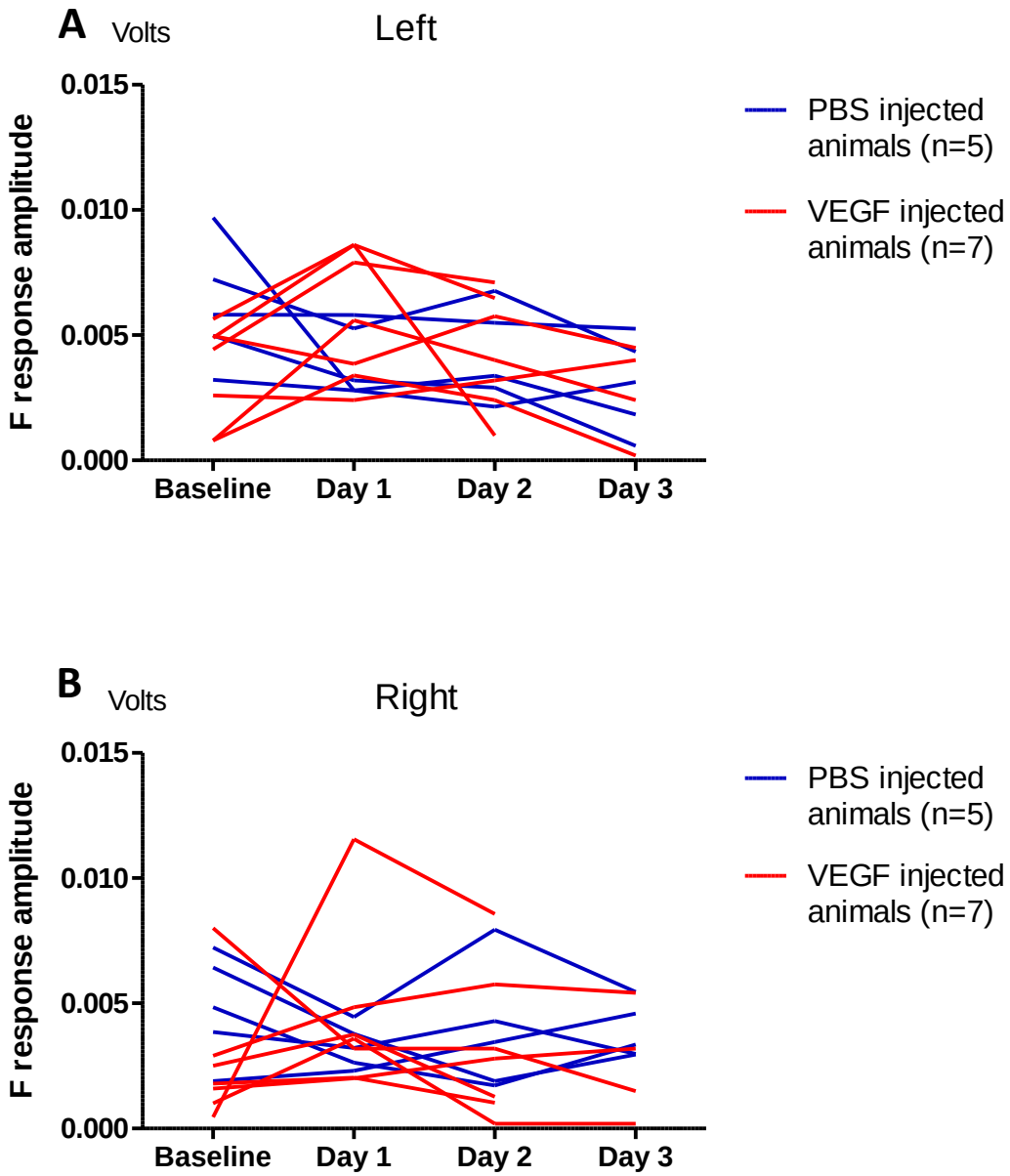

Figure V.10: *F response amplitude recorded in the left (top) and right (bottom) foot muscle of individual animals injected with PBS (n=5) or VEGF (n=7). Day 0 corresponds to the date of surgery.*

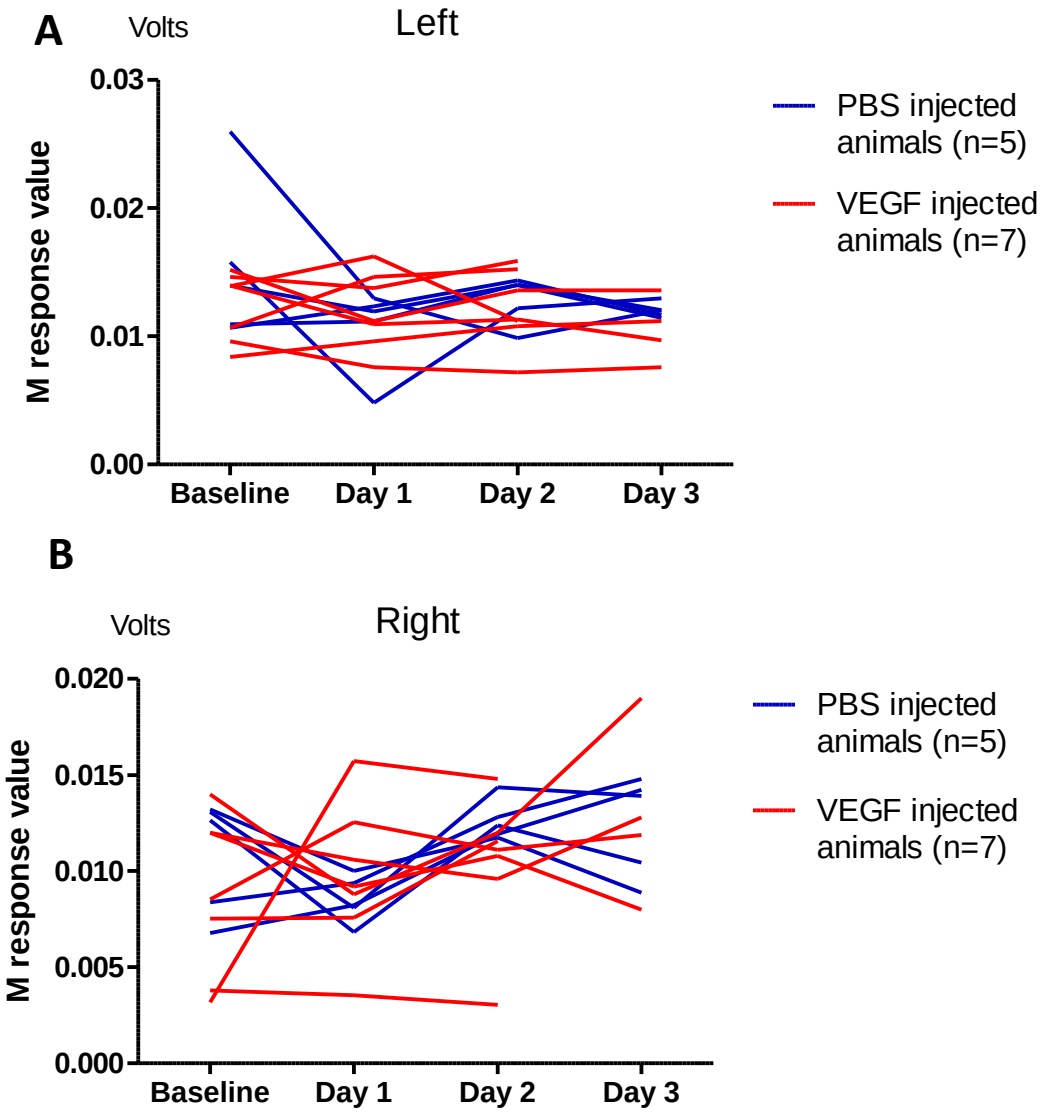

Figure V.11: *M response amplitude recorded in the left (top) and right (bottom) foot muscle of individual animals injected with PBS (n=5) or VEGF (n=7). Day 0 corresponds to the date of surgery.*

V.4.2- Synaptic markers

Following these observations, we investigated whether changes in synaptic properties were responsible for these changes in excitability. We thus looked at the expression of synaptophysin and PSD-95, respectively a pre-synaptic and a post-synaptic marker, two days following surgery. Figure V.12 shows a typical image obtained from double-labelling for synaptophysin and PSD-95 in the ventral horn, where motor neurons are located. An interesting observation is that synaptophysin is broadly expressed in the grey matter, and not only around motor neurons. Also, PSD-95 is more localized in clusters which are not only present around motor neurons, but also on other cells in the grey matter. Neuron cell bodies that are not located in the motor nuclei of the ventral horn are positive for PSD-95 within their cytoplasm whereas motor neurons of the motor nuclei are not. It has been shown the ventral horn and dendrites in the adjacent white matter develop synaptic pathology in EAE (Zhu, 2003). We therefore looked at the expression pattern of synaptophysin and PSD-95 in the ipsilateral ventral horn and the white matter lateral to the horn column where motor neurons develop their dendrites. No difference could be observed between tissue injected with VEGF and tissue injected with PBS (figure V.13),

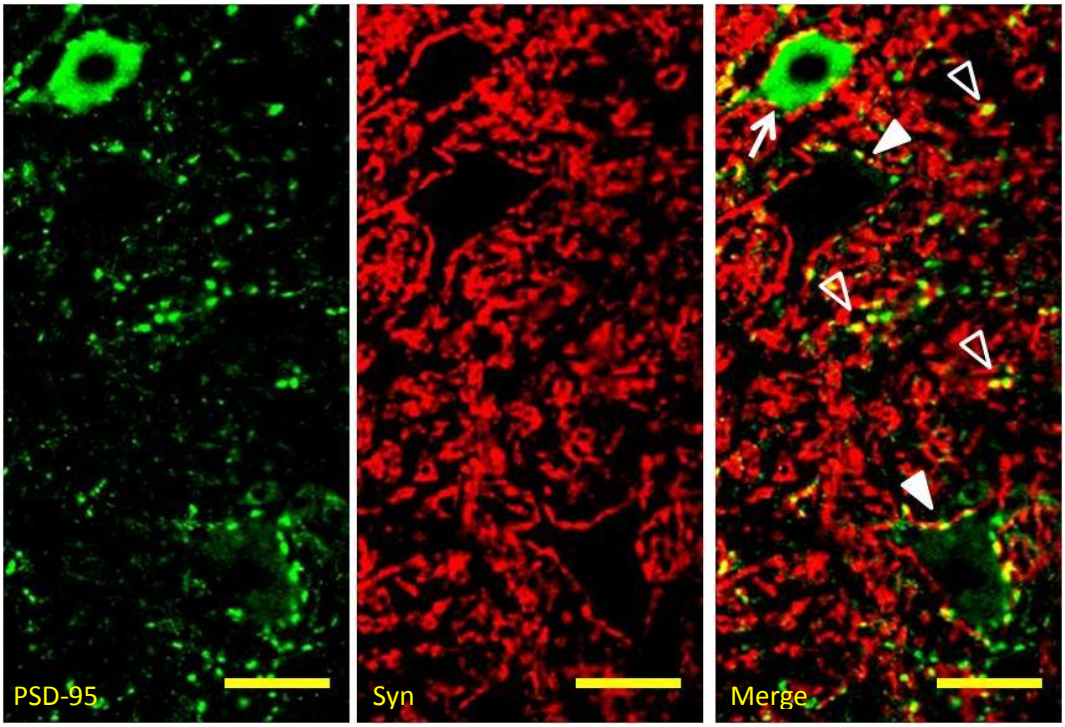

Figure V.12: *Representative labelling of the ventral horn for PSD-95 (left panel, green), synaptophysin (middle panel, red) and the merged pictures (right panel). Colocalization of PSD-95 clusters with synaptophysin positive tissue was present around the motor neurons of the motor nuclei (filled arrow head) but also elsewhere in the tissue (empty arrow heads), possibly on other cell types. Cell bodies of motor neurons out of the motor nuclei had their cytoplasm PSD-95-positive (arrow). Scale bar: 10µm.*

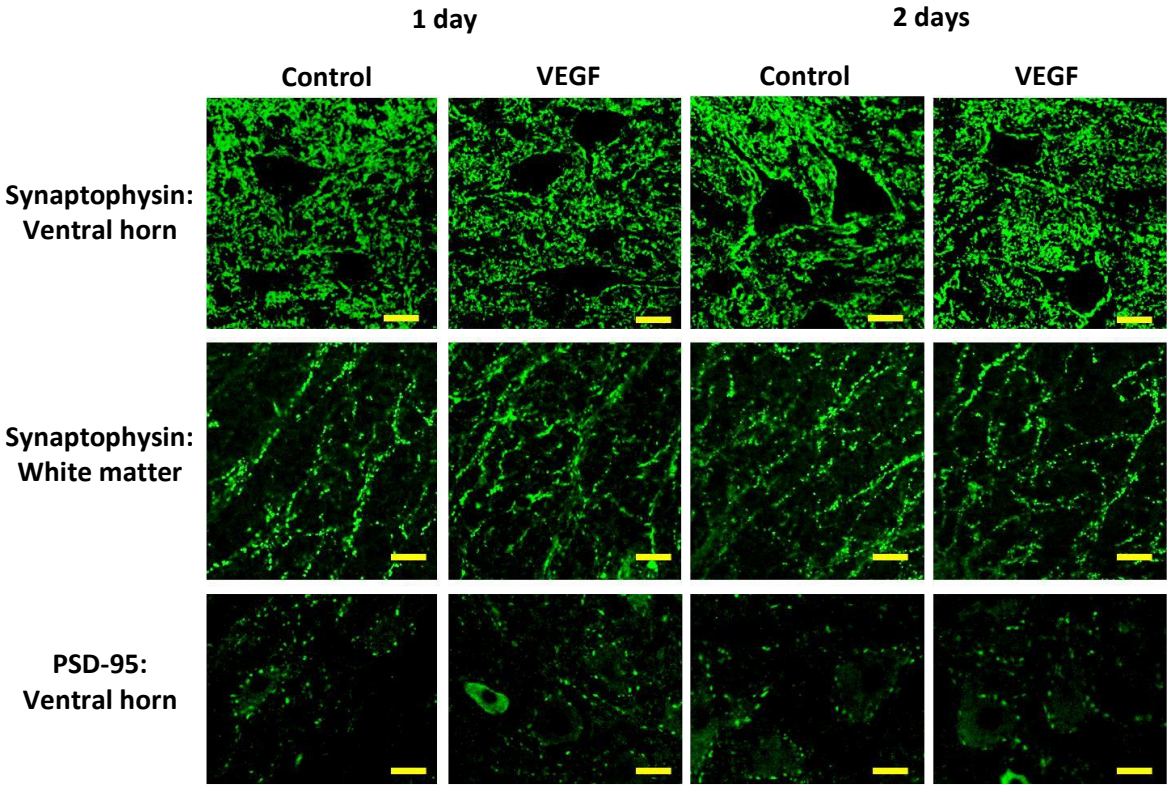

Figure V.13: *Synaptophysin and PSD-95 labelling in the ventral horn (synaptophysin and PSD-95) and adjacent white matter (synaptophysin) in VEGF and control animals at one day and two days following surgery. Scale bar: 10µm.*

suggesting that synapses pathology is not responsible for the deficit observed two days following injection of VEGF.

V.5- Astrocyte activation induced by injection of VEGF

We investigated whether injection of VEGF into the spinal cord had detectable effects on astrocytes, as detectable by their expression of GFAP. In a time course study, spinal cord sections of animals injected with VEGF or PBS were labelled for GFAP, an astrocytic marker. Different areas of the spinal cord were assessed, namely the dorsal column, dorsal horns and ventral horns. Sections of animals injected with VEGF showed a more intense labelling compared to control animals injected with PBS, as shown in figure V.14. GFAP intensity was higher in all areas investigated at day one and two following surgery. Labelling on sections taken three days after surgery was similar to the labelling observed in control tissue. Interestingly, the ipsilateral side was more strongly labelled compared to the contralateral side. In VEGF-treated animals, astrocytes marked with GFAP were ramified with long and thick processes.

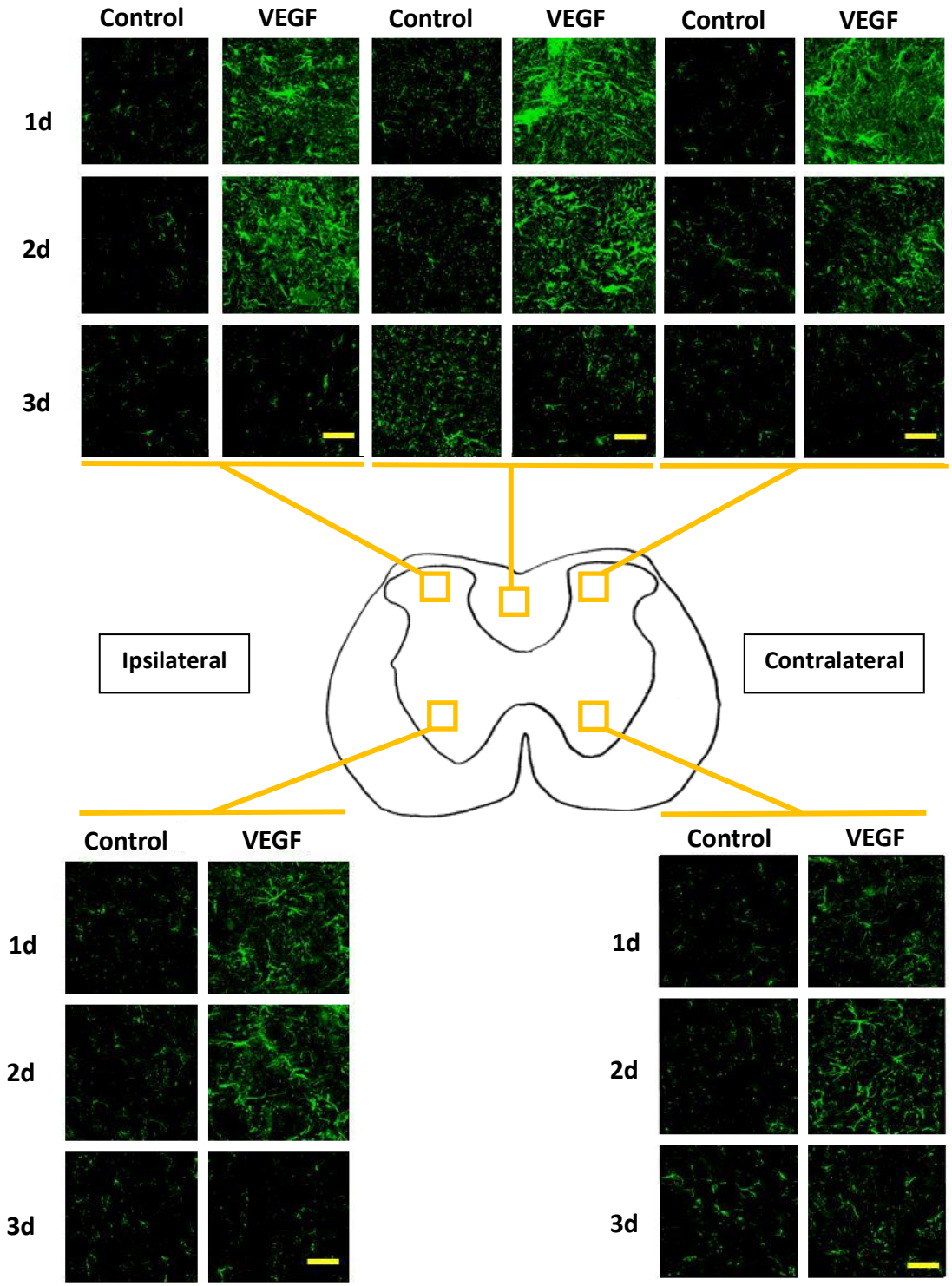

Figure V.14: *GFAP labelling in spinal cords of animals treated with VEGF (right column) or PBS (left column) at one day (top row), two days (middle row) and three days (bottom row) post-surgery. Pictures were taken in the left dorsal horn (top left panel), the dorsal column (top middle panel), the right dorsal horn (top right panel), the left ventral horn (bottom left panel) and the right ventral horn (bottom right panel). Scale: 10µm. Injections were made on the left side of the dorsal column.*

Chapter VI: Discussion

The findings reveal that an intraspinal injection of VEGF provoked a breakdown of the blood-brain barrier localised to the injection site. The barrier dysfunction was present at 24 hours, and persisted for two days. On the first day after injection, there was an increase in neuronal excitability, which returned to normal within 24 hours. On the second day there was an obvious neurological deficit, consisting of a spastic weakness of the hindlimbs, with a tendency for the ipsilateral limb to be more profoundly affected. The loss of motor function was accompanied by a reduction in sensory function consisting of a decrease in sensitivity as assessed by von Frey stimulation. The motor and sensory deficits were significant, but expressed for only one day. Histochemical studies showed that inflammation (as revealed by the presence of macrophages and activation of microglia and astrocytes) correlated both temporally and spatially with the breakdown of the blood-brain barrier. During this time the tissue suffered from hypoxia, as determined by an increase in binding of systemically-administered pimonidazole. The gross structure of the parenchyma remained unchanged and there was no evidence of demyelination or degeneration.

VI.1- Characterization of the blood-brain barrier breakdown

VI.1.1- IgG leakage

We found that the intraspinal injection of VEGF at the T13-L1 vertebral level caused blood-brain barrier breakdown as assessed by IgG leakage at days one and two post-surgery. A similar observation had been made by Benton and Whittemore (Benton and Whittemore, 2003) except that they found that the peak of leakage was on the first day following injection of VEGF, although we could not distinguish an obvious difference between days

one and two. This may be due to the difference in method used to assess the leakage of blood components into the CNS. Whereas Benton and Whittemore used horseradish peroxidase (HRP) injected intravenously, we measured the leakage of IgG, which has a different molecular weight (150kDa compared with 44kDa for HRP), but may also have different properties when considering the blood-brain barrier. Moreover, we used rat VEGF whereas the other group used recombinant human VEGF, which may have a different potency in terms of blood-brain barrier disruption. Consistently, the blood-brain barrier was repaired three days after the injection. IgG was found mainly in the grey matter, consistent with the greater density of blood vessels in the grey vs. the white matter. Also, IgG was present throughout the whole spinal cord cross-section, and not only around the dorsal column where VEGF had been injected. It is not clear from the current study whether the VEGF diffuses away from the dorsal column to affect blood vessels across the spinal cord, or whether the IgG diffuses from the dorsal column into the surrounding tissue. Rather than focus on this issue we have studied the mechanism leading to the deficit, once the lesion had been characterized both immunohistochemically and functionally. In any case, this observation means that the blood components entering the CNS after injection of VEGF can interact with the CNS cells in any part of the spinal cord and are able to influence many pathways. Moreover, at day three post-surgery, most IgG has disappeared but the base of the dorsal column consistently revealed some positive labelling in animals injected with VEGF. This suggests that a higher concentration of IgG is present at this location and takes longer to be removed or that the blood barrier is still open at day three. The latter possibility is unlikely since it is known that VEGF-induced blood-brain barrier stops after 72h (Benton and Whittemore, 2003).

VI.1.2- Fibrinogen extravasation

MS lesions show a transient blood-brain barrier breakdown characterized by leakage of fibrinogen (Kermode et al., 1990; Kirk et al., 2003). We investigated this feature of MS lesions in our model and showed that intraspinal injection of VEGF leads to fibrinogen extravasation into the CNS, confirming the observation that a blood-brain barrier breakdown occurs. This is in line with other studies showing that direct injection of VEGF into the retina leads to a breakdown of the blood-retina barrier, and, therefore, fibrinogen leakage into the retina (Hofman et al., 2000). Similarly to IgG, fibrinogen was present in the whole section, in the grey matter and the dorsal column. Less fibrinogen was present at day three, suggesting that some of the fibrinogen that leaked during the first two days had been removed.

VI.1.3 Evans blue leakage

The last marker we used to assess the blood barrier leakage was Evans blue. Evans blue leakage was apparent around the injection site, delimitating a lesion 6mm in length along the spinal cord, similar to other studies (Sasaki et al., 2010). The lesion induced is large enough to affect the spinal roots leading to the sciatic nerve, which enter the spinal cord in the same area (Gelderd and Chopin, 1977). This anatomical proximity provided the basis for our study of hind limb motor function.

Leakage of Evans blue was observed two days following the injection of VEGF but it was not studied at days one and three due to limited animals available at these time points (since a clear focus was made on the second day for immunohistochemical studies). As it can be argued that the presence of IgG in the spinal cord may be due to an immunological

activation, we are aware of the necessity to characterize further the blood brain barrier breakdown at other time points (namely one and three days) thanks to specific markers such as Evans blue or HRP, as done in another study (Benton and Whittemore, 2003). HRP would allow a better localisation of the leakage compared to Evans blue, as it can be precisely localised via immunohistochemical labelling. Moreover, using such a marker at different time points would confirm the timing of the blood brain barrier leakage we observe and increase the consistency we obtain using IgG and fibrinogen labelling.

Overall, an intraspinal injection of VEGF is able to induce a focal breakdown of the blood-brain barrier, thus allowing for the selection of particular parts of the body by choosing the site of injection along the spinal cord. Interestingly, the breakdown was also delimitated in time. Both these characteristics are similar to what has been observed in brains of patients with MS lesions (Cotton et al., 2003; Kermode et al., 1990; Kirk et al., 2003; Leech et al., 2007). Since no symptom is present before the plasma leakage into the CNS (Kermode et al., 1990), inducing a leakage in naive animal is relevant to understand the pathogenesis leading to MS symptoms.

VI.2- Characterization of the motor deficit induced by VEGF

VI.2.1- Effect of VEGF injection on trained walking ability

We investigated the functional consequences of an injection of VEGF in the spinal cord by testing the animals on the horizontal ladder test, as described elsewhere (Metz and Whishaw, 2009). Animals injected with VEGF showed a motor deficit in hind limb function two days following surgery, and recovered the next day. This result is comparable with Sasaki and colleagues' observations, i.e. animals intraspinally injected with VEGF show a

deficit in the next three days after injection (Sasaki et al., 2010). We believe that Sasaki and colleagues misinterpreted their finding in that they attributed the deficit to the surgical trauma associated with the injection (even though no control group was used for comparison).

In the current study, some animals were tested for up to a year following the injection and no deficit could be observed after the two day time point. The blood-brain barrier breakdown induced by VEGF follows a similar timing. It is present the first two days following surgery and stops at day three. This correlation suggests that the barrier leakage in the CNS may have a role in the motor deficit observed. Moreover, both hind limbs were affected by this motor impairment, as expected given that blood components (IgG and fibrinogen) were present across the whole width of the spinal cord, despite the injection being made on the left side of the dorsal column. Thus although each side of the spinal cord primarily controls the ipsilateral hind limb (Nicolopoulos-Stournaras and Iles, 1983), the blood components affected both sides of the cord.

VI.2.2- Effect of VEGF injection on response to tactile stimuli

We investigated the effect of injection of VEGF on nociception. We showed that animals injected with VEGF had a significantly reduced sensitivity in their hind paws at day two following surgery. This result correlates temporally with the motor deficit. The pathway for innocuous and noxious sensations is mediated by neurons in the dorsal horns (Christensen and Hulsebosch, 1997; Giesler and Cliffer, 1985), and although VEGF is injected into the nearby dorsal columns, its effects are known to spread to the nearby dorsal horns, as evidenced by the presence of IgG and fibrinogen in this part of the grey matter. It thus can be inferred that the alterations in sensory function occur mainly at the lesion site in

response to the barrier breakdown. Interestingly, this desensitization was stronger on the ipsilateral side, suggesting that even though no side-specificity was observed with the horizontal ladder test, a slight sensory difference is present. The strength of the tactile stimuli applied to the hind paws of the animals are above the threshold for nociception. The results presented here therefore suggest that animals injected with VEGF are hypoallergesic. However, it must be borne in mind that the same animals show signs of motor dysfunction. Thus, the decreased sensitivity to tactile stimulation could simply be due to weakness in the hind limbs which prevents the animals from lifting their paw.

VI.2.3- Effect of VEGF injection on natural behaviour

Rats, amongst other species such as mice, gerbils or hamsters, have a natural tendency to burrow. We exploited this ability to assess any difference in natural behaviour between control animals and animals injected with VEGF, as described by Deacon (Deacon, 2006, 2009). After a period of adaptation to the new enriched environment, all of the animals burrowed to eject 100% of the woodchip bedding when left with a burrowing tube overnight. Animals injected with VEGF displayed a reduced burrowing activity (only 50% of the woodchip bedding was ejected) for the first three days following surgery. Although the first two days of reduced activity correlate well with the motor deficit observed, the decreased in burrowing activity at day three was not expected, since the motor functions are restored at this point. We suggest that at three days, the motor deficit was not severe enough to be detected by observation, but it was nevertheless sufficiently strong to prevent normal burrowing activity. Another possible explanation is that the animals had sufficient motor power to eject the woodchips, but were not motivated to do so. One potential reason for a lack of motivation may be loss of visceral motor function and, for example, stomach cramps.

VI.2.4- Effect of VEGF injection on hind-limb strength

The inclined plane test was originally conceived to evaluate the consequences of spinal cord injury on motor functions (Rivlin and Tator, 1977), and it can be used as an index of animal strength (Gale et al., 1985; von Euler et al., 1997). We assessed hind limb strength by placing the animals on the inclined plane facing upward, although it is possible to place them in different orientations (Pearse et al., 2005). In our model, animals injected with VEGF were unable to maintain their position on the inclined plane from a lower angle compared to their control counterparts, confirming the presence of a motor deficit. Similarly to the horizontal ladder test, and the time course of blood-brain barrier breakdown, the deficit on the inclined plane appeared at two days following surgery and disappeared the following day.

VI.2.5- Effect of VEGF injection on positioning of the tail

While analysing the locomotor properties of animals on the horizontal ladder test, it was noticeable that animals injected with VEGF were not able to lift their tail in a natural manner while walking, as naive animals can. We therefore measured the tail angle from videos taken during the ladder test. We observed that animals injected with VEGF were dragging their tail, leading to an angle of 0° compared to baseline. The tail is controlled at the low sacral level (S2) of the spinal cord (Bennett et al., 1999), which is located under the L2-L3 vertebrae. Although the VEGF lesion was induced more rostrally, it is likely that more caudal functions will still be affected as the pathways responsible for voluntary tail function have first to pass through the injected region. Thus in a manor analogous to spinal cord

injury, a lesion in the thorax can cause loss of tail reflex in cats (Cavallari and Pettersson, 1989).

VI.2.6- Effect of VEGF injection on gait

Gait analysis is useful to quantify locomotor behaviour in an objective manner thanks to an automated data analysis system. Such systems also allow control of the inter-animal variability in walking speed. Using the Treadscan system as described elsewhere (Beare et al., 2009), we quantified several gait parameters of animals injected with VEGF. The outcome of this study was a non-significant but consistent trend towards an impairment in balance and posture at day two following surgery, only in animals injected with VEGF. Indeed, animals injected with VEGF showed a decrease in rear track width and gait angle at day two post-surgery, indicative of a lack of balance and altered posture: the paws were positioned closer to the longitudinal midline. Stride frequency and stance time were reduced while minimal longitudinal reach and feet base were increased. This shows that the animals injected with VEGF were making smaller steps at a higher frequency to maintain their speed. This can also be indicative of balance problems, since smaller and faster steps help maintain balance, but it could also come from an inability to perform bigger steps because of a motor impairment. The analysis performed in this study does not allow for the discrimination between the two hypotheses since both of them are interrelated.

VI.2.7- Complementarity of behavioural tests

In accordance with Muir and Webb's view on the implementation of behavioural tests (Muir and Webb, 2000), we performed a comprehensive analysis with functional tests

including three components: a measure of motor abilities during trained behavioural tasks (ladder test, tail angle), a measure of motor abilities during spontaneous locomotion (treadmill, inclined plane, burrowing) and an assessment of reflex function (von Frey hair test). Overall, the different behavioural and locomotor tests all lead to the same observations and bring complementary conclusions. At day one following surgery, a hint of motor deficit is present in animals injected with VEGF and is detectable using the burrowing and tail-angle test. However, this deficit is not yet strong enough to be revealed by other tests. At day two, all tests reveal a significant deficit which has a locomotor component (inclined plane, ladder test) linked to a problem in balance and posture (treadmill, tail angle). Finally, the sensory motor pathway seems also to be altered (von Frey). All these impairments lead to a modification in general behaviour, as assessed by the burrowing activity test. Most functions recovered at day three, although the burrowing activity was not restored at this time point, suggesting that impairments not detectable with other tests may still be present.

VI.3- Discrimination between a direct action of VEGF on the CNS tissue, and the consequences of blood-brain barrier leakage

It is thought that VEGF can have a direct effect on the CNS independently of its effect on the blood brain barrier. Indeed, VEGF has a trophic role on the neuronal cell population. It can enhance neuronal survival and neurite outgrowth in the brain cortex and the substantia nigra (Rosenstein et al., 2003; Silverman et al., 1999) and in cultured dorsal root ganglia (Sondell et al., 1999; Sondell et al., 2000). VEGF also protects neurons during hypoxia (Jin et al., 2000b) and glutamate-induced excitotoxicity (Matsuzaki et al., 2001). However, it is not yet clear whether these effects are due to a direct action of VEGF (Rosenstein et al., 2010) or whether it is acting indirectly, perhaps through glia (Krum et al., 2002).

To distinguish between direct and indirect effects of VEGF on neurons we have sought to inhibit its indirect effects (i.e. effects on the blood-brain barrier) to determine whether the loss of function persisted. It has been shown that VEGF exerts its vascular permeability action via eNOS (Argaw et al., 2012), an enzyme selectively expressed in endothelial cells. Specific inhibition of this pathway is thus a good opportunity to prevent the blood-brain barrier leakage while allowing any potential direct action of VEGF on other cell types and thereby to discriminate between the two hypotheses described earlier. Cavtratin, a cell-permeable fusion protein made from caveolin-1, selectively blocks eNOS without affecting other isoforms of the enzyme (Bernatchez et al., 2005; Bucci et al., 2000; Gratton et al., 2003). It had previously been shown in mice that blood-brain barrier breakdown induced by direct microinjection of VEGF in the brain was abrogated by peripheral injection of cavtratin at a dose of 2.5 mg/kg (Argaw et al., 2012). In another study, 1 mg/kg was able to reduce vascular permeability induced by inflammation (Bucci et al., 2000; Hatakeyama et al., 2006). Studies involving cavtratin injections in rats have also been published (Bauser-Heaton et al., 2008; Li et al., 2009) but none of them concerned vascular permeability. Given this lack of experience in rats and the high purchase price of cavtratin (and its scrambled peptide control), we decided to conduct a preliminary experiment based on the highest dose we found in the literature (2.5 mg/kg i.p. every 24h) in order to optimize the chances of successful inhibition of blood-brain barrier breakdown. Unfortunately, the animal group injected with cavtratin displayed a similar deficit and similar IgG leakage following VEGF injection as the group injected with the scrambled peptide, so the cavtratin appeared ineffective in our model. Despite this disappointing outcome in pilot experiments, we believe on the basis of the published work that this pharmacological method may be a good tool to investigate the events leading to the motor deficit we observed, and thus that a pharmacokinetic study would help in finding an effective dose in

blocking the blood vessel leakage. This would however be a very expensive method and we decided to stop this study and investigate other pathways. Although we know that VEGF can act directly on neurons, there is no literature suggesting the presence of negative actions that could explain the loss of function that we observe. On the contrary, it has been extensively documented that VEGF can have positive actions on neurons, acting as a trophic factor and promoting growth and survival. Although it obviously needs further investigation; the latter observation points towards an indirect role of VEGF in the deficit we observe, reinforcing the hypothesis that it is caused by breakdown of the blood-brain barrier.

VI.4- Structural changes induced by injection of VEGF

VI.4.1- Oedema

Blood-brain barrier leakage in the CNS often leads to the formation of oedema. In patients with spinal cord injury, it has been shown that the magnitude and extent of oedema following injury correlates with the severity and extent of recovery from the motor deficit (Flanders et al., 1999). In our model, the time course of blood-brain barrier breakdown correlates strongly with the temporal course of the neurological deficit and the following recovery, suggesting that it may be causally related to the motor deficit. In animals with EAE, an animal model of MS, the blood-brain barrier is altered and this leads to oedema formation and exacerbation of symptoms (Claudio et al., 1990). Since the course of disease in EAE is made of acute phases of motor deficit during which severe oedema occurs (Kaneyama et al., 2013), we investigated whether, in our model of acute motor deficit followed by remission, such oedema was present during the blood-brain barrier breakdown. We discovered that no oedema was present at the time of functional deficit undergone by animals injected by VEGF, suggesting that the leakage of blood components,

as confirmed by the presence of IgG and fibrinogen, was not large enough to induce any oedema that could be seen directly on toluidine blue-stained spinal cross-sections. The hypothesis suggesting that oedema is the cause of the functional deficit can thus be discounted.

VI.4.2- Demyelination and axonal loss

In EAE, animals typically experience a relapsing-remitting onset during which they undergo one or more acute peaks of disease, before they enter a more chronic phase during which disabilities persist or increase progressively. Similar phenomena occur in MS. During the acute phase, inflammation is thought to be primarily responsible for the symptoms observed, whereas demyelination and axonal loss are the primary causes of the progressive impairments seen in the chronic phase (Wujek et al., 2002). Accordingly, during the acute deficit we observe in our model, we did not see any axonal loss or demyelination in spinal cords injected with VEGF, consistent with the rapidly evolving but also rapidly reversing deficit.

This absence of demyelination in the VEGF model is in contrast to the presence of this pathology when LPS is injected into the spinal cord (Felts et al., 2005; Marik et al., 2007), despite the fact that in both cases there is breakdown of the blood-brain barrier following the injection. However, the duration of the blood-brain barrier deficit is longer (more than five days) in the LPS lesion, resulting in prolonged inflammation and plasma protein deposition in the CNS (Felts et al., 2005; Marik et al., 2007), and this is followed by demyelination after two days. We suggest that the intensity of the VEGF lesion, and the limited duration of plasma leakage induced by VEGF (two days) is not long enough to

trigger any axonal loss or demyelination within one month, nor indeed within one year, as revealed in our long-term study.

VI.5- Possible role of hypoxia

It has been shown in our lab (Davies et al., 2013) that hypoxia is linked to the neurological deficits observed in the acute phase of EAE. Indeed, pimonidazole labelling and spinal cord tissue oxygen concentration were both strongly correlated with the severity of the disease in animals with EAE. We have therefore considered whether hypoxia may also play a role in the loss of function following VEGF injection. We found that, in VEGF-injected tissue (but not in PBS-injected control tissue), the grey matter was positive for pimonidazole, although to a lesser extent than in the EAE tissue used as a positive control. This labelling was present at days one and two following surgery but not at day three, so the presence of hypoxia correlated temporally with the expression of deficits. We investigated whether the hypoxia may be responsible for the loss of function by attempting to reverse the hypoxia by the administration of inspired oxygen, i.e. normobaric hyperoxia. Indeed, Davies et al treated animals suffering of EAE for 1h with 95% oxygen and saw an improvement of neurological score in the animals treated with oxygen compared to the ones treated with room air. In our model, after 1h of oxygen treatment, most of the animals showed some improvement on the horizontal ladder test. However, the same was true for the animals treated with room air. These findings thus suggest that the improvement in function was due to practise rather than therapy, i.e. that the animals were performing better simply because of the short period of time separating the two trials on the horizontal ladder. Since the amplitude of improvement was similar for both the room air and the oxygen group, we concluded that normobaric hyperoxia does not improve the clinical deficit observed in animals injected with VEGF.

We decided to use a second marker of hypoxia to confirm the hypoxic state of the tissue at the time of deficit. Using HIF-1α immunolabelling, we showed that this transcriptional inducible factor was expressed at day two after injection, consistent with the (seemingly more sensitive) pimonidazole result suggesting that the tissue of animals injected with VEGF is hypoxic. HIF-1α was labelled in the dorsal column, the dorsal horn and the ventral horn (mainly in motor neurons). However, not all sections of animals injected with VEGF and showing a neurological deficit illustrated this labelling. Thus, the HIF-1α expression is not necessarily correlated with the deficit we observe, suggesting that hypoxia, which induces HIF-1α expression, is not always present when the animals suffer from a functional deficit. However, for these animals, pimonidazole labelling was present, highlighting a partial discrepancy between the two hypoxia markers which is best explained by a different sensitivity of their expression.

Although the findings with pimonidazole can potentially explain the neurological deficit observed, it is wise to be cautious before accepting this explanation: i.e. the possibility that the labelling is simply an artefact must be considered. First to consider is the possibility that more pimonidazole passes into the tissue when the blood-brain barrier is disrupted, i.e. that pimonidazole is normally only sparingly permeable across the intact blood-brain barrier. This remains a concern, but against it must be balanced the fact that, according to the relevant literature, pimonidazole will not bind to tissue irrespective of its concentration, unless the oxygen concentration is low. If so, then an increased pimonidazole concentration is not only speculative, it is also irrelevant. Another potential artefact can also be discounted by similar argument. Thus there is a potential concern that haem-iron complexes present in blood can prevent the oxidation of pimonidazole into its oxygen-insensitive N-oxide metabolite (Walton et al., 1985). Potential leakage of haem-iron

complexes into the CNS following disruption of the blood-brain barrier may therefore increase the concentration of detectable pimonidazole within the tissue, but if the pimonidazole concentration is partly irrelevant, this concern is diminished. Also, inflammatory cells, which are present in the spinal cord of animals injected with VEGF, may produce nitroreductases which are enzymes capable of reducing pimonidazole in an oxygen-insensitive manner, thus leading to hypoxia-independent labelling. The presence of inflammatory cells could therefore provide a false positive labelling of pimonidazole in VEGF-injected spinal cord compared with control tissue. This complication remains a theoretical concern in the brain, but the issue has been directly addressed in the liver (Arteel et al., 1995) where it has been shown that the presence of nitroreductase enzymes does not affect pimonidazole labelling, which seems to be solely dependent on the oxygen gradient.

We used several methods to assess whether hypoxia caused the functional deficit we observe, but none of them provided a clear answer. At least three hypotheses are consistent with the data.

1. The tissue is not hypoxic, which explains why the oxygen therapy is ineffective. In this case the pimonidazole labelling is an artefact (potential mechanisms have been discussed above). The labelling for HIF-1α, when present, would also be an artefact, perhaps induced by a non-hypoxic pathway.

2. Hypoxia is present but not very severe, yet its effects are slowly cumulative so that over two days it results in a functional deficit. This would explain the mild pimonidazole labelling at one day, which correlates with a weak, non-significant neurological deficit, but accumulating over two days to produce a significant

deficit. Such a low level of hypoxia may not be sufficient to induce the strong expression of HIF-1α, hence the variability of HIF labelling in animals injected with VEGF. However, if this explanation is correct, oxygen treatment would be expected to result in an alleviation of neurological deficit, which did not occur.

3. Hypoxia is sufficiently severe to induce labelling by pimonidazole, but this severity is insufficient to cause a loss of function. Such borderline hypoxia would explain the variability in HIF-1α expression, and also the inability of oxygen treatment to reverse the neurological deficit.

Further investigation is needed to confirm or refute any of these hypotheses. However, it is notable that the normal spinal cord does not label for hypoxia and has normal function, that the VEGF lesion labels lightly for hypoxia and has partial function, and the EAE spinal cord labels strongly for hypoxia and has no function. In this view, the hypoxia in the VEGF lesion falls on a continuum of loss of function.

VI.6- Potential triggers of inflammation

An interesting feature of our model is the presence of inflammatory cells (ED1-positive macrophages, MHC-II-positive microglia and Ox-42-positive microglia) within the spinal cord of animals presenting a hind limb motor deficit. We can confidently infer that this inflammatory reaction is not due to the surgical trauma caused by the injection since control animals show no inflammation despite experiencing the injection. Several hypotheses can explain the inflammation within the CNS.

VI.6.1- VEGF

It is known that via VEGFR-1 expressed on monocytes and macrophages, VEGF plays a role in the activation (Clauss et al., 1996; Sawano et al., 2001) and recruitment of inflammatory cells (Bottomley et al., 2000; Lemstrom et al., 2002; Luttun et al., 2002). Accordingly, VEGF is upregulated in inflamed tissues and provides recruitment signals for the infiltration of inflammatory cells, and inhibition of the VEGFR-1 pathway diminishes inflammatory cell infiltration and reduces the production of pro-inflammatory cytokines (MCP-1, TNF-α) by macrophages (Luttun et al., 2002). VEGF can thus directly stimulate an inflammatory process that could have deleterious consequences and trigger the deficit we observe.

VI.6.2- Fibrinogen, thrombin and albumin

Another hypothesis explaining the presence of inflammation in animals injected with VEGF is the abnormal presence of blood proteins in the CNS following breakdown of the blood-brain barrier. It has been shown that fibrinogen can directly activate macrophages (Akassoglou et al., 2004; Sobel and Mitchell, 1989) such that it stimulates chemokine secretion by these cells at sites of inflammation (Smiley et al., 2001). Pharmacologic depletion of fibrinogen also decreases inflammation in a mouse model of MS (Akassoglou et al., 2004). The presence of fibrinogen we observe in VEGF-injected tissue and the correlation with the inflammation we observe suggest that fibrinogen will contribute to inflammatory cell activation and infiltration.

Thrombin may also be involved in the induction of an inflammatory response as intra-cortical injection of thrombin induces microglial activation (Lee da et al., 2006; Moller et al., 2000) that can be inhibited with anti-inflammatory agents (Choi et al., 2005a). It is thus

possible that the presence of thrombin following the blood-brain barrier leakage, if shown, may trigger the inflammatory response we observe.

Albumin is another plasma component that can lead to microglial activation, inducing the release of pro-inflammatory cytokines such as IL-1β (Ralay Ranaivo and Wainwright, 2010) or TNF-α (Hooper et al., 2009).

In summary, the presence of each of these vascular factors in the parenchyma can promote inflammatory changes.

VI.6.3- Does inflammation play a role in the functional deficit

The presence and magnitude of the inflammatory changes correlates quite precisely with the expression of neurological deficit, implying that the inflammation and deficit may be causally related. Moreover, inflammation as revealed by ED1-positive cells is most severe in the side ipsilateral to the injection, which correlates with the ipsilateral expression of deficit. The dorsal cord is involved in proprioception (Jordan and Schmidt, 2002) and accordingly the desensitization of the hind paw was stronger on the ipsilateral side.

VI.6.4- Nitric oxide

NO is a potent cause of mitochondrial dysfunction (Witte et al., 2010) and activated microglia can produce abundant NO (and hence loss of excitability) via the induction of iNOS (Galea et al., 1992). However, we found that iNOS was not expressed at the injection site during at least the three days following surgery, indicating that NO plays no role in the loss of function. However, to ensure that other sources of NO may not be playing a role, we

labelled for nitrotyrosine as a “foot print” of the earlier presence of peroxynitrite, formed when NO combines with superoxide. However, as with iNOS, no nitrotyrosine was present in either VEGF-injected or PBS-injected tissue. We therefore conclude that microglia-induced NO does not play a role in the functional deficit we observed.

VI.6.5- T-cells

T-cells can express VEGFR-2 in inflammatory conditions and VEGF action via this receptor can lead to a pro-inflammatory Th1 phenotype (Mor et al., 2004). It has also been shown that VEGF is functional for CD-3-positive lymphocyte recruitment (Reinders et al., 2003). We therefore investigated whether an intraspinal injection of VEGF could lead to CD-3 positive lymphocyte entry into the CNS, in conjunction with the inflammatory pattern we observed. No T-cell could be found in the spinal cord injected with VEGF, at any time point. This result contrasts with the involvement of T-cells in EAE pathogenesis, where they contribute to the tissue damage observed (Gold et al., 2006). However, even though chronic and acute MS lesions show T-cell infiltration (Stadelmann et al., 2011), it has also been shown that some early lesions are devoid of T-cell infiltration (Barnett and Prineas, 2004). Thus, it is possible that the lesion we induced with the injection of VEGF possesses the characteristics of early pre-demyelinating lesions that could be induced by vascular abnormalities such as a blood-brain barrier breakdown (Ge et al., 2008).

VI.7- Hyperexcitability

VI.7.1- Change in H/M and F/M ratio

During the behavioural testing of the animals it was noticed that one day following surgery, in absence of any deficit, the animals injected with VEGF presented an unexpected tremor in the hind limbs, indicating a change in motor neuron excitability. We confirmed this possibility by showing an increase in H/M and F/M ratios at one day post-surgery, and this change returned to normal at day two, when the deficit was present. Only the H and F components of these ratios were increased, while the M response did not show any consistent change. This observation was expected since the M response is the direct response to stimulation, and the pathway does not involve the spinal cord. Moreover, changes in M response such as temporal dispersion or decreased amplitude are hallmarks of demyelination or axonal neuropathy respectively (Argyriou et al., 2010). An absence of change is thus in line with our findings that neither demyelination nor axonal loss occur in our model. On the other hand, both H and F signals pass through the VEGF-lesioned part of the spinal cord (one via the sensory pathway located in the dorsal horn, the other through the cell body of the motor neurons located in the ventral horn) explaining the EMG results obtained.

Care must be taken in the interpretation of EMG data, especially the F-wave parameters. Indeed, a controversy is still on-going as to whether F-wave measurements are good indicators of motor neurons excitability. Several studies have suggested that a reduction of the incidence of F-waves can be obtained by both an increase and a decrease in motor neuron excitability (Espiritu et al., 2003; Hultborn and Nielsen, 1995) whereas others consider the study of the recurrent discharge produced by the F-wave as a valid mechanism to assess motor neuron excitability (Rossi et al., 2012; Salih et al., 2011). Several hypotheses can explain this discrepancy between the F-wave parameters and motor

neuron excitability. It has been suggested (Burke, 2014) that the supramaximal stimulus used to study F-waves can also elicit a Ia afferent signal that triggers an H-reflex mediated response in the low-threshold motor neurons. Therefore, the reflex discharge and the anti-dromic F-wave in these motor neurons would collide and prevent the H-reflex from being measured (in accord with observation) but also preventing the assessment of the F-wave. Therefore, the F-wave signal only takes into account the high-threshold motor neurons (where no H-reflex occurs) and so it is not useful to measure the change in excitability in low-threshold motor neurons. Moreover, backfiring of neurons is not completely understood and may well not be correlated with the intrinsic neuronal excitability (Lin and Floeter, 2004). Another assessment is usually needed to confirm the evolution of the F-wave parameters and its correlation with excitability. The H-reflex is considered more accurate in this view as it accesses the same population of motor neurons as the majority of excitatory afferents and is correlated with the number of motor neurons recruited (Lin and Floeter, 2004). Regarding our study, we can confidently infer that we have an increase in excitability at day one following injection of VEGF as the increase in the F/M ratio is confirmed by an even greater increase in H/M ratio.

VI.7.2- Role of astrocytes in hyperexcitability

Several recent reports provide an explanation for why the leakage of blood components induced by VEGF could be responsible for the increase in excitability, and they have proposed different pathways that may be involved.

First, it has been proposed that the release of vascular components by blood-brain barrier dysfunction can act on astroglial cells with consequences on neuronal excitability (Ivens et al., 2007; Seiffert et al., 2004). Astrocytes and endothelial cells are closely linked, being part

of the so-called neurovascular unit (Abbott et al., 2006). It is thus expected that alteration of the blood-brain barrier will affect astrocytic function. Indeed, leakage of albumin, which we showed by Evans blue leakage, can lead to its uptake by astrocytes (Ivens et al., 2007) and their activation (as assessed by GFAP over-expression) (Seiffert et al., 2004). Thrombin has also been shown to signal through PAR-1 receptors located on astrocytes (Junge et al., 2004), which are receptors involved in astrocytic glutamate release (Lee and Haydon, 2007). In our study, we showed that VEGF injection induces astroglial activation and GFAP over-expression, as described elsewhere (Krum et al., 2002). Astroglial activation can act on neuronal excitability through several mechanisms. Downregulation of the abundant astrocytic inward rectifying potassium channels (Kir4.1) and water channels (aquaporin 4) can have consequences on the extra-cellular ionic balance in the CNS, and this can affect neuronal excitability. For example, the failure of astrocytes to take up potassium results in an increase in external potassium which in turn leads to an increase of neuronal excitability by lowering the firing threshold, reducing the speed of repolarisation and facilitating activation of NMDA receptors (David et al., 2009).

Astrocytes are also important for glutamate uptake and metabolism and evidence supports the hypothesis that impairment of astrocytic glutamate transporters can lead to development of epileptic seizures (Wetherington et al., 2008).

VI.7.3- Role of inflammation

A role of inflammation and more precisely of inflammatory cytokines released by astroglial and microglial cells, has also been investigated (Weissberg et al., 2011). IL-1β, cyclooxygenase-2, TNF-α, IL-6 and TGF-β have been shown to directly affect synaptic signalling and plasticity (Yu and Shinnick-Gallagher, 1994). For example, IL-1β reduces

glutamate uptake by astrocytes (Ye and Sontheimer, 1996) and enhances their TNF-α mediated glutamate release (Bezzi et al., 2001), and has been shown to exacerbate seizures in rodents (Vezzani et al., 1999) by enhancing NMDA mediated excitability (Vezzani and Baram, 2007). Inflammatory cells themselves have also been shown to release glutamate (Piani and Fontana, 1994). Albumin may also act on microglia to induce glutamate release (Hooper et al., 2009), thereby increasing neuronal excitability.

VI.7.4- Direct role of plasma proteins in hyperexcitability

Plasma proteins may also directly increase neuronal excitability. For example, IgG is present in the spinal cord of animals injected with VEGF at the time of hyperexcitability, and it can accumulate in neurons of epileptic patients (Rigau et al., 2007). Indeed, such accumulation has been linked to neuronal hyperexcitability (Michalak et al., 2012), and since IgG is present in the dorsal and ventral horns of animals injected with VEGF one day following surgery, it may be involved in the correlated increase in H/M and F/M ratios.

Also, thrombin has been shown to potentiate NMDA receptor function and to increase neuronal excitability via binding to the PAR-1 receptor, thereby indicating a possible direct action on neurons (Gingrich et al., 2000). Moreover, thrombin can enhance the neuronal response to afferent stimulation (Maggio et al., 2008), and hence enhance the H reflex following sciatic nerve stimulation. We therefore hypothesize that the increase in H reflex amplitude following VEGF injection may be due to thrombin-induced excitability.

The normal range of glutamate concentration in plasma is 50-100 µmol/L, but it is normally only 0.5-2 µmol/L in the extracellular fluid in the CNS (Hawkins, 2009). Leakage of plasma in

the CNS would therefore dramatically increase the extra-cellular glutamate concentration, thus contributing further to an increase in excitability.

VI.7.5- Synaptic alterations in animals injected with VEGF

Loss of the pre-synaptic marker synaptophysin occur in acute lesions in the grey matter of MS patients (Vercellino et al., 2005), associated with a high density of activated microglia (Vercellino et al., 2007). Furthermore, in EAE, a loss of these two synaptic markers occurred in the ventral horn and on dendrites located in the adjacent white matter, in correlation with inflammation and NMDA receptor activation (Zhu et al., 2003). These changes may be significant because in AD, loss of the synaptophysin is associated with reduction in glutamate uptake and excitotoxicity (Masliah et al., 1996), and degradation of PSD-95 resulting from NMDA administration to organotypic hippocampal cultures is also associated with excitotoxicity (Lu et al., 2000). In light of the increase in excitability observed at day one following injection of VEGF, we characterized the synaptic state of neurons in the spinal cord by labelling sections for synaptophysin and PSD-95. Unexpectedly, no difference in either marker could be observed between animals injected with VEGF and controls at day one, when an increase in excitability is present, nor at day two, when a neurological deficit is present. This suggests that changes in neuronal conduction occurring at least at day one are not mediated by synaptic modification. As discussed earlier, an increase in extracellular glutamate without a decrease in synaptic function (i.e. the same amount of synaptophysin and PSD-95) would be expected to lead to an increase in excitability.

The fact that the changes in electrophysiological properties observed at day one returned to baseline by day two, makes it less surprising that no change was detected at the synaptic level. However, this is in contrast to observations in MS patients and particularly in EAE,

where synaptic stripping and decreases in synaptic proteins have been reported (Trapp et al., 2007). The changes in MS have understandably been interpreted as an explanation for at least some of the loss of function, but the findings from our study suggest that such severe changes are not required. It seems that the structural changes in MS and EAE may require much stronger inflammation around neurons and dendrites than observed in our study, but that loss of function occurs even without these changes.

VI.8- Relevance of this model to MS

We believe that the lesion induced by VEGF is very relevant to understanding the pathophysiology of MS, especially with regard to the consequences of blood-brain barrier breakdown.

VI.8.1- Blood-brain barrier breakdown

Transient breakdown of the blood-brain barrier is a prominent feature of MS lesions (Leech et al., 2007), particularly during the relapsing/remitting phase of the disease where it is recognised as an early event during the formation of a new lesion (Cotton et al., 2003; Kermode et al., 1990) by MRI detection the leakage of gadolinium contrast medium (Kermode et al., 1990). Such blood-brain barrier breakdown is associated with the onset of neurological deficit, at least in optic neuritis, which often the first sign of MS (Youl et al., 1991). This time course is comparable to ours since blood-brain barrier breakdown occurs before the onset of deficit. In other MS animal models, the leakage of plasma components into the CNS is also present. Again, it is often present before the onset of neurological deficit in EAE animals and disappears with the functional problems (Floris et al., 2004) as seen in our model.

VI.8.2- Functional deficit

Second, the functional deficit we observed is consistently limited to the hind limbs and consists of an acute phase occurring two days following injection of VEGF followed by a remission the next day. This acute phase followed by remission is also observed in patients suffering from relapsing/remitting MS but also in animal models of MS, EAE (Hawkins et al., 1991) and LPS (Felts et al., 2005; Marik et al., 2007). Our model can thus be a tool to explore the pathogenesis of this transient deficit.

VI.8.3- VEGF

The expression of VEGF has been shown to correlate with relapses in MS patients. Indeed, an increased concentration of VEGF is found in the serum of patients undergoing relapses, and this returns to normal during the remission phase (Su et al., 2006). In EAE, an increased expression of VEGF is also present and it is correlated with the inflammatory process observed in the tissue (Proescholdt et al., 2002a). These studies suggest that VEGF itself may play a role in the pathogenesis of MS, not only by opening the blood-brain barrier and exposing the brain to compounds it is normally shielded from, but also by inducing inflammation and attracting monocytes. Inducing a blood-brain barrier leakage in naive animals by injecting VEGF is therefore a useful tool to reproduce the blood-brain barrier alterations observed in MS. Moreover, the use of VEGF avoids the use of non-physiological agents that could lead to the triggering of non-physiological mechanisms and pathologies.

VI.8.4- Spasticity

Spasticity is a very common symptom of MS, reported in 84% of patients (Rizzo et al., 2004). Spasticity is thought to be due to a hyperexcitable state of the stretch reflex arc (Heckmann et al., 2005). The determination of the amplitudes of the H-reflex (Voerman et al., 2005) and F-wave (Argyriou et al., 2006; Lin and Floeter, 2004) provide quantitative methods available in the clinic to assess over excitability of neurons and thus spasticity, and these methods have already been used in MS patients to detect spasticity (Argyriou et al., 2010; Bischoff et al., 1992; Smith et al., 1989; Voerman et al., 2005). Our results are in line with what has been found in MS patients, i.e. an increase in H-reflex and F-wave amplitudes occurs, while the M response remains constant (Argyriou et al., 2010). The VEGF lesion may prove to be an excellent model in later studies to investigate the pathways involved in spasticity.

VI.8.5- Features of the preactive lesion

As discussed in the introduction, MS lesions present some heterogeneity in their structure. Staging of MS lesions is a subject of controversy (van der Valk and De Groot, 2000) because of the difficulties to characterize a time frame of lesion evolution. One specific type or stage of lesion, called the (p)reactive lesion (De Groot et al., 2001), is thought to precede the demyelination that characterises active lesions (van der Valk and De Groot, 2000). In this type of lesion, there are clusters of activated microglia, but in the absence of T-cells and demyelination (van der Valk and Amor, 2009; van Horssen et al., 2012; van Noort et al., 2011). This cellular pattern has similarities with what we observe in the VEGF lesion, suggesting that breakdown of the blood-brain barrier may trigger the formation of preactive lesions in MS. Whether the preactive lesions evolve into the classical ‘actively

demyelinating' lesion is uncertain, although current belief is that many preactive lesions subside without any persistent pathology.

The intraspinal injection of VEGF induces a transient (2-three days) breakdown of the blood-brain barrier breakdown, which is shorter than occurs in many MS lesions, based on gadolinium leakage (Cotton et al., 2003). It seems likely that such more chronic leakage would, of course, lead to a longer exposure of the CNS to plasma compounds and that this would exacerbate any damage. Particularly, it has been shown that blood components have toxic effects on oligodendrocytes and myelin protein expression (Juliet et al., 2009) and it seems likely that prolonged blood-brain barrier breakdown may contribute to, or even cause, the degeneration of oligodendrocytes in actively demyelinating lesions.

VI.9- Concluding remark

It is sometimes said that all animal models are wrong, but that some are useful. We agree, and believe that the VEGF lesion may not only prove to be more useful than many models, but also that it may illuminate the mechanisms operating in MS to cause the potentially devastating symptoms. If so, the lesion may provide an avenue to elucidate the underlying mechanisms, and thereby provide the information needed to devise novel and effective therapeutic strategies.

References

Abbott, N.J., Patabendige, A.A., Dolman, D.E., Yusof, S.R., and Begley, D.J. (2010). Structure and function of the blood-brain barrier. Neurobiology of Disease *37*, 13-25.

Abbott, N.J., Ronnback, L., and Hansson, E. (2006). Astrocyte-endothelial interactions at the blood-brain barrier. Nature Reviews Neuroscience *7*, 41-53.

Aboul-Enein, F., Rauschka, H., Kornek, B., Stadelmann, C., Stefferl, A., Bruck, W., Lucchinetti, C., Schmidbauer, M., Jellinger, K., and Lassmann, H. (2003). Preferential loss of Myelin-Associated Glycoprotein reflects hypoxia like white matter damge in stroke and inflammatory brain disease. Journal of Neuropathology and Experimental Neurology *62*, 25-33.

Abraham, C.S., Deli, M.A., Joo, F., Megyeri, P., and Torpier, G. (1996). Intracarotid tumor necrosis factor-alpha administration increases the blood-brain barrier permeability in cerebral cortex of the newborn pig: quantitative aspects of double-labelling studies and confocal laser scanning analysis. Neuroscience letters *208*, 85-88.

Adams, R.A., Schachtrup, C., Davalos, D., Tsigelny, I., and Akassoglou, K. (2007). Fibrinogen signal transduction as a mediator and therapeutic target in inflammation: lessons from multiple sclerosis. Current medicinal chemistry *14*, 2925-2936.

Adhya, S., Johnson, G., Herbert, J., Jaggi, H., Babb, J.S., Grossman, R.I., and Inglese, M. (2006). Pattern of hemodynamic impairment in multiple sclerosis: dynamic susceptibility contrast perfusion MR imaging at 3.0 T. Neuroimage *33*, 1029-1035.

Afifi, A.K., Bergman, R.A. (2005). Functional neuroanatomy: text and atlas, 2nd edn.

Akassoglou, K., Adams, R.A., Bauer, J., Mercado, P., Tseveleki, V., Lassmann, H., Probert, L., and Strickland, S. (2004). Fibrin depletion decreases inflammation and delays the onset of demyelination in a tumor necrosis factor transgenic mouse model for multiple sclerosis. Procedings of the National Academy Science U S A *101*, 6698-6703.

Allt, G., and Lawrenson, J.G. (2001). Pericytes: cell biology and pathology. Cells Tissues Organs *169*, 1-11.

Alusi, S.H., Worthington, J., Glickman, S., and Bain, P.G. (2001). A study of tremor in multiple sclerosis. Brain *124*, 720-730.

Anderson, C.M., and Nedergaard, M. (2003). Astrocyte-mediated control of cerebral microcirculation. Trends in Neurosciences *26*, 340-344; author reply 344-345.

Angelov, L., Doolittle, N.D., Kraemer, D.F., Siegal, T., Barnett, G.H., Peereboom, D.M., Stevens, G., McGregor, J., Jahnke, K., Lacy, C.A*., et al.* (2009). Blood-brain barrier disruption and intra-arterial methotrexate-based therapy for newly diagnosed primary CNS lymphoma: a multi-institutional experience. Journal of clinical oncology : official journal of the American Society of Clinical Oncology *27*, 3503-3509.

Aoyama, M., Hongo, T., and Kudo, N. (1988). Sensory input to cells of origin of uncrossed spinocerebellar tract located below Clarke's column in the cat. Journal of Physiology *398*, 233-257.

Araque, A., Parpura, V., Sanzgiri, R.P., and Haydon, P.G. (1998). Glutamate-dependent astrocyte modulation of synaptic transmission between cultured hippocampal neurons. European Journal of Neuroscience *10*, 2129-2142.

Argaw, A.T., Asp, L., Zhang, J., Navrazhina, K., Pham, T., Mariani, J.N., Mahase, S., Dutta, D.J., Seto, J., Kramer, E.G*., et al.* (2012). Astrocyte-derived VEGF-A drives blood-brain barrier disruption in CNS inflammatory disease. Journal of Clinical Investigation *122*, 2454-2468.

Argyriou, A.A., Karanasios, P., Makridou, A., and Makris, N. (2010). F-wave characteristics as surrogate markers of spasticity in patients with secondary progressive multiple sclerosis. Journal of Clinical Neurophysiology *27*, 120-125.

Argyriou, A.A., Polychronopoulos, P., Talelli, P., and Chroni, E. (2006). F wave study in amyotrophic lateral sclerosis: assessment of balance between upper and lower motor neuron involvement. Clinical Neuropharmacology *117*, 1260-1265.

Armulik, A., Abramsson, A., and Betsholtz, C. (2005). Endothelial/pericyte interactions. Circulation Research *97*, 512-523.

Arteel, G.E., Thurman, R.G., and Raleigh, J.A. (1998). Reductive metabolism of the hypoxia marker pimonidazole is regulated by oxygen tension independent of the pyridine nucleotide redox state. European Journal of Biochemistry *253*, 743-750.

Arteel, G.E., Thurman, R.G., Yates, J.M., and Raleigh, J.A. (1995). Evidence that hypoxia markers detect oxygen gradients in liver: pimonidazole and retrograde perfusion of rat liver. British journal of cancer *72*, 889-895.

Arundine, M., and Tymianski, M. (2003). Molecular mechanisms of calcium-dependent neurodegeneration in excitotoxicity. Cell Calcium *34*, 325-337.

Autiero, M., Luttun, A., Tjwa, M., and Carmeliet, P. (2003). Placental growth factor and its receptor, vascular endothelial growth factor receptor-1: novel targets for stimulation of ischemic tissue revascularization and inhibition of angiogenic and inflammatory disorders. Journal of Thrombosis and Haemostasis *1*, 1356-1370.

Banks, W.A., and Kastin, A.J. (1997). The role of the blood-brain barrier transporter PTS-1 in regulating concentrations of methionine enkephalin in blood and brain. Alcohol *14*, 237-245.

Banks, W.A., Kastin, A.J., Horvath, A., and Michals, E.A. (1987). Carrier-mediated transport of vasopressin across the blood-brain barrier of the mouse. Journal of Neurology Research *18*, 326-332.

Barleon, B., Sozzani, S., Zhou, D., Weich, H.A., Mantovani, A., and Marme, D. (1996). Migration of human monocytes in response to vascular endothelial growth factor (VEGF) is mediated via the VEGF receptor flt-1. Blood *87*, 3336-3343.

Barnett, M.H., and Prineas, J.W. (2004). Relapsing and remitting multiple sclerosis: pathology of the newly forming lesion. Annals of Neurology *55*, 458-468.

Barrera, C.M., Kastin, A.J., and Banks, W.A. (1987). D-[Ala1]-peptide T-amide is transported from blood to brain by a saturable system. Brain Research Bulletin *19*, 629-633.

Barrera, C.M., Kastin, A.J., Fasold, M.B., and Banks, W.A. (1991). Bidirectional saturable transport of LHRH across the blood-brain barrier. The American journal of physiology *261*, E312-318.

Bates, D.O., and Harper, S.J. (2002). Regulation of vascular permeability by vascular endothelial growth factors. Vascular pharmacology *39*, 225-237.

Bauser-Heaton, H.D., Song, J., and Bohlen, H.G. (2008). Cerebral microvascular nNOS responds to lowered oxygen tension through a bumetanide-sensitive cotransporter and sodium-calcium exchanger. American journal of physiology Heart and circulatory physiology *294*, H2166-2173.

Bazzoni, G., Martinez-Estrada, O.M., Mueller, F., Nelboeck, P., Schmid, G., Bartfai, T., Dejana, E., and Brockhaus, M. (2000a). Homophilic interaction of junctional adhesion molecule. Journal of Biochemical Chemistry *275*, 30970-30976.

Bazzoni, G., Martinez-Estrada, O.M., Orsenigo, F., Cordenonsi, M., Citi, S., and Dejana, E. (2000b). Interaction of junctional adhesion molecule with the tight junction components ZO-1, cingulin, and occludin. Journal of Biological Chemistry *275*, 20520-20526.

Beare, J.E., Morehouse, J.R., DeVries, W.H., Enzmann, G.U., Burke, D.A., Magnuson, D.S., and Whittemore, S.R. (2009). Gait analysis in normal and spinal contused mice using the TreadScan system. Journal of Neurotrauma *26*, 2045-2056.

Bell, R.D., and Zlokovic, B.V. (2009). Neurovascular mechanisms and blood-brain barrier disorder in Alzheimer's disease. Acta Neuropathol *118*, 103-113.

Ben-Nun, A., Mendel, I., Bakimer, R., Fridkis-Hareli, M., Teitelbaum, D., Arnon, R., Sela, M., and Kerlero de Rosbo, N. (1996). The autoimmune reactivity to myelin oligodendrocyte

glycoprotein (MOG) in multiple sclerosis is potentially pathogenic: effect of copolymer 1 on MOG-induced disease. Journal of neurology *243*, S14-22.

Bennett, D.J., Gorassini, M., Fouad, K., Sanelli, L., Han, Y., and Cheng, J. (1999). Spasticity in rats with sacral spinal cord injury. Journal of Neurotrauma *16*, 69-84.

Bennett, J., Basivireddy, J., Kollar, A., Biron, K.E., Reickmann, P., Jefferies, W.A., and McQuaid, S. (2010). Blood-brain barrier disruption and enhanced vascular permeability in the multiple sclerosis model EAE. Journal of Neuroimmunology *229*, 180-191.

Benton, R.L., and Whittemore, S.R. (2003). VEGF165 therapy exacerbates secondary damage following spinal cord injury. Neurochemical Research *28*, 1693-1703.

Bernacki, J., Dobrowolska, A., Nierwinska, K., and Malecki, A. (2008). Physiology and pharmacological role of the blood-brain barrier. Pharmacological Reports *60*, 600-622.

Bernatchez, P.N., Bauer, P.M., Yu, J., Prendergast, J.S., He, P., and Sessa, W.C. (2005). Dissecting the molecular control of endothelial NO synthase by caveolin-1 using cell-permeable peptides. Procedings of the National Academy of Science U S A *102*, 761-766.

Berse, B., Brown, L.F., Van de Water, L., Dvorak, H.F., and Senger, D.R. (1992). Vascular permeability factor (vascular endothelial growth factor) gene is expressed differentially in normal tissues, macrophages, and tumors. Molecular Biology of the Cell *3*, 211-220.

Bezzi, P., Carmignoto, G., Pasti, L., Vesce, S., Rossi, D., Rizzini, B.L., Pozzan, T., and Volterra, A. (1998). Prostaglandins stimulate calcium-dependent glutamate release in astrocytes. Nature *391*, 281-285.

Bezzi, P., Domercq, M., Brambilla, L., Galli, R., Schols, D., De Clercq, E., Vescovi, A., Bagetta, G., Kollias, G., Meldolesi, J.*, et al.* (2001). CXCR4-activated astrocyte glutamate release via TNFalpha: amplification by microglia triggers neurotoxicity. Nature neuroscience *4*, 702-710.

Bischoff, C., Schoenle, P.W., and Conrad, B. (1992). Increased F-wave duration in patients with spasticity. Electromyogr Clin Neurophysiol *32*, 449-453.

Bitsch, A., Schuchardt, J., Bunkowski, S., Kuhlmann, T., and Bruck, W. (2000). Acute axonal injury in multiple sclerosis. Correlation with demyelination and inflammation. Brain *123 (Pt 6)*, 1174-1183.

Black, J.A., Felts, P., Smith, K.J., Kocsis, J.D., and Waxman, S.G. (1997). Distribution of sodium channels in chronically demyelinated spinal cord axons: immunoultrastructural localization and electrophysiological observations. Brain Research 544 (1991) 59-70. Brain research *761*, 1.

Blamire, A.M., Anthony, D.C., Rajagopalan, B., Sibson, N.R., Perry, V.H., and Styles, P. (2000). Interleukin-1beta -induced changes in blood-brain barrier permeability, apparent

diffusion coefficient, and cerebral blood volume in the rat brain: a magnetic resonance study. Journal of neuroscience *20*, 8153-8159.

Bo, L., Dawson, T.M., Wesselingh, S., Mork, S., Choi, S., Kong, P.A., Hanley, D., and Trapp, B.D. (1994). Induction of nitric oxide synthase in demyelinating regions of multiple sclerosis brains. Annals of Neurology *36*, 778-786.

Bolton, S.J., Anthony, D.C., and Perry, V.H. (1998). Loss of the tight junction proteins occludin and zonula occludens-1 from cerebral vascular endothelium during neutrophil-induced blood-brain barrier breakdown in vivo. Neuroscience *86*, 1245-1257.

Bottomley, M.J., Webb, N.J., Watson, C.J., Holt, L., Bukhari, M., Denton, J., Freemont, A.J., and Brenchley, P.E. (2000). Placenta growth factor (PlGF) induces vascular endothelial growth factor (VEGF) secretion from mononuclear cells and is co-expressed with VEGF in synovial fluid. Clinical Experimental Immunology *119*, 182-188.

Breviario, F., Caveda, L., Corada, M., Martin-Padura, I., Navarro, P., Golay, J., Introna, M., Gulino, D., Lampugnani, M.G., and Dejana, E. (1995). Functional properties of human vascular endothelial cadherin (7B4/cadherin-5), an endothelium-specific cadherin. Arteriosclerosis, thrombosis, and vascular biology *15*, 1229-1239.

Brightman, M.W., and Reese, T.S. (1969). Junctions between intimately apposed cell membranes in the vertebrate brain. Journal of Cellular Biology *40*, 648-677.

Brown, P.D., Davies, S.L., Speake, T., and Millar, I.D. (2004). Molecular mechanisms of cerebrospinal fluid production. Neuroscience *129*, 957-970.

Bucci, M., Gratton, J.P., Rudic, R.D., Acevedo, L., Roviezzo, F., Cirino, G., and Sessa, W.C. (2000). In vivo delivery of the caveolin-1 scaffolding domain inhibits nitric oxide synthesis and reduces inflammation. Nature medicine *6*, 1362-1367.

Burke, D. (2014). Inability of F waves to control for changes in the excitability of the motoneurone pool in motor control studies. Clinical Neurophysiology *125*, 221-222.

Burstein, R., Dado, R.J., and Giesler, G.J., Jr. (1990). The cells of origin of the spinothalamic tract of the rat: a quantitative reexamination. Brain research *511*, 329-337.

Bushell, T. (2007). The emergence of proteinase-activated receptor-2 as a novel target for the treatment of inflammation-related CNS disorders. Journal of Physiology *581*, 7-16.

Butter, C., Baker, D., O'Neill, J.K., and Turk, J.L. (1991). Mononuclear cell trafficking and plasma protein extravasation into the CNS during chronic relapsing experimental allergic encephalomyelitis in Biozzi AB/H mice. Journal of Neurological Sciences *104*, 9-12.

Cataldo, A.M., and Broadwell, R.D. (1986). Cytochemical identification of cerebral glycogen and glucose-6-phosphatase activity under normal and experimental conditions. II. Choroid

plexus and ependymal epithelia, endothelia and pericytes. Journal of Neurocytology *15*, 511-524.

Cavallari, P., and Pettersson, L.G. (1989). Tonic suppression of reflex transmission in low spinal cats. Experimental Brain Research *77*, 201-212.

Cerasa, A., Fera, F., Gioia, M.C., Liguori, M., Passamonti, L., Nicoletti, G., Vercillo, L., Paolillo, A., Clodomiro, A., Valentino, P.*, et al.* (2006). Adaptive cortical changes and the functional correlates of visuo-motor integration in relapsing-remitting multiple sclerosis. Brain Research Bulletins *69*, 597-605.

Charcot, M. (1868). Histologie de la sclerose en pnaques. Gaz Hosp *121*, 554-555, 557-558.

Choi, S.H., Lee, D.Y., Chung, E.S., Hong, Y.B., Kim, S.U., and Jin, B.K. (2005a). Inhibition of thrombin-induced microglial activation and NADPH oxidase by minocycline protects dopaminergic neurons in the substantia nigra in vivo. Journal of Neurochemistry *95*, 1755-1765.

Choi, S.H., Lee, D.Y., Kim, S.U., and Jin, B.K. (2005b). Thrombin-induced oxidative stress contributes to the death of hippocampal neurons in vivo: role of microglial NADPH oxidase. J Journal of Neuroscience *25*, 4082-4090.

Christensen, M.D., and Hulsebosch, C.E. (1997). Chronic central pain after spinal cord injury. Journal of Neurotrauma *14*, 517-537.

Claudio, L., Kress, Y., Factor, J., and Brosnan, C.F. (1990). Mechanisms of edema formation in experimental autoimmune encephalomyelitis. The contribution of inflammatory cells. The American journal of pathology *137*, 1033-1045.

Clauss, M., Weich, H., Breier, G., Knies, U., Rockl, W., Waltenberger, J., and Risau, W. (1996). The vascular endothelial growth factor receptor Flt-1 mediates biological activities. Implications for a functional role of placenta growth factor in monocyte activation and chemotaxis. Journal of Biochemical Chemistry *271*, 17629-17634.

Compston, A., and Coles, A. (2002). Multiple sclerosis. Lancet *359*, 1221-1231.

Conta, A.C.S., D.J. (2009). The propriospinal system. In The spinal cord, pp. 180-190.

Cotter, T.G., Lennon, S.V., Glynn, J.G., and Martin, S.J. (1990). Cell death via apoptosis and its relationship to growth, development and differentiation of both tumour and normal cells. Anticancer research *10*, 1153-1160.

Cotton, F., Weiner, H.L., Jolesz, F.A., and Guttmann, C.R. (2003). MRI contrast uptake in new lesions in relapsing-remitting MS followed at weekly intervals. Neurology *60*, 640-646.

D'Arcangelo, G., Grassi, F., Ragozzino, D., Santoni, A., Tancredi, V., and Eusebi, F. (1991). Interferon inhibits synaptic potentiation in rat hippocampus. Brain research *564*, 245-248.

Daneman, R., Zhou, L., Kebede, A.A., and Barres, B.A. (2010). Pericytes are required for blood-brain barrier integrity during embryogenesis. Nature *468*, 562-566.

David, Y., Cacheaux, L.P., Ivens, S., Lapilover, E., Heinemann, U., Kaufer, D., and Friedman, A. (2009). Astrocytic dysfunction in epileptogenesis: consequence of altered potassium and glutamate homeostasis? Journal of neuroscience *29*, 10588-10599.

Davies, A.L., Desai, R.A., Bloomfield, P.S., McIntosh, P.R., Chapple, K.J., Linington, C., Fairless, R., Diem, R., Kasti, M., Murphy, M.P*., et al.* (2013). Neurological deficits caused by tissue hypoxia in neuroinflammatory disease. Annals of Neurology.

De Groot, C.J., Bergers, E., Kamphorst, W., Ravid, R., Polman, C.H., Barkhof, F., and van der Valk, P. (2001). Post-mortem MRI-guided sampling of multiple sclerosis brain lesions: increased yield of active demyelinating and (p)reactive lesions. Brain *124*, 1635-1645.

Deacon, R.M. (2006). Burrowing in rodents: a sensitive method for detecting behavioral dysfunction. Nature protocols *1*, 118-121.

Deacon, R.M. (2009). Burrowing: a sensitive behavioural assay, tested in five species of laboratory rodents. Behavioural brain research *200*, 128-133.

Del Maschio, A., De Luigi, A., Martin-Padura, I., Brockhaus, M., Bartfai, T., Fruscella, P., Adorini, L., Martino, G., Furlan, R., De Simoni, M.G*., et al.* (1999). Leukocyte recruitment in the cerebrospinal fluid of mice with experimental meningitis is inhibited by an antibody to junctional adhesion molecule (JAM). Journal of Experimental Medicine *190*, 1351-1356.

del Zoppo, G.J., and Milner, R. (2006). Integrin-matrix interactions in the cerebral microvasculature. Arteriosclerosis, thrombosis, and vascular biology *26*, 1966-1975.

Del Zoppo, G.J., Milner, R., Mabuchi, T., Hung, S., Wang, X., and Koziol, J.A. (2006). Vascular matrix adhesion and the blood-brain barrier. Biochemical Society Transactions *34*, 1261-1266.

Desai, B.S., Monahan, A.J., Carvey, P.M., and Hendey, B. (2007). Blood-brain barrier pathology in Alzheimer's and Parkinson's disease: implications for drug therapy. Cell Transplant *16*, 285-299.

Devinsky, O., Vezzani, A., Najjar, S., De Lanerolle, N.C., and Rogawski, M.A. (2013). Glia and epilepsy: excitability and inflammation. Trends in Neurosciences *36*, 174-184.

Dheen, S.T., Kaur, C., and Ling, E.A. (2007). Microglial activation and its implications in the brain diseases. Current medicinal chemistry *14*, 1189-1197.

Dux, E., Temesvari, P., Joo, F., Adam, G., Clementi, F., Dux, L., Hideg, J., and Hossmann, K.A. (1984). The blood-brain barrier in hypoxia: ultrastructural aspects and adenylate cyclase activity of brain capillaries. Neuroscience *12*, 951-958.

Ehrlich, P. (1904). Ueber die beziehungen von chemischer constiution, verteilung und pharmakologisher wirkung. Gesammelte Arbeiten zur Immunitaetsforschung, 574.

Engelhardt, B., and Wolburg, H. (2004). Mini-review: Transendothelial migration of leukocytes: through the front door or around the side of the house? European Journal of Immunology *34*, 2955-2963.

Espiritu, M.G., Lin, C.S., and Burke, D. (2003). Motoneuron excitability and the F wave. Muscle & nerve *27*, 720-727.

Fabis, M.J., Scott, G.S., Kean, R.B., Koprowski, H., and Hooper, D.C. (2007). Loss of blood-brain barrier integrity in the spinal cord is common to experimental allergic encephalomyelitis in knockout mouse models. Procedings of the National Academy of Science U S A *104*, 5656-5661.

Fanning, A.S., Jameson, B.J., Jesaitis, L.A., and Anderson, J.M. (1998). The tight junction protein ZO-1 establishes a link between the transmembrane protein occludin and the actin cytoskeleton. Journal of Biological Chemistry *273*, 29745-29753.

Farkas, E., Donka, G., de Vos, R.A., Mihaly, A., Bari, F., and Luiten, P.G. (2004). Experimental cerebral hypoperfusion induces white matter injury and microglial activation in the rat brain. Acta Neuropathol *108*, 57-64.

Felts, P.A., Woolston, A.M., Fernando, H.B., Asquith, S., Gregson, N.A., Mizzi, O.J., and Smith, K.J. (2005). Inflammation and primary demyelination induced by the intraspinal injection of lipopolysaccharide. Brain *128*, 1649-1666.

Ferrara, N., and Henzel, W.J. (1989). Pituitary follicular cells secrete a novel heparin-binding growth factor specific for vascular endothelial cells. Biochemical and Biophysical Research Commun *161*, 851-858.

Fischer, S., Wobben, M., Marti, H.H., Renz, D., and Schaper, W. (2002). Hypoxia-induced hyperpermeability in brain microvessel endothelial cells involves VEGF-mediated changes in the expression of zonula occludens-1. Microvasc Res *63*, 70-80.

Flanders, A.E., Spettell, C.M., Friedman, D.P., Marino, R.J., and Herbison, G.J. (1999). The relationship between the functional abilities of patients with cervical spinal cord injury and the severity of damage revealed by MR imaging. American Journal of Neuroradiology *20*, 926-934.

Flick, M.J., Du, X., and Degen, J.L. (2004a). Fibrin(ogen)-alpha M beta 2 interactions regulate leukocyte function and innate immunity in vivo. Experimental Biology and Medicine (Maywood) *229*, 1105-1110.

Flick, M.J., Du, X., Witte, D.P., Jirouskova, M., Soloviev, D.A., Busuttil, S.J., Plow, E.F., and Degen, J.L. (2004b). Leukocyte engagement of fibrin(ogen) via the integrin receptor alphaMbeta2/Mac-1 is critical for host inflammatory response in vivo. Journal of Clinical Investigation *113*, 1596-1606.

Floris, S., Blezer, E.L., Schreibelt, G., Dopp, E., van der Pol, S.M., Schadee-Eestermans, I.L., Nicolay, K., Dijkstra, C.D., and de Vries, H.E. (2004). Blood-brain barrier permeability and monocyte infiltration in experimental allergic encephalomyelitis: a quantitative MRI study. Brain *127*, 616-627.

Fossier, P., Blanchard, B., Ducrocq, C., Leprince, C., Tauc, L., and Baux, G. (1999). Nitric oxide transforms serotonin into an inactive form and this affects neuromodulation. Neuroscience *93*, 597-603.

Frigerio, F., Frasca, A., Weissberg, I., Parrella, S., Friedman, A., Vezzani, A., and Noe, F.M. (2012). Long-lasting pro-ictogenic effects induced in vivo by rat brain exposure to serum albumin in the absence of concomitant pathology. Epilepsia *53*, 1887-1897.

Fukumura, D., Gohongi, T., Kadambi, A., Izumi, Y., Ang, J., Yun, C.O., Buerk, D.G., Huang, P.L., and Jain, R.K. (2001). Predominant role of endothelial nitric oxide synthase in vascular endothelial growth factor-induced angiogenesis and vascular permeability. Proceedings of the National Academy of Sciences of the United States of America *98*, 2604-2609.

Fukumura, D., and Jain, R.K. (1998). Role of nitric oxide in angiogenesis and microcirculation in tumors. Cancer Metastasis Review *17*, 77-89.

Fulton, D., Gratton, J.P., McCabe, T.J., Fontana, J., Fujio, Y., Walsh, K., Franke, T.F., Papapetropoulos, A., and Sessa, W.C. (1999). Regulation of endothelium-derived nitric oxide production by the protein kinase Akt. Nature *399*, 597-601.

Furuse, M., Fujita, K., Hiiragi, T., Fujimoto, K., and Tsukita, S. (1998). Claudin-1 and -2: novel integral membrane proteins localizing at tight junctions with no sequence similarity to occludin. Journal of Cellular Biology *141*, 1539-1550.

Furuse, M., Hirase, T., Itoh, M., Nagafuchi, A., Yonemura, S., and Tsukita, S. (1993). Occludin: a novel integral membrane protein localizing at tight junctions. Journal of Cellular Biology *123*, 1777-1788.

Gale, K., Kerasidis, H., and Wrathall, J.R. (1985). Spinal cord contusion in the rat: behavioral analysis of functional neurologic impairment. Experimental Neurology *88*, 123-134.

Galea, E., Feinstein, D.L., and Reis, D.J. (1992). Induction of calcium-independent nitric oxide synthase activity in primary rat glial cultures. Procedings of the National Academy of Science U S A *89*, 10945-10949.

Ge, Y., Zohrabian, V.M., and Grossman, R.I. (2008). Seven-Tesla magnetic resonance imaging: new vision of microvascular abnormalities in multiple sclerosis. Arch Neurol *65*, 812-816.

Gelderd, J.B., and Chopin, S.F. (1977). The vertebral level of origin of spinal nerves in the rat. Anatomical Record *188*, 45-47.

Giesler, G.J., Jr., and Cliffer, K.D. (1985). Postsynaptic dorsal column pathway of the rat. II. Evidence against an important role in nociception. Brain research *326*, 347-356.

Gijbels, K., Van Damme, J., Proost, P., Put, W., Carton, H., and Billiau, A. (1990). Interleukin 6 production in the central nervous system during experimental autoimmune encephalomyelitis. European Journal of Immunology *20*, 233-235.

Gingrich, M.B., Junge, C.E., Lyuboslavsky, P., and Traynelis, S.F. (2000). Potentiation of NMDA receptor function by the serine protease thrombin. Journal of neuroscience *20*, 4582-4595.

Gold, R., Linington, C., and Lassmann, H. (2006). Understanding pathogenesis and therapy of multiple sclerosis via animal models: 70 years of merits and culprits in experimental autoimmune encephalomyelitis research. Brain *129*, 1953-1971.

Goldmann, E.E. (1913). Vitalfarbung am Zentral-nerbensystem. Abh Preuss Akad Wissensch, Physkol Mathem Klasse *60*.

Gratton, J.P., Lin, M.I., Yu, J., Weiss, E.D., Jiang, Z.L., Fairchild, T.A., Iwakiri, Y., Groszmann, R., Claffey, K.P., Cheng, Y.C.*, et al.* (2003). Selective inhibition of tumor microvascular permeability by cavtratin blocks tumor progression in mice. Cancer Cell *4*, 31-39.

Gumbiner, B., Lowenkopf, T., and Apatira, D. (1991). Identification of a 160-kDa polypeptide that binds to the tight junction protein ZO-1. Procedings of the National Academy of Science U S A *88*, 3460-3464.

Hansen, A.J. (1985). Effect of anoxia on ion distribution in the brain. Physiological reviews *65*, 101-148.

Hatakeyama, T., Pappas, P.J., Hobson, R.W., 2nd, Boric, M.P., Sessa, W.C., and Duran, W.N. (2006). Endothelial nitric oxide synthase regulates microvascular hyperpermeability in vivo. Journal of Physiology *574*, 275-281.

Hattori, K., Heissig, B., Wu, Y., Dias, S., Tejada, R., Ferris, B., Hicklin, D.J., Zhu, Z., Bohlen, P., Witte, L.*, et al.* (2002). Placental growth factor reconstitutes hematopoiesis by recruiting VEGFR1(+) stem cells from bone-marrow microenvironment. Nature medicine *8*, 841-849.

Haugland, H.K., Vukovic, V., Pintilie, M., Fyles, A.W., Milosevic, M., Hill, R.P., and Hedley, D.W. (2002). Expression of hypoxia-inducible factor-1alpha in cervical carcinomas: correlation with tumor oxygenation. International journal of radiation oncology, biology, physics *53*, 854-861.

Hawkins, B.T., and Davis, T.P. (2005). The blood-brain barrier/neurovascular unit in health and disease. Pharmacol Rev *57*, 173-185.

Hawkins, C.P., Mackenzie, F., Tofts, P., du Boulay, E.P., and McDonald, W.I. (1991). Patterns of blood-brain barrier breakdown in inflammatory demyelination. Brain *114 (Pt 2)*, 801-810.

Hawkins, R.A. (2009). The blood-brain barrier and glutamate. American Journal of Clinical Nutrition *90*, 867S-874S.

Hawkins, R.A., O'Kane, R.L., Simpson, I.A., and Vina, J.R. (2006). Structure of the blood-brain barrier and its role in the transport of amino acids. The Journal of nutrition *136*, 218S-226S.

Heckmann, C.J., Gorassini, M.A., and Bennett, D.J. (2005). Persistent inward currents in motoneuron dendrites: implications for motor output. Muscle & nerve *31*, 135-156.

Heinemann, U., Kaufer, D., and Friedman, A. (2012). Blood-brain barrier dysfunction, TGFbeta signaling, and astrocyte dysfunction in epilepsy. Glia *60*, 1251-1257.

Hickey, W.F., and Kimura, H. (1988). Perivascular microglial cells of the CNS are bone marrow-derived and present antigen in vivo. Science *239*, 290-292.

Hillman, N.J., Whittles, C.E., Pocock, T.M., Williams, B., and Bates, D.O. (2001). Differential effects of vascular endothelial growth factor-C and placental growth factor-1 on the hydraulic conductivity of frog mesenteric capillaries. J Vasc Res *38*, 176-186.

Hirase, T., Kawashima, S., Wong, E.Y., Ueyama, T., Rikitake, Y., Tsukita, S., Yokoyama, M., and Staddon, J.M. (2001). Regulation of tight junction permeability and occludin phosphorylation by Rhoa-p160ROCK-dependent and -independent mechanisms. Journal of Biological Chemistry *276*, 10423-10431.

Hiratsuka, S., Minowa, O., Kuno, J., Noda, T., and Shibuya, M. (1998). Flt-1 lacking the tyrosine kinase domain is sufficient for normal development and angiogenesis in mice. Procedings of the National Academy of Science U S A *95*, 9349-9354.

Hofman, P., Blaauwgeers, H.G., Tolentino, M.J., Adamis, A.P., Nunes Cardozo, B.J., Vrensen, G.F., and Schlingemann, R.O. (2000). VEGF-A induced hyperpermeability of blood-retinal barrier endothelium in vivo is predominantly associated with pinocytotic vesicular transport and not with formation of fenestrations. Vascular endothelial growth factor-A. Curr Eye Res *21*, 637-645.

Hofstetter, L., Naegelin, Y., Filli, L., Kuster, P., Traud, S., Smieskova, R., Mueller-Lenke, N., Kappos, L., Gass, A., Sprenger, T.*, et al.* (2013). Progression in disability and regional grey matter atrophy in relapsing-remitting multiple sclerosis. Multiple Sclerosis.

Hoftberger, R., Aboul-Enein, F., Brueck, W., Lucchinetti, C., Rodriguez, M., Schmidbauer, M., Jellinger, K., and Lassmann, H. (2004). Expression of major histocompatibility complex class I molecules on the different cell types in multiple sclerosis lesions. Brain pathology *14*, 43-50.

Holland, C.M., Charil, A., Csapo, I., Liptak, Z., Ichise, M., Khoury, S.J., Bakshi, R., Weiner, H.L., and Guttmann, C.R. (2012). The relationship between normal cerebral perfusion patterns and white matter lesion distribution in 1,249 patients with multiple sclerosis. Journal of Neuroimmaging *22*, 129-136.

Holmes, K., Roberts, O.L., Thomas, A.M., and Cross, M.J. (2007). Vascular endothelial growth factor receptor-2: structure, function, intracellular signalling and therapeutic inhibition. Cellular signalling *19*, 2003-2012.

Hooper, C., Pinteaux-Jones, F., Fry, V.A., Sevastou, I.G., Baker, D., Heales, S.J., and Pocock, J.M. (2009). Differential effects of albumin on microglia and macrophages; implications for neurodegeneration following blood-brain barrier damage. Journal of Neurochemistry *109*, 694-705.

Hooper, C., Taylor, D.L., and Pocock, J.M. (2005a). Pure albumin is a potent trigger of calcium signalling and proliferation in microglia but not macrophages or astrocytes. Journal of Neurochemistry *92*, 1363-1376.

Hooper, C., Taylor, D.L., and Pocock, J.M. (2005b). Pure albumin is a potent trigger of calcium signalling and proliferation in microglia but not macrophages or astrocytes. Journal of Neurochemistry *92*, 1363-1376.

Hultborn, H., and Nielsen, J.B. (1995). H-reflexes and F-responses are not equally sensitive to changes in motoneuronal excitability. Muscle & nerve *18*, 1471-1474.

Hutchison, G.J., Valentine, H.R., Loncaster, J.A., Davidson, S.E., Hunter, R.D., Roberts, S.A., Harris, A.L., Stratford, I.J., Price, P.M., and West, C.M. (2004). Hypoxia-inducible factor 1alpha expression as an intrinsic marker of hypoxia: correlation with tumor oxygen, pimonidazole measurements, and outcome in locally advanced carcinoma of the cervix. Clinical cancer research : an official journal of the American Association for Cancer Research *10*, 8405-8412.

Igarashi, Y., Utsumi, H., Chiba, H., Yamada-Sasamori, Y., Tobioka, H., Kamimura, Y., Furuuchi, K., Kokai, Y., Nakagawa, T., Mori, M.*, et al.* (1999). Glial cell line-derived neurotrophic factor induces barrier function of endothelial cells forming the blood-brain barrier. Biochemical and Biophysical Research Commun *261*, 108-112.

Itoh, M., Nagafuchi, A., Yonemura, S., Kitani-Yasuda, T., and Tsukita, S. (1993). The 220-kD protein colocalizing with cadherins in non-epithelial cells is identical to ZO-1, a tight junction-associated protein in epithelial cells: cDNA cloning and immunoelectron microscopy. Journal of Cellular Biology *121*, 491-502.

Ivens, S., Kaufer, D., Flores, L.P., Bechmann, I., Zumsteg, D., Tomkins, O., Seiffert, E., Heinemann, U., and Friedman, A. (2007). TGF-beta receptor-mediated albumin uptake into astrocytes is involved in neocortical epileptogenesis. Brain *130*, 535-547.

Jefferies, W.A., Brandon, M.R., Hunt, S.V., Williams, A.F., Gatter, K.C., and Mason, D.Y. (1984). Transferrin receptor on endothelium of brain capillaries. Nature *312*, 162-163.

Jeong, S.M., Hahm, K.D., Shin, J.W., Leem, J.G., Lee, C., and Han, S.M. (2006). Changes in magnesium concentration in the serum and cerebrospinal fluid of neuropathic rats. Acta Anaesthesiologica Scandinavica *50*, 211-216.

Jin, K.L., Mao, X.O., and Greenberg, D.A. (2000a). Vascular endothelial growth factor rescues HN33 neural cells from death induced by serum withdrawal. Journal of Molecular Neuroscience *14*, 197-203.

Jin, K.L., Mao, X.O., and Greenberg, D.A. (2000b). Vascular endothelial growth factor: direct neuroprotective effect in in vitro ischemia. Procedings of the National Academy of Science U S A *97*, 10242-10247.

Jordan, L.M., and Schmidt, B.J. (2002). Propriospinal neurons involved in the control of locomotion: potential targets for repair strategies? Progress in Brain Research *137*, 125-139.

Juliet, P.A., Frost, E.E., Balasubramaniam, J., and Del Bigio, M.R. (2009). Toxic effect of blood components on perinatal rat subventricular zone cells and oligodendrocyte precursor cell proliferation, differentiation and migration in culture. Journal of Neurochemistry *109*, 1285-1299.

Junge, C.E., Lee, C.J., Hubbard, K.B., Zhang, Z., Olson, J.J., Hepler, J.R., Brat, D.J., and Traynelis, S.F. (2004). Protease-activated receptor-1 in human brain: localization and functional expression in astrocytes. Experimental Neurology *188*, 94-103.

Juvin, L., Simmers, J., and Morin, D. (2005). Propriospinal circuitry underlying interlimb coordination in mammalian quadrupedal locomotion. Journal of neuroscience *25*, 6025-6035.

Kalaria, R.N., Cohen, D.L., Premkumar, D.R., Nag, S., LaManna, J.C., and Lust, W.D. (1998). Vascular endothelial growth factor in Alzheimer's disease and experimental cerebral ischemia. Molecular Brain Research *62*, 101-105.

Kaneyama, T., Takizawa, S., Tsugane, S., Yanagisawa, S., Takeichi, N., Ehara, T., Ichikawa, M., and Koh, C.S. (2013). Downregulation of water channel aquaporin-4 in rats with experimental autoimmune encephalomyeritis induced by myelin basic protein. Cellular immunology *281*, 91-99.

Kang, J., Jiang, L., Goldman, S.A., and Nedergaard, M. (1998). Astrocyte-mediated potentiation of inhibitory synaptic transmission. Nature neuroscience *1*, 683-692.

Kanno, S., Oda, N., Abe, M., Terai, Y., Ito, M., Shitara, K., Tabayashi, K., Shibuya, M., and Sato, Y. (2000). Roles of two VEGF receptors, Flt-1 and KDR, in the signal transduction of VEGF effects in human vascular endothelial cells. Oncogene *19*, 2138-2146.

Kayalioglu, G. (2009). Projections from the spinal cord to the brain. In The spinal cord, pp. 148-167.

Kerlero de Rosbo, N., Milo, R., Lees, M.B., Burger, D., Bernard, C.C., and Ben-Nun, A. (1993). Reactivity to myelin antigens in multiple sclerosis. Peripheral blood lymphocytes respond predominantly to myelin oligodendrocyte glycoprotein. Journal of Clinical Investigation *92*, 2602-2608.

Kermode, A.G., Thompson, A.J., Tofts, P., MacManus, D.G., Kendall, B.E., Kingsley, D.P., Moseley, I.F., Rudge, P., and McDonald, W.I. (1990). Breakdown of the blood-brain barrier precedes symptoms and other MRI signs of new lesions in multiple sclerosis. Pathogenetic and clinical implications. Brain : a journal of neurology *113 (Pt 5)*, 1477-1489.

Kiba, A., Sagara, H., Hara, T., and Shibuya, M. (2003). VEGFR-2-specific ligand VEGF-E induces non-edematous hyper-vascularization in mice. Biochemical and Biophysical Research Commun *301*, 371-377.

Kirk, J., Plumb, J., Mirakhur, M., and McQuaid, S. (2003). Tight junctional abnormality in multiple sclerosis white matter affects all calibres of vessel and is associated with blood-brain barrier leakage and active demyelination. Journal of Pathology *201*, 319-327.

Klimova, T., and Chandel, N.S. (2008). Mitochondrial complex III regulates hypoxic activation of HIF. Cell Death and Differentiation *15*, 660-666.

Kniesel, U., and Wolburg, H. (2000). Tight junctions of the blood-brain barrier. Cellular and Molecular Neurobiology *20*, 57-76.

Knudsen, K.A., Soler, A.P., Johnson, K.R., and Wheelock, M.J. (1995). Interaction of alpha-actinin with the cadherin/catenin cell-cell adhesion complex via alpha-catenin. Journal of Cellular Biology *130*, 67-77.

Kroll, J., and Waltenberger, J. (1999). A novel function of VEGF receptor-2 (KDR): rapid release of nitric oxide in response to VEGF-A stimulation in endothelial cells. Biochemical and Biophysical Research Commun *265*, 636-639.

Krum, J.M., Mani, N., and Rosenstein, J.M. (2002). Angiogenic and astroglial responses to vascular endothelial growth factor administration in adult rat brain. Neuroscience *110*, 589-604.

Kuchler, M., Fouad, K., Weinmann, O., Schwab, M.E., and Raineteau, O. (2002). Red nucleus projections to distinct motor neuron pools in the rat spinal cord. Journal of Computational Neurology *448*, 349-359.

Lampugnani, M.G., and Dejana, E. (2007). Adherens junctions in endothelial cells regulate vessel maintenance and angiogenesis. Thrombosis research *120 Suppl 2*, S1-6.

Lando, D., Peet, D.J., Gorman, J.J., Whelan, D.A., Whitelaw, M.L., and Bruick, R.K. (2002). FIH-1 is an asparaginyl hydroxylase enzyme that regulates the transcriptional activity of hypoxia-inducible factor. Genes and Development *16*, 1466-1471.

Law, M., Saindane, A.M., Ge, Y., Babb, J.S., Johnson, G., Mannon, L.J., Herbert, J., and Grossman, R.I. (2004). Microvascular abnormality in relapsing-remitting multiple sclerosis: perfusion MR imaging findings in normal-appearing white matter. Radiology *231*, 645-652.

Lee da, Y., Park, K.W., and Jin, B.K. (2006). Thrombin induces neurodegeneration and microglial activation in the cortex in vivo and in vitro: proteolytic and non-proteolytic actions. Biochemical and Biophysical Research Commun *346*, 727-738.

Lee, S.W., Kim, W.J., Choi, Y.K., Song, H.S., Son, M.J., Gelman, I.H., Kim, Y.J., and Kim, K.W. (2003). SSeCKS regulates angiogenesis and tight junction formation in blood-brain barrier. Nature medicine *9*, 900-906.

Lee, S.Y., and Haydon, P.G. (2007). Astrocytic glutamate targets NMDA receptors. Journal of Physiology *581*, 887-888.

Leech, S., Kirk, J., Plumb, J., and McQuaid, S. (2007). Persistent endothelial abnormalities and blood-brain barrier leak in primary and secondary progressive multiple sclerosis. Neuropathology and applied neurobiology *33*, 86-98.

Lemstrom, K.B., Krebs, R., Nykanen, A.I., Tikkanen, J.M., Sihvola, R.K., Aaltola, E.M., Hayry, P.J., Wood, J., Alitalo, K., Yla-Herttuala, S.*, et al.* (2002). Vascular endothelial growth factor enhances cardiac allograft arteriosclerosis. Circulation *105*, 2524-2530.

Li, Q.X., Xiong, Z.Y., Hu, B.P., Tian, Z.J., Zhang, H.F., Gou, W.Y., Wang, H.C., Gao, F., and Zhang, Q.J. (2009). Aging-associated insulin resistance predisposes to hypertension and its reversal by exercise: the role of vascular vasorelaxation to insulin. Basic Res Cardiol *104*, 269-284.

Lin, J.Z., and Floeter, M.K. (2004). Do F-wave measurements detect changes in motor neuron excitability? Muscle & nerve *30*, 289-294.

Lok, J., Gupta, P., Guo, S., Kim, W.J., Whalen, M.J., van Leyen, K., and Lo, E.H. (2007). Cell-cell signaling in the neurovascular unit. Neurochemical Research *32*, 2032-2045.

Loscher, W., and Potschka, H. (2005). Drug resistance in brain diseases and the role of drug efflux transporters. Nature Review of Molecular and Cellular Biology *6*, 591-602.

Lu, X., Rong, Y., and Baudry, M. (2000). Calpain-mediated degradation of PSD-95 in developing and adult rat brain. Neuroscience letters *286*, 149-153.

Lucchinetti, C., Bruck, W., Parisi, J., Scheithauer, B., Rodriguez, M., and Lansmann, H. (2000). Heterogeneity of Multiple Sclerosis Lesions: Implications for Pathogenesis of Demyelination. Annals of Neurology *47*, 707-717.

Luttun, A., Tjwa, M., Moons, L., Wu, Y., Angelillo-Scherrer, A., Liao, F., Nagy, J.A., Hooper, A., Priller, J., De Klerck, B.*, et al.* (2002). Revascularization of ischemic tissues by PlGF

treatment, and inhibition of tumor angiogenesis, arthritis and atherosclerosis by anti-Flt1. Nature medicine *8*, 831-840.

MacMicking, J.D., Willenborg, D.O., Weidemann, M.J., Rockett, K.A., and Cowden, W.B. (1992). Elevated secretion of reactive nitrogen and oxygen intermediates by inflammatory leukocytes in hyperacute experimental autoimmune encephalomyelitis: enhancement by the soluble products of encephalitogenic T cells. Journal of Experimental Medicine *176*, 303-307.

Maggio, N., Shavit, E., Chapman, J., and Segal, M. (2008). Thrombin induces long-term potentiation of reactivity to afferent stimulation and facilitates epileptic seizures in rat hippocampal slices: toward understanding the functional consequences of cerebrovascular insults. Journal of neuroscience *28*, 732-736.

Man, S., Ubogu, E.E., and Ransohoff, R.M. (2007). Inflammatory cell migration into the central nervous system: a few new twists on an old tale. Brain pathology *17*, 243-250.

Mankertz, J., Tavalali, S., Schmitz, H., Mankertz, A., Riecken, E.O., Fromm, M., and Schulzke, J.D. (2000). Expression from the human occludin promoter is affected by tumor necrosis factor alpha and interferon gamma. Journal of Cellular Science *113 (Pt 11)*, 2085-2090.

Marik, C., Felts, P.A., Bauer, J., Lassmann, H., and Smith, K.J. (2007). Lesion genesis in a subset of patients with multiple sclerosis: a role for innate immunity? Brain *130*, 2800-2815.

Martin, R.J., Apkarian, A.V., and Hodge, C.J., Jr. (1990). Ventrolateral and dorsolateral ascending spinal cord pathway influence on thalamic nociception in cat. Journal of Neurophysiology *64*, 1400-1412.

Masliah, E., Alford, M., DeTeresa, R., Mallory, M., and Hansen, L. (1996). Deficient glutamate transport is associated with neurodegeneration in Alzheimer's disease. Annals of Neurology *40*, 759-766.

Matsuzaki, H., Tamatani, M., Yamaguchi, A., Namikawa, K., Kiyama, H., Vitek, M.P., Mitsuda, N., and Tohyama, M. (2001). Vascular endothelial growth factor rescues hippocampal neurons from glutamate-induced toxicity: signal transduction cascades. FASEB Journal *15*, 1218-1220.

Maxwell, P.H., Wiesener, M.S., Chang, G.W., Clifford, S.C., Vaux, E.C., Cockman, M.E., Wykoff, C.C., Pugh, C.W., Maher, E.R., and Ratcliffe, P.J. (1999). The tumour suppressor protein VHL targets hypoxia-inducible factors for oxygen-dependent proteolysis. Nature *399*, 271-275.

McDonald, J.W., Althomsons, S.P., Hyrc, K.L., Choi, D.W., and Goldberg, M.P. (1998). Oligodendrocytes from forebrain are highly vulnerable to AMPA/kainate receptor-mediated excitotoxicity. Nature medicine *4*, 291-297.

McHanwell, S.W., C. (2009). Localization of motorneurons in the spinal cord. In The spinal cord, pp. 94-114.

McKenna, M.C., Gruetter, R. Sonnewald, U. Waagepetersen, H. Schousboe, A. (2006). Energy metabollism of the brain: Molecular, cellular and medical aspects. In Basic Neurochemistry (San Diego: Academic Press), pp. 531-558.

Meli, R., Raso, G.M., Cicala, C., Esposito, E., Fiorino, F., and Cirino, G. (2001). Thrombin and PAR-1 activating peptide increase iNOS expression in cytokine-stimulated C6 glioma cells. Journal of Neurochemistry *79*, 556-563.

Metz, G.A., and Whishaw, I.Q. (2002a). Cortical and subcortical lesions impair skilled walking in the ladder rung walking test: a new task to evaluate fore- and hindlimb stepping, placing, and co-ordination. Journal of neuroscience methods *115*, 169-179.

Metz, G.A., and Whishaw, I.Q. (2002b). Drug-induced rotation intensity in unilateral dopamine-depleted rats is not correlated with end point or qualitative measures of forelimb or hindlimb motor performance. Neuroscience *111*, 325-336.

Metz, G.A., and Whishaw, I.Q. (2009). The ladder rung walking task: a scoring system and its practical application. Journal of visualized experiments : JoVE.

Michalak, Z., Lebrun, A., Di Miceli, M., Rousset, M.C., Crespel, A., Coubes, P., Henshall, D.C., Lerner-Natoli, M., and Rigau, V. (2012). IgG leakage may contribute to neuronal dysfunction in drug-refractory epilepsies with blood-brain barrier disruption. Journal of Neuropathology and Experimental Neurology *71*, 826-838.

Minassian, K., Jilge, B., Rattay, F., Pinter, M.M., Binder, H., Gerstenbrand, F., and Dimitrijevic, M.R. (2004). Stepping-like movements in humans with complete spinal cord injury induced by epidural stimulation of the lumbar cord: electromyographic study of compound muscle action potentials. Spinal Cord *42*, 401-416.

Miyakawa, T. (2010). Vascular pathology in Alzheimer's disease. Psychogeriatrics : the official journal of the Japanese Psychogeriatric Society *10*, 39-44.

Molander, C., and Grant, G. (1987). Spinal cord projections from hindlimb muscle nerves in the rat studied by transganglionic transport of horseradish peroxidase, wheat germ agglutinin conjugated horseradish peroxidase, or horseradish peroxidase with dimethylsulfoxide. Journal of Computational Neurology *260*, 246-255.

Moller, T., Hanisch, U.K., and Ransom, B.R. (2000). Thrombin-induced activation of cultured rodent microglia. Journal of Neurochemistry *75*, 1539-1547.

Mor, F., Quintana, F.J., and Cohen, I.R. (2004). Angiogenesis-inflammation cross-talk: vascular endothelial growth factor is secreted by activated T cells and induces Th1 polarization. Journal of Immunology *172*, 4618-4623.

Moreau, T., Coles, A., Wing, M., Isaacs, J., Hale, G., Waldmann, H., and Compston, A. (1996). Transient increase in symptoms associated with cytokine release in patients with multiple sclerosis. Brain *119 (Pt 1)*, 225-237.

Muir, G.D., and Webb, A.A. (2000). Mini-review: assessment of behavioural recovery following spinal cord injury in rats. European Journal of Neuroscience *12*, 3079-3086.

Muller, D.M., Pender, M.P., and Greer, J.M. (2005). Blood-brain barrier disruption and lesion localisation in experimental autoimmune encephalomyelitis with predominant cerebellar and brainstem involvement. Journal of Neuroimmunology *160*, 162-169.

Nadal, A., Fuentes, E., Pastor, J., and McNaughton, P.A. (1995). Plasma albumin is a potent trigger of calcium signals and DNA synthesis in astrocytes. Procedings of the National Academy of Science U S A *92*, 1426-1430.

Nagy, Z., Kolev, K., Csonka, E., Pek, M., and Machovich, R. (1995). Contraction of human brain endothelial cells induced by thrombogenic and fibrinolytic factors. An in vitro cell culture model. Stroke; a journal of cerebral circulation *26*, 265-270.

Nakamura, Y., Si, Q.S., Takaku, T., and Kataoka, K. (2000). Identification of a peptide sequence in albumin that potentiates superoxide production by microglia. Journal of Neurochemistry *75*, 2309-2315.

Nasdala, I., Wolburg-Buchholz, K., Wolburg, H., Kuhn, A., Ebnet, K., Brachtendorf, G., Samulowitz, U., Kuster, B., Engelhardt, B., Vestweber, D.*, et al.* (2002). A transmembrane tight junction protein selectively expressed on endothelial cells and platelets. Journal of Biological Chemistry *277*, 16294-16303.

Nave, K.A., and Trapp, B.D. (2008). Axon-glial signaling and the glial support of axon function. Annual Review in Neuroscience *31*, 535-561.

Newman, E.A. (1996). Acid efflux from retinal glial cells generated by sodium bicarbonate cotransport. J Journal of Neuroscience *16*, 159-168.

Nicolopoulos-Stournaras, S., and Iles, J.F. (1983). Motor neuron columns in the lumbar spinal cord of the rat. Journal of Computational Neurology *217*, 75-85.

Nielsen, S., Nagelhus, E.A., Amiry-Moghaddam, M., Bourque, C., Agre, P., and Ottersen, O.P. (1997). Specialized membrane domains for water transport in glial cells: high-resolution immunogold cytochemistry of aquaporin-4 in rat brain. Journal of neuroscience *17*, 171-180.

Nischwitz, V., Berthele, A., and Michalke, B. (2008). Speciation analysis of selected metals and determination of their total contents in paired serum and cerebrospinal fluid samples: An approach to investigate the permeability of the human blood-cerebrospinal fluid-barrier. Anal Chimica Acta *627*, 258-269.

Nitta, T., Hata, M., Gotoh, S., Seo, Y., Sasaki, H., Hashimoto, N., Furuse, M., and Tsukita, S. (2003). Size-selective loosening of the blood-brain barrier in claudin-5-deficient mice. Journal of Cellular Biology *161*, 653-660.

O'Donnell, M.E., Tran, L., Lam, T.I., Liu, X.B., and Anderson, S.E. (2004). Bumetanide inhibition of the blood-brain barrier Na-K-Cl cotransporter reduces edema formation in the rat middle cerebral artery occlusion model of stroke. Journal of Cerebral Blood Flow and Metabolism *24*, 1046-1056.

Ohtsuki, S., and Terasaki, T. (2007). Contribution of carrier-mediated transport systems to the blood-brain barrier as a supporting and protecting interface for the brain; importance for CNS drug discovery and development. Pharm Res *24*, 1745-1758.

Olsson, A.K., Dimberg, A., Kreuger, J., and Claesson-Welsh, L. (2006). VEGF receptor signalling - in control of vascular function. Nature Review of Molecular and Cellular Biology *7*, 359-371.

Oosthuyse, B., Moons, L., Storkebaum, E., Beck, H., Nuyens, D., Brusselmans, K., Van Dorpe, J., Hellings, P., Gorselink, M., Heymans, S*., et al.* (2001). Deletion of the hypoxia-response element in the vascular endothelial growth factor promoter causes motor neuron degeneration. Nat Genet *28*, 131-138.

Palmieri, R.M., Ingersoll, C.D., and Hoffman, M.A. (2004). The hoffmann reflex: methodologic considerations and applications for use in sports medicine and athletic training research. J Athl Train *39*, 268-277.

Pantano, P., Mainero, C., and Caramia, F. (2006). Functional brain reorganization in multiple sclerosis: evidence from fMRI studies. Journal of Neuroimmaging *16*, 104-114.

Pardridge, W.M. (2007). Blood-brain barrier delivery. Drug Discovery Today *12*, 54-61.

Pardridge, W.M., Eisenberg, J., and Yang, J. (1985). Human blood-brain barrier insulin receptor. Journal of Neurochemistry *44*, 1771-1778.

Park, H.J., Won, C.K., Pyun, K.H., and Shin, H.C. (1995). Interleukin 2 suppresses afferent sensory transmission in the primary somatosensory cortex. Neuroreport *6*, 1018-1020.

Pasti, L., Zonta, M., Pozzan, T., Vicini, S., and Carmignoto, G. (2001). Cytosolic calcium oscillations in astrocytes may regulate exocytotic release of glutamate. Journal of neuroscience *21*, 477-484.

Patel, J., and Balabanov, R. (2012). Molecular mechanisms of oligodendrocyte injury in multiple sclerosis and experimental autoimmune encephalomyelitis. Int J Mol Sci *13*, 10647-10659.

Patrizio, M., and Levi, G. (1994). Glutamate production by cultured microglia: differences between rat and mouse, enhancement by lipopolysaccharide and lack effect of HIV coat protein gp120 and depolarizing agents. Neuroscience letters *178*, 184-189.

Paul, J., Strickland, S., and Melchor, J.P. (2007). Fibrin deposition accelerates neurovascular damage and neuroinflammation in mouse models of Alzheimer's disease. Journal of Experimental Medicine *204*, 1999-2008.

Pearse, D.D., Lo, T.P., Jr., Cho, K.S., Lynch, M.P., Garg, M.S., Marcillo, A.E., Sanchez, A.R., Cruz, Y., and Dietrich, W.D. (2005). Histopathological and behavioral characterization of a novel cervical spinal cord displacement contusion injury in the rat. Journal of Neurotrauma *22*, 680-702.

Peppiatt, C.M., Howarth, C., Mobbs, P., and Attwell, D. (2006). Bidirectional control of CNS capillary diameter by pericytes. Nature *443*, 700-704.

Perez, R.L., Ritzenthaler, J.D., and Roman, J. (1999). Transcriptional regulation of the interleukin-1beta promoter via fibrinogen engagement of the CD18 integrin receptor. American Journal of Respiratory Cellular and Molecular Biology *20*, 1059-1066.

Petty, M.A., and Lo, E.H. (2002). Junctional complexes of the blood-brain barrier: permeability changes in neuroinflammation. Progress in Neurobiology *68*, 311-323.

Piani, D., and Fontana, A. (1994). Involvement of the cystine transport system xc- in the macrophage-induced glutamate-dependent cytotoxicity to neurons. Journal of Immunology *152*, 3578-3585.

Piani, D., Frei, K., Do, K.Q., Cuenod, M., and Fontana, A. (1991). Murine brain macrophages induced NMDA receptor mediated neurotoxicity in vitro by secreting glutamate. Neuroscience letters *133*, 159-162.

Piontek, J., Winkler, L., Wolburg, H., Muller, S.L., Zuleger, N., Piehl, C., Wiesner, B., Krause, G., and Blasig, I.E. (2008). Formation of tight junction: determinants of homophilic interaction between classic claudins. FASEB Journal *22*, 146-158.

Pitt, D., Nagelmeier, I.E., Wilson, H.C., and Raine, C.S. (2003). Glutamate uptake by oligodendrocytes: Implications for excitotoxicity in multiple sclerosis. Neurology *61*, 1113-1120.

Pitt, D., Werner, P., and Raine, C.S. (2000). Glutamate excitotoxicity in a model of multiple sclerosis. Nature medicine *6*, 67-70.

Plumb, J., McQuaid, S., Mirakhur, M., and Kirk, J. (2002). Abnormal endothelial tight junctions in active lesions and normal-appearing white matter in multiple sclerosis. Brain pathology *12*, 154-169.

Pompeiano, O. (1972). Spinovestibular relations: anatomical and physiological aspects. Progress in Brain Research *37*, 263-296.

Pouly, S., Becher, B., Blain, M., and Antel, J.P. (2000). Interferon-gamma modulates human oligodendrocyte susceptibility to Fas-mediated apoptosis. Journal of Neuropathology and Experimental Neurology *59*, 280-286.

Proescholdt, M.A., Jacobson, S., Tresser, N., Oldfield, E.H., and Merrill, M.J. (2002a). Vascular endothelial growth factor is expressed in multiple sclerosis plaques and can induce inflammatory lesions in experimental allergic encephalomyelitis rats. Journal of Neuropathology and Experimental Neurology *61*, 914-925.

Proescholdt, M.G., Chakravarty, S., Foster, J.A., Foti, S.B., Briley, E.M., and Herkenham, M. (2002b). Intracerebroventricular but not intravenous interleukin-1beta induces widespread vascular-mediated leukocyte infiltration and immune signal mRNA expression followed by brain-wide glial activation. Neuroscience *112*, 731-749.

Rahimi, N. (2006). Vascular endothelial growth factor receptors: molecular mechanisms of activation and therapeutic potentials. Exp Eye Res *83*, 1005-1016.

Ralay Ranaivo, H., and Wainwright, M.S. (2010). Albumin activates astrocytes and microglia through mitogen-activated protein kinase pathways. Brain research *1313*, 222-231.

Rausche, G., Igelmund, P., and Heinemann, U. (1990). Effects of changes in extracellular potassium, magnesium and calcium concentration on synaptic transmission in area CA1 and the dentate gyrus of rat hippocampal slices. Pflugers Archives *415*, 588-593.

Ravizza, T., Gagliardi, B., Noe, F., Boer, K., Aronica, E., and Vezzani, A. (2008). Innate and adaptive immunity during epileptogenesis and spontaneous seizures: evidence from experimental models and human temporal lobe epilepsy. Neurobiology of Disease *29*, 142-160.

Redford, E.J., Kapoor, R., and Smith, K.J. (1997). Nitric oxide donors reversibly block axonal conduction: demyelinated axons are especially susceptible. Brain *120 (Pt 12)*, 2149-2157.

Reese, T.S., and Karnovsky, M.J. (1967). Fine structural localization of a blood-brain barrier to exogenous peroxidase. Journal of Cellular Biology *34*, 207-217.

Reinders, M.E., Sho, M., Izawa, A., Wang, P., Mukhopadhyay, D., Koss, K.E., Geehan, C.S., Luster, A.D., Sayegh, M.H., and Briscoe, D.M. (2003). Proinflammatory functions of vascular endothelial growth factor in alloimmunity. Journal of Clinical Investigation *112*, 1655-1665.

Reinke, E.K., Lee, J., Zozulya, A., Karman, J., Muller, W.A., Sandor, M., and Fabry, Z. (2007). Short-term sPECAM-Fc treatment ameliorates EAE while chronic use hastens onset of symptoms. Journal of Neuroimmunology *186*, 86-93.

Rigau, V., Morin, M., Rousset, M.C., de Bock, F., Lebrun, A., Coubes, P., Picot, M.C., Baldy-Moulinier, M., Bockaert, J., Crespel, A.*, et al.* (2007). Angiogenesis is associated with blood-brain barrier permeability in temporal lobe epilepsy. Brain *130*, 1942-1956.

Rivlin, A.S., and Tator, C.H. (1977). Objective clinical assessment of motor function after experimental spinal cord injury in the rat. Journal of Neurosurgery *47*, 577-581.

Rizzo, M.A., Hadjimichael, O.C., Preiningerova, J., and Vollmer, T.L. (2004). Prevalence and treatment of spasticity reported by multiple sclerosis patients. Multiple Sclerosis *10*, 589-595.

Robinson, C.J., and Stringer, S.E. (2001). The splice variants of vascular endothelial growth factor (VEGF) and their receptors. Journal of Cellular Science *114*, 853-865.

Rosenstein, J.M., Krum, J.M., and Ruhrberg, C. (2010). VEGF in the nervous system. Organogenesis *6*, 107-114.

Rosenstein, J.M., Mani, N., Khaibullina, A., and Krum, J.M. (2003). Neurotrophic effects of vascular endothelial growth factor on organotypic cortical explants and primary cortical neurons. Journal of neuroscience *23*, 11036-11044.

Rossi, A., Rossi, S., and Ginanneschi, F. (2012). Activity-dependent changes in intrinsic excitability of human spinal motoneurones produced by natural activity. Journal of Neurophysiology *108*, 2473-2480.

Rothstein, J.D., Dykes-Hoberg, M., Pardo, C.A., Bristol, L.A., Jin, L., Kuncl, R.W., Kanai, Y., Hediger, M.A., Wang, Y., Schielke, J.P.*, et al.* (1996). Knockout of glutamate transporters reveals a major role for astroglial transport in excitotoxicity and clearance of glutamate. Neuron *16*, 675-686.

Ruiz de Almodovar, C., Lambrechts, D., Mazzone, M., and Carmeliet, P. (2009). Role and therapeutic potential of VEGF in the nervous system. Physiological reviews *89*, 607-648.

Sahara, Y., Xie, Y.K., and Bennett, G.J. (1990). Intracellular records of the effects of primary afferent input in lumbar spinoreticular tract neurons in the cat. Journal of Neurophysiology *64*, 1791-1800.

Saija, A., Princi, P., Lanza, M., Scalese, M., Aramnejad, E., and De Sarro, A. (1995). Systemic cytokine administration can affect blood-brain barrier permeability in the rat. Life Science *56*, 775-784.

Saitou, M., Furuse, M., Sasaki, H., Schulzke, J.D., Fromm, M., Takano, H., Noda, T., and Tsukita, S. (2000). Complex phenotype of mice lacking occludin, a component of tight junction strands. Molecular Biology of the Cell *11*, 4131-4142.

Sakakibara, A., Furuse, M., Saitou, M., Ando-Akatsuka, Y., and Tsukita, S. (1997). Possible involvement of phosphorylation of occludin in tight junction formation. Journal of Cellular Biology *137*, 1393-1401.

Salih, F., Steinheimer, S., and Grosse, P. (2011). Excitability and recruitment patterns of spinal motoneurons in human sleep as assessed by F-wave recordings. Experimental Brain Research *213*, 1-8.

Sarchielli, P., Greco, L., Floridi, A., and Gallai, V. (2003). Excitatory amino acids and multiple sclerosis: evidence from cerebrospinal fluid. Arch Neurol *60*, 1082-1088.

Sasaki, M., Lankford, K.L., Brown, R.J., Ruddle, N.H., and Kocsis, J.D. (2010). Focal experimental autoimmune encephalomyelitis in the Lewis rat induced by immunization with myelin oligodendrocyte glycoprotein and intraspinal injection of vascular endothelial growth factor. Glia *58*, 1523-1531.

Sawano, A., Iwai, S., Sakurai, Y., Ito, M., Shitara, K., Nakahata, T., and Shibuya, M. (2001). Flt-1, vascular endothelial growth factor receptor 1, is a novel cell surface marker for the lineage of monocyte-macrophages in humans. Blood *97*, 785-791.

Schachtrup, C., Ryu, J.K., Helmrick, M.J., Vagena, E., Galanakis, D.K., Degen, J.L., Margolis, R.U., and Akassoglou, K. (2010). Fibrinogen triggers astrocyte scar formation by promoting the availability of active TGF-beta after vascular damage. Journal of neuroscience *30*, 5843-5854.

Schell, M.J., Molliver, M.E., and Snyder, S.H. (1995). D-serine, an endogenous synaptic modulator: localization to astrocytes and glutamate-stimulated release. Procedings of the National Academy of Science U S A *92*, 3948-3952.

Schinkel, A.H., Smit, J.J., van Tellingen, O., Beijnen, J.H., Wagenaar, E., van Deemter, L., Mol, C.A., van der Valk, M.A., Robanus-Maandag, E.C., te Riele, H.P.*, et al.* (1994). Disruption of the mouse mdr1a P-glycoprotein gene leads to a deficiency in the blood-brain barrier and to increased sensitivity to drugs. Cell *77*, 491-502.

Schinkel, A.H., Wagenaar, E., Mol, C.A., and van Deemter, L. (1996). P-glycoprotein in the blood-brain barrier of mice influences the brain penetration and pharmacological activity of many drugs. Journal of Clinical Investigation *97*, 2517-2524.

Schofield, C.J., and Zhang, Z. (1999). Structural and mechanistic studies on 2-oxoglutarate-dependent oxygenases and related enzymes. Current Opinions in Structural Biology *9*, 722-731.

Schulze, C., and Firth, J.A. (1993). Immunohistochemical localization of adherens junction components in blood-brain barrier microvessels of the rat. Journal of Cellular Science *104 (Pt 3)*, 773-782.

Seifert, G., Schilling, K., and Steinhauser, C. (2006). Astrocyte dysfunction in neurological disorders: a molecular perspective. Nature Review of Molecular and Cellular Biology *7*, 194-206.

Seiffert, E., Dreier, J.P., Ivens, S., Bechmann, I., Tomkins, O., Heinemann, U., and Friedman, A. (2004). Lasting blood-brain barrier disruption induces epileptic focus in the rat somatosensory cortex. Journal of neuroscience *24*, 7829-7836.

Senger, D.R., Galli, S.J., Dvorak, A.M., Perruzzi, C.A., Harvey, V.S., and Dvorak, H.F. (1983). Tumor cells secrete a vascular permeability factor that promotes accumulation of ascites fluid. Science *219*, 983-985.

Shortland, P., and Woolf, C.J. (1993). Morphology and somatotopy of the central arborizations of rapidly adapting glabrous skin afferents in the rat lumbar spinal cord. Journal of Computational Neurology *329*, 491-511.

Silverman, W.F., Krum, J.M., Mani, N., and Rosenstein, J.M. (1999). Vascular, glial and neuronal effects of vascular endothelial growth factor in mesencephalic explant cultures. Neuroscience *90*, 1529-1541.

Simpson, I.A., Carruthers, A., and Vannucci, S.J. (2007). Supply and demand in cerebral energy metabolism: the role of nutrient transporters. Journal of Cerebral Blood Flow and Metabolism *27*, 1766-1791.

Smiley, S.T., King, J.A., and Hancock, W.W. (2001). Fibrinogen stimulates macrophage chemokine secretion through toll-like receptor 4. Journal of Immunology *167*, 2887-2894.

Smith, S.J., Claus, D., Hess, C.W., Mills, K.R., Murray, N.M., and Schriefer, T. (1989). F responses and central motor conduction in multiple sclerosis. Electroencephalography and Clinincal Neurophysiology *74*, 438-443.

Sobel, R.A., and Mitchell, M.E. (1989). Fibronectin in multiple sclerosis lesions. The American journal of pathology *135*, 161-168.

Soker, S., Takashima, S., Miao, H.Q., Neufeld, G., and Klagsbrun, M. (1998). Neuropilin-1 is expressed by endothelial and tumor cells as an isoform-specific receptor for vascular endothelial growth factor. Cell *92*, 735-745.

Sokolova, E., and Reiser, G. (2008). Prothrombin/thrombin and the thrombin receptors PAR-1 and PAR-4 in the brain: localization, expression and participation in neurodegenerative diseases. Thrombosis and haemostasis *100*, 576-581.

Sondell, M., Lundborg, G., and Kanje, M. (1999). Vascular endothelial growth factor has neurotrophic activity and stimulates axonal outgrowth, enhancing cell survival and Schwann cell proliferation in the peripheral nervous system. Journal of neuroscience *19*, 5731-5740.

Sondell, M., Sundler, F., and Kanje, M. (2000). Vascular endothelial growth factor is a neurotrophic factor which stimulates axonal outgrowth through the flk-1 receptor. European Journal of Neuroscience *12*, 4243-4254.

Spector, R., and Johanson, C.E. (2007). Vitamin transport and homeostasis in mammalian brain: focus on Vitamins B and E. Journal of Neurochemistry *103*, 425-438.

Srinivasan, R., Sailasuta, N., Hurd, R., Nelson, S., and Pelletier, D. (2005). Evidence of elevated glutamate in multiple sclerosis using magnetic resonance spectroscopy at 3 T. Brain *128*, 1016-1025.

Stadelmann, C., Wegner, C., and Bruck, W. (2011). Inflammation, demyelination, and degeneration - recent insights from MS pathology. Biochimica et biophysica acta *1812*, 275-282.

Stelzner, D.J., and Cullen, J.M. (1991). Do propriospinal projections contribute to hindlimb recovery when all long tracts are cut in neonatal or weanling rats? Experimental Neurology *114*, 193-205.

Stevenson, B.R., Siliciano, J.D., Mooseker, M.S., and Goodenough, D.A. (1986). Identification of ZO-1: a high molecular weight polypeptide associated with the tight junction (zonula occludens) in a variety of epithelia. Journal of Cellular Biology *103*, 755-766.

Stolp, H.B., and Dziegielewska, K.M. (2009). Review: Role of developmental inflammation and blood-brain barrier dysfunction in neurodevelopmental and neurodegenerative diseases. Neuropathology and applied neurobiology *35*, 132-146.

Striggow, F., Riek, M., Breder, J., Henrich-Noack, P., Reymann, K.G., and Reiser, G. (2000). The protease thrombin is an endogenous mediator of hippocampal neuroprotection against ischemia at low concentrations but causes degeneration at high concentrations. Procedings of the National Academy of Science U S A *97*, 2264-2269.

Strukova, S.M. (2001). Thrombin as a regulator of inflammation and reparative processes in tissues. Biochemistry (Mosc) *66*, 8-18.

Su, J.J., Osoegawa, M., Matsuoka, T., Minohara, M., Tanaka, M., Ishizu, T., Mihara, F., Taniwaki, T., and Kira, J. (2006). Upregulation of vascular growth factors in multiple sclerosis: correlation with MRI findings. Journal of Neurological Sciences *243*, 21-30.

Suh, S.W., Bergher, J.P., Anderson, C.M., Treadway, J.L., Fosgerau, K., and Swanson, R.A. (2007). Astrocyte glycogen sustains neuronal activity during hypoglycemia: studies with the glycogen phosphorylase inhibitor CP-316,819 ([R-R*,S*]-5-chloro-N-[2-hydroxy-3-(methoxymethylamino)-3-oxo-1-(phenylmethyl)pro pyl]-1H-indole-2-carboxamide). Journal of Pharmacology and Experimental Therapeutics *321*, 45-50.

Takahashi, C., Muramatsu, R., Fujimura, H., Mochizuki, H., and Yamashita, T. (2013). Prostacyclin promotes oligodendrocyte precursor recruitment and remyelination after spinal cord demyelination. Cell death & disease *4*, e795.

Takahashi, H., Hattori, S., Iwamatsu, A., Takizawa, H., and Shibuya, M. (2004). A novel snake venom vascular endothelial growth factor (VEGF) predominantly induces vascular permeability through preferential signaling via VEGF receptor-1. Journal of Biological Chemistry *279*, 46304-46314.

Takahashi, H., and Shibuya, M. (2005). The vascular endothelial growth factor (VEGF)/VEGF receptor system and its role under physiological and pathological conditions. Clinical science *109*, 227-241.

Takumi, T., Ishii, T., Horio, Y., Morishige, K., Takahashi, N., Yamada, M., Yamashita, T., Kiyama, H., Sohmiya, K., Nakanishi, S.*, et al.* (1995). A novel ATP-dependent inward rectifier potassium channel expressed predominantly in glial cells. Journal of Biological Chemistry *270*, 16339-16346.

Tancredi, V., D'Arcangelo, G., Grassi, F., Tarroni, P., Palmieri, G., Santoni, A., and Eusebi, F. (1992). Tumor necrosis factor alters synaptic transmission in rat hippocampal slices. Neuroscience letters *146*, 176-178.

Taylor, C.J., Nicola, P.A., Wang, S., Barrand, M.A., and Hladky, S.B. (2006). Transporters involved in regulation of intracellular pH in primary cultured rat brain endothelial cells. Journal of Physiology *576*, 769-785.

Thorburne, S.K., and Juurlink, B.H. (1996). Low glutathione and high iron govern the susceptibility of oligodendroglial precursors to oxidative stress. Journal of Neurochemistry *67*, 1014-1022.

Tomas-Camardiel, M., Venero, J.L., Herrera, A.J., De Pablos, R.M., Pintor-Toro, J.A., Machado, A., and Cano, J. (2005). Blood-brain barrier disruption highly induces aquaporin-4 mRNA and protein in perivascular and parenchymal astrocytes: protective effect by estradiol treatment in ovariectomized animals. Journal of neuroscience research *80*, 235-246.

Trapp, B.D., Wujek, J.R., Criste, G.A., Jalabi, W., Yin, X., Kidd, G.J., Stohlman, S., and Ransohoff, R. (2007). Evidence for synaptic stripping by cortical microglia. Glia *55*, 360-368.

Umeda, K., Matsui, T., Nakayama, M., Furuse, K., Sasaki, H., Furuse, M., and Tsukita, S. (2004). Establishment and characterization of cultured epithelial cells lacking expression of ZO-1. Journal of Biological Chemistry *279*, 44785-44794.

van Bruggen, N., Thibodeaux, H., Palmer, J.T., Lee, W.P., Fu, L., Cairns, B., Tumas, D., Gerlai, R., Williams, S.P., van Lookeren Campagne, M.*, et al.* (1999). VEGF antagonism reduces edema formation and tissue damage after ischemia/reperfusion injury in the mouse brain. Journal of Clinical Investigation *104*, 1613-1620.

van der Valk, P., and Amor, S. (2009). Preactive lesions in multiple sclerosis. Current Opinions in Neurology *22*, 207-213.

van der Valk, P., and De Groot, C.J. (2000). Staging of multiple sclerosis (MS) lesions: pathology of the time frame of MS. Neuropathology and applied neurobiology *26*, 2-10.

van Horssen, J., Singh, S., van der Pol, S., Kipp, M., Lim, J.L., Peferoen, L., Gerritsen, W., Kooi, E.J., Witte, M.E., Geurts, J.J.*, et al.* (2012). Clusters of activated microglia in normal-appearing white matter show signs of innate immune activation. J Neuroinflammation *9*, 156.

van Noort, J.M., van den Elsen, P.J., van Horssen, J., Geurts, J.J., van der Valk, P., and Amor, S. (2011). Preactive multiple sclerosis lesions offer novel clues for neuroprotective therapeutic strategies. CNS and Neurological Disorders - Drug Targets *10*, 68-81.

Vartanian, T., Li, Y., Zhao, M., and Stefansson, K. (1995). Interferon-gamma-induced oligodendrocyte cell death: implications for the pathogenesis of multiple sclerosis. Molecular Medicine *1*, 732-743.

Veikkola, T., Jussila, L., Makinen, T., Karpanen, T., Jeltsch, M., Petrova, T.V., Kubo, H., Thurston, G., McDonald, D.M., Achen, M.G.*, et al.* (2001). Signalling via vascular endothelial growth factor receptor-3 is sufficient for lymphangiogenesis in transgenic mice. EMBO Journal *20*, 1223-1231.

Vercellino, M., Merola, A., Piacentino, C., Votta, B., Capello, E., Mancardi, G.L., Mutani, R., Giordana, M.T., and Cavalla, P. (2007). Altered glutamate reuptake in relapsing-remitting and secondary progressive multiple sclerosis cortex: Correlation with microglia infiltration, demyelination, and neuronal and synaptic damage. Journal of Neuropathology and Experimental Neurology *66*, 732-739.

Vercellino, M., Plano, F., Votta, B., Mutani, R., Giordana, M.T., and Cavalla, P. (2005). Grey matter pathology in multiple sclerosis. Journal of Neuropathology and Experimental Neurology *64*, 1101-1107.

Vezzani, A., and Baram, T.Z. (2007). New roles for interleukin-1 Beta in the mechanisms of epilepsy. Epilepsy Currents *7*, 45-50.

Vezzani, A., Conti, M., De Luigi, A., Ravizza, T., Moneta, D., Marchesi, F., and De Simoni, M.G. (1999). Interleukin-1beta immunoreactivity and microglia are enhanced in the rat hippocampus by focal kainate application: functional evidence for enhancement of electrographic seizures. Journal of neuroscience *19*, 5054-5065.

Vincent, P.A., Xiao, K., Buckley, K.M., and Kowalczyk, A.P. (2004). VE-cadherin: adhesion at arm's length. American journal of physiology Cell physiology *286*, C987-997.

Virgintino, D., Girolamo, F., Errede, M., Capobianco, C., Robertson, D., Stallcup, W.B., Perris, R., and Roncali, L. (2007). An intimate interplay between precocious, migrating pericytes and endothelial cells governs human fetal brain angiogenesis. Angiogenesis *10*, 35-45.

Voerman, G.E., Gregoric, M., and Hermens, H.J. (2005). Neurophysiological methods for the assessment of spasticity: the Hoffmann reflex, the tendon reflex, and the stretch reflex. Disability Rehabilitation *27*, 33-68.

von Euler, M., Seiger, A., and Sundstrom, E. (1997). Clip compression injury in the spinal cord: a correlative study of neurological and morphological alterations. Experimental Neurology *145*, 502-510.

von Tell, D., Armulik, A., and Betsholtz, C. (2006). Pericytes and vascular stability. Exp Cell Res *312*, 623-629.

Wallstrom, E., Diener, P., Ljungdahl, A., Khademi, M., Nilsson, C.G., and Olsson, T. (1996). Memantine abrogates neurological deficits, but not CNS inflammation, in Lewis rat experimental autoimmune encephalomyelitis. Journal of Neurological Sciences *137*, 89-96.

Walton, M.I., Bleehen, N.M., and Workman, P. (1985). The reversible N-oxidation of the nitroimidazole radiosensitizer Ro 03-8799. Biochemical pharmacology *34*, 3939-3940.

Watson, C.H., A.R. (2009). Projections from the brain to the spinal cord. In The spinal cord, pp. 168-179.

Waxman, S.G., Black, J.A., Ransom, B.R., and Stys, P.K. (1994). Anoxic injury of rat optic nerve: ultrastructural evidence for coupling between Na+ influx and Ca(2+)-mediated injury in myelinated CNS axons. Brain research *644*, 197-204.

Waxman, S.G., and Ritchie, J.M. (1993). Molecular dissection of the myelinated axon. Annals of Neurology *33*, 121-136.

Weinshenker, B.G. (1996). Epidemiology of multiple sclerosis. Neurol Clin *14*, 291-308.

Weissberg, I., Reichert, A., Heinemann, U., and Friedman, A. (2011). Blood-brain barrier dysfunction in epileptogenesis of the temporal lobe. Epilepsy Research Treatment *2011*, 143908.

Werner, P., Pitt, D., and Raine, C.S. (2000). Glutamate excitotoxicity--a mechanism for axonal damage and oligodendrocyte death in Multiple Sclerosis? Journal of Neural Transmission Supplementa, 375-385.

Werner, P., Pitt, D., and Raine, C.S. (2001). Multiple sclerosis: altered glutamate homeostasis in lesions correlates with oligodendrocyte and axonal damage. Annals of Neurology *50*, 169-180.

Wetherington, J., Serrano, G., and Dingledine, R. (2008). Astrocytes in the epileptic brain. Neuron *58*, 168-178.

Whitaker, G.B., Limberg, B.J., and Rosenbaum, J.S. (2001). Vascular endothelial growth factor receptor-2 and neuropilin-1 form a receptor complex that is responsible for the

differential signaling potency of VEGF(165) and VEGF(121). Journal of Biological Chemistry *276*, 25520-25531.

Whitlock, B.B., Gardai, S., Fadok, V., Bratton, D., and Henson, P.M. (2000). Differential roles for alpha(M)beta(2) integrin clustering or activation in the control of apoptosis via regulation of akt and ERK survival mechanisms. Journal of Cellular Biology *151*, 1305-1320.

Whittles, C.E., Pocock, T.M., Wedge, S.R., Kendrew, J., Hennequin, L.F., Harper, S.J., and Bates, D.O. (2002). ZM323881, a novel inhibitor of vascular endothelial growth factor-receptor-2 tyrosine kinase activity. Microcirculation *9*, 513-522.

Willenborg, D.O., Staykova, M., Fordham, S., O'Brien, N., and Linares, D. (2007). The contribution of nitric oxide and interferon gamma to the regulation of the neuro-inflammation in experimental autoimmune encephalomyelitis. Journal of Neuroimmunology *191*, 16-25.

Wilson, V.J., Wylie, R.M., and Marco, L.A. (1967). Projection to the spinal cord from the medial and descending vestibular nuclei of the cat. Nature *215*, 429-430.

Witte, M.E., Geurts, J.J., de Vries, H.E., van der Valk, P., and van Horssen, J. (2010). Mitochondrial dysfunction: a potential link between neuroinflammation and neurodegeneration? Mitochondrion *10*, 411-418.

Wolburg, H., and Lippoldt, A. (2002). Tight junctions of the blood-brain barrier: development, composition and regulation. Vascular pharmacology *38*, 323-337.

Wujek, J.R., Bjartmar, C., Richer, E., Ransohoff, R.M., Yu, M., Tuohy, V.K., and Trapp, B.D. (2002). Axon loss in the spinal cord determines permanent neurological disability in an animal model of multiple sclerosis. Journal of Neuropathology and Experimental Neurology *61*, 23-32.

Ye, Z.C., and Sontheimer, H. (1996). Cytokine modulation of glial glutamate uptake: a possible involvement of nitric oxide. Neuroreport *7*, 2181-2185.

Youl, B.D., Turano, G., Miller, D.H., Towell, A.D., MacManus, D.G., Moore, S.G., Jones, S.J., Barrett, G., Kendall, B.E., Moseley, I.F.*, et al.* (1991). The pathophysiology of acute optic neuritis. An association of gadolinium leakage with clinical and electrophysiological deficits. Brain *114 (Pt 6)*, 2437-2450.

Yu, B., and Shinnick-Gallagher, P. (1994). Interleukin-1 beta inhibits synaptic transmission and induces membrane hyperpolarization in amygdala neurons. Journal of Pharmacology and Experimental Therapeutics *271*, 590-600.

Yuan, L., Moyon, D., Pardanaud, L., Breant, C., Karkkainen, M.J., Alitalo, K., and Eichmann, A. (2002). Abnormal lymphatic vessel development in neuropilin 2 mutant mice. Development *129*, 4797-4806.

Zhang, Z.G., Zhang, L., Jiang, Q., Zhang, R., Davies, K., Powers, C., Bruggen, N., and Chopp, M. (2000). VEGF enhances angiogenesis and promotes blood-brain barrier leakage in the ischemic brain. Journal of Clinical Investigation *106*, 829-838.

Zhao, T.Z., Xia, Y.Z., Li, L., Li, J., Zhu, G., Chen, S., Feng, H., and Lin, J.K. (2009). Bovine serum albumin promotes IL-1beta and TNF-alpha secretion by N9 microglial cells. Neurological Science *30*, 379-383.

Zhong, H., Chiles, K., Feldser, D., Laughner, E., Hanrahan, C., Georgescu, M.M., Simons, J.W., and Semenza, G.L. (2000). Modulation of hypoxia-inducible factor 1alpha expression by the epidermal growth factor/phosphatidylinositol 3-kinase/PTEN/AKT/FRAP pathway in human prostate cancer cells: implications for tumor angiogenesis and therapeutics. Cancer research *60*, 1541-1545.

Zhu, B., Luo, L., Moore, G.R., Paty, D.W., and Cynader, M.S. (2003). Dendritic and synaptic pathology in experimental autoimmune encephalomyelitis. The American journal of pathology *162*, 1639-1650.

Zhu, C.S., Hu, X.Q., Xiong, Z.J., Lu, Z.Q., Zhou, G.Y., and Wang, D.J. (2008). Adenoviral delivery of soluble VEGF receptor 1 (sFlt-1) inhibits experimental autoimmune encephalomyelitis in dark Agouti (DA) rats. Life Science *83*, 404-412.

Zlokovic, B.V. (2008). The blood-brain barrier in health and chronic neurodegenerative disorders. Neuron *57*, 178-201.

Zlotnik, A., Gurevich, B., Tkachov, S., Maoz, I., Shapira, Y., and Teichberg, V.I. (2007). Brain neuroprotection by scavenging blood glutamate. Experimental Neurology *203*, 213-220.

Zonta, M., Angulo, M.C., Gobbo, S., Rosengarten, B., Hossmann, K.A., Pozzan, T., and Carmignoto, G. (2003). Neuron-to-astrocyte signaling is central to the dynamic control of brain microcirculation. Nature neuroscience *6*, 43-50.